# THE ANALYSIS OF ENGINE OILS AND ENGINE OIL ADDITIVES BY MASS SPECTROMETRY

A thesis presented by

STEPHEN GRAHAM O'HAGAN, B.Sc, M.Sc.

In fulfilment of the requirements of

**the University of Warwick**

for the degree of

**Doctor of Philosophy**

Department of Chemistry,

University of Warwick,

Coventry, U.K.

March 1988.

# PREFACE

The work reported here was carried out at the Department of Chemistry of the University of Warwick under the supervision of Professor K. R. Jennings, and at the ESSO Research Centre, Abingdon, under the supervision of Mr. E. K. Kendrick.

The work was carried out completely by the author, except where indicated in the text.

This thesis is not substantially the same as any other submitted for a degree or qualification to this, or any other, institution of learning.

ACKNOWLEDGEMENTS

First and foremost I would like to thank Prof. K. R. Jennings for his supervision and helpful advice during my stay at the University of Warwick.

Special thanks must also go to Mr. E. K. Kendrick, of ESSO Research Centre, Abingdon, for his help and guidance during my visits to ESSO Research Centre.

I would also like to thank Mr. Inder Kaytal for his help with the MS80 mass spectrometer and for providing the example spectra used in chapter I.

Additional thanks go to Dave Mitchell, Colin Moore, Dave Newton, Richard Gallagher, Richard Bowen and Rod Mason.

Very special thanks must go to Miss Chiu Yi Li.

# ABSTRACT

Chapter I presents an overview of mass spectrometry on double focusing instruments. Special attention is paid to ionisation methods which may be of use in mixture analysis.

In chapter II, following a brief introduction to chemometrics, results of the application of factor analysis to the problem of determining the components of a mixture from mass spectra of simple mixtures are given. After applying the technique to simulated data, the results of applying the technique to simple mixtures and to the deconvolution of overlapping GC/MC spectra are given. It is concluded that provided the pure compounds have 'unique' peaks in their mass spectra, and that the statistical variations in the intensities of peaks due to different mixtures are not correlated, then the technique will yield good results.

Chapter III deals with the application of CI techniques and factor analysis to the analysis of engine oils.

Attempts to use the factor analysis technique to yield a meaningful 'type' analysis of engine oil fractions was not successful.

The use of proton transfer reagents and charge transfer reagents for CI spectra of engine oil fractions was also unsuccessful. It is concluded that the complexity of engine oil mixtures and the chemical similarity of the constituent molecules makes them difficult to differentiate by CI mass spectrometry.

In the final chapter, details are give of an investigation into the use of CI mass spectrometry and FAB mass spectrometry for the analysis of engine oil additives. The additives studied were calcium 2,2'-bis (4-alkylphenyl) sulphides.

The FAB mass spectrometry of these sulphurised phenates gave poor results with glycerol, triethanolamine, triethanolamine / sodium sulphate or squalane used as FAB matrix.

Of the CI techniques used, electron capture ionisation of the hydrolysed sample gave the most promising results. The molecular ion peak intensities were higher than those encountered in the EI spectra. In addition, the fragmentation in the EC spectra was simpler than the fragmentation in the EI spectrum.

Metastable ion studies of the EI and EC spectra of the sulphurised phenols, using the technique of metastable mapping, gave some useful results, but the poor mass resolving power and the long run times were a major drawback. It is concluded that the technique of metastable mapping is of no use where mass resolution is important, and the use of inlet systems, such as an AGHIS, which allow long sample lifetimes is recommended.

Where possible, the use of tandem mass spectrometry or Fourier transform mass spectrometry for metastable ion studies for mixture analysis, is also recommended.

CONTENTS

CHAPTER I



CHAPTER II

FIGURES

CHAPTER I



CHAPTER II

CHAPTER III

TABLES

ABREVIATIONS

| | |
|---|---|
| $\Delta E$ | EXOERGICITY OF REACTION |
| $\Delta H$ | ENTHALPY OF REACTION |
| $\Delta M$ | MASS DEFECT |
| CI | CHEMICAL IONISATION |
| DCI | DIRECT CHEMICAL IONISATION |
| DIP | DIRECT INSERTION PROBE |
| EC | ELECTRON CAPTURE IONISATION |
| EI | ELECTRON IONISATION |
| ESA | ELECTROSTATIC ANALYSER |
| FA | FACTOR ANALYSIS |
| FAB | FAST ATOM BOMBARDMENT (IONISATION) |
| FAB/MS | FAST ATOM BOMBARDMENT MASS SPECTROMETRY |
| FTMS | FOURIER TRANSFORM MASS SPECTROMETRY |
| GC | GAS CHROMATOGRAPHY |
| GC/MS | GAS CHROMATOGRAPHY - MASS SPECTROMETRY |
| HPLC | HIGH PERFORMANCE LIQUID CHROMATOGRAPHY |
| I(M) | INTENSITY OF PEAK DUE TO SPECIES OF RELATIVE MOLECULAR MASS M |
| IE | IONISATION ENERGY |
| IE(X) | IONISATION ENERGY OF SPECIES X |
| LC | LIQUID CHROMATOGRAPHY |
| LC/FABMS | LIQUID CHROMATOGRAPHY - FAST ATOM BOMBARDMENT MASS SPECTROMETRY |
| LC/MS | LIQUID CHROMATOGRAPHY - MASS SPECTROMETRY |
| M | SPECIES OF RELATIVE MOLECULAR MASS M, OR RELATIVE MOLECULAR MASS |
| M/Z | MASS / CHARGE RATIO |
| MS | MASS SPECTROMETRY |
| MS/MS | TANDEM MASS SPECTROMETRY |
| NMR | NUCLEAR MAGNETIC RESONANCE (SPECTROMETRY) |
| PA | PROTON AFFINITY |
| PCA | PRINCIPAL COMPONENT ANALYSIS |
| SIMS | SECONDARY ION MASS SPECTROMETRY |
| TIC | TOTAL ION CURRENT |
| TOF | TIME OF FLIGHT (MASS SPECTROMETRY) |

# CHAPTER I

# THE MASS SPECTROMETER.

## 1.0 The Mass Spectrometer

The mass spectrometer is an analytical instrument designed to measure the mass/charge ratio and relative abundances of gaseous ions derived from a sample compound. A plot of relative ion abundance versus mass/charge ratio is known as a mass spectrum of the sample, and since there are several methods of sample introduction and ionisation, there are several types of mass spectra. Since the ions are derived from an element, compound or mixture of interest, and, given that the ions are related to the original material, one can then answer a number of questions about that material. In order fully to answer these questions, an understanding of the relationship between the gaseous ions and the original material is needed. This will involve an understanding of the method of ion production, the mass analyser and the ion detector. The functions of ion production, mass analysis, and ion detection can often be considered separately, as shown in figure 1.1.

In a general introduction it is pertinent to enquire what advantages the technique of mass spectrometry offers over other analytical techniques. The mass spectrometer provides, in favourable cases, information about the relative molecular mass of a compound, structural information and possibly information about the compound's elemental composition. Mass spectrometry is highly sensitive, sample sizes in the order of a microgram or less are common, and detection limits down to the nanogram level are achievable without difficulty.

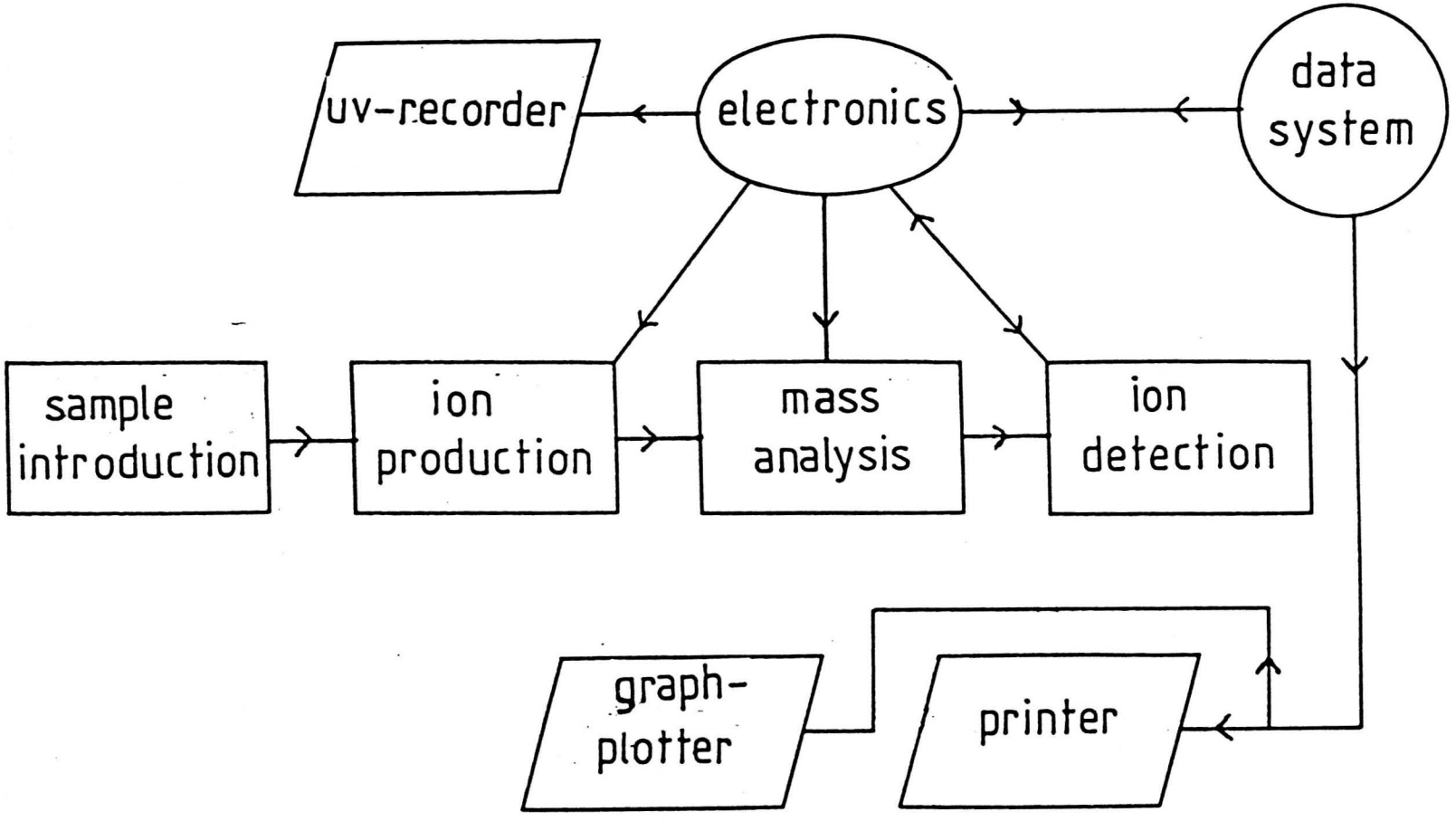


FIGURE 1.1: Mass Spectrometer System Schematic Diagram.

## 1.1 Ion Production

Many samples can be volatilised without decomposition and enter the ion source in the form of a vapour. The function of an ion source is to produce as many structurally significant ions as possible from the sample and to eject these ions, as an ion beam into the mass analyser. The most commonly used ion source is the electron ionisation source.

### 1.1.1 Positive Electron Ionisation

The electron ionisation (EI) source employs a beam of electrons to achieve ionisation of the sample molecules. The EI source is shown schematically in figure 1.2.

Electrons are accelerated through a known potential difference and collide with sample molecules, imparting some of their translational energy as internal energy.

Ions may be classified as fragment ions or molecular ions, and the type of ions produced depends on the source temperature, the nature of the sample molecules and the energy transfered to the molecules by the electrons.

A typical set of ionisation efficiency curves is shown in figure 1.3. These show relative ion abundances of ions as a function of electron energy. At the onset of ionisation, characterised by the adiabatic ionisation potential of the molecule, production of the 'molecular ion' begins, provided the molecular ion is stable with respect to decomposition:-

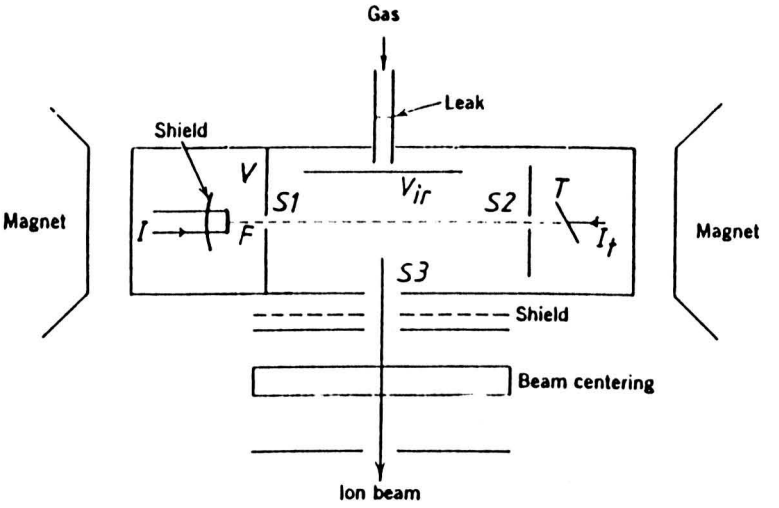


**FIGURE 1.2: Electron Ionisation Source.**
(after Roboz, Ref.8, p119)

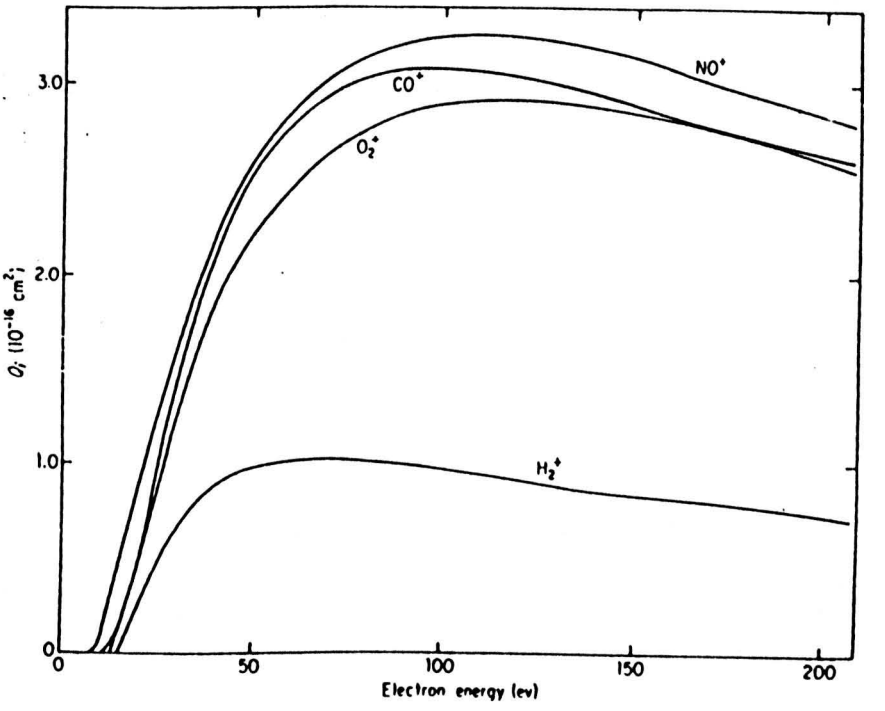


**FIGURE 1.3: Electron Ionisation Efficiency Curves.**
(from Kiser, Ref.6, p164)

$$M + e^- \rightarrow M^+ + 2e^-$$

The efficiency of ionisation increases with increasing electron energy, reaching a peak in the region 50 - 90 eV. For reasons of maximising sensitivity and reproducibility, operation of EI sources at an electron energy of 70 eV is standard. Ionisation potentials are, for most molecules, of the order of 10 eV, and energy transfer from the ionising electrons in excess of this will result in the production of ions in excited states. Some of these excited ions will have sufficient internal energy for fragmentation of the molecular ion. These features can be understood in terms of the Frank-Condon principle.

A simple calculation shows that the time taken for a 70 eV electron to traverse molecular distances is about two orders of magnitude less than typical molecular vibrational periods, so that electron ionisation obeys the Frank-Condon principle. Thus the initially produced molecular ion has the same structure as the neutral molecule. This often corresponds to a vibrationally excited state of the molecular ion, which may then undergo unimolecular decomposition to produce fragment ions which may also be formed in excited states. Figure 1.4 illustrates the Frank-Condon principle as applied to the electron ionisation of diatomic molecules.

The structure of the molecular ion or fragment ion may re-arrange to a more stable structure if the internal energy is sufficient to overcome the activation energy of isomerisation. Structural re-arrangements accompanying decomposition often encountered are 1-2 hydride or alkyl shifts, for example, the $C_3H_7^+$ ion formed

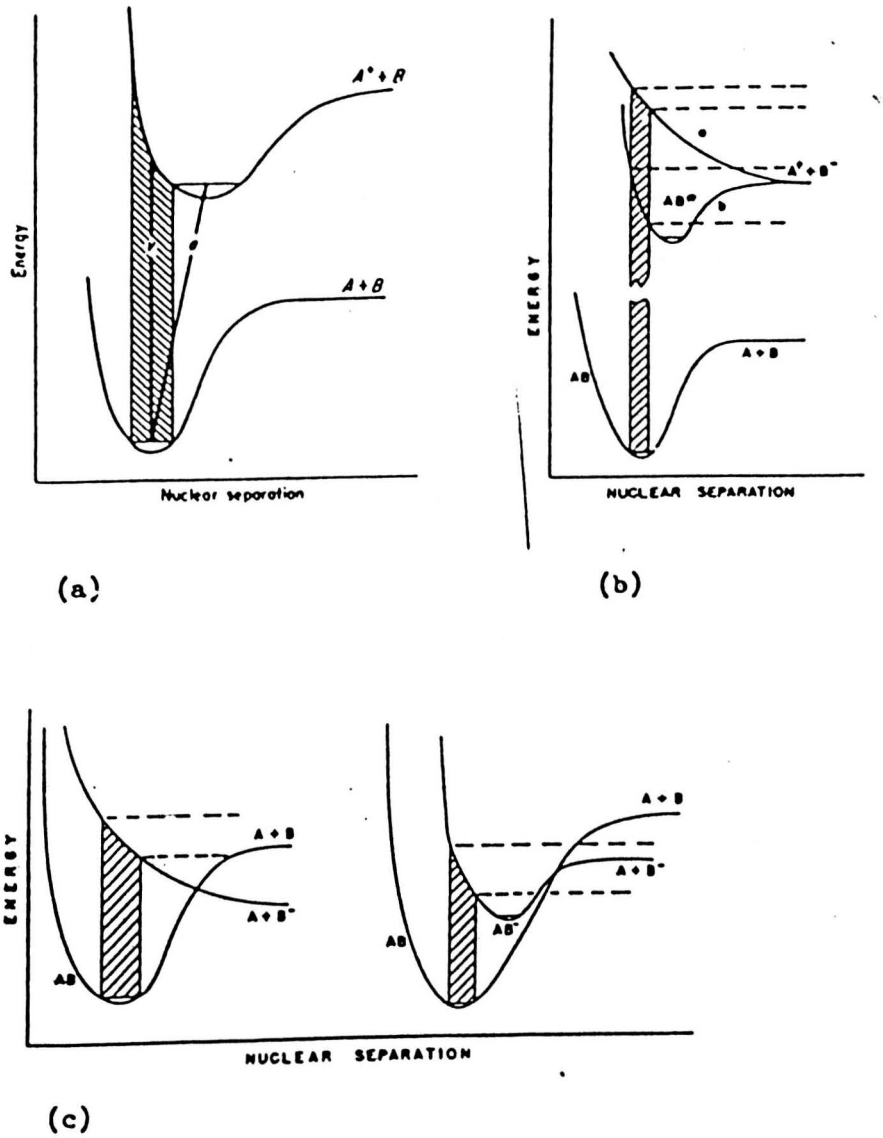


FIGURE 1.4: Frank-Condon Principle

(a) Illustrating the adiabatic and vertical transitions. The Frank-Condon region (shaded) is the region where transitions have the highest probability of occurrence.(b) Curves for ion-pair production. (c) Curves for resonance electron capture and dissociative resonance capture.

(from Kiser, Ref.6, p120 and Field and Franklin, Ref.9, p146)

from electron ionisation of n-butane has been shown to have the $s\text{-}C_3H_7^+$ structure (1). Whether these rearrangments accompanying decomposition arise during the decomposition or are a result of a molecular ion isomerisation followed by decomposition it is difficult to say on the available evidence.

For some types of molecules, then, the molecular ion may undergo complete fragmentation:-

$$M^+ \rightarrow f_1^+ + n_1$$

$$M^+ \rightarrow f_2^+ + n_2$$

etc.

Where 'f' and 'n' refer to fragment ions and neutral species respectively.

We may also have further fragmentation:-

$$F_1^+ \rightarrow f'^+_1 + n'_1$$

$$F_2^+ \rightarrow f'^+_2 + n'_2$$

etc.

Thus the E.I mass spectrum of a compound results from a series of competing, consecutive unimolecular decompositions arising from the transfer of energy ranging from the ionisation energy up to about the ionisation energy plus 10 eV or so.

The mass spectrum can provide a 'fingerprint' of the particular

compound if the mass spectrum is reproducible. In favourable cases, however, the fragment ions provide clues to the structural features of the unknown compound under investigation.

In cases where excessive fragmentation, or absence of a molecular ion is a problem, an early technique was to operate the ion source at low electron energies. Typically, the source was operated at electron energies in the region of 10 eV; under these conditions the spectrum often consists essentially of molecular ions. The major drawback is that the sensitivity is vastly reduced due to the low ionisation efficiency at low electron energy.

The operation of the EI source will now be considered. Referring to figure 1.2, the filament, F, which is heated by the filament current, I, produces electrons by thermionic emission. The filament is negative with respect to the source block, and this voltage, V, determines the electron energy. The electron beam enters the source via hole, S1, and leaves the source via hole, S2, to be collected by the anode or trap, T. The electron beam is collimated by an external magnetic field of about 300-400 Gauss. This magnetic field maintains the alignment of the electron beam along a spiral path, so that the ionisation region within the source is well defined. The trap current, $I_t$, is the current flowing to the anode trap, T, and is a measure of the electron current available for ionisation and therefore strongly influences the ion beam current. For this reason the trap current is electronically regulated by applying appropriate feedback to the filament current. The emission current, $I_e$, measured between the filament and the source block, allows one to judge the operating condition of the source. Thus when the source accumulates a layer of pyrolysis products, and is in need of

cleaning, its efficiency will be reduced, and this will be reflected in excessively large emission currents.

The positive ions formed in the ionisation region of the electron beam are repelled by a small positive voltage, $V_{ir}$, on the ion repeller. A proportion of these ions then leave via the exit hole, S3. In some designs of EI source (e.g. on the MS80) a small negative voltage on the extraction plates provides further control of the ion beam.

Because ion residence time has a great effect upon the fragmentation pattern observed, the ion repeller and extraction voltages have a large effect upon the fragmentation pattern, as well as the over-all sensitivity. The residence time of an ion within the source is important because a longer residence time allows a greater proportion of ions to undergo unimolecular decomposition reactions and to undergo reactions at metal surfaces.

The ion beam next encounters a series of focusing and centering plates before being accelerated to the required ion beam energy. These centering and focusing plates allow the ion beam to be correctly aligned and focused on to the entrance slit of the following analyser.

Another important factor in the nature of the fragmentation pattern is the source temperature. The temperature contributes to the internal energy of the ions, and thus affects the degree of fragmentation observed. For this reason the source block is fabricated out of a comparatively bulky piece of metal, and the source block and ion repeller are both heated electrically, with the temperature thermostatically maintained.

Sample pressures in the EI source are usually in the range $10^{-6}$

to $10^{-5}$ Torr. Maximum sample pressure is about $10^{-4}$ Torr, above which, the ions begin to undergo ion-molecule reactions, and the reproducibility of the spectrum suffers since these ion-molecule reactions occur in uncontrolled conditions.

### 1.1.2 Negative Electron Ionisation

Negative ions may be formed from some neutral molecules upon electron ionisation by the following three mechanisms:-

(A) Resonance electron capture.

$$AB + e^- \rightarrow AB^-$$

(B) Dissociative resonance capture.

$$AB + e^- \rightarrow A + B^-$$

(C) Ion pair production.

$$AB + e^- \rightarrow A^+ + B^- + e^-$$

In the first two processes electron capture occurs over a very narrow range of electron energies, as there is no product electron to carry away the excess energy. Thus the ionisation efficiency curves typically show a sharp peak at low electron energies (0 - 10 eV). Process (B) may be regarded as electron capture followed by dissociation

of the negative ion formed, any excess energy may be carried away either by the dissociation process or by the reverse of process (A) - electron loss. Electron loss will always be the preferred reaction in that case. In addition, the amount of excess energy which may be removed as translational energy of the product particles is limited by the constraints of the Frank-Condon principle and the topologies of the potential energy hypersufaces involved.

The ionisation efficiency curves for ion pair production show a broad maximum, as the product electron can take away the excess energy. Figure 1.5 shows an example of an ionisation efficiency curve for which dissociative resonance capture and ion pair production processes play a part. Since the first two processes predominate, negative electron ionisation ionisation is sometimes referred to as electron capture (EC).

The negative ion current measured with an EI source operating with 70 eV electrons (with the appropriate voltages reversed) is almost negligible. In order to observe negative ions the ion source must be operated with a buffer gas present to provide a wide spread of electron energies. The buffer gas may also provide some degree of collisional stabilisation of the newly formed ions. The buffer gas must be effectively chemically inert to the sample molecules and ions. Buffer gas pressures of 0.1 - 1.0 Torr are used. To achieve this the source must be constructed so that it is more gas tight than an EI source, and the pumping speed of the source region must be greater. The use of differential pumping for the source and analyser regions of the mass spectrometer is advantageous. Because of the high gas pressure, the electrons do not penetrate into the source very far, this has two effects: the electron energies used often need to be in the range 100 -

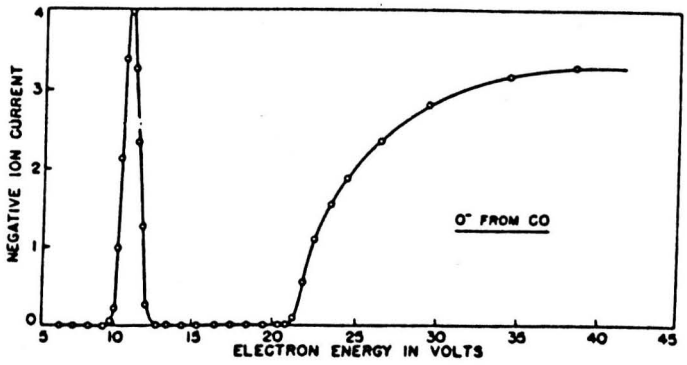


FIGURE 1.5: Electron Capture Ionisation Efficiency Curves.

150 eV, or more, and the electrons do not reach the trap electrode. Thus the electron beam must be controlled by monitoring the emission current instead of the trap current. These requirements in source design are also of use for the technique of chemical ionisation (CI) (see section 1.1.3, below) which also operates at high source pressures. Such an ion source may be referred to as a CI source, but may be used for electron capture as long as it is possible to monitor negative ions. It is possible to design a source which can operate in both EI and CI modes, the electron beam control circuits and the electron energy control circuits being changed over at the press of a button. An EI/CI source of this type often allows alternate EI and CI scans to be taken.

The main attractions of electron capture spectra are their simplicity when compared to conventional EI spectra. This is thought to be partly due to the narrow range of electron energies that produce the ions. An electron with excess energy is simply not captured by the neutral molecule. Additionally operation of the source at high pressure allows collisional de-activation of excited species.

Another plus point is that for electronegative molecules, the electron capture spectrum can be much more sensitive than EI. It may even be possible to determine the relative molecular mass of particular molecules contained within complex mixtures because of preferential ionisation. Electron capture is referred to as a 'soft' ionisation technique, because of the virtual absence of fragmentation peaks, thus it finds use where relative molecular weight determination are analytically important.

The selectivity of electron capture ionisation for those molecules

which have a high electron affinity, for example compounds containing an electronegative hetero-atom or an aromatic system capable of accepting an electron, may also be regarded as a disadvantage as those species which do not have a high electron affinity will give rise to very poor electron capture ionisation spectra.

### 1.1.3 Chemical Ionisation

In chemical ionisation use is made of ion-molecule reactions to achieve ionisation. Thus CI is perhaps potentially the most versatile technique, since the choice of ion-molecule reactions is large. However it is possible to identify several categories of reaction which have proved to be useful. In all types of CI certain conditions have to be met for reproducible results to be obtained. In the CI technique, ions, the 'reagent ions', are allowed to undergo ion-molecule reactions with the sample molecules to give product ions which are passed to the mass analyser. The reagent ions are produced from initial electron ionisation of the reagent gas, ionisation of the sample molecules must be by the reagent ions, with little or no contribution from the direct ionisation of the sample by the electron beam. This is achieved by having the reagent gas pressure to sample pressure ratio of the order 1000:1, and reagent gas pressure of the order of 1 Torr. A general scheme for chemical ionisation is summarised below:-

$$\text{gas} \rightarrow A^+$$

$$A^+ + \text{gas} \rightarrow RG^+$$

$$RG^+ + \text{gas} \rightarrow \text{no further reaction.}$$

$$RG^+ + \text{sample} \rightarrow \text{ion of interest}$$

Here, $A^+$ is an intermediate ion, $RG^+$ is the reagent ion, and 'gas' refers to the CI reagent gas.

The exact nature of the CI spectrum for a given molecule will depend upon the particular type of ion-molecule reaction occurring.

**Proton Transfer**

The most commonly used CI reagent gases give rise to reagent ions which undergo proton transfer reactions with the sample molecule:-

$$M + RH^+ \rightarrow MH^+ + R$$

Careful choice of reagent ion enables one to achieve 'soft' ionisation for particular types of sample molecules, as the excess energy deposited into the product ion depends upon the proton affinities of the molecule and the conjugate base of the reagent ion. The exothermicity, $\Delta E$, of the reaction is given by:-

$$\Delta E = -\Delta H = PA(M) - PA(R)$$

Thus one can interpret proton transfer reactions in terms of

Bronsted acid ($AH^+$) / base (M) behaviour. A strong acid, $AH^+$, will produce spectra which exhibit a larger degree of fragmentation than exhibited by the spectra of the same sample with weakly acidic reagent ions. If $MH^+$ is a stronger acid than $AH^+$, no proton transfer will occur, alternative ion-molecule reactions may then occur.

Table 1.1 shows a list of commonly used proton transfer reagent gases and the corresponding reagent ions with their proton affinities.

Proton transfer reactions may also be observed in negative ion CI spectra. However, in this case the sample molecules are behaving as the Bronsted acids, and the reagent ions as the bases:-

$$MH + R^- \rightarrow M^- + RH$$

Positive CI spectra which involve proton transfer reagent ions often show so-called pseudo-molecular ions at $(M+1)^+$, and negative CI may show pseudo-molecular ions at $(M-1)^-$. The term 'pseudo-molecular' ion is used to refer to any ion which is derived from sample molecules and reagent ions in a simple and repeatable manner, irrespective of the nature of the sample molecules. These pseudo-molecular ions are often valuable for the confirmation of the relative molecular mass of the sample when compared with the EI spectrum. In certain cases, when the EI spectrum shows no molecular ion, the pseudo-molecular ions in the CI spectra are the only guide to the relative molecular mass of the sample molecules. An illustrative example is shown in fig. 1.6.

TABLE 1.1: CHEMICAL IONISATION PROTON TRANFER REAGENTS

| Reagent Gas | Reagent Ion | Proton Affinity /kJ $mol^{-1}$ |
|---|---|---|
| Methane | $CH_5^+$, | 552 |
| | $C_2H_5^+$, | 680 |
| | $C_3H_7^+$ | 628 |
| iso-Butane | $t\text{-}C_4H_9^+$ | 751 |
| Ammonia | $NH_4^+$ | 854 |
| Methylamine | $CH_3NH_3^+$ | 896 |

FIGURE 1.6(a): Ammonia CI Spectrum.

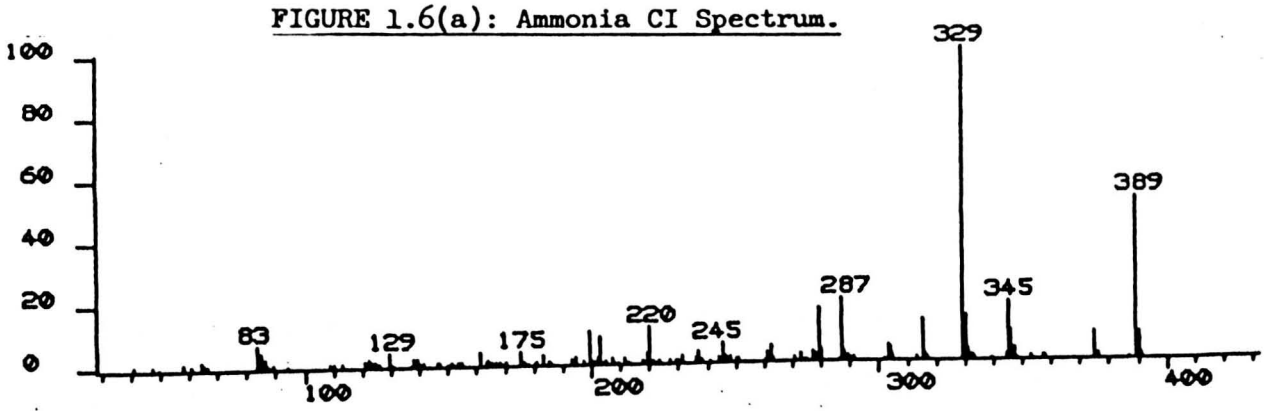


FIGURE 1.6(b): Electron Ionisation Spectrum.

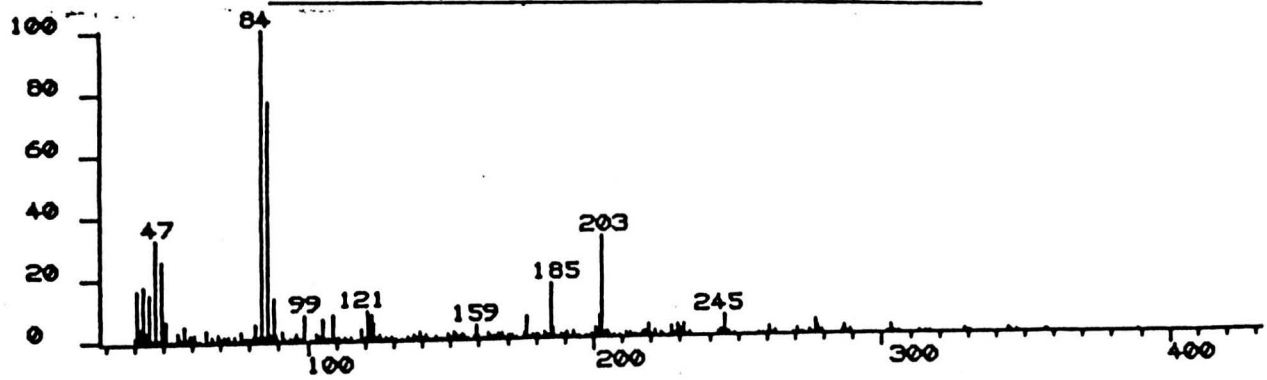


FIGURE 1.6: Comparison of Ammonia CI and EI Spectra of:

3-hydroxy-propyl di-(t-butyl) phosphate IV,

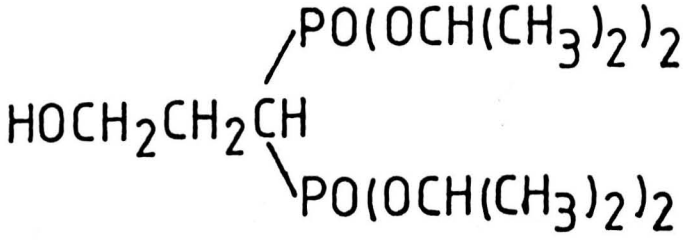

**Association Reactions**

Bimolecular association reactions often occur in positive CI spectra using methane or isobutane. More commonly they occur in ammonia CI, as the reagent ions are only weakly acidic; the alternative reaction pathway may be energetically favoured:-

$$M + NH_4^+ \rightarrow (MNH_4)^+$$

Consequently, in ammonia CI spectra, one may observe pseudo-molecular ions at $(M+18)^+$ as well as, or instead of, the pseudo-molecular ion at $(M+1)^+$. This is typical of oxygen compounds, for example see figure 1.7.

Association reactions also occur in negative CI and in certain cases may be very useful. For example the chloride ion attachment reactions are useful for the analysis of certain organo-metallic compounds.

**Charge Transfer**

A bimolecular ion-molecule reaction of the type:-

$$M + R^+ \rightarrow M^+ + R$$

is termed a charge transfer reaction. The exothermicity of the reaction is dependent upon the ionisation energies thus:-

**TABLE 1.2.**

Ionisation energies of selected atoms and molecules

| Species Produced | IE/eV |
|---|---|
| Argon: | |
| $Ar^{+}$ | 15.8 |
| $Ar^{2+}$ | 43.3 |
| $Ar^{3+}$ | 84.0 |
| $Ar^{4+}$ | 150. |
| n-hexane: | |
| $n\text{-}C_6H_4^{+}$ | 10.2 |
| Toluene: | |
| $C_7H_8^{+}$ | 8.8 |
| $C_7H_8^{2+}$ | 23.5 |
| $C_7H_8^{3+}$ | 42. |
| Propanone: | |
| $C_3H_6O^{+}$ | 9.7 |
| Anthracene: | |
| $C_{14}H_{10}^{+}$ | 7.4 |
| $C_{14}H_{10}^{2+}$ | 21.1 |

FIGURE 1.7(a): Ammonia CI Spectrum.

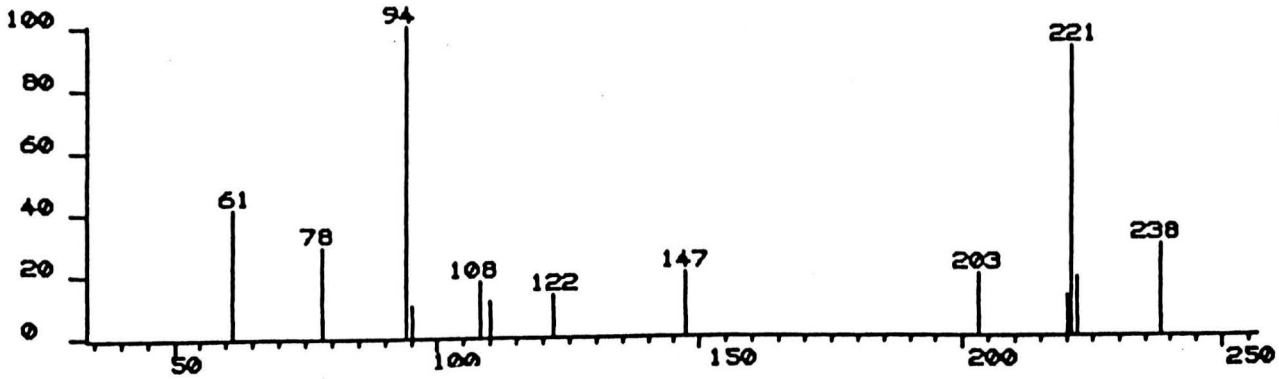


FIGURE 1.7(b): Electron Ionisation Spectrum.

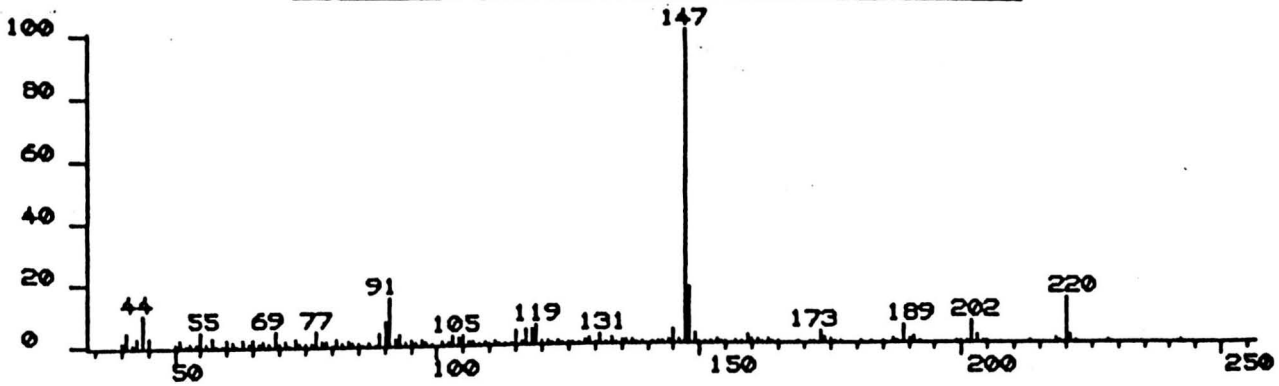


FIGURE 1.7: Comparison of Ammonia CI and EI Spectra of 4-(4'-propylphenyl)-4-one-oic Acid

$$\Delta H = IE(M) - IE(R)$$

and

$$\text{exothermicity,} \quad \Delta E = -\Delta H$$

The exothermicity of the reaction appears as the internal energy of the products, thus, highly exothermic reactions will produce products in highly excited states - these will tend to undergo unimolecular fragmentation reactions. Conversely, reactions of low exothermicity will produce products which do not undergo fragmentation reactions.

Thus, charge tranfer is another CI technique which offers the possibility of selective ionisation in a mixture or controlled fragmentation.

### 1.1.4 Fast Atom Bombardment

Fast atom bombardment mass spectrometry (FAB) is a relatively new technique which has proved to be successful in ionising compounds which hitherto had been difficult to ionise using either EI or CI mass spectrometry.

EI and CI both produce ions from the sample vapour, so that samples which are difficult to volatilise do not yield good results with these techniques. In particular samples which contain ions in solution tend to give EI spectra of their pyrolysis products rather than spectra of the original sample.

It is this type of sample for which FAB is especially suited. For

these types of sample it is required to get ions in solution into the gas phase, or to ionise both the sample molecules and get the resultant ions into the gas phase. This can be achieved by bombarding the sample with an energetic beam of ions or atoms.

The process producing the ions from the sample is the phenomenon of sputtering. At the simplest level of understanding, this is the ejection of material into the gas phase because of the transfer of energy into the sample from the impinging atoms or ions via multiple collisions in the sample. Sputtering is observed to occur when the impinging particles have kinetic energies in the range $10^{+2}$ to $10^{+8}$ eV; also the efficiency of the sputtering process increases as the mass of the bombarding particle increases.

When a beam of ions is used to perform the ionisation, the technique is generally referred to as secondary ion mass spectrometry (SIMS). In SIMS, the sample is generally deposited upon the surface of a solid matrix, and the secondary ions mass analysed by either a quadrupole or time-of-flight mass spectrometer.

In FAB, a beam of ions is accelerated to an energy of 4 - 6 kV, and then passed through a buffer gas, in which charge exchange occurs, to give atoms of essentially the same kinetic energy as the ion. The heavier inert gases, Xenon, Krypton or Argon, are usually used, both for the buffer gas and for generating the initial energetic ions. The resonance charge exchange process is particularly efficient:-

$$Xe^{+} + Xe \rightarrow Xe + Xe^{+}$$

and

$$\Delta E = 0$$

Residual ions, which do not undergo charge exchange, are

removed by electrostatic deflection.

The sample is dissolved in a liquid matrix, and the secondary ions mass analysed using a double focusing mass spectrometer.

Whether the bombarding particles are atoms or ions, the sputtering process is virtually the same, on either a solid or liquid matrix.

The design of a typical FAB source is shown schematically in fig.1.8.

For practical reasons, the liquid used for the matrix in FAB has to have a low vapour pressure, as it has to survive in the low pressure environment of the mass spectrometer source. For best results, the sample is dissolved in a solvent of high dielectric constant, such as glycerol, thioglycerol etc. This is generally understood in terms of the "preformed ion" model of secondary ion emmission. In terms of this model, a matrix of high dielectric constant promotes the formation of sample ions in solution, and these are ejected from the matrix surface by the impinging atoms. This model also finds support in SIMS, for example, the metal ion emmission from a metal oxide is many orders of magnitude higher than the metal ion emission from the pure metal.

Calculations and experimental evidence suggests that the phenomenon of sputtering occurs only within the surface layers of the matrix. Consequently, the surfactant properties of the particular matrix/sample combination has a great influence on the success of the technique. Optimum sensitivity would be obtained if the surfactant properties are such that the sample forms a surface monolayer on the matrix. Indeed, it has been found that in some cases suitable

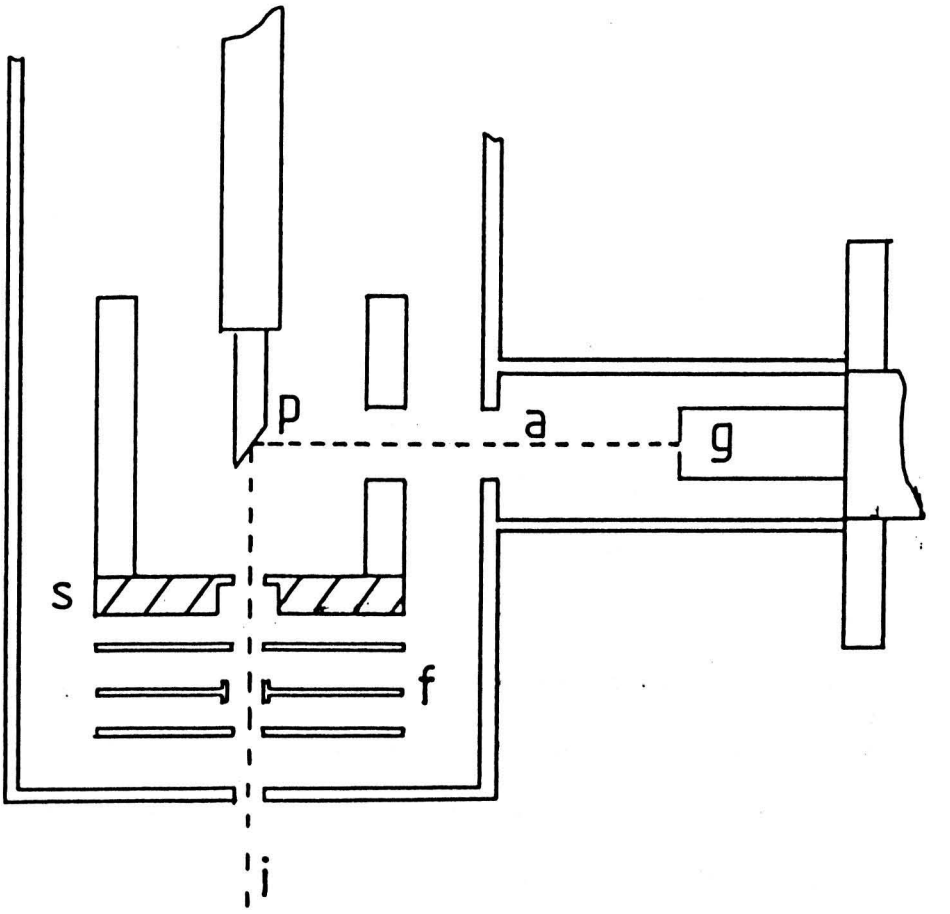


**FIGURE 1.8: Schematic Diagram of a Fast Atom Bombardment Ion Source.**

**KEY:**

| | | |
|---|---|---|
| a | - | atom beam. |
| f | - | ion centering plates. |
| g | - | FAB gun. |
| i | - | ion beam. |
| p | - | probe tip. |
| s | - | source block. |

surfactant properties give rise to spectra in which the solvent mass peaks are totally absent. Another function of the matrix is that it provides a constantly renewable surface to the atom beam: the sample should be soluble in the matrix so that the surface monolayer can be replenished from sample molecules from the bulk of the liquid.

A feature of the sputtering process is that the energy transfer from bombarding particle to matrix is very fast - of the order $10^{-12}$ sec., this results in FAB and SIMS being relatively 'soft' ionisation techniques. In this respect FAB and SIMS are very similar to laser induced ionisation, and the spectra of thermally labile molecules and clusters from all three techniques are very similar.

The technique of FAB has proved useful in obtaining spectra of highly polar or highly involatile (high relative molecular mass) samples. It is, however, not a fully understood process. The spectra of compounds like squalane and other aliphatic hydrocarbons show that pre-ionisation of the sample is not as essential as was once thought, but it is desirable for reasons of sensitivity.

The 'pre-formed ion' model of FAB ionisation provides a good basis for understanding some of the observed correlations between ions found in the FAB spectra and the ionic equilibria occuring in the matrix. For example, the use of acids and bases to alter the position of acid/base equilibria of the sample to enhance the intensity of sample ions in the FAB spectrum is quite common.

Interactions between the sample and the matrix are quite important; for example, when used as a matrix, glycerol almost always gives rise to $(M-H)^-$ ions in the negative FAB spectrum and $MH^+$ ions in the positive FAB spectrum. This has been attributed to acid/base equilibria

between sample and matrix in solution:-

$$(M-H)^- + (glycerol+H)^+ \rightleftharpoons M + glycerol$$

and

$$M + glycerol \rightleftharpoons MH^+ + (glycerol-H)^-$$

It is noteworthy that glycerol is both a moderately good proton acceptor and proton donor. Occasionally, glycerol adduct ions, for example $(MH+glycerol)^+$, are also observed.

The effects due to solution chemistry are not always easy to predict. It has been noted that for some samples the presence of alkali metal ions suppresses the sample ions in the FAB spectrum, whilst for other samples, the deliberate addition of sodium chloride to the matrix results in an enhancement in the intensity of the sodium / sample adduct ions, $MNa^+$, which are regarded as useful pseudo-molecular ions. There is no straight-forward correlation between equilibria in solution and the intensity of secondary ions in FAB; reports in the literature are conflicting, for example a recent report (2) suggests that secondary ion intensities are more a reflection of the fast atom bombardment induced reactions in solution than a reflection of the ionic equilibria that exists in the bulk solution, whilst the extensive work on the measurement of acid/base equilibrium constants by Caprioli, suggests that the ion abundances in FAB spectra do reflect the equilibria that exist in bulk solution (3).

As mentioned above, the surface activity of the sample / matrix system also has an important effect on the ions observed in FAB spectra. Important correlations between the types of ions observed in the FAB

spectrum and the concentration / surface-tension characteristics of surfactant samples has been observed (4). The concentration / surface-tension characteristics may be divided into three regions; the pre-monolayer region, the monolayer region, and the micelle region. Ions derived from the matrix are predominant in the FAB spectrum when the sample concentration corresponds to the pre-monolayer region. In the monolayer region, the FAB spectra exhibit ions due to the sample, whilst in the micelle region, matrix / sample adduct ions are observed in addition to sample ions.

The complex solution and surface chemistry that occurs can lead to apparently large differences in sensitivity for quite similar compounds, making quantitative analysis difficult, as generalised sensitivity / structure relationships usually can not be applied.

## 1.2 Mass Analysis & Ion Detection

The separation of the ions according to their mass/charge ratio is generally referred to as mass analysis, as the occurrence of multiply charged ions is usually negligible. In EI mass spectra the intensities observed for doubly charged ions are about two orders of magnitude below those of typical singly charged ions. Further ionisation to give triply charged ions, etc, is still more difficult, and thus they are even less abundant. In table 1.2 are shown the relative ionisation energies of some typical atoms and molecules. It will be noted that although multiply charged ions usually have relative intensities less than 1% of the base peak, for some aromatic molecules and molecules containing conjugated systems, multiply charged ions occur in greater abundance, as

much as 20% for doubly charged ions.

### 1.2.1 The Magnetic Analyser

The ions produced in the ion source are accelerated by falling through a potential difference, V , so that the kinetic energy, T, gained by an ion of charge, q, is given by:-

$$T = mv^2/2 = qV \qquad (1.1)$$

Here, m, is the mass and v is the velocity of the ion. On entering a magnetic field of flux density, B, perpendicular to the direction of ion motion, the ion experiences a force, F, given by:-

$$F = Bqv \qquad (1.2)$$

The force, F, is perpendicular to both the magnetic field and the ion motion, and may be equated with the centripetal force of circular motion, of radius, r:-

$$F = mv^2/r \qquad (1.3)$$

Hence,

$$mv^2/r = Bqv \qquad (1.4)$$

Rearranging, (1.4) gives:-

$$v = Bqr/m \qquad (1.5)$$

Inserting into Eqn. (1.1), we have:-

$$(Bqr)^2/2m = eV \qquad (1.6)$$

or

$$m/q = (Br)^2/2V \qquad (1.7)$$

Equation (1.7) indicates that, for a given radius,r, mass analysis may be achieved either by changing the magnetic flux density, B, or the accelerating potential, V. In early instruments the accelerating potential was used to scan the mass spectrum. However, as the sensitivity of the instrument depends upon the accelerating potential, the magnetic scan is preferred.

### 1.2.2 The Double Focusing Instrument

The magnetic analyser suffers from the problem of limited resolving power, $m/\Delta m$, where $\Delta m$ may be defined in several ways. Two convenient definitions of $\Delta m$ are the "5% peak width" definition, and the "10% valley" definition. In the former definition, $\Delta m$ is given by the width of the peak at 5% of its height, and for the latter definition, $\Delta m$ is given by the separation between two peaks of the same intensity such that the valley between them is 10% of the peak height, in other words,

each peak contributes 5% of its height to the valley height. For peaks which are gaussian in shape, these definitions give the same answer. These definitions of resolving power are illustrated in figure 1.9. For a given resolving power, $m/\Delta m$, two adjacent peaks will be resolved if their difference in masses is greater than or equal to $\Delta m$. For a magnetic analyser of 20 - 30 cm radius, resolving powers of about 2000 are typical. The origin of this problem is that the assumption that we have monoenergetic ions is not strictly true. The ions have a thermal distribution of energies which contributes to a final energy distribution after the ions have been accelerated, also, energy release during fragmentation, and the presence of electric fields within the source add to this. Equation (1.5) may be re-arranged as follows:-

$$mv = Bqr \qquad (1.5b)$$

This equation indicates that the magnetic sector is a momentum filter, only when the velocity, v, is the same for all ions of a given mass, m, does the magnetic sector become a mass filter. The addition of a second analyser, the electrostatic analyser, provides this extra criterion.

#### 1.2.2.1 The Electrostatic Analyser

The electrostatic analyser consists of two concentric cylindrical electrodes with a radial electric field, E, maintained between them. In such a field an ion of charge, q, experiences a force, f, parallel to the field, given by:-

$$f = qE \qquad (1.8)$$

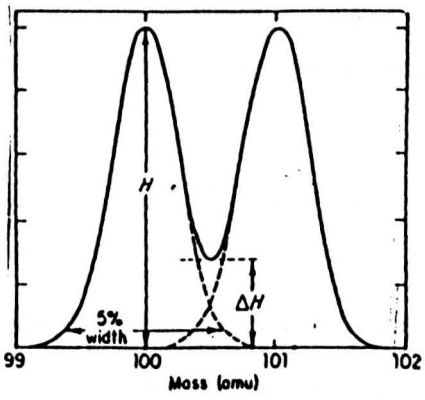


**FIGURE 1.9:**

**Resolving Power.**

(after Kiser, Ref.6, p55)

Equating this with the centripetal force of circular motion of radius, R, we obtain:-

$$R = mv^2/qE \qquad (1.9)$$

Combining this with Eqn. (1.1), one obtains:-

$$R = 2V/E$$

Thus the electrostatic analyser acts as an energy filter, so that when used in conjunction with a magnetic mass analyser superior resolving power may obtained.

**Double Focusing**

The beam of ions ejected from the ion source does not only exhibit an energy distribution, but also an angular distribution. By proper combination of magnetic and electostatic analysers one may achieve correction for both the velocity and the directional distribution. Such an instrument is termed double focusing. The angular dispersion of the ions is characterised by an angle, $\alpha$, and the energy dispersion is characterised by a parameter, $\beta$, such that ions of a given mass have velocity, $v = v_o(1+\beta)$. It can be shown that the expressions for the widths of the image focused by electric and magnetic fields are polynomials in a and b. If it assumed that a and b are small, terms in $\alpha^2$ and $\beta^2$ or higher can be neglected. This is termed first

order double focusing. Double focusing mass spectrometers with higher-order focusing have been designed.

Two of the commonest designs for double focusing instruments are the Nier-Johnson instrument with double focusing first order and direction focusing second order, and the so-called 'reverse geometry' instruments. Schematic diagrams of these are shown in figure 1.10.

Ion Detectors

Probably the most commonly used ion detector is the electron multiplier (see figure 1.11). This detector relies for its operation upon the phenomenon of secondary electron emmision. Energetic positive ions impinge upon a metal cathode, held at a high negative potential, causing the emission of a large number of secondary electrons. These electrons are then accelerated so as to impinge upon a metal dynode, causing further secondary electron emission. This process can be repeated from ten to twenty times until the final cascade of electrons is collected on the anode. By this means, current gains in the range of $10^{+5}$ - $10^{+6}$ can be obtained. The sensitivity of the detector is controlled by varying the negative voltage on the cathode. One advantage of the electron multiplier is its rapid response time, about $10^{-9}$ to $10^{-8}$ seconds, corresponding to a bandwidth of ca 100 MHz, and this is important where fast scan times are required. The detection of negative ions requires the reversal of the initial acceleration voltages before the first dynode. This dynode, referred to as the conversion dynode, ejects positive ions due to the impact of the negative ions from the mass analyser; amplification then proceeds in

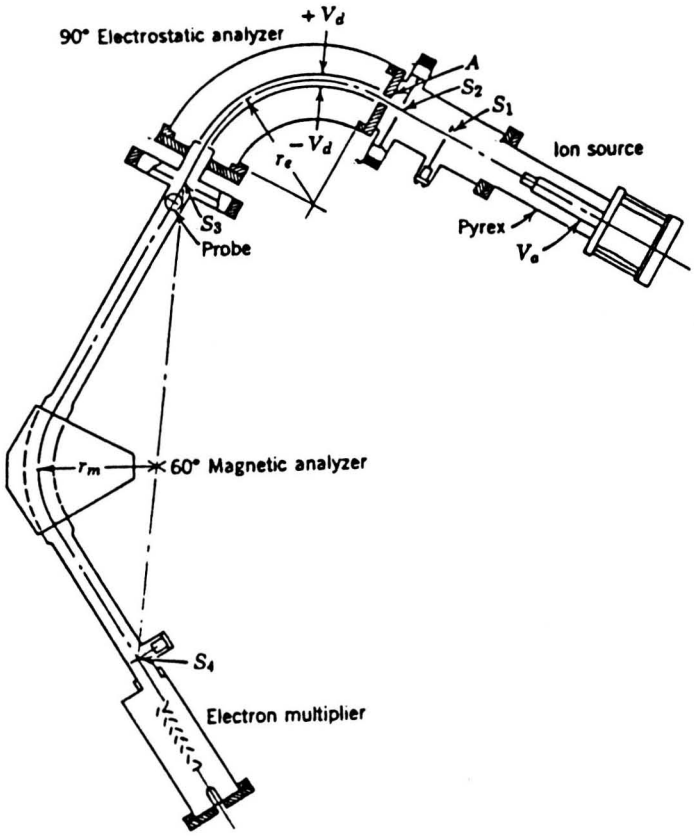


**FIGURE 1.10(a):**

**Nier-Johnson Double Focusing Mass Spectrometer.**
(from Roboz, Ref.8, p90)

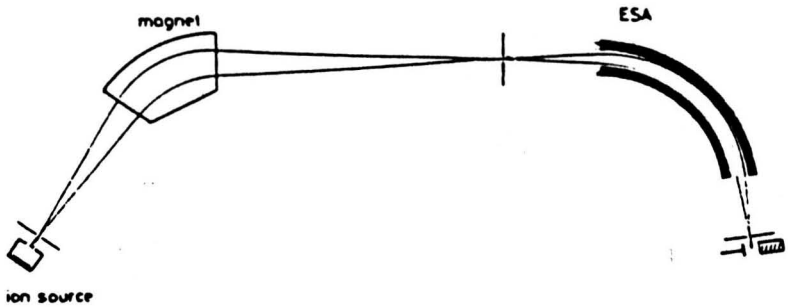


**FIGURE 1.10(b):**

**Reverse Geometry Double Focusing Mass Spectrometer.**

(after Porter et al., Ref.10)

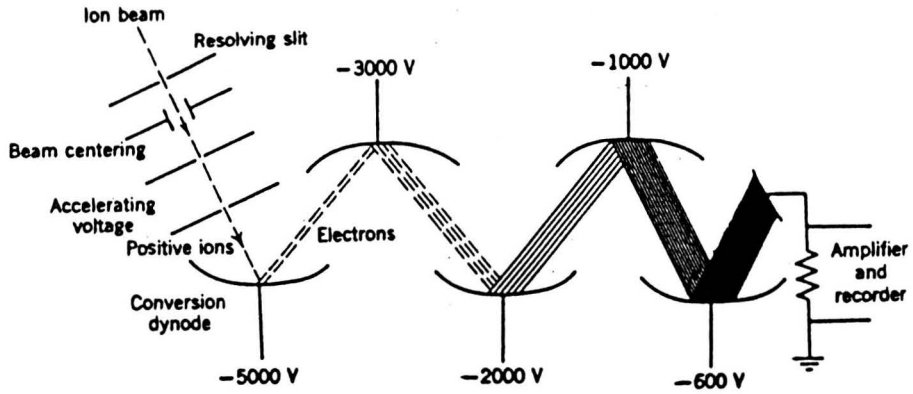


**FIGURE 1.11: Schematic Diagram of The Electron Multiplier Ion Detector**
(from Roboz, Ref.8, p160)

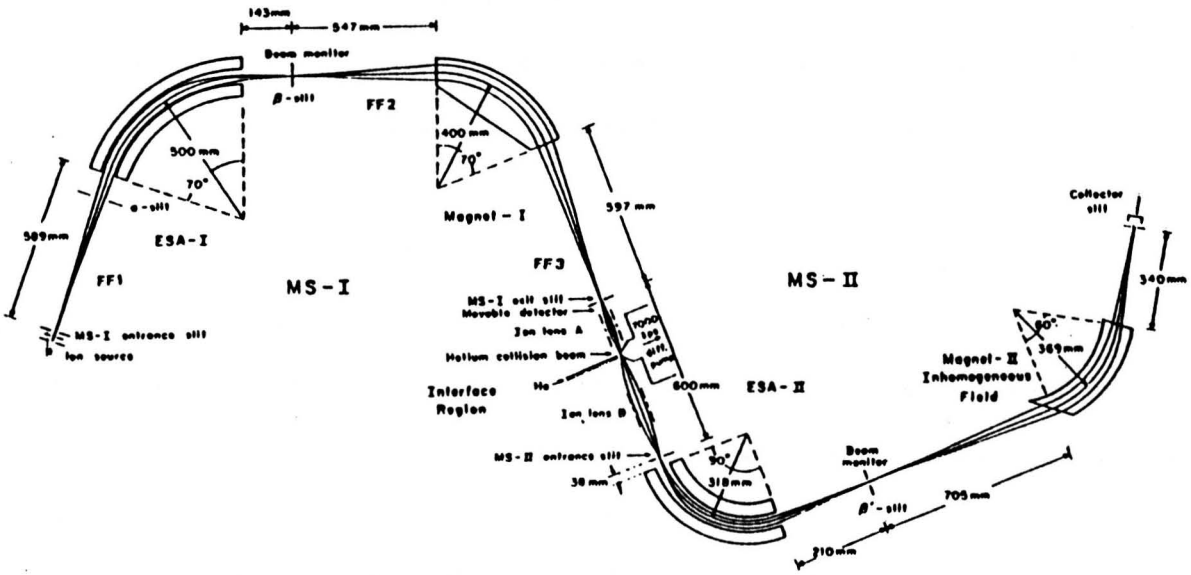


**FIGURE 1.12: Schematic Diagram of Tandem Mass Spectrometer, with two electric Sectors & two Magnetic Sectors**
(from McLafferty, Ref.7)

the manner described above for the detection of positive ions.

Another common ion detector, the Daly detector, utilises a photomultiplier to achieve the high gain required. The positive ions are first accelerated and allowed to impinge upon a cathode, causing secondary electron emission, as in the electron multiplier. The secondary electrons are then accelerated and allowed to strike a phosphorescent screen, which emits photons which enter the photomultiplier.

Other detectors include the channel electron multiplier, or channeltron, the Faraday cup and various designs of electron multipliers which utilise a magnetic field (5).

### 1.2.3 Multiple Mass Analyser Instruments

In recent years mass spectrometers which incorporate two or more mass analysers have proved useful research tools in the study of ion-molecule reactions and for analytical applications.

A typical example is shown in fig. 1.12. Numerous types of scans can be carried out on these instruments. As an example, one may use a soft ionisation technique to produce molecular ions for each component of a complex mixture. The first mass analyser is used to select one of these molecular ions. Introduction of a collision cell in the beam path after the first mass analyser allows fragmentation of the molecular ion to take place. The second mass analyser is used to scan the fragment ions. In favourable cases, structural information can be obtained for each component of the mixture.

The main disadvantage with such instruments is their great cost,

and their complexity.

### 1.2.5 Other Types of Mass Spectrometer

Of the other types of mass spectrometer available, only a brief mention will be given as none of them were used in this study.

The quadrupole mass analyser (8) is favoured in small low resolution instruments where fast scan times are required, such as for GC/MS applications.

The phenomenon of ion cyclotron resonance is utilised in the Fourier Transform Mass Spectrometer (FTMS, 7). Mass is determined by measuring cyclotron frequency and mass measurements are made simultaneously over the whole mass range by Fourier Transform Analysis. The main advantage of these instruments is their high mass resolution (typically, resolution = 100 000 at 1000 Daltons; 1000 000 at 100 Daltons).

In time-of-flight (TOF, 8) mass spectrometers the time required for an ion to travel a predetermined distance is measured. For a monoenergetic pulsed beam of ions the flight time is proportional to the square root of the mass/charge ratio. These instruments are used with ionisation techniques which readily provide a pulsed beam of ions, such as laser ionisation and secondary ion mass spectrometry (SIMS).

## CHAPTER ONE: REFERENCES


1) McAdoo, D. J., McLafferty, F. W. & Bente III, P.. F., J. Amer. Chem. Soc., 94, 2027, (1972).

2) Connolly, M. J. & Orth, R. G., Anal. Chem., 59, 903, (1987).

3) Caprioli, R. M., Anal. Chem., 55, 2387, (1983).

4) Barber, M., Bordoli, R. R., Elliott, G. J., Sedgwick, R. D. & Tyler, A. N., J. Chem. Soc., Faraday Trans. 1, 79, 1249, (1983).

5) Roboz, J., 'Introduction to Mass Spectrometry Instrumentation and Techniques', Chap. 5, Interscience Publishers (1968).

6) Kiser, R. W., 'Introduction to Mass Spectrometry and Its Applications', Chap.4, Sec. 4.9, Prentice-Hall Inc. (1965).

7) McIver Jr., R. T. & Bowers, W. D., 'Tandem Mass Spectrometry', Ed. McLafferty, F. W., p287, Wiley-Interscience Publication, (1983).

8) Roboz, J., 'Introduction to Mass Spectrometry Instrumentation and Techniques', Chap.2 Sect. IV, Interscience Publishers, (1968).

9) Field, F. H. & Franklin, J. L., 'Electron Impact Phenomena and The Properties of Gaseous Ions', Academic Press, (1957).

10) Porter, C. J., Beynon, J. H. and Ast, T, Org. Mass Spec., Vol. 16, No.3, 101, (1981).

# CHAPTER II

# CHEMOMETRICS - FACTOR ANALYSIS.

## 2.0 Introduction.

The application of data processing techniques to analytical problems is becoming more widespread. This chapter will give a short review of this topic, with special attention to the technique of 'factor analysis', which is especially applicable to the problem of mixture analysis.

## 2.1 'Chemometrics'.

Chemometrics has been described as the interface between chemistry and mathematics; more explicitly, it is the development and application of mathematical and statistical techniques to the extraction of useful information from chemical data.

Developments in the field have evolved in response to the need to process the increasingly more complex data generated by modern analytical instrumentation, and they have been realised because of the exceptional increase in the sophistication of easily available computer hardware and software.

Many of the developments in chemometrics have the common feature that they treat chemical data as multivariate systems - gone are the days when chemical experiments were designed to reduce the measurements to one or two variables by holding all other 'variables' constant. In effect chemometrics is the extension of mathematical and statistical techniques beyond 'linear least squares' and simple curve fitting to data processing applications such as parameter estimation (1), calibration (2), image analysis (3), factor analysis, pattern

recognition (4), optimisation (5), library searching (6), and chemical structure handling (7). Thus the field of chemometrics finds application throughout all branches of chemistry from the theoretical organic chemist's attempt to the design of 'tailor-made' drugs using structure manipulation, to the experimental physical chemist's concern with signal recovery and enhancement.

## 2.2 Pattern recognition and Factor analysis.

Pattern recognition and factor analysis are techniques which are of special interest in analytical chemistry. These two areas of chemometrics can be applied to the problem of mixture analysis.

Probably the two most fundamental questions an analytical chemist can ask about a chemical mixture are:-

(1) Is the mixture identical with a previously known mixture?

(2) What are the components of the mixture, and in what proportions are they present?

Pattern recognition tries to answer the first question, whilst factor analysis tries to answer the latter question. Which question we are able to answer depends to some extent on the nature of the sample and the analytical techniques used. For example, analytical techniques, such as pyrolysis mass spectrometry(8), which tend to give quantitative results only with difficulty, and so may be viewed more as 'fingerprint' techniques, are more easily analysed using pattern recognition. Indeed, pattern recognition techniques have become routine analytical procedures for the interpretation of pyrolysis mass spectra (8).

### 2.2.1 Cluster Analysis.

The pattern recognition technique known as 'cluster analysis', of which there are several different versions, as used in the interpretation of pyrolysis mass spectra, may be regarded as an extension of the 'scatter diagram' used for two and three dimensional data sets. In two or three dimensions it is easy to visualise the clustering of data points into regions where neighbouring data points are in some way related. Thus the distances between the data points are numerical expressions of the degree of similarity between different measurements. Extension of this idea to multidimensional space raises two problems: finding the 'real' dimensionality of the data and the corresponding unit vectors; and visualising the resultant 'distance' measurements. The first problem has a straightforward mathematical solution, the second problem is more difficult. Frequently the raw data are transformed into statistical functions such as the correlation coefficients, standard deviations, chi squared coefficients etc. (see table 2.1). These are all so-called 'similarity coefficients', and are more appropriate functions upon which to base the distance measurements (see below). Finding the dimensionality of the data is simply achieved by eigenvector analysis of the matrix of similarity coefficients. In geometrical terms, eigenvector analysis seeks to find the mutually orthogonal unit vectors which, in the three dimensional case, correspond to the three co-ordinate axes. In an analogous way, in 'm' dimensional space, there are 'm' co-ordinate axes. A series of mass spectra may be represented by a vector in 'n' dimensional space, where the 'n' different mass peaks in the spectra define the unit vectors. However,

TABLE 2.1: Correlation Coefficients etc.

For two mixtures, l and m, with mass spectra containing n mass peaks, the correlation coefficient, $C_{lm}$, is given by:-

$$C_{lm} = \sum_{i=1}^{n} [\, I_{li} \cdot I_{mi} \,] / [\, \sum_{i=1}^{n} I_{li} \cdot \sum_{i=1}^{n} I_{mi} \,]$$

Where $I_{li}$ is the intensity of the $i^{th}$ mass peak in the spectrum of mixture l. Similarly, the co-variance, $V_{lm}$, is defined by:-

$$V_{lm} = \sum_{i=1}^{n} I_{li} \cdot I_{mi}$$

Alternatively, one may define the peak-to-peak correlation and co-variance for mass peaks i and j:-

$$C_{ij} = \sum_{l=1}^{k} [\, I_{il} \cdot I_{jl} \,] / [\, \sum_{l=1}^{k} I_{il} \sum_{l=1}^{k} I_{jl}$$

and

$$V_{ij} = \sum_{l=1}^{k} I_{il} \cdot I_{jl}$$

Where $I_{il}$ is the intensity of mass peak i in the $l^{th}$ mixture, and k is the number of mixtures.

The coefficients $C_{lm}$ and $V_{lm}$ may be regarded as measures of the similarity of the mass spectra of mixtures l and m, whereas, the coefficients $C_{ij}$ and $V_{ij}$ are better regarded as measures of the correlation between the statistical variations in the intensities of mass peak i and mass peak j.

the true dimensionality of the data may be less than 'n'. Consider for simplicity a set of spectra from mixtures of two pure compounds, containing three mass peaks; all of the mixture spectra will lie in a plane defined by the vectors representing the spectra of the pure compounds, as illustrated in figure 2.1a, so that the true dimensionality of the data is two. Eigenvector analysis will yield two orthogonal unit vectors in the same plane as that defined by the pure compound's vectors. It will be seen below that eigenvector analysis is also the first step of the factor analysis technique.

In the vector representation of spectra, the covariance and the correlation have simple interpretations. The correlation coefficient is the normalised dot product of two vectors, $A.B/|A||B|$, and the covariance is the dot product of the two vectors, A.B. Thus, the correlation coefficient will be unity if the vectors are in the same direction, i.e. if the two vectors represent spectra of the same compound or mixture, and the covariance will be large if the vectors are nearly parallel and have large magnitudes.

Extension of these ideas to real data in which there are many mixture spectra each containing hundreds of mass peaks presents problems due the amount of data involved. It is difficult to interpret a large table of similarity distances, so that special visualisation techniques are required. The use of 'non-linear maps' to visualise cluster analysis results is probably the most favoured technique. This reduces the multidimensional data to a two or three dimensional diagram. It is not merely a projection of multidimensional space onto two or three dimensions, but an iterative technique which aims to preserve the nearest neighbour sequence of the data in the non-linear map (9).

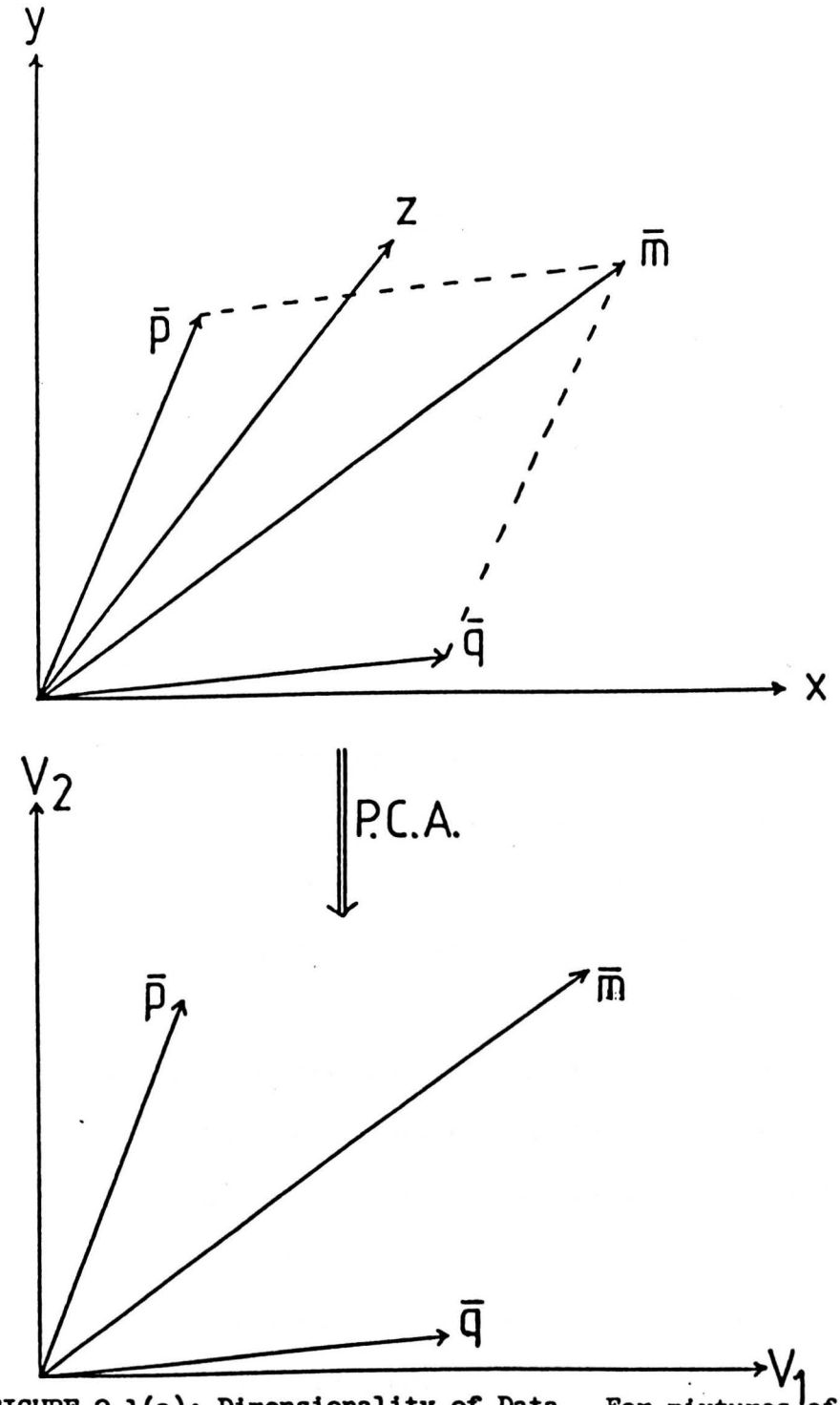


**FIGURE 2.1(a): Dimensionality of Data** For mixtures of two substances, with a total of three mass peaks, a mixture can be represented by a vector, $\bar{m}$, in 3-dimensional space, the three mass peaks defining the co-ordinate axes, x, y and z. All possible vectors, $\bar{m}$, will however, lie in the plane defined by the vectors, $\bar{p}$ and $\bar{q}$, representing the pure components. Principal component analysis will yield orthogonal vectors $V_1$ and $V_2$ in the same plane as $\bar{p}$ and $\bar{q}$.

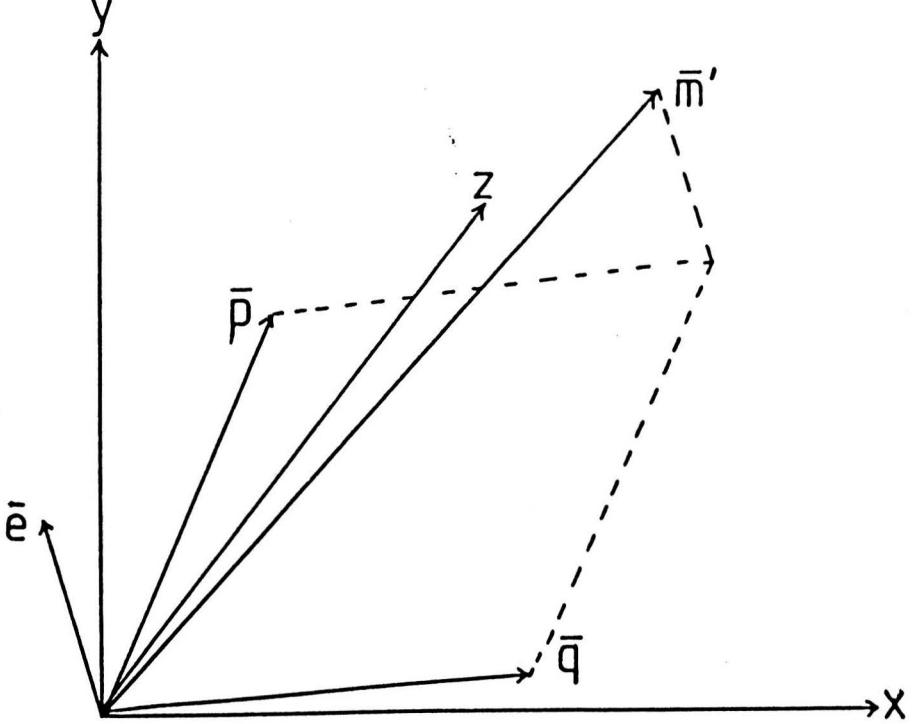


**FIGURE 2.1(b): Dimensionality of Data** In experimental data, errors will generally be present in the measurement of the x, y and z co-ordinates, represented above by the vector $\bar{e}$. This results in the vector $\bar{m}'$ no longer being confined to the plane defined by $\bar{p}$ and $\bar{q}$. If the error is symmetric about the plane defined by $\bar{p}$ and $\bar{q}$, the first two principal components will define the plane, and the third principal component will represent the out-of-plane error. The components of the error vector, $\bar{e}$, in the plane however, will be mixed in with the first two principal components.

It is to be expected that pattern recognition techniques will play a more important part in the interpretation of FAB mass spectra, especially as the techniques have already been fully developed for pyrolysis mass spectrometry. Figure 2.2 illustrates the kind of diagrams produced by the procedure.

### 2.2.2 Factor analysis.

Factor analysis is an extension of principal component analysis which has been used in the social sciences for many years (10). Principal component analysis, also referred to as abstract factor analysis, is basically a data reduction technique. Factor analysis seeks to identify the components of an unknown mixture by a mathematical analysis of the statistical variations in the data. It can be applied to any analytical technique in which the measured intensities of the parameters are a concentration-weighted sum of the intensities due to the individual components. In recent years factor analysis has been applied to many chemical problems, such as gas chromatography (11), nuclear magnetic resonance (12), infra-red and ultra-violet spectroscopy (13,14), and mass spectrometry including GC/MS (15). For mass spectroscopic analysis, factor analysis requires the measurement of several spectra of unknown mixtures of different composition of the same components. The mixture spectra are represented as the columns of the data matrix, [D], the rows of [D] may then be referred to as mass profiles.

The spectra of the pure components are represented as the columns

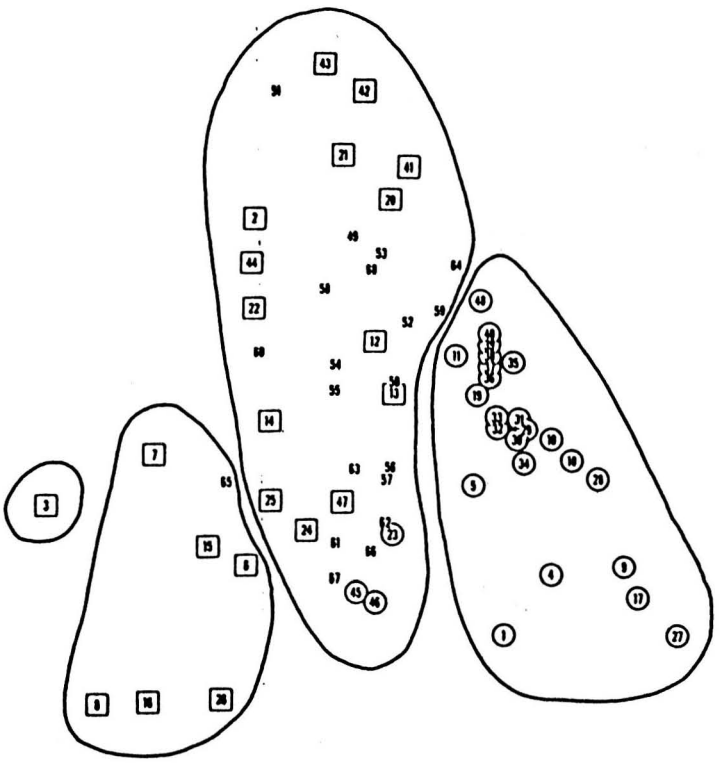

**FIGURE 2.2: Non-Linear Map** Illustrated here, is a two-dimensional non-linear map of six-dimensional data for the elements. The six variables used were; the highest valence, the melting point, the covalent radius, the ionic radius, the electronegativety and $\Delta H$ fusion. The highest oxide is acidic if the element is represented by a square, and basic, if it is represented by a circle, otherwise it is amphoteric. Ref. Kowalski & Fender (9).

of an unknown matrix [R], and the composition of the mixtures as the columns of an unknown matrix [C], thus:-

$$[D]=[R][C] \qquad (2.1)$$

The problem is, given the data matrix [D], we need to calculate the matrices [R] and [C]. A difficulty arises because the above equation has an infinite number of solutions:-

$$[D]=[R].[C]$$
$$=[R].[B].[B]^{-1}.[C]$$

where [B] is any non-singular matrix.

Thus,

$$[D]=[R]^{*}.[C]^{*}$$

where $[R]^{*}$ and $[C]^{*}$ are new solutions, given by:-

$$[R]^{*}=[R].[B]$$
$$[C]^{*}=[B]^{-1}.[C]$$

Obviously, this process could be repeated indefinitely. In order to solve this matrix equation additional information is required.

2.2.2.1 Target factor analysis.

One of the first pieces of additional information that was used to help solve this problem, was the fact that all of the intensities are positive or zero, i.e. no solutions are permissible that give negative intensities (16). This simplification did not help sufficiently - a range of solutions still existed.

Another approach is to hypothesise one or more of the components of the

mixture, the hypothetical component can be represented by a 'target' vector, occasionally referred to as the 'test' vector. Solutons of equation (2.1) are then generated so as to give a result closest to the hypothetical component. This technique, known as 'Target Factor Analysis', TFA, has two objectives, to find a suitable hypothetical target vector, and to reject or confirm the hypothesis on the basis of the difference between the target vector and the factor analysis regenerated target vector. Several proposed schemes exist for the statistical measurement of the acceptability of the test vector (17). However, probably the main difficulty is the initial selection of the most likely target vectors. For the analysis of closely related mixtures, the TFA method is particularly useful, as the test vectors will be the same for each mixture (18). The TFA method has also been used as the basis of a library search procedure (19). Perhaps the simplest idea is to introduce one or more internal standards into the mixture, and to use the spectra of the internal standards as the target vector(s).

#### 2.2.2.2 The 'pure peaks method'

For analytical systems for which it is difficult or impossible to find a selection of target vectors, obviously the TFA method can not be applied.

A consideration of the behaviour of peaks which are unique to a given component, i.e. that have zero intensity in all components except one, leads to the conclusion that if such a peak can be found for each component, then this is the information which is required to 'pin-down'

the nature of [R] and [C] unambiguously.

The analysis proceeds in two stages, first the number of factors, i.e. components in the mixture, has to be determined. This first step is common to all factor analysis and related techniques. In effect this first step determines the 'true' dimensionality of the data. Next the data are decomposed into spectra of the pure components and concentrations - a process which involves the identification of the unique peaks.

The number of components is determined by accounting for the statistical variations in the data. Two measures of statistical variation have been used in factor analysis. These are the correlation coefficient and the covariance, both measured about the origin. Note that these are similarity coefficients as are used in the first stage of cluster analysis.

#### 2.2.2.3 Weighting

The correlation coefficient gives all variables equal weighting, no matter how relatively small some of them may be, i.e. some of the smaller variables are given too much weight.

For this reason, and due to the ease with which subsequent analysis is performed, the covariance about the origin is to be preferred.

The covariance matrix, [M], is calculated from the data matrix as:-

$$[M]=[D]^T.[D]$$

So that element $m_{kl}$ of this matrix gives the covariance of mixture k with mixture l.

### 2.2.2.4 Eigenvector Analysis.

The covariance matrix is symmetric about the main diagonal. From the results of matrix algebra, it can be shown that such symmetric matrices can be diagonalised by the similarity transformation (20):-

$$[Q].^{-1}[M].[Q] = l_j \delta_{jk}$$

where

$$\delta_{jk} = 1 : \text{for } i = j$$
$$\delta_{jk} = 0 : \text{for } i \neq j$$

Here [Q] is an eigenvector matrix, whose columns are the eigenvector, $Q_j$, of the equation:

$$[M].Q_j = l_j Q_j$$

and $l_j$ is the eigenvalue corresponding to $Q_j$.

For each factor which contributes to the covariance in the data, there exists an eigenvector, the relative importance of which depends upon the magnitude of the corresponding eigenvalue. Thus if we have 'm' mixture spectra forming the data matrix (assumed to be error free) and 'n' factors, only the first 'n' eigenvalues will have non-zero values, the remaining (m-n) eigenvalues will be zero (or nearly so, due to computational rounding errors).

As shown by Malinowski (21), the [R] and [C] matrices can be represented in terms of the eigenvector matrix [Q], which is derived from the covariance matrix [M]. Malinowski finds that:-

$$[D] = [U].[Q]^T$$

where

$$[U] = [D].[Q]$$

Now if [Q] is constructed using only the first 'n' non-zero eigenvalued eigenvectors, the [U] matrix will be of dimension r by n, where 'r' is the number of mass peaks in each spectrum, and 'n' is the number of factors. Also the $[Q]^T$ matrix will have dimension n by m, where m is the number of mixtures.

The matrix, [U], may be regarded as an abstract representation of the [R] matrix, and $[Q]^T$ a representation of the [C] matrix. These eigenvector representations, [U] and $[Q]^T$, have no physical significance, however, the matrix of abstract factors, can sometimes be of use in identifying components of the mixture. The abstract factors, or principal components provide the mathematical description of the statistical variations in the data, and it may be the case that the statistical variations yield principal components that are close to the 'true' factors or be related to them (22).

The 'true' [C] matrix, as shown by Knorr and Futrell (23), is equal to a non-orthogonal rotation of $[Q]^T$:-

$$[C] = [Q]^T.[A]$$

Where [A] is a non-orthogonal rotation matrix.

Because [C] is a non-square matrix, it has no inverse, and [R] has to be obtained via the so-called 'pseudo-inverse' :-

$$[R] = [D].[C]^T.([C].[C]^T)^{-1}$$

### 2.2.2.5 Theory of error in abstract factor analysis

The errors associated with experimental data introduce more factors which contribute to the variations in the data, and hence introduce more non-zero eigenvalues of [M] than the case of error free data. For example, in the simple case of mixtures of two components with a total of three mass peaks, illustrated in figure 2.1a, experimental error in the measurement of the mass peaks will extend the dimensionality of the data to three, as in figure 2.1b.

It has been shown (21) that the first 'n' eigenvalues correspond to the data, and that the remaining eigenvalues represent the errors.

The theory of error in factor analysis shows that the error is composed of two parts, the imbedded error, IE, and the extracted error, XE.

The real error RE is the difference between the pure data, free from error, and the raw data which contains experimental error. The real error is related to the imbedded error and the extracted error as follows:-

$$RE^2 = XE^2 + IE^2$$

The extracted error is a measure of the amount of error which can be extracted by factor analysis. This error, XE, can be equated with the difference between the factor analysis regenerated data and the raw data:-

$$[XE] = [D] - [U].[Q]^T$$

Here [XE] is the extracted error matrix, and [Q] is the eigenvector matrix composed of only the first 'n' eigenvectors which represent data + imbedded error only.

The imbedded error is the difference between the factor analysis regenerated data and the pure data, and represents the error which cannot be removed by factor analysis. The Malinowski theory of error shows that these errors are given by the equations in table 2.2.

These considerations of the errors associated with factor analysis hint at another application of the technique. Slight modification of the technique allows one to use it for signal enhancement. If one eigen-analyses a data matrix to find the 'true' dimensionality of the data, and then re-creates the data using the abstract [R] and [C] matrices of the correct dimensionality, then the data will be re-created with the extracted error removed (21).

Returning, now, to the discussion of factor analysis, the first task in using factor analysis for mixture analysis is to decide upon the number of factors which contribute to the data.

If an estimate of the experimental error is known, then we proceed by starting with the smallest eigenvalue, i.e. the least important, and

TABLE 2.2: FACTOR ANALYSIS ERROR PARAMETERS

$$RE = \sum_{j=n+1}^{j=c} [l_j/r(c-n)]^{1/2}$$

$$XE = \sum_{j=n+1}^{j=c} [l_j/rc]^{1/2}$$

$$IE = \sum_{j=n+1}^{j=c} [l_j/rc(c-n)]^{1/2}$$

Where:

$r,c$ - number of rows and columns respectively in the data matrix, $r \geq c$ assumed.

$l_j$ - the $j^{th}$ eigenvalue of the equation:-

$$[M].Q_j = l_j.Q_j$$

$n$ - the number of factors.

Note: if $r < c$, then r and c must be interchanged in these equations.

calculate the real error, as given in table 2.2. We then repeat the calculation using the two smallest eigenvalues, then the three smallest values, and so forth. The real error calculated in this manner is then compared to the estimated error. The point at which the calculated real error is closest to the estimated error reveals the number of factors.

This method requires an accurate estimate of the experimental error. In many situations it is difficult to obtain such information, and an alternative method is required to estimate the number of factors.

Possible methods available to estimate the number of factors which contribute to the data are given below:-

(1) The real error

If the errors are distributed uniformly and randomly throughout the data matrix, then each error eigenvalue should be approximately the same. Thus we may expect that RE as a function of n should become approximately constant at the transition between data eigenvalues and error eigenvalues.

(2) The Malinowski 'IND' function.

The Malinowski 'IND' function, which is defined by:-

$$IND = RE / (c-n)^2$$

and is an empirical function which has been observed to reach a minimum when the correct number of factors have been used (24).

(3) Ratio of successive eigenvalues.

The ratio of each eigenvalue to the proceeding one can be used as an indication of the correct number of factors (25). This function will reach a maximum at the boundary between the primary set of eigenvalues and the secondary set.

### 2.2.2.6 Other effects of error.

A feature of principal component analysis and factor analysis is that they tend to exaggerate the non-uniformity of the error distribution, placing heavy emphasis on bad data points. Deviations will occur if:-

(1) The error is not truly random.

(2) Sporadic errors occur.

(3) Systematic errors exist.

(4) The error is not fairly uniform.

### 2.2.2.7 Finding the [A] matrix.

If 'n' unique peaks can be found where 'n' is the number of components, then it is possible to construct the [A] matrix by considering the behaviour of the unique peaks.

Suppose that by some means we have located the 'n' required unique peaks, then we may construct the [A] matrix by a method developed by Futrell (23). First the the eigenvector representation of the [C] matrix, [U], is calculated. Each element, $u_{ik}$, of this matrix

represents the amount of the $k^{th}$ eigenvector which contributes to the $i^{th}$ mass peak. The [U] matrix is normalised such that the sum of the squares of the elements across each row is unity. The elements of the normalised [U] matrix then represent the relative contribution of each eigenvector to each mass peak. If the element of the normalised [U] matrix represents a unique peak, then this element also represents the contribution of the eigenvector to the corresponding pure compound. Thus the rows of the normalised [U] matrix corresponding to unique peaks can be used to construct the columns of the [A] matrix.

### 2.2.2.8 Identifying the unique peaks

Two methods are available for locating the unique peaks. The first, due to Knorr and Futrell (23), is computationally faster, but has been shown by Malinowski to fail frequently if there are more than three factors. Malinowski gives an alternative procedure, which appears not to suffer from this problem (26). In both methods use is made of the normalised [U] matrix and the fact that, because of their uniqueness, pure mass peaks will be least like the average, and least like each other.

In the Knorr-Futrell method the first unique mass is chosen to correspond to the smallest element of the first column of the normalised [U] matrix. This may be rationalised as follows. The first column of [U], $u_{i1}$, represents the contribution to each mass, i, of the first eigenvector, i.e. the most important eigenvector with the largest corresponding eigenvalue. This first column represents the average behaviour of the mass peaks, so that the smallest element in this first

column represents the mass peak least like the average. The second pure mass peak is taken to be the mass peak which has the greatest difference between it and the first unique mass, chosen for the values of the elements of the second column of [U], $u_{i2}$. The third pure mass is chosen on the basis of the third eigenvector, $u_{i3}$, as that peak which has the greatest difference between it and the average of the first two unique peaks. The remaining unique peaks are found by continuing this procedure, i.e. the $k^{th}$ pure peak (k>2) is that which, on the basis of the elements of the $k^{th}$ normalised eigenvector, maximizes the difference between it and the average of the previous k-1 pure mass peaks.

As with the Knorr-Futrell method, in the Malinowski method the first unique peak is taken to be that corresponding to the element of the first column of the normalised [U] matrix which is closest to zero. However, subsequent unique peaks are calculated in a different manner. If the second unique peak is 'j', then in the Malinowski method this is chosen such that the $j^{th}$ row vector,

$$V_j = (v_{j1}, v_{j2})$$

in two dimensional space is most nearly orthogonal to

$$V_i = (v_{i1}, v_{i2})$$

where i corresponds to the first unique peak. Hence the dot product between $V_i$ and $V_j$ should be a minimum. To find the third unique peak, we consider the row vectors in three dimensional space, i.e. we now include elements which correspond to the third most important normalised eigenvector. The cross product of the the vectors $V_i$ and $V_j$ is a vector which is mutually perpendicular to both $V_i$ and $V_j$, where now we are using

$$V_i = (v_{i1}, v_{i2}, v_{i3})$$

and

$$V_j = (v_{j1}, v_{j2}, v_{j3}).$$

Thus the three dimensional row vector $V_k$, corresponding to the the third unique peak is taken to be that vector which gives the maximum dot product with the above cross product. Thus the determinant constructed from the three dimensional row vectors for the first, second, and third unique peaks will be a maximum when the correct third unique peak has been chosen.

In a similar manner each successive unique peak can be found by selecting that row vector which maximises the determinant constructed from itself and the previously found unique peak row vectors in 'm' dimensional space where 'm' refers to the $m^{th}$ unique peak.

## 2.3 Computing

A factor analysis program was available at the ESSO Research Centre, Abingdon. This was programmed in compiled BASIC on the site PDP11/70 computer, and was a transcript of a factor analysis program written in Sharp BASIC (27).

Because of the complexity of the program it was decided to produce a BASIC program that could generate test data.

The test data program generates a data matrix, [D], which is stored as a file compatible with the factor analysis program's input requirements. The data matrix was calculated from:-

$$[D] = [R].[C] + [E]$$

The matrices [R], [C], and [E] are the spectra matrix, the concentration matrix, and the error matrix respectively.

Since the bulk of the present work was carried out at the University of Warwick Department of Chemistry, it was decided to write a FORTRAN IV version of the factor analysis program for use on the MS80 data system. Initially this program was written for the Department's Data General Nova II computer, however, this was replaced by a Data General Eclipse S120 computer, so that the factor analysis program had to be re-written. An advantage of using FORTRAN was that several memory saving techniques could be used, so that it is possible that in future, the program could be extended to allow a greater data set to be processed, or more elaborate pre-processing of the data. Furthermore, a simple program was written to prepare data files, compatible with the factor analysis program, from the stored mass spectra. This program used library subroutines to access Kratos DS55 format mass files.

It was proposed that a factor analysis program be implemented on the University's main-frame computer; however, as a result of the University upgrading it's mainframe computer, very little time was available for this work, and it was not completed.

## 2.4 Test Results

As the final part of this chapter, the results and conclusions from a series of test experiments will be presented. The first series of test experiments, performed at the ESSO Research Centre Abingdon, were designed to test the factor analysis program using computer generated test data.

The second series of experiments, performed at the University of Warwick, used simple test mixtures to generate spectra on the MS80. These spectra were then analysed using the factor analysis program.

The results obtained when using the factor analysis programs to analyse data for more specific problems will be presented in later chapters.

### 2.4.1 Computer Generated Test Data.

In agreement with the observations of Malinowski, it was found that the Knorr-Futrell method of unique peak selection often failed to give the correct results. The Malinowski method always found unique peaks when they were present, although when two or more unique peaks occurred for a given component, the one chosen was not always the most characteristic unique peak i.e. it was not always the most intense unique peak.

With little or no error, and unique peaks for each component, the factor analysis program was able to give good results. A typical example is shown in table 2.3. This shows the results for eight mixtures, each of three components. The RMS error was 358 intensity units (about 2% of the mean intensity). All three methods of finding the number of factors clearly indicate that there are three factors. The agreement between the actual spectra and mixture concentrations is quite good.

The results for the factor analysis of data corresponding to six mixtures, each of four components, and not having unique peaks, is shown in table 2.4. Again the three methods available to determine the dimensionality of the system all showed that four components were

TABLE 2.3: FACTOR ANALYSIS RESULTS

| PEAK £ | COMPONENT 1 ACTUAL | COMPONENT 1 FOUND | COMPONENT 2 ACTUAL | COMPONENT 2 FOUND | COMPONENT 3 ACTUAL | COMPONENT 3 FOUND |
|---|---|---|---|---|---|---|
| 1 | 44 | 44 | 0 | 0 | 41 | 42 |
| 2 | 0 | 0 | 48 | 49 | 0 | 0 |
| 3 | 100 | 100 | 0 | 0 | 0 | 0 |
| 4 | 0 | 1 | 85 | 85 | 24 | 22 |
| 5 | 27 | 27 | 0 | 0 | 20 | 22 |
| 6 | 0 | 1 | 93 | 95 | 0 | 0 |
| 7 | 24 | 25 | 99 | 100 | 42 | 39 |
| 8 | 0 | 1 | 80 | 81 | 0 | 0 |
| 9 | 0 | 0 | 0 | 0 | 100 | 100 |
| 10 | 0 | 1 | 100 | 100 | 0 | 0 |

| MIXTURE £ | % COMPONENT 1 ACTUAL | % COMPONENT 1 FOUND | % COMPONENT 2 ACTUAL | % COMPONENT 2 FOUND | % COMPONENT 3 ACTUAL | % COMPONENT 3 FOUND |
|---|---|---|---|---|---|---|
| 1 | 72 | 67 | 15 | 15 | 13 | 18 |
| 2 | 80 | 76 | 11 | 11 | 9 | 13 |
| 3 | 70 | 66 | 17 | 16 | 13 | 18 |
| 4 | 45 | 40 | 33 | 30 | 22 | 30 |
| 5 | 40 | 36 | 36 | 33 | 23 | 31 |
| 6 | 11 | 10 | 67 | 61 | 21 | 28 |
| 7 | 5 | 4 | 76 | 70 | 20 | 26 |
| 8 | 8 | 6 | 25 | 19 | 67 | 75 |

| £ FACTORS | REAL ERROR | 'IND' FUNCTION | RATIO OF EIGEN VALUES |
|---|---|---|---|
| 1 | 17308 | 353 | - |
| 2 | 9796 | 272 | 6 |
| 3 | 320 | 12 | 3 |
| 4 | 289 | 18 | 3257 |
| 5 | 246 | 27 | 1 |
| 6 | 197 | 49 | 1 |
| 7 | 150 | 150 | 2 |

TABLE 2.4: FACTOR ANALYSIS RESULTS

| PEAK NO. | COMP. 1 ACT. | COMP. 1 FND. | COMP. 2 ACT. | COMP. 2 FND. | COMP. 3 ACT. | COMP. 3 FND. | COMP. 4 ACT. | COMP. 4 FND. |
|---|---|---|---|---|---|---|---|---|
| 1 | 93 | 76 | 0 | 0 | 0 | 0 | 5 | 0 |
| 2 | 0 | 5 | 41 | 37 | 6 | 20 | 0 | 3 |
| 3 | 100 | 100 | 100 | 100 | 0 | 37 | 0 | 0 |
| 4 | 75 | 40 | 0 | 0 | 62 | 31 | 49 | 66 |
| 5 | 94 | 43 | 0 | 0 | 94 | 49 | 71 | 100 |
| 6 | 62 | 30 | 0 | 0 | 38 | 34 | 0 | 37 |
| 7 | 21 | 36 | 96 | 99 | 0 | 34 | 0 | 0 |
| 8 | 0 | 0 | 50 | 0 | 100 | 100 | 0 | 92 |
| 9 | 28 | 11 | 11 | 0 | 29 | 29 | 0 | 27 |
| 10 | 6 | 0 | 0 | 0 | 53 | 0 | 100 | 65 |

| MIX. NO. | COMP. 1 ACT. | COMP. 1 FND. | COMP. 2 ACT. | COMP. 2 FND. | COMP. 3 ACT. | COMP. 3 FND. | COMP. 4 ACT. | COMP. 4 FND. |
|---|---|---|---|---|---|---|---|---|
| 1 | 0 | 1 | 43 | 21 | 39 | 23 | 18 | 54 |
| 2 | 28 | 29 | 21 | 16 | 42 | 13 | 9 | 42 |
| 3 | 11 | 13 | 35 | 20 | 42 | 19 | 12 | 48 |
| 4 | 36 | 38 | 24 | 6 | 7 | 15 | 32 | 42 |
| 5 | 18 | 19 | 15 | 16 | 46 | 9 | 21 | 56 |
| 6 | 53 | 56 | 41 | 7 | 5 | 26 | 2 | 10 |

| PURE PEAK | COMP. 1 | COMP. 2 | COMP. 3 | COMP. 4 |
|---|---|---|---|---|
| 1 | 818 | 0 | 0 | 42 |
| 8 | 0 | 399 | 952 | 0 |
| 7 | 184 | 767 | 0 | 0 |
| 10 | 57 | 0 | 508 | 717 |

present. The RMS error for the data was 31 intensity units (about 0.3% of the mean intensity). Here the spectra, and concentrations of component 1 have been quite well reproduced. Consideration of the unique peaks that the program produced shows that the first 'unique' peak is only significantly intense for component 1. Thus we may consider that a unique peak is a peak for which the relative intensity is high for only one component. The intensities of the unique peak for the other components need not be zero, but should be small in relation to the intensity of the unique peak for that one component.

In cases where there are no unique peaks, or where the errors are large, the factor analysis program will, not surprisingly, fail to reproduce the spectra and concentrations reliably. In fact the program will, in such a situation, produce bogus spectra, and it is up to the operator to use his 'chemical intuition' and experience to spot such a situation.

In some cases non-uniform errors can introduce 'phantom' components into the mixtures. However it is sometimes possible that these appear as secondary maxima in the ratio of eigenvalues, and as secondary minima in the 'IND' function. Such a case is shown in table 2.5, which represents data for eight mixtures, each of three components, with an RMS error of 299 intensity units. The lowest minimum of the IND function, and the highest maxima of the ratio of the eigenvalues suggest six factors. If we consider the first encountered minima and maxima of these functions, however, then only three factors are indicated. Comparison of the real error with the actual RMS error correctly indicates three components. The concentrations and spectra of the three components were quite well reproduced.

TABLE 2.5: FACTOR ANALYSIS RESULTS

| PEAK £ | COMPONENT 1 ACTUAL | COMPONENT 1 FOUND | COMPONENT 2 ACTUAL | COMPONENT 2 FOUND | COMPONENT 3 ACTUAL | COMPONENT 3 FOUND |
|---|---|---|---|---|---|---|
| 1 | 100 | 100 | 0 | 0 | 0 | 0 |
| 2 | 5 | 15 | 100 | 100 | 0 | 0 |
| 3 | 0 | 0 | 0 | 0 | 49 | 57 |
| 4 | 0 | 3 | 44 | 44 | 56 | 52 |
| 5 | 0 | 8 | 85 | 85 | 0 | 0 |
| 6 | 31 | 35 | 51 | 51 | 100 | 100 |

| MIXTURE £ | % COMPONENT 1 ACTUAL | % COMPONENT 1 FOUND | % COMPONENT 2 ACTUAL | % COMPONENT 2 FOUND | % COMPONENT 3 ACTUAL | % COMPONENT 3 FOUND |
|---|---|---|---|---|---|---|
| 1 | 92 | 87 | 3 | 5 | 5 | 7 |
| 2 | 98 | 97 | 5 | 1 | 1 | 2 |
| 3 | 51 | 42 | 12 | 17 | 36 | 41 |
| 4 | 10 | 8 | 6 | 7 | 84 | 85 |
| 5 | 16 | 11 | 15 | 19 | 68 | 69 |
| 6 | 0 | 10 | 99 | 99 | 1 | 1 |
| 7 | 9 | 5 | 80 | 84 | 11 | 10 |
| 8 | 27 | 19 | 48 | 56 | 25 | 24 |

| £ FACTORS | REAL ERROR | 'IND' FUNCTION | | RATIO OF EIGEN VALUES | |
|---|---|---|---|---|---|
| 1 | 19862 | 405 | | - | |
| 2 | 12113 | 336 | | 4 | |
| 3 | 172 | 7 | 1 MIN. | 2 | |
| 4 | 144 | 9 | | 13675 | 1 MAX. |
| 5 | 114 | 12 | | 1 | |
| 6 | 0.18 | 0.04 | 2 MIN. | 1 | |
| 7 | 0.18 | 0.1 | | 1E+06 | 2 MAX. |

### 2.4.2 Factor Analysis of Simple Mixtures

Factor analysis was applied to data generated on the MS80 mass spectrometer. However, as the factor analysis program was the newly written FORTRAN IV version, two sets of data were used to test the program prior to using it on actual mass spectra.

The first test data set was used to compare the performance of the program with that of the previously used BASIC version of the program mensioned above. The second data set used was that quoted by Malinowski (26), and the results obtained were found to be in agreement with his results.

Having confirmed that the factor analysis program was functioning correctly, it was used to analyse several mass spectra of simple mixtures.

#### 2.4.2.1 Mass Selection.

The factor analysis program can, at present, process up to ten spectra, each containing up to thirty mass peaks. Thus, since mass spectra will generally have more than thirty mass peaks, and a given run will often contain more than ten scans, some form of mass selection and scan selection is required.

A program was written to access the Kratos DS-55 format mass files and select the required mass peaks from the required scans. Due to lack of time whilst writing this program, it is not able to perform all the

functions one may wish: mass peak and scan selection are achieved manually, i.e. the program asks the user to input the required mass peaks, and the scans input via the DS-55 'scan-queuing' system (28). The mass peaks can be normalised, if required, this is simply achieved by reading the 'software total ion current (TIC)' from the scan statistics block of the mass file, and using this to scale the intensities of the peaks used.

A simple procedure was adopted to select the mass peaks to be used:-

(1) Peak average all the scans in the run. The intensity limit being set so as to reject all peaks with intensity less than 2% of the base peak, and the minimum peak limit set so as to reject all peaks that occur in fewer than four scans. (Recall that the factor analysis technique is prone to be over influenced by sporadic errors - so that spurious mass peaks must be rejected).

(2) Select those mass peaks from the peak averaged result which have intensity greater than 2% of the base peak, or the thirty most intense peaks if the above gives more than thirty peaks.

This procedure was carried out manually, using the DS-55 peak averaging software, listing the result, and supplying the appropriate mass peaks to the peak selection program. If more time had been available it would have been possible to carry out this procedure automatically in the peak selection program.

Obviously, the above procedure is not the optimum peak selection method, for example, it does not take into account that statistically important peaks may have a very low intensity relative to the base peak. The peak selection procedure is just as important as the factor analysis

procedure itself, so that a much more elaborate peak selection procedure is necessary, more will mentioned on this point below.

### 2.4.2.2 Results.

The mass spectra were run on the MS80 mass spectrometer as probe samples, therefore, one cannot expect quantitative results for the mixture composition. For this reason the first test mixture consisted of four components, and was of arbitrary composition (but roughly equal proportions of each). The pure components were 2,4,6-trichlorophenol, 1-chloro-2-nitrobenzene, phenylethanoic acid and methyl benzoate, their spectra are shown in figures 2.3 - 2.6 respectively.

Factor analysis was applied to the mixture spectra in two stages, in the first stage, scans were selected at regular intervals from the sample run. Factor analysis was then used to identify the unique peaks. In the second stage, scans were selected from the sample run, so as to include those scans that maximised the pure peak intensity profiles. In this fashion, one may include the most statistically relevant scans in the data processing procedure. It was noted that a small improvement in the results obtained from factor analysis was achieved by this two stage process.

The factor analysis results are shown in table 2.6 and in figures 2.7 - 2.11. The values of the eigenvalue ratio, the real error, and the 'IND' function are shown in the table, whilst the spectra are shown in the figures. It will be noticed that the factor analysis program identifies an additional component with major peaks at m/z = 32, and m/z = 28, obviously due to air. The extra pure component may be identified

TABLE 2.6: FACTOR ANALYSIS RESULTS

SIMPLE MIXTURE - FOUR COMPONENTS

| EIGENVALUE RATIOS | |
|---|---|
| 1 | 2.90 |
| 2 | 1.45 |
| 3 | 1.11 |
| 4 | 9.81 |
| 5 | 61.07 |
| 6 | 2.02 |
| 7 | 3.02 |
| 8 | 6.46 |
| 9 | 1.76 |

| IND FUNCTION | |
|---|---|
| 1 | 510 |
| 2 | 521 |
| 3 | 514 |
| 4 | 233 |
| 5 | 60 |
| 6 | 68 |
| 7 | 75 |
| 8 | 91 |
| 9 | 311 |

| REAL ERROR | |
|---|---|
| 1 | 41279 |
| 2 | 33342 |
| 3 | 25171 |
| 4 | 8373 |
| 5 | 1509 |
| 6 | 1082 |
| 7 | 675 |
| 8 | 365 |
| 9 | 311 |

UNIQUE PEAKS

| FACTOR | PEAK NO. | MASS |
|---|---|---|
| 1 | 23 | 196 |
| 2 | 10 | 91 |
| 3 | 1 | 28 |
| 4 | 14 | 105 |
| 5 | 21 | 157 |

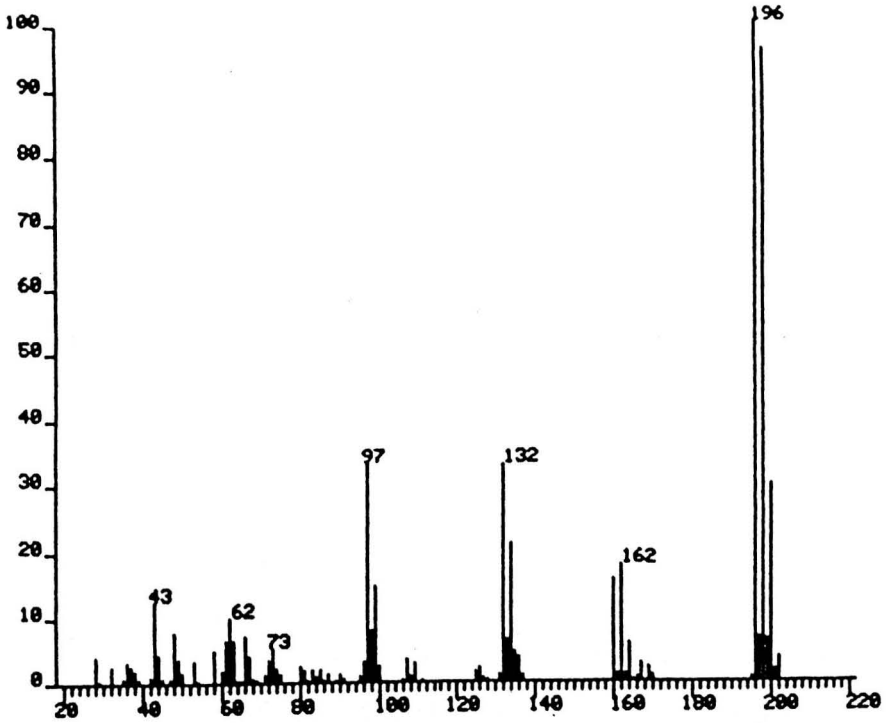


FIGURE 2.3: Electron Ionisation Spectrum of 2,4,6-trichlorophenol.

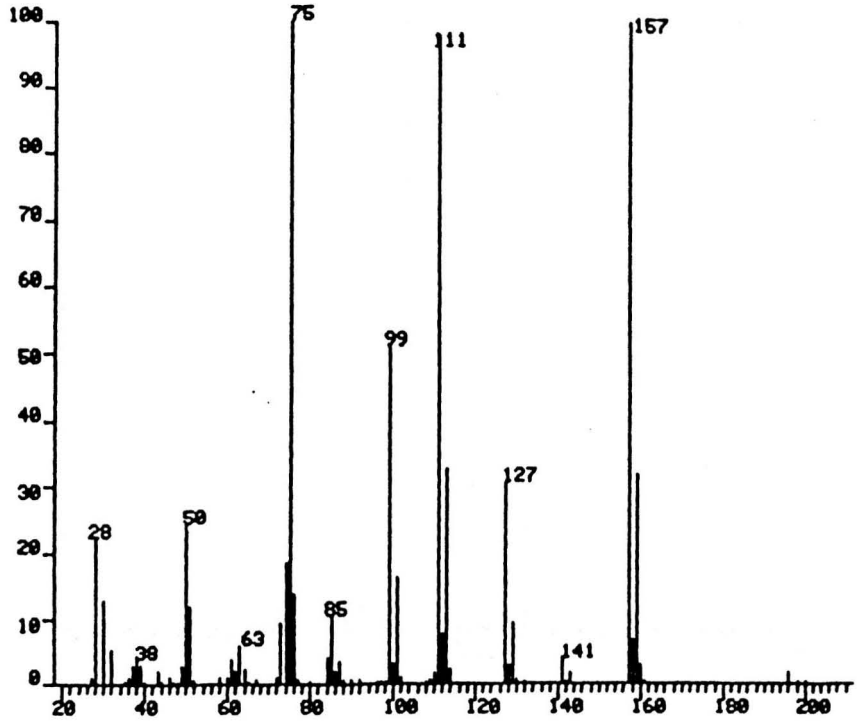


FIGURE 2.4: Electron Ionisation Spectrum of 1-chloro-2-nitrobenzene.

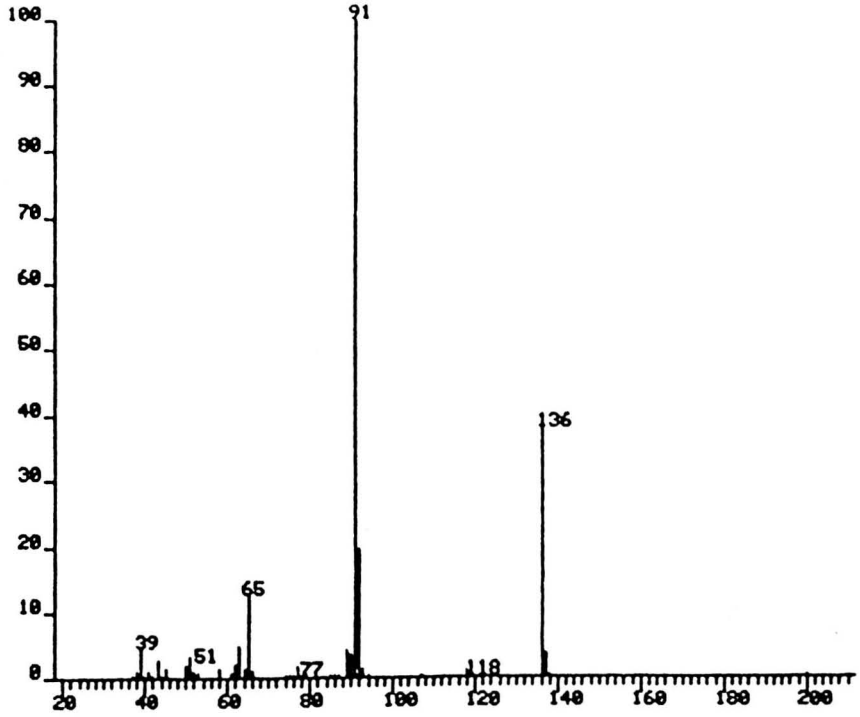


FIGURE 2.5: Electron Ionisation Spectrum of phenylethanoic acid.

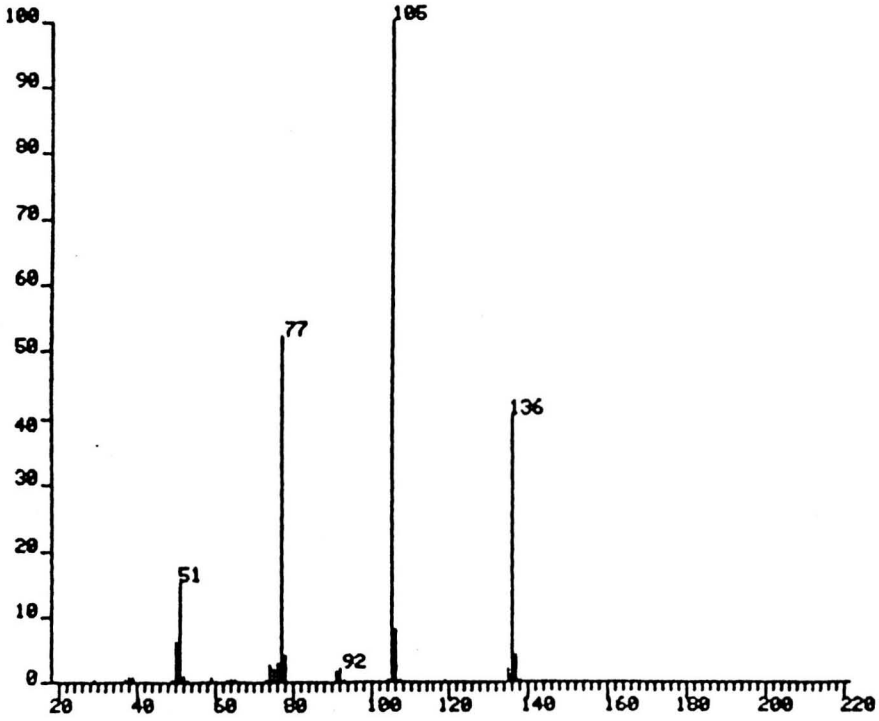


FIGURE 2.6: Electron Ionisation Spectrum of methyl benzoate.

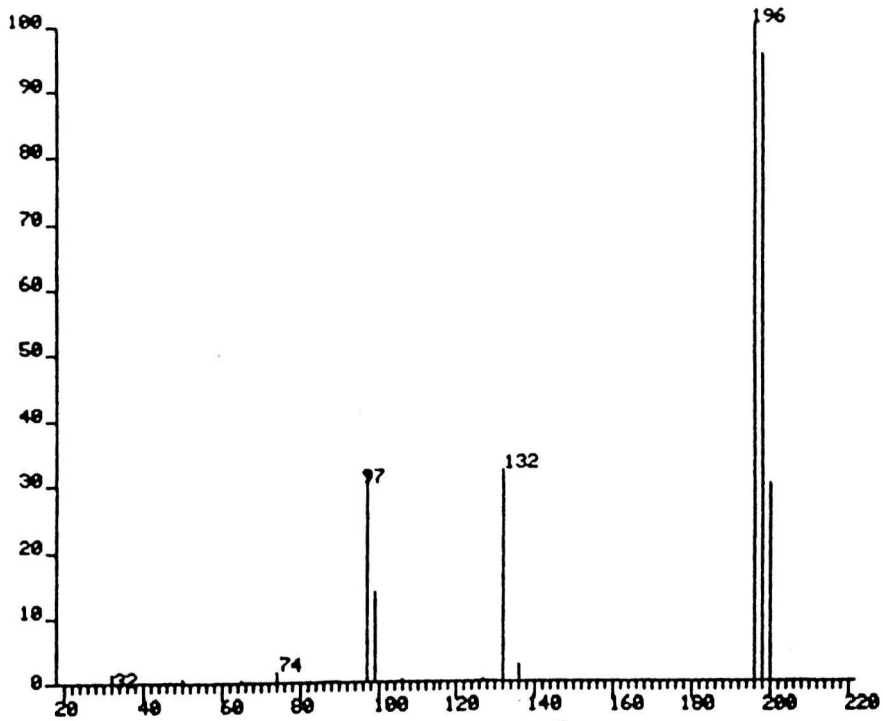


FIGURE 2.7: Factor Analysis Generated Spectrum: Component No.1.

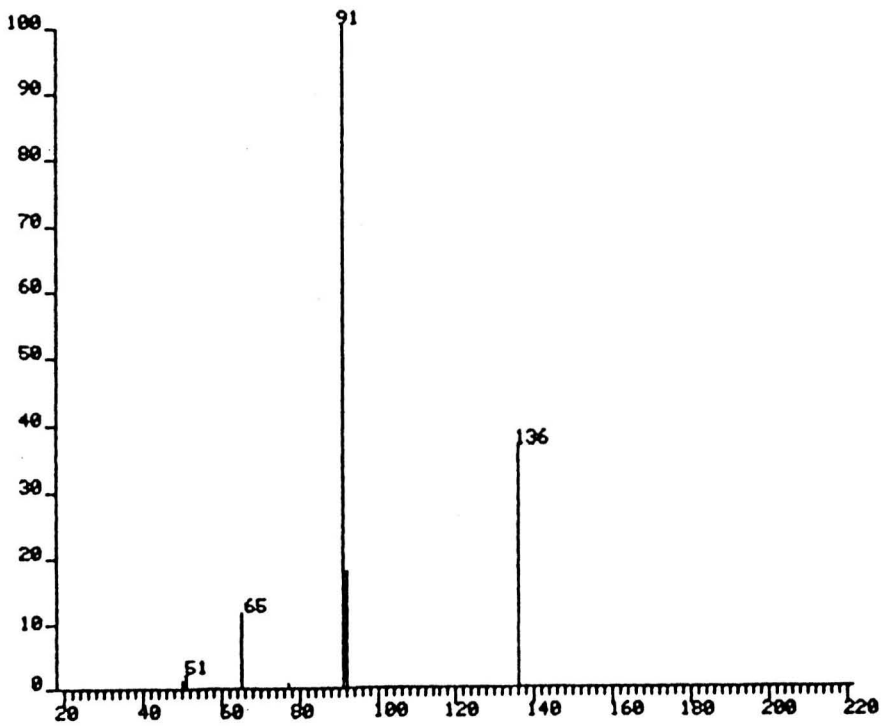


FIGURE 2.8: Factor Analysis Generated Spectrum: Component No.2.

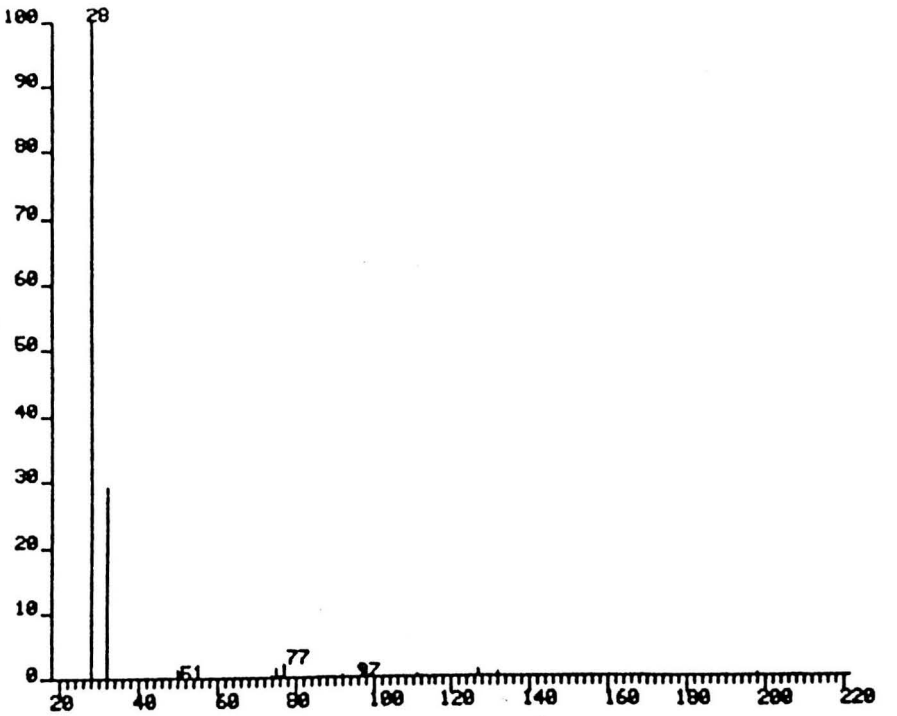


FIGURE 2.9: Factor Analysis Generated Spectrum: Component No.3.

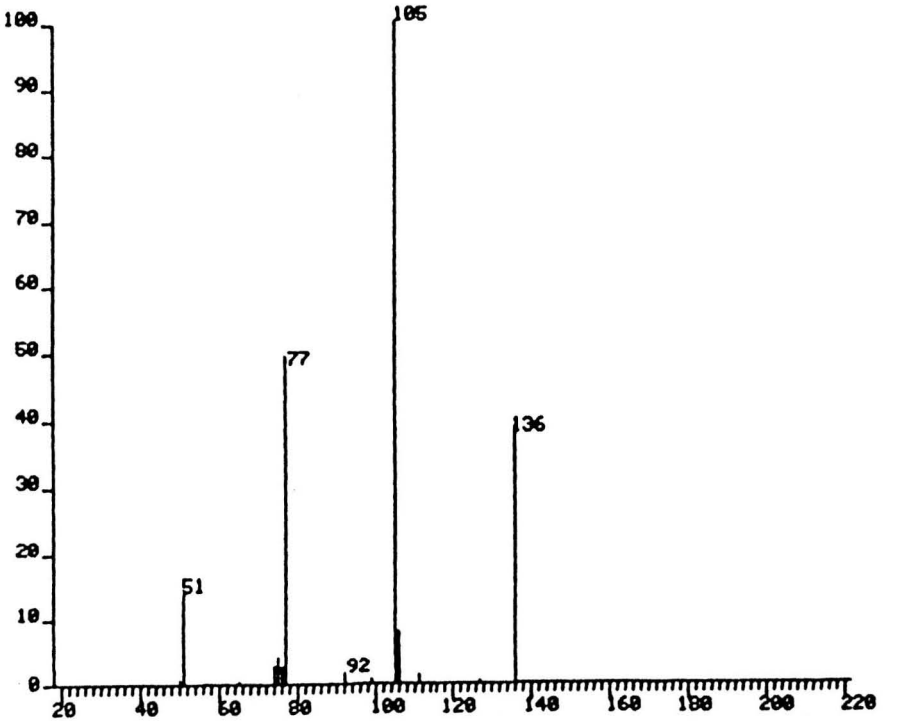


FIGURE 2.10: Factor Analysis Generated Spectrum:

Component No.4.

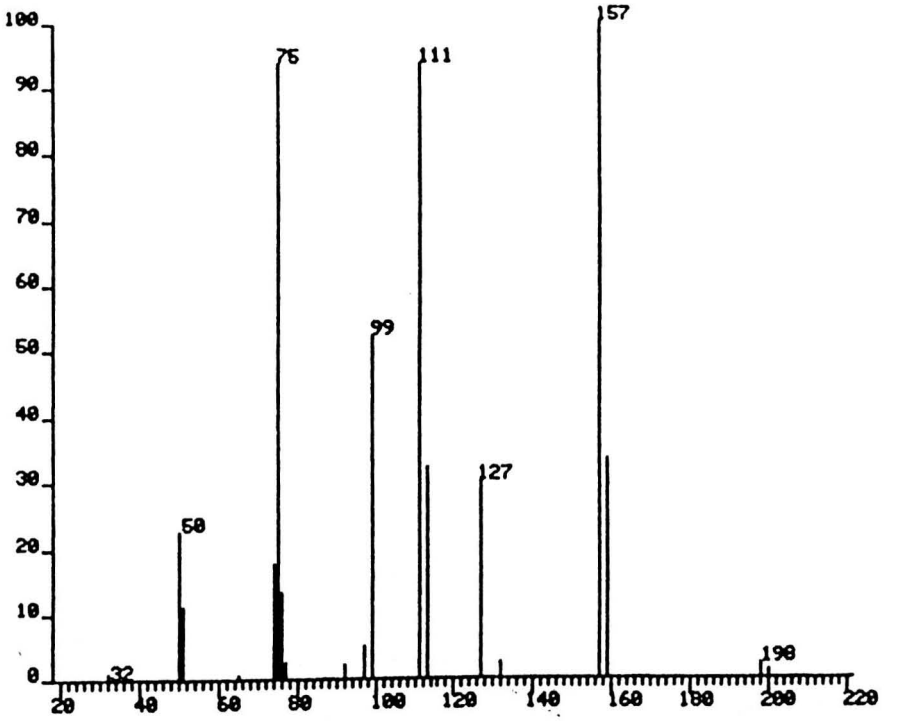


FIGURE 2.11: Factor Analysis Generated Spectrum: Component No.5.

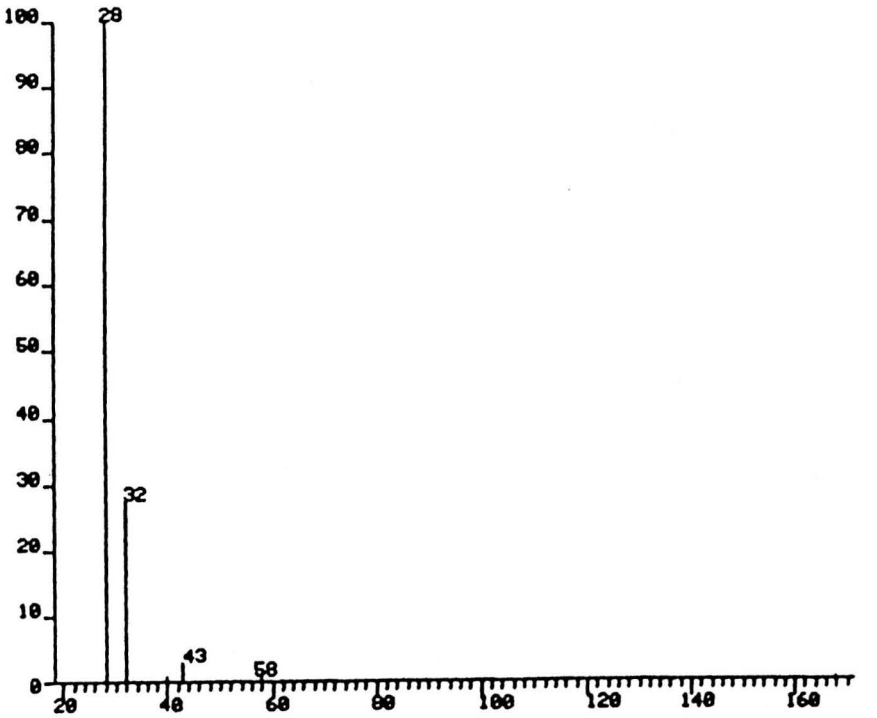


FIGURE 2.12: Electron Ionisation Spectrum: Simple Mixture: Scan 2.

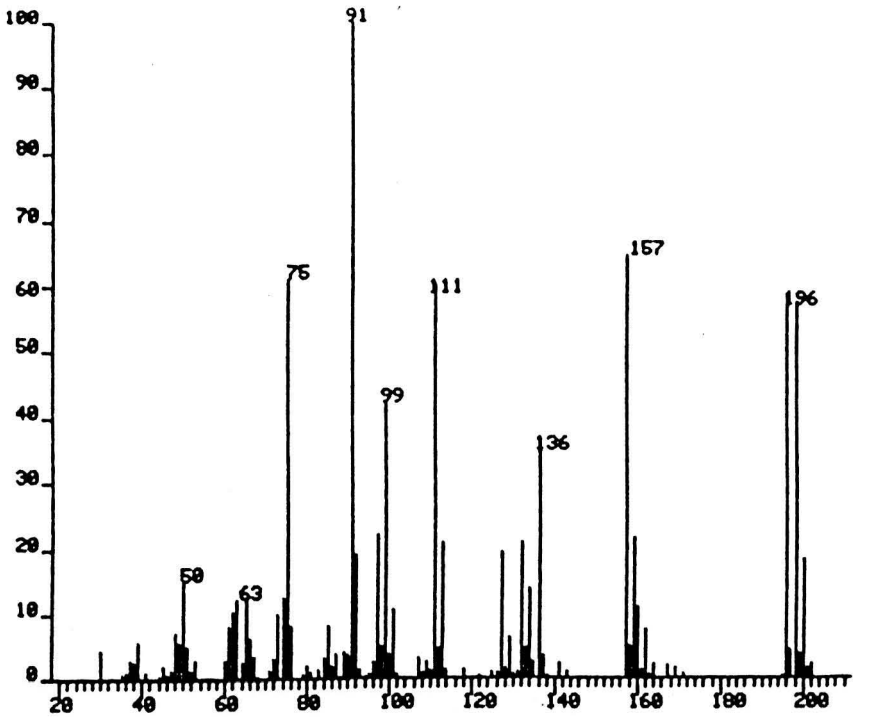


FIGURE 2.13: Electron Ionisation Spectrum: Simple Mixture: Scan 12.

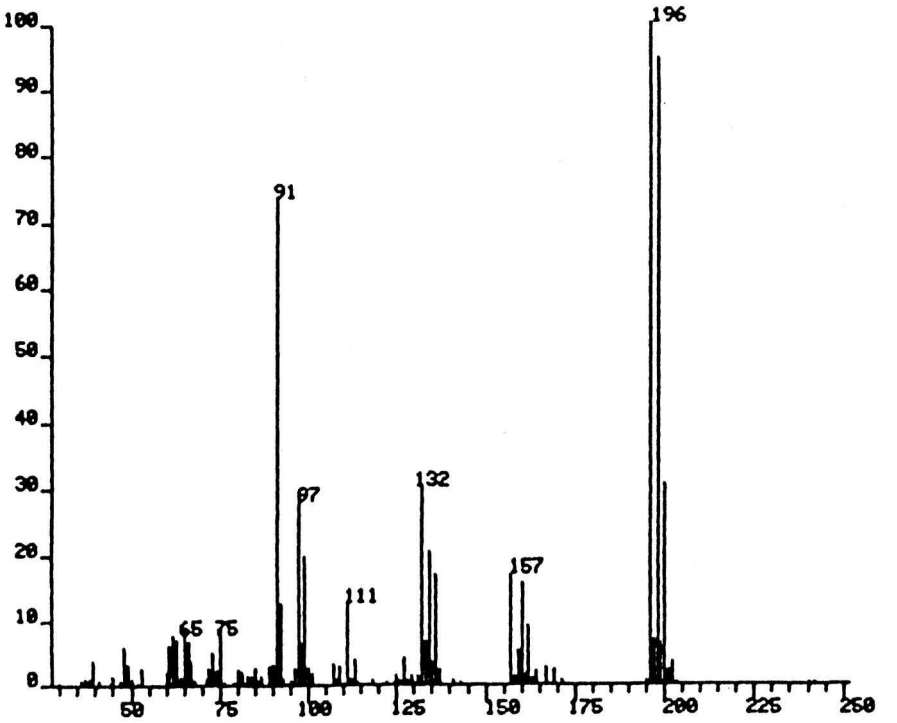


FIGURE 2.14: Electron Ionisation Spectrum: Simple Mixture: Scan 13.

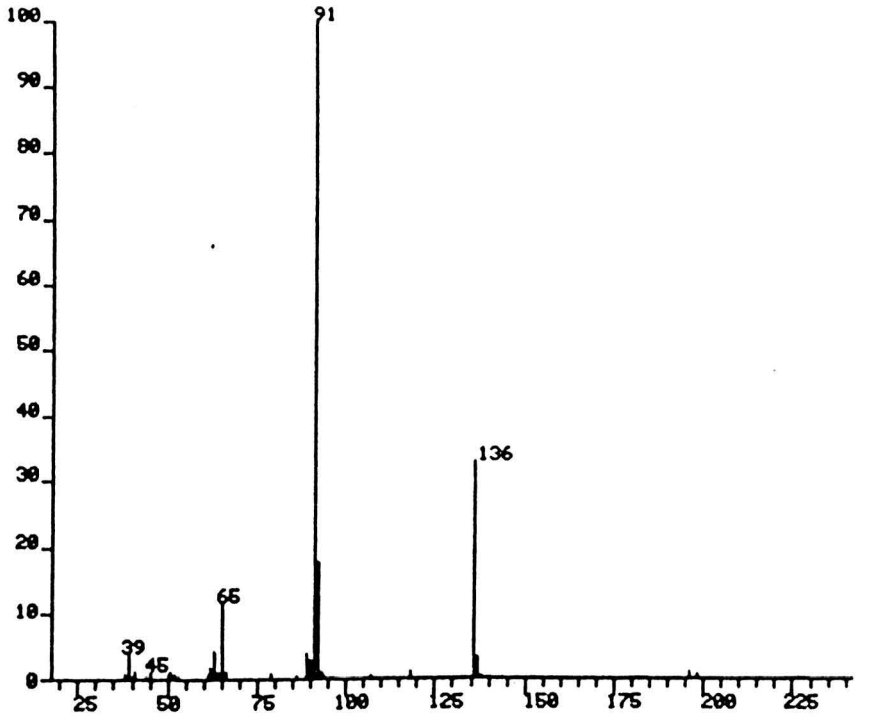


FIGURE 2.15: Electron Ionisation Spectrum: Simple Mixture: Scan 15.

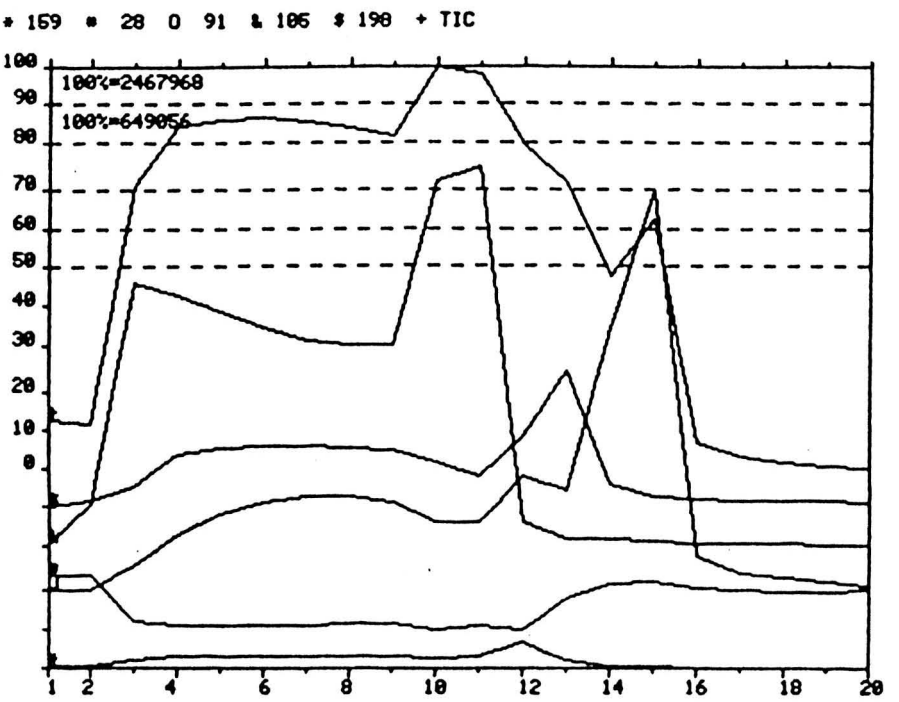


FIGURE 2.16: Cross Scan Plot of Simple Mixture Run.

with the back-ground spectrum, in effect, factor analysis automatically performs background subtraction - provided that one or other of the background mass peaks is a 'unique' peak.

The spectra of the components are very well reproduced, however, this particular mixture was quite well separated due to the relatively large vapour pressure differences between the four components. This is illustrated in figures 2.12 - 2.15, which show those spectra of the mixture which maximise the 'pure peak' intensity as a function of scan number (see figure 2.16, which shows the mass profiles of the pure peak intensities versus scan number).

A second test mixture was made up for use as a probe sample, it consisted of toluene, oct-1-ene, n-dodecane, and n-hexadecane. The ratio of eigenvalues and the IND function are shown graphically in figures 2.17 and 2.18 respectively. The maximum in the eigenvalue ratios and the minimum in the IND function, both show that there are seven components in the mixture; however, as noted previously, data that have relatively large errors often show another maximum in the eigenvalue ratio and another minimum in the IND function at lower component numbers corresponding to the 'real' number of components. Figures 2.17 and 2.18 show these features at a number of components, No. CMP = 4. It may also be noted that at No. CMP = 4, the reproduced spectrum for the background (i.e. air) is closer to what one would expect. The factor analysis generated spectrum for air is shown in figure 2.19.

The four spectra generated by the factor analysis program are shown in figures 2.19 to 2.22. As noted above, figure 2.19 may be identified with the background spectrum. Only two spectra have been well reproduced. These are n-dodecane, shown in figure 2.20, and

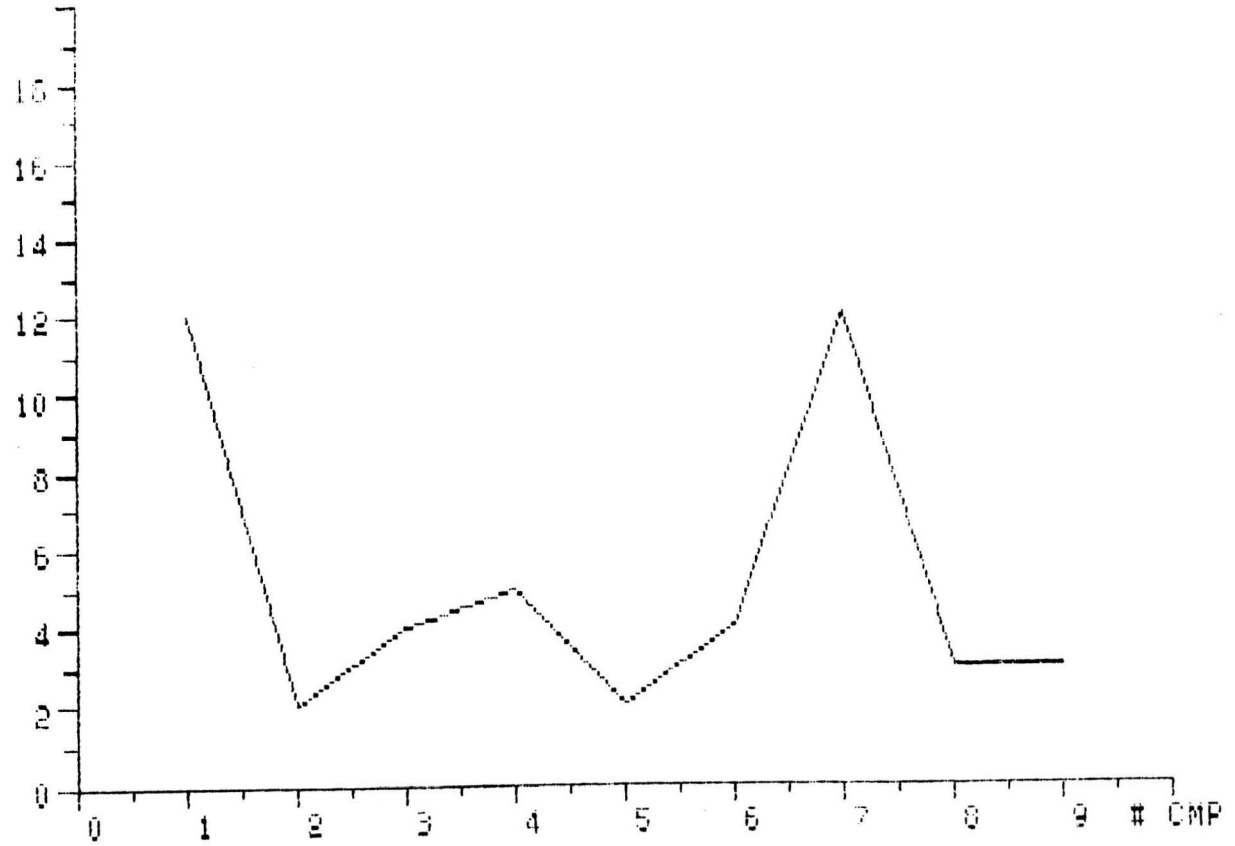


**FIGURE 2.17: Ratio of Eigenvalues: Test Mixture Two.**

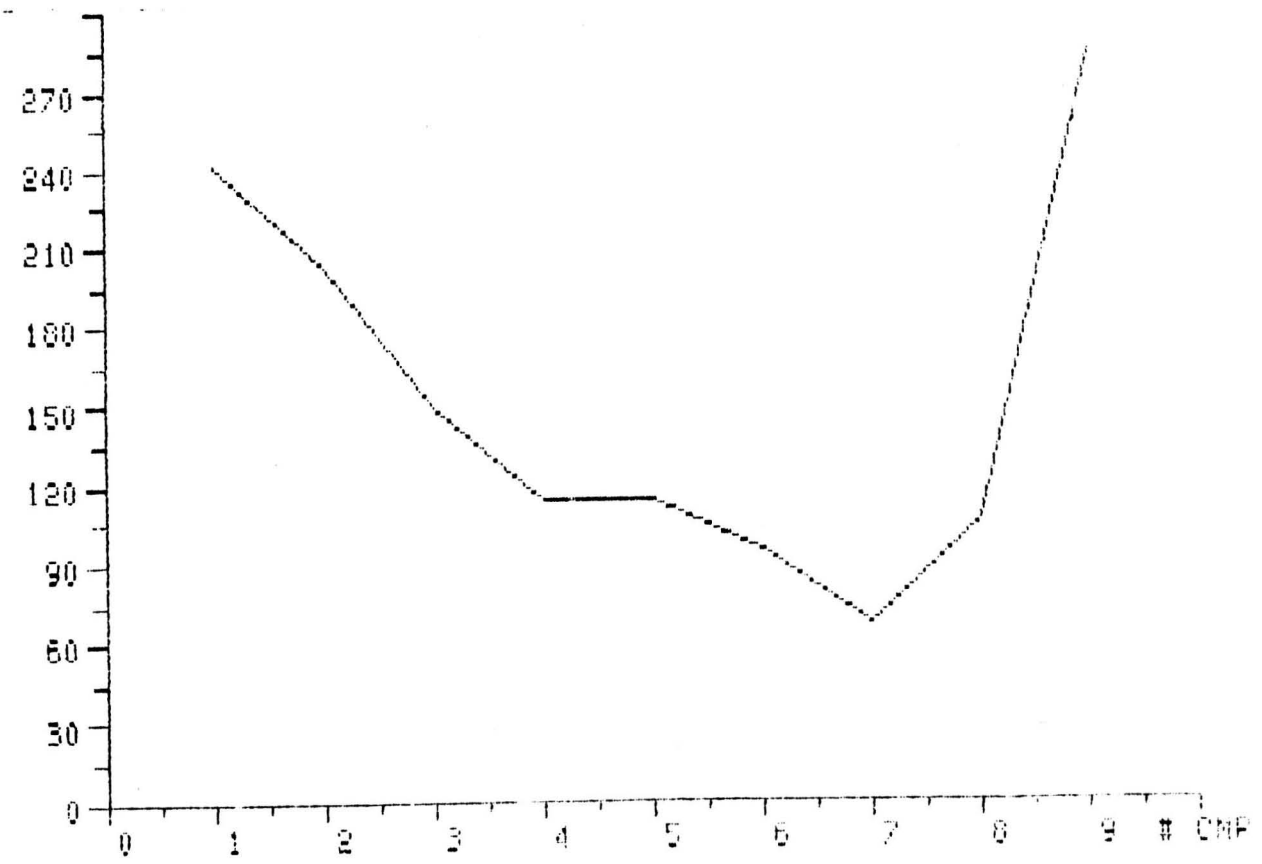


**FIGURE 2.18: Ind Function vs No. of Components: Test Mixture Two.**

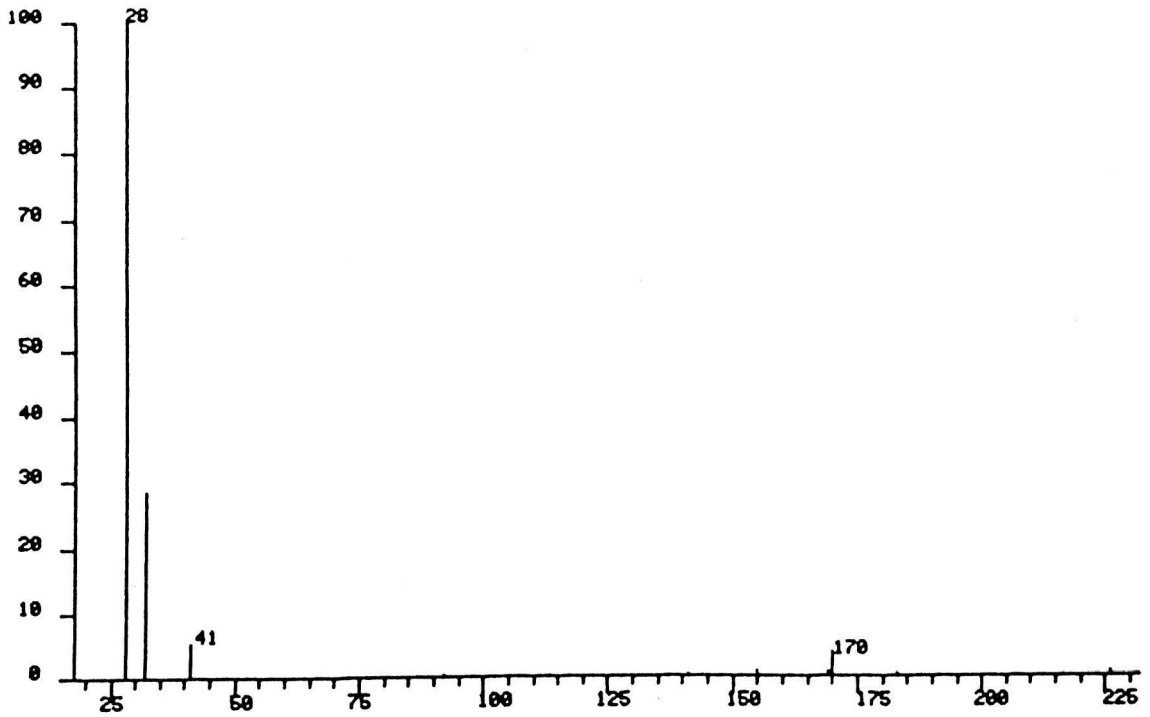


FIGURE 2.19: Factor Analysis Generated Spectrum: Test Mixture Two, Component No.1.

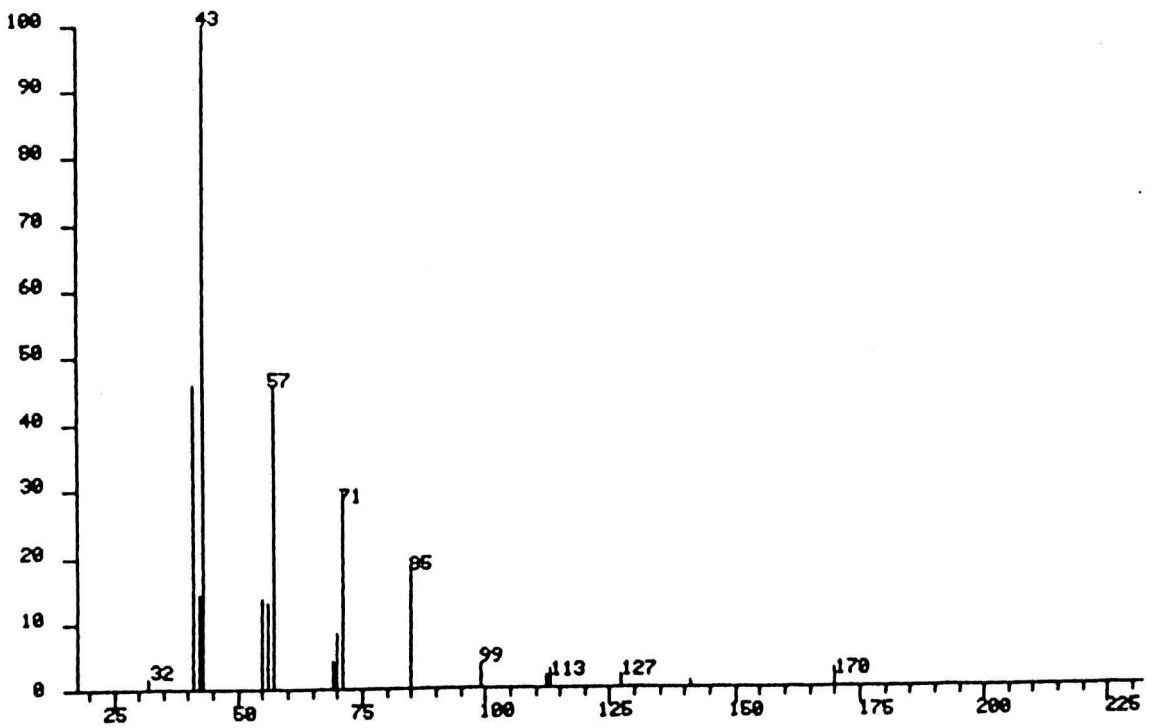


FIGURE 2.20: Factor Analysis Generated Spectrum: Test Mixture Two, Component No.2.

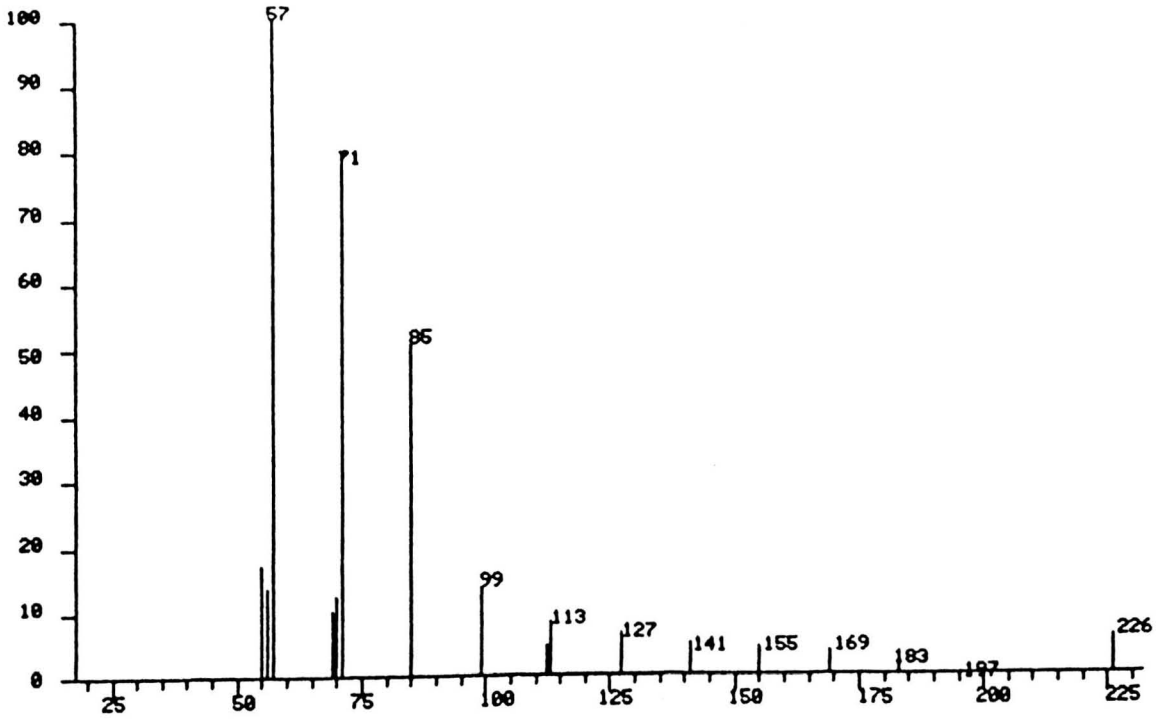


FIGURE 2.21: Factor Analysis Generated Spectrum: Test Mixture Two, Component No.3.

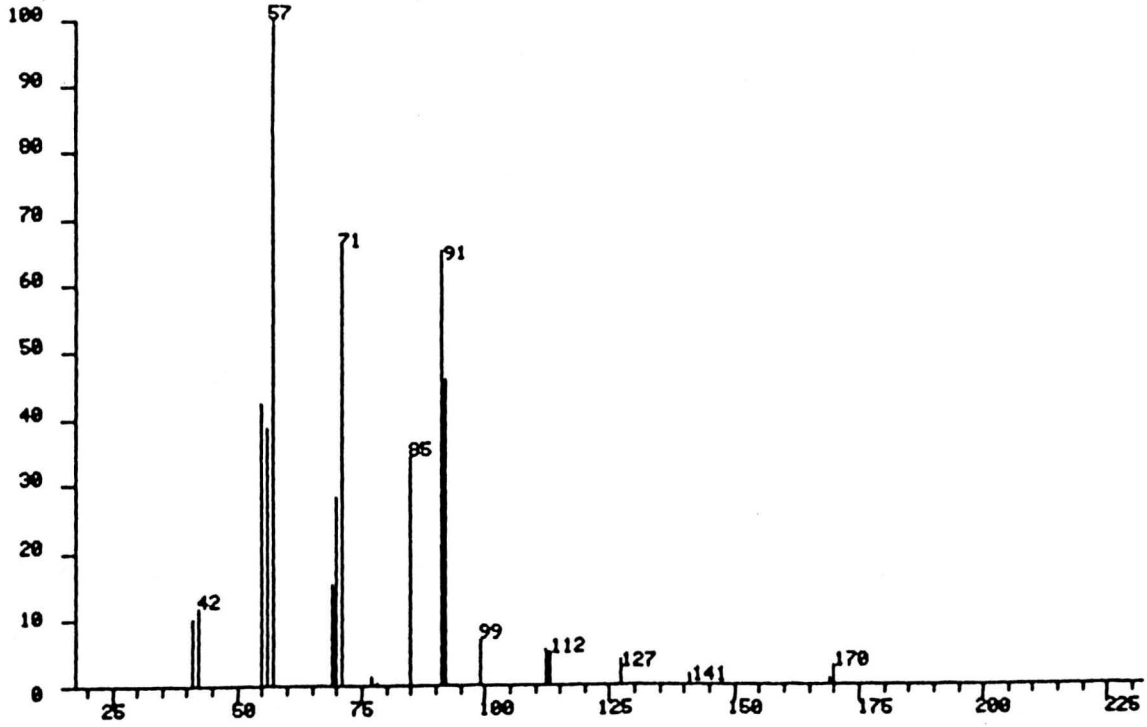


FIGURE 2.22: Factor Analysis Generated Spectrum: Test Mixture Two, Component No.4.

n-hexadecane, shown in figure 2.21. One may expect that the oct-1-ene component would not be well 'recognised', as it's unique peak at m/z = 112, would be easily masked by the fragment ions from the two alkanes. It is more of a surprise that the toluene was not identified by the program, as this has a well defined unique peak at m/z = 91. As can be seen from figure 2.22, the fourth factor identified by the factor analysis program consists of a mixture of toluene, oct-1-ene and n-dodecane peaks. It is important to note that factor analysis results may represent spectra of components which undergo correlated changes. In the case of probe samples, components of the mixture which have similar vapour pressure / temperature characteristics are not likely to be differentiated from each other, especially if statistical variations swamp the small differences that do exist between the components. We may note here that oct-1-ene and toluene are likely to have similar vapour pressure / temperature characteristics.

Using the factor analysis program simply to identify the 'unique' peaks present in a complex mixture spectrum is a useful end in itself. For example, one may identify the unique peaks in a set of GC/MS spectra, and then use these to generate mass profiles, from which more accurate retention times and peak areas may be calculated. Generation of the spectra of the pure components may then be regarded as a bonus.

A simple example is shown in figure 2.23, where a GC/MS cross-scan report (i.e. graph of TIC vs scan number) shows that the third GC peak overlaps with the fourth GC peak. Applying the factor analysis program to the data for scans twenty to twenty-nine gives m/z = 58, 31, and 32 as unique peaks when three factors are chosen. The mass profiles for these mass peaks are also shown in figure 2.23. The resultant spectra

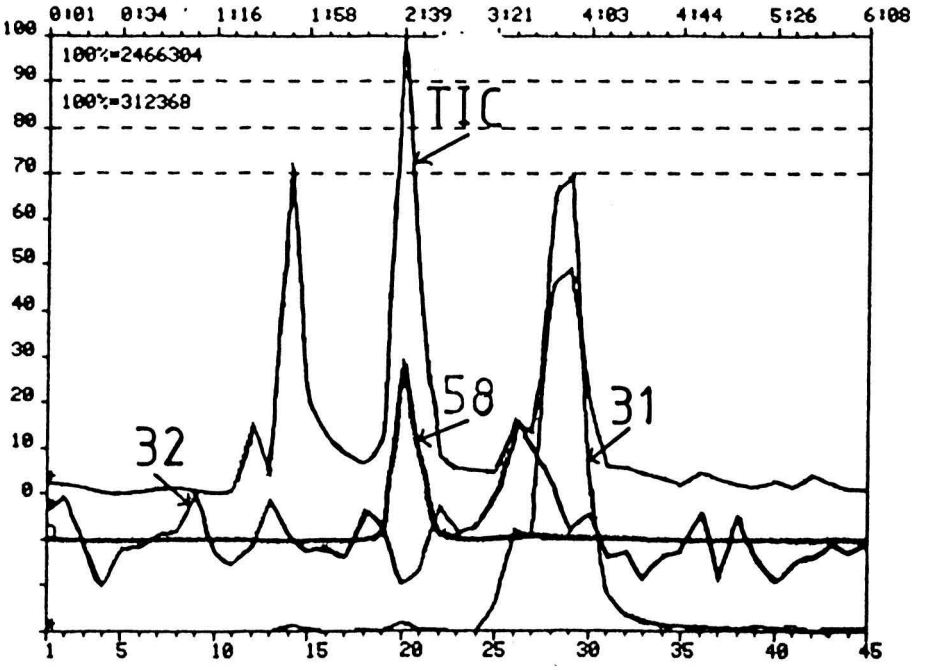


FIGURE 2.23: GC/MS Cross Scan Plot.

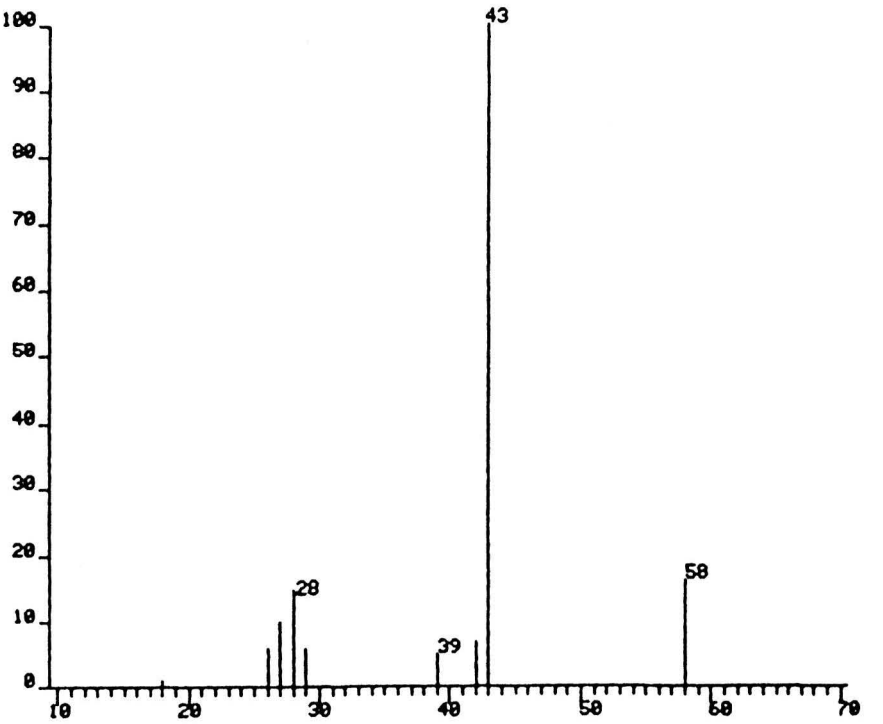


FIGURE 2.24: Factor Analysis Generated Spectrum: GC/MS Data, Component No.1.

are shown in figures. 2.24 to 2.26. These may be identified with propanone, ethanol, and air, respectively. In the present case, the third GC peak was, in fact, not a 'real' GC peak, but due to an air leak in the vacuum system.

## 2.5 Conclusions

It is most apparent that for factor analysis to be of use on a day-to-day basis as an aid to mixture analysis, then the importance of data pre-processing needs to be recognised.

The aspects of data pre-processing that need to be considered are:-

### (1) Normalisation.

Normalisation, (often referred to as 'pattern scaling'), is performed so as to eliminate effects, such as instrumental sensitivity, sample size, etc, which are of no analytical importance from the point of view of using factor analysis to identify the unknown components of mixtures. Simple normalisation, using the total ion current to scale the ion intensities, suffers from the disadvantage that very large peaks, especially if they exhibit a high degree of deviation, can over influence the total ion current, so that the smaller, perhaps statistically significant, mass peaks are undervalued. (see ref. 8, chapter six).

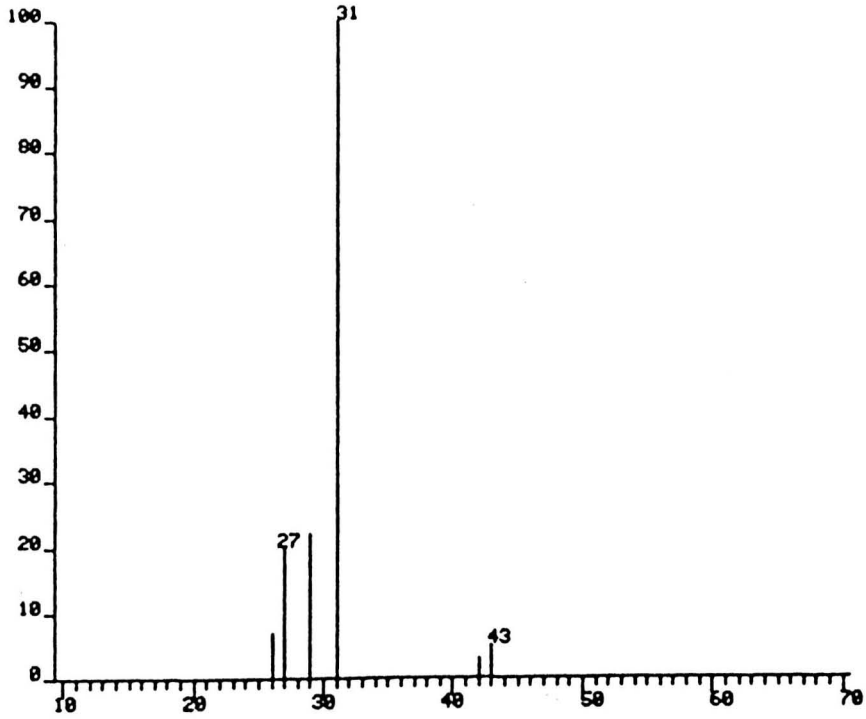


FIGURE 2.25: Factor Analysis Generated Spectrum: GC/MS Data, Component No.2.

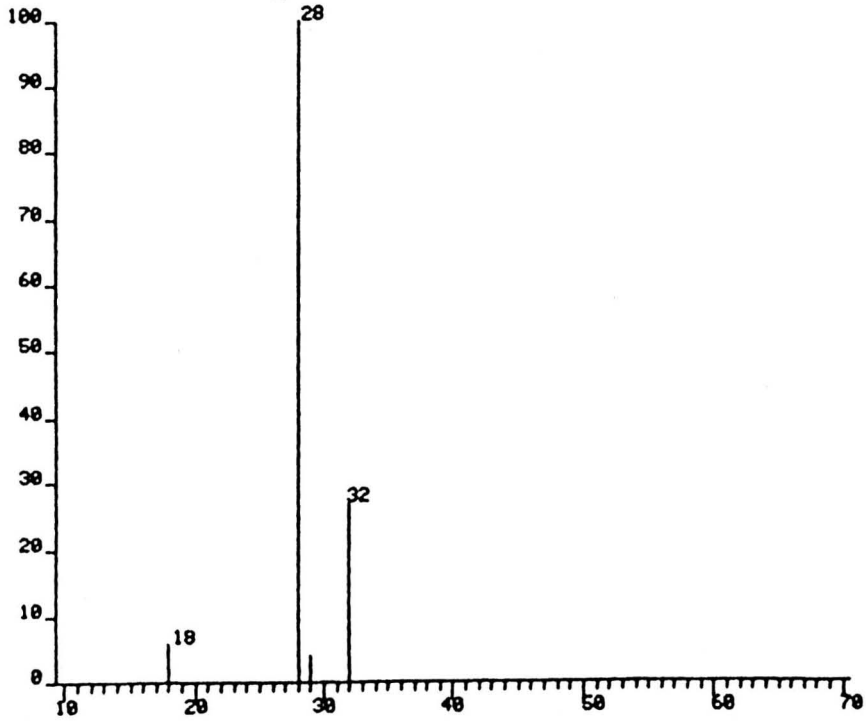


FIGURE 2.26: Factor Analysis Generated Spectrum: GC/MS Data, Component No.3.

(2) Feature scaling.

This is effectively a method that attempts to compensate for the fact that the statistically relevent mass peaks may have a small relative intensity, so that they require a statistical weighting. In other words one attempts to base the analysis of the data on the most reliable and most characteristic mass peaks rather than on the largest. (see ref. 29).

As well as these data pre-processing procedures, there are a number of closely related factor analysis techniques which could be incorporated into a suite of mixture analysis programs. Pattern recognition, as mentioned in the introduction, is an obvious example.

Factor analysis itself has a number of variations, the previously mentioned technique of target factor analysis, and also alternative methods of constructing the rotation matrix are of interest.

As an example of the latter variation on the factor analysis technique, Windig et. al. have devised a method of constructing the rotation matrix which does not require the presence of 'pure' mass peaks in the component compounds (30). This would have obvious advantages for the analysis of complex biological samples, for example, for which the condition of 'pure' mass peaks generally does not hold.

Finally, as most of the factor analysis software has been extensively used for the analysis of pyrolysis mass spectra, it seems likely that with little or no modification, its application to FAB mass spectrometry in particular, and mass spectrometry in general, should be relatively straight-forward.

## CHAPTER TWO: REFERENCES


1) Karrer, L. M., Gordon, H. L., Rothstein, S. M., Miller, J. M. & Jones, R. B., Anal. Chem., 55, 1723, (1983).

2) VanArendonk, M. D., Skogerboe, R. K. & Grant, C. L., Anal. Chem., 53, 2349, (1981).

3) Patkin, A. J. & Morrison, G. H., Anal. Chem., 54, 2, (1982).

4) Derde, M. P. & Massart, D. L., Z. Anal. Chem., 313, 484, (1982).

5) Eckschlager, K. & Stepanek, V., Anal. Chem., 54, 1115A, (1982).

6) Clerc, J. T., Z. Anal. Chem., 313, 480, (1983).

7) Figueras, J., Anal. Chim. Acta., 146, 29, (1983).

8) Meuzelaar H. L. C., Haverkamp, J. & Hileman, F. D., 'Pyrolysis Mass Spectrometry of Recent & Fossil Biomaterials; Compendium & Atlas', Elsevier, (1982).

9) Kowalski, B. R., & Bender, C. F., J. Amer. Chem. Soc., 94, 5632, (1972).

10) Rummel, R. J., "Applied Factor Analysis", Northwestern University Press, Evanston, III., (1970).

11) Slezer, R. B. & Howery, D. G., J. Chromatogr., 115, 139, (1975).

12) Weiner, P. H., Malinowsky, E. R. & Levinstone, A. R., J. Phys. Chem., 74, 4537, (1970).

13) Bulmer, J. T. & Shurvell, H. F., J. Phys. Chem., 77, 256, (1973).

14) Hugus Jr., Z. Z. & El-Awardy, J. Phys. Chem., 75, 2954, (1971).

15) Sharaf, M. A. & Kowalski, B. R., Anal. Chem., 53, 518, (1981).

16) Martens, H., Anal. Chim. Acta, 112, 423, (1979).

17) Lorber, A., Anal. Chem., 56, 1004, (1984).

18) Malinowski, E. R., Anal. Chim. Acta, 103, 339, (1978).

19) Rasmussen, G. T., Hohne, B. A., Weiboldt, R. C. & Isenhour, T. L., Anal. Chim. Acta, 112, 151, (1979).

20) Stoll, R. R., 'Linear Algebra and Matrix Theory', Mcgraw-Hill, (1952).

21) Malinowski, E. R., Anal. Chem., 49, 606, (1977).

22) Ritter, G. L., Lowry, S. R., Isenhour, T. L. & Wilkins, C. L., Anal. Chem., 48, 591, (1976).

23) Knorr, F. J. & Futrell, J. H., Anal. Chem., 51, 1236, (1979).

24) Malinowski, E. R., Anal. Chem., 49, 612, (1977).

25) Farncombe, M. J., Ph.D Thesis, University of Warwick, (1984).

26) Malinowski, E. R., Anal. Chim. Acta, 134, 129, (1982).

27) Farncombe, M. J., University of Warwick.

28) DS-55 Data System, Kratos Analytical, Barton Dock Rd., Manchester.

29) Eshuis, W., Kistemaker, P. G. & Meuzelaar, H. L. C., "Analytical Pyrolysis", Elsevier, Amsterdam, p151-166, (1977).

30) Windig, W. & Meuzelaar, H.L.C., Anal. Chem., 56, 2297, (1984).

# CHAPTER III

## MASS SPECTROMETRY OF ENGINE OIL FRACTIONS.

## 3.1 INTRODUCTION

The use of the mass spectrometer as an analytical instrument in commercial applications started in the late 1930's with its use in the petroleum industry, and is still in use throughout the petroleum industry today. In the intervening time, many innovations have developed in mass spectrometry, techniques such as Fourier Transform Mass Spectrometry; Fast Atom Bombardment; Chemical Ionisation; and Gas Chromatography/Mass Spectrometry. Industry has, however, been relatively slow in taking up these new techniques - many of the standard analytical techniques date from the mid 60's or earlier.

The analytical needs of the petroleum industry range from the analysis of crude oils and crude oil spills - yielding information for the geochemist and helping to minimise environmental polution, to the analysis of hydrocarbon composition of process streams and petroleum products - useful in following the effect of process variables, diagnosing plant upsets and in evaluating the effect of changes in composition on product performance. The mass spectrometer helps to provide this information on composition - and so is being applied to the analysis of the whole range of petroleum chemicals from crude oils to refinery products.

### 3.1.1 STRUCTURE OF PETROLEUM MOLECULES

Crude oil is a complex mixture of hydrocarbons, mainly alkanes, cycloalkanes, aromatic and polyaromatic in nature, with only trace amounts of alkenes and alkynes. (Large quantities of alkenes are produced, however, in refinery cracking processes). In addition, there

are trace amounts of organic compounds of sulphur, nitrogen, oxygen and organo-metallic compounds of transition metals, mainly titanium and manganese.

A typical crude oil contains tens of thousands of compounds. In such a sample, each of these compounds consists of essentially one long chain. In paraffin waxes, the molecules are mostly n-alkanes along with some slightly branched iso-alkanes, cycloalkanes and traces of aromatics. In lubricating oils, the iso-alkanes have slightly longer branches, and the monocycloalkanes and monoaromatics have several methyl groups on the ring. Lubricating oils may also have short branches at the opposite end of the long chain. Polyaromatics generally have all of their rings in a single nucleus, whilst polycycloalkanes may have ring systems at both ends of the chain (1-3). A summary of the main crude oil fractions is given in table 3.1.

Crude oils generally contain molecules of the steroid type - the so-called 'bio-markers', these compounds usually give rise to characteristic mass peaks which are easy to pick out from the smooth background distribution of peaks. The distribution of these bio-markers is often characteristic of crude oil from a particular source, and are the basis of some of the recent analyses of crude oil spillage.

The high boiling residues from crude oils contain coloured pigments which are related in structure to chlorophyll and the haem group. These are known as 'geoporphyrins' and occur in trace amounts as complexes of transition metals such as titanium. Studies of these compounds and the biomarkers provides valuable clues to the processes which are involved in the transformation of plant and animal material

TABLE 3.1: Main Crude Oil Fractions

| Fraction | Distillation Temp. / C | Carbon Number |
|---|---|---|
| Gas | Below 20 | C1-C4 |
| Petroleum ether | 20-60 | C5-C6 |
| Light naphtha | 60-100 | C6-C7 |
| Gasoline | 40-205 | C5-C10, and cyclo-alkanes |
| Kerosine | 175-325 | C12-C18, + aromatics |
| Gas oil | above 275 | C12 and higher |
| Lubricating oil | Non-volatile liquids | Long chains + cyclic structures |
| Asphalt | Non-volatile solids | Polycyclic structures |

into crude oil (4,5).

## MASS SPECTROMETRIC ANALYSIS OF ENGINE OILS

### QUANTITATIVE MASS SPECTRAL ANALYSIS

In the quantitative analysis of mixtures of organic materials using electron ionisation mass spectrometry, several assumptions are made:

(1) The mass spectrum of each chemical compound in the mixture is characteristic of that compound. This usually the case, but where compounds are similar, eg cis-2-butene and trans-2-butene, there may be insufficient differences in the spectrum to allow analysis. Obviously, as the complexity and relative molecular weight of the compound increases, this is more likely to be a problem.

(2) The sensitivity and cracking patterns are constant, as long as experimental conditions are maintained. The stability of the cracking pattern over time depends upon the condition of the source - such as the temperature of the filament and source housing, as well as spurious potential changes within the source due the deposition of insulating layers within the source.

Different regions of a spectrum may show greater or less than average fluctuations of the cracking pattern. For example, isotope peaks are generally quite reproducible, whilst fragment peaks which correspond to fragments where many hydrogens are stripped off may exhibit much greater variability.

The sensitivity of the instrument is also affected by source conditions in much the same way.

(3) Each component of the mixture behaves as if it were present alone. This asssumption is valid in electron ionisation mass spectrometry provided the sample pressure is not too high. At higher sample pressures the sample begins to undergo "self C.I.", where the pressure is sufficiently high for sample ions to participate in ion-molecule reactions - in other words chemical ionisation occurs. A more frequent cause of interference is due to the effect of certain kinds of sample on the filament; filament 'conditioning', usually alleviates this problem. Filament conditioning uses an unsaturated hydrocarbon sample to deposit tungsten carbide uniformly on the (tungsten) filament surface, thus protecting the filament.

(4) The measured ion intensities of the various components are proportional to the partial pressures in the sample reservoir. Here, one may have problems if the sample is difficult to volatilise, for example very high molecular weight petroleum samples are difficult to analyse even with use of all glass heated inlet systems which can be heated up to 350 $^{o}$C.

Despite the difficulties with these requirements, the quantitative analysis of complex mixtures using electron ionisation mass spectrometry is remarkably reliable.

The principle of linear additivity of peaks allows one to set up a system of linear equations, with the peak heights contributed by the individual components as the unknowns, the measured peak heights the constants, and the cracking pattern ratios multiplied by sensitivities as the coefficients. The calculation of the results is relatively straight-foward with today's computer technology. The difficult part of the procedure is the measurement of the cracking pattern ratios and sensitivities; and the choice of the 'best' peaks to use for the analysis. The measurement of the cracking pattern and sensitivities requires the use of sample of the pure compounds or the use of a standard mixture. The choice of what peaks to use in the calculation involves considerations of the pattern variability and possible impurity peaks as well as an attempt to use peaks which are monoisotopic or nearly so (6).

### 3.1.2 COMPOUND 'TYPE' ANALYSIS

When one is confronted with the analysis of mixtures of such complexity as crude oil fractions, it is obviously practically impossible to perform even a qualitative analysis of each particular compound. The only possible analysis is one that attempts to analyse the sample in terms of the classes of compounds present. The question

that then arises is how specific are compound classes for which one is to analyse?

Quantitative analysis of crude oil fractions and refinery products in terms of their aromatic, cycloalkane and alkane/alkene content can be achieved using high performance liquid chromatography, HPLC (12). This also has the advantage that preparative scale HPLC allows further analysis of these classes; ultimately LC/MS would be highly advantageous.

The use of electron impact mass spectrometry for the determination of compound classes, referred to as 'type' analysis, was first suggested by Brown (7) when he observed that the spectra of the principal compound classes, such as alkanes, cycloalkanes, cycloalkenes etc, could be quantitatively characterised by using sums of specific mass peaks for each class. Many different type analysis procedures now exist, a typical example, developed by Cook and Robinson (8), and the basis of ASTM method D3239, (9), analyses petroleum aromatics in terms of 21 compound classes, these are shown in table 3.2 It is important to note that the names given to the compounds in table 3.2 are those of compounds believed most likely to occur, and that the presence of other compounds of the same empirical formula is not excluded. In this method the sum of two series of masses is used for each compound type, the M+ series and the $(M-1)^+$ series, the $(M-1)^+$ intensities are corrected for their C-13 content. Overlap types are resolved using empirical relationships between the intensity of the (M-1)+ and M. Empirical adjustments are also made to the intensities at masses 175,176,189,190,200, and 213, which have anomalous intensities because they are due to the presence of the 'unusual' biomarker compounds.

TABLE 3.2: D3239 Compound Types

| CLASS | TYPE | FORMULAE |
|---|---|---|
| I | 0 | Alkylbenzenes, CnH2n-6 |
| I | 1 | Benzothiophenes, CnH2n-10S |
| I | 2 | Naphthenephenanthrenes, CnH2n-20 |
| II | 0 | Naphthenebenzenes, CnH2-8 |
| II | 1 | Pyrenes, CnH2n-22 |
| II | 2 | Unidentified |
| III | 0 | Dinaphthenebenzenes, CnH2n-10 |
| III | 1 | Chrysenes, CnH2n-24 |
| III | 2 | Unidentified |
| IV | 0 | Naphthalenes, CnH2n-12 |
| IV | 1 | Dibenzothiophenes, CnH2n-16S |
| IV | 2 | Unidentified |
| V | 0 | Acenaphthenes + dibenzofurans CnH2n-14 and CnH2n-16O |
| V | 1 | Perylenes, CnH2n-28 |
| V | 2 | Unidentified |
| VI | 0 | Fluorenes, CnH2n-16 |
| VI | 1 | Dibenzanthracenes, CnH2n-30 |
| VI | 2 | Unidentified |
| VII | 0 | Phenanthrenes, CnH2n-18 |
| VII | 1 | Naphthobenzothiophenes, CnH2n-22S |
| VII | 2 | Unidentified |

Calculations are carried out by the use of inverted matrices which are derived from ion intensity calibration sensitivities.

The extensive use of empirical relationships, including those implicit in the calibration procedure, means that type analysis procedures can only be applied to a limited range of samples. This range may be extended by providing several inverted matrices, for example the type analysis procedure for the analysis of gas-oil saturates fractions, (ASTM 2786, 10), ten inverse matrices are provided which are selected on the basis of the mean carbon number of the sample, and on the basis of an empirical test, designed to distinguish between predominantly n-alkane samples and predominantly iso-alkane samples.

Together with the procedures for separating oil fractions into their saturate and aromatic components (11,12), the above mentioned type analysis procedures, ASTM methods D3239 and D2786 provide detailed analysis of the hydrocarbon composition of gas-oil fractions.

As mentioned in the introduction, the 'type' analysis procedures date from the early 1960's, the calibration and empirical data were based upon the performance characteristics of the CEC 21-103 mass spectrometer. Use of the type analysis procedures on more modern mass spectrometers often requires that the operating parameters of the modern instrument are adjusted to be quite far from their optimum setting. The nature of this non-optimum tuning will be illustrated in the following section.

## 3.2 PRELIMINARY EXPERIMENTS ON THE MS-80 MASS SPECTROMETER

In any quantitative analysis in mass spectrometry it is important to ensure the reproducibility of the experimental procedures involved in the analysis. For "type-analysis" the reproducibility of the analysis is based upon the attainment of standard source conditions such that the cracking pattern of an n-hexadecane sample is reproduced within certain limits. The criteria used to measure the cracking pattern are the ratio of the intensities at m/z = 127 to the intensity at m/z = 226, and the ratio S(69)/S(71), defined such that:-

$$S(69) = I(69) + I(83) + I(97) + I(111) + I(125) + I(139)$$

and

$$S(71) = I(71) + I(85) + I(99) + I(113)$$

The standardisation procedure calls for the I(127)/I(226) ratio to be in the range 1.40 to 1.54, and the S(69)/S(71) ratio to in the range 0.18 to 0.22, although it is has been found that it is often not possible to obtain values of the above ratio greater than 0.18 under normal conditions (13).

The I(127)/I(226) ratio is a measure of the molecular ion fragmentation, and depends upon the interplay between the ion residence time in the source and the source temperature. As the ion repeller voltage is increased, this should decrease the ion residence time. Thus by adjusting the ion repeller voltage and the source temperature it

is usually possible to tune the source operating conditions to the required I(127)/I(226) ratio. We would expect the I(127)/I(226) to be approximately inversely proportional to the ion repeller voltage, and proportional to the source temperature.

The other parameter, S(69)/S(71), is a rough measure of the degree of thermal degradation which the sample undergoes, so that we should expect this ratio to follow roughly an inverse relationship to that of the I(127)/I(226) ratio as functions of ion repeller voltage and source temperature.

A number of experiments were carried out on the MS-80 mass spectrometer to investigate the behaviour of these ratios as functions of ion repeller voltage and source temperature, as well as other parameters, such as sample pressure.

Three main ways of sample introduction are available on the MS-80 which are of interest for the introduction of oil samples. They are the direct insertion probe, the 'liquid' probe (also referred to as the 'gas' probe), and the GC interface. Results of initial experiments with the liquid probe were unpromising. The n-hexadecane samples were sufficiently involatile to require excessive heating of the liquid probe in order to obtain reasonable source pressures. It was also found difficult to remove excess sample from the probe. It required one - two hours to remove the excess sample, and it was found that the sample had a tendency to condense on the cooler parts of the instrument, so introducing large backgrounds for several hours. In view of these drawbacks, and the fact that 'real' samples are likely to of a much higher average molecular weight all experiments utilizing the liquid probe were suspended.

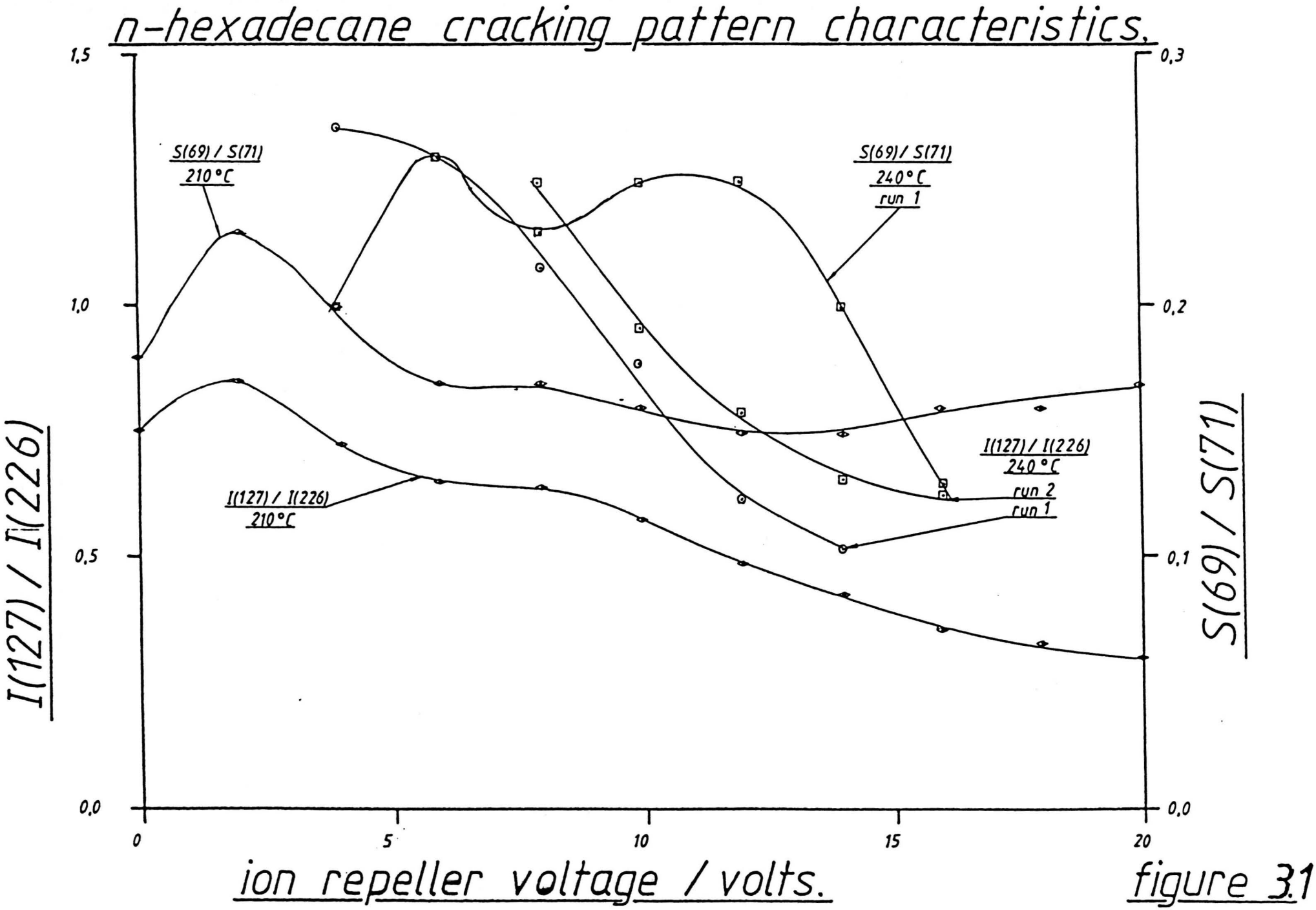
n-hexadecane cracking pattern characteristics.
S(69) / S(71)
210 °C
S(69) / S(71)
240 °C
run 1
I(127) / I(226)
240 °C
run 2
run 1
I(127) / I(226)
210 °C
I(127) / I(226)
S(69) / S(71)
1,5
1,0
0,5
0,0
0,3
0,2
0,1
0,0
0
5
10
15
20
ion repeller voltage / volts.

figure 3.1

# n-hexadecane cracking pattern characteristics.

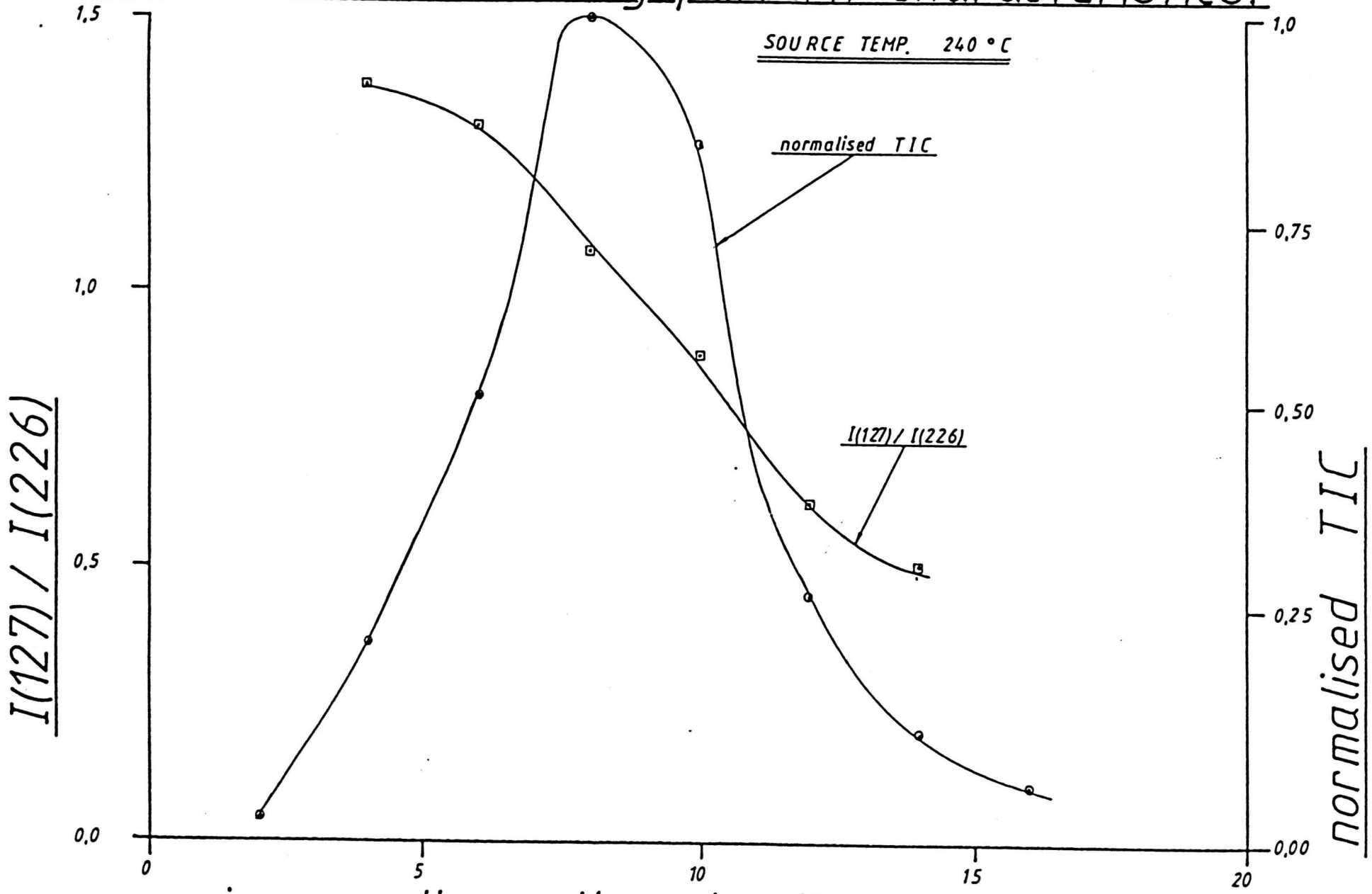


figure 3.2

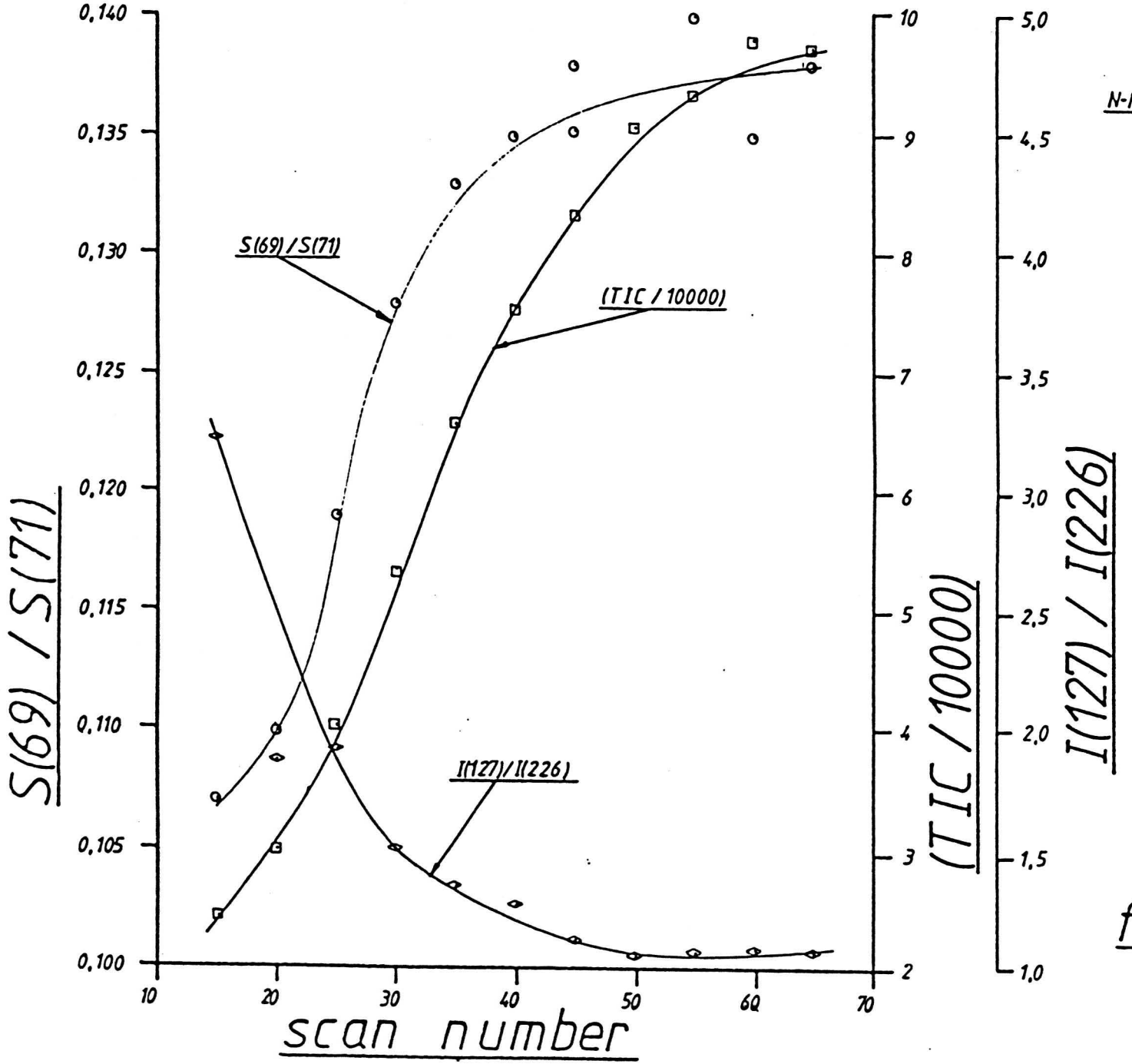
N-HEXADECANE CRACKING PATTERN
CHARACTERISTICS
source temp. 220°C
S(69) / S(71)
(TIC / 10000)
I(127) / I(226)
S(69) / S(71)
(TIC / 10000)
I(127) / I(226)
scan number
0,140
0,135
0,130
0,125
0,120
0,115
0,110
0,105
0,100
10
9
8
7
6
5
4
3
2
5,0
4,5
4,0
3,5
3,0
2,5
2,0
1,5
1,0
10
20
30
40
50
60
70

figure 3.3

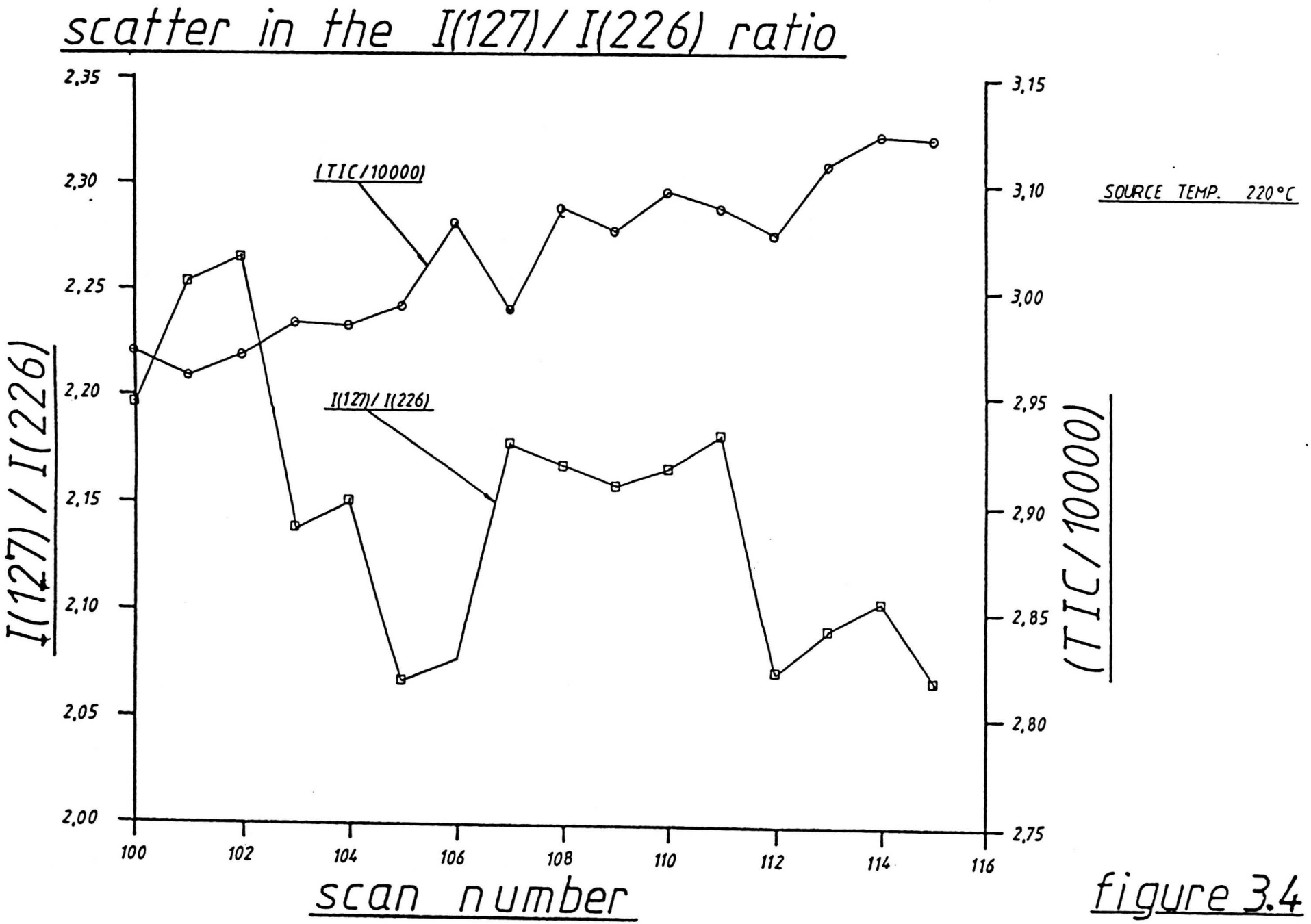
scatter in the I(127)/I(226) ratio
(TIC/10000)
I(127)/I(226)
SOURCE TEMP. 220°C
I(127) / I(226)
(TIC/10000)
2,35
2,30
2,25
2,20
2,15
2,10
2,05
2,00
3,15
3,10
3,00
2,95
2,90
2,85
2,80
2,75
100
102
104
106
108
110
112
114
116
scan number

figure 3.4

The experiments quoted here, have made use of the direct insertion probe. This has the advantage of ease of use, but one is not able to keep the sample pressure steady enough for quantitative analysis. However the 'DIP' has provided some useful preliminary data on the behaviour of the n-hexadecane cracking pattern on the MS-80. Typical results are shown in the diagrams (fig. 3.1 - 3.4). Figure 3.1 shows the ratios I(127)/I(226) and S(69)/S(71) as functions of ion repeller voltage and source temperature. The ratios show the expected functionality, and also it is apparent that the desired I(127)/I(226) ratio range is attainable, although at a higher source temperature than is the usual practice. The need for an alternative sample introduction system is illustrated in figures 3.3 and 3.4. Here we see that both the ratios are strongly dependent upon the sample pressure (it is assumed that the TIC - total ion current - is a measure of the sample pressure). It is also evident that the ratios fluctuate greatly from scan to scan.

As an alternative to the direct insertion probe, it is feasible to connect a heated glass bulb to the GC inlet system. This allows the sample at a moderate stagnation pressure to leak into the jet separator region of the GC interface. A separate pump-out line allows excess sample to be removed. This does, however, have the disadvantage that the GC interface could become contaminated, this would be especially troublesome when oil samples are used. In view of this problem, this technique of sample introduction was not used.

One may interpret the results displayed in figure 3.2, as showing the relative sensitivity of the mass spectrometer, if we equate relative sensitivity with the ratio TIC / TIC(max). If one recalls that the

type-analysis calibration procedure requires that the ratio I(127)/I(226) is in the range 1.4 - 1.54, one can see that the performance of the mass spectrometer is far from optimum; in this case, the mass spectrometer is operating at only about 20% of its optimum sensitivity.

It would be quite straightforward to update the type analysis procedures by using new calibration data taken from more modern mass spectrometers. This would not, however, take advantage of any of the new analytical techniques in mass spectrometry, nor would it take advantage of the advances that have been made in data processing.

## 3.3 FACTOR ANALYSIS APPLIED TO THE ANALYSIS OF ENGINE OIL FRACTIONS

The use of factor analysis, and related procedures, for the analysis of mixtures in terms of compound types does not occur very much in the chemical literature.

In an attempt to utilise the factor analysis program available at the ESSO RESEARCH CENTRE, ABINGDON, a short data preparation program was written to compress mass spectrometry data from engine oil samples into the mass groups as used in the conventional 'type' analysis procedures. These mass groups where then used as the data for the factor analysis program. The mass groups used are shown in table 3.3

The samples used for this analysis are shown in table 3.4, with the corresponding 'type' analysis results given in appendix A.

In using the factor analysis program in this way the assumption is that the characteristic compound types will have characteristic mass

TABLE 3.3: Mass Groups For

Factor Analysis

| GROUP | SUMMATION SERIES |
|---|---|
| 1 | Total Alkane (M-1)+ |
| 2 | Total 1-ring (M-1)+ |
| 3 | Total 2-ring (M-1)+ |
| 4 | Total 3-ring (M-1)+ |
| 5 | Total 4-ring (M-1)+ |
| 6 | Total 5-ring (M-1)+ |
| 7 | Total 6-ring (M-1)+ |
| 8 | Alkane M+ to M/Z=170 |
| 9 | 1-Ring M+ to M/Z=196 |
| 10 | 2-Ring M+ to M/Z=208 |
| 11 | 3-Ring M+ to M/Z=220 |
| 12 | 4-Ring M+ to M/Z=232 |
| 13 | 5-Ring M+ to M/Z=244 |
| 14 | 6-Ring at M/Z=270 |
| 15 | D2786 Alkane |
| 16 | D2786 1-ring |
| 17 | D2786 2-ring |
| 18 | D2786 3-ring |
| 19 | D2786 4-ring |
| 20 | D2786 5-ring |
| 21 | D2786 6-ring |
| 22 | D2786 Mono-aromatics |
| 23 | D3239 class I |
| 24 | D3239 class II |
| 25 | D3239 class III |
| 26 | D3239 class IV |
| 27 | D3239 class V |
| 28 | D3239 class VI |
| 29 | D3239 class VII |

TABLE 3.4: Samples For Factor Analysis

(All are aromatic fractions)

| NO. | SAMPLE | COMMENT |
|---|---|---|
| 1 | m-Xylene | |
| 2 | G4 | |
| 3 | G5 | |
| 4 | G6 | High in naphthalenes |
| 5 | G7 | |
| 6 | G8 | |
| 7 | G9 | high in naphthalenes, phenanthrenes and fluorenes |
| 8 | G10 | High in phenanthrenes and fluorenes |
| 9 | G11 | |
| 10 | G3B | |

group patterns, and will have most of their ion intensity in one particular mass group. This would be analogous to a normal mass spectrum with one 'pure' peak in the case of a specific compound.

One draw-back of using this factor analysis program is that almost by definition it will be unable to resolve 'overlap' types, i.e. it will not resolve into separate compound types those compound types which all give their major ion intensity in the same mass group.

The factor analysis was carried out on a variety of different combinations of sample spectra. As with conventional type analysis, the samples consisted of oil fractions which had been separated into an aromatic fraction and a saturates fraction either by elution chromatography or HPLC. The factor analysis program used data corresponding to the following cases:

(1) All aromatic samples.

(2) All saturates samples.

(3) A mixture of saturate and aromatic samples.

(4) successive spectra from one aromatic or one saturate sample taken from runs using a direct insertion probe for sample introduction.

The results of the factor analysis program applied to the mass group data were not encouraging. A typical example is illustrated in table 3.5 and table 3.6, the latter gives the factor analysis results and the former the mass group data.

From appendix A, it will be observed that the 'type' analysis results for samples 7 and 8 show high concentrations of phenathrenes and fluorenes, whilst sample 4 is high in naphthalenes. Now the factor

# Table 3.5: Mass group data for factor analysis

| MIX. No. :- | | 1 | 2 | 3 | 4 | 5 | 6 | 7 | 8 | 9 | 10 |
|---|---|---|---|---|---|---|---|---|---|---|---|
| GROUP No. | V | | | | | | | | | | |
| 1 | 1 | 0.0 | 0.0 | 0.0 | 0.0 | 0.0 | 0.0 | 0.0 | 0.0 | 0.0 | 0.0 |
| 2 | 2 | 0.0 | 0.0 | 0.0 | 0.0 | 0.0 | 0.0 | 0.0 | 0.0 | 0.0 | 0.0 |
| 3 | 3 | 0.0 | 0.0 | 0.0 | 0.0 | 0.0 | 0.0 | 0.0 | 0.0 | 0.0 | 0.0 |
| 4 | 4 | 0.0 | 0.0 | 0.0 | 0.0 | 0.0 | 0.0 | 0.0 | 0.0 | 0.0 | 0.0 |
| 5 | 5 | 0.0 | 0.0 | 0.0 | 0.0 | 0.0 | 0.0 | 0.0 | 0.0 | 0.0 | 0.0 |
| 6 | 6 | 0.0 | 0.0 | 0.0 | 0.0 | 0.0 | 0.0 | 0.0 | 0.0 | 0.0 | 0.0 |
| 7 | 7 | 0.0 | 0.0 | 0.0 | 0.0 | 0.0 | 0.0 | 0.0 | 0.0 | 0.0 | 0.0 |
| 8 | 8 | 0.0 | 3.2 | 3.6 | 96.0 | 6.4 | 6.2 | 1.2 | 7.4 | 3.8 | 4.0 |
| 9 | 9 | 0.0 | 5.4 | 7.7 | 4.5 | 10.7 | 4.8 | 10.7 | 8.8 | 3.1 | 8.3 |
| 10 | 10 | 0.0 | 1.5 | 2.7 | 0.4 | 4.1 | 2.5 | 14.3 | 14.2 | 1.5 | 2.5 |
| 11 | 11 | 0.0 | 0.5 | 0.9 | 0.0 | 1.1 | 0.9 | 3.5 | 9.6 | 0.5 | 0.7 |
| 12 | 12 | 0.0 | 1.1 | 1.8 | 2.4 | 1.9 | 2.3 | 11.9 | 16.0 | 1.1 | 1.3 |
| 13 | 13 | 0.0 | 0.3 | 0.4 | 0.0 | 0.6 | 1.7 | 2.3 | 3.0 | 0.2 | 0.3 |
| 14 | 14 | 0.0 | 0.1 | 0.2 | 0.0 | 0.3 | 0.7 | 0.7 | 0.8 | 0.1 | 0.1 |
| 15 | 15 | 0.0 | 13.4 | 17.4 | 0.2 | 17.2 | 12.3 | 0.1 | 5.2 | 9.3 | 19.0 |
| 16 | 16 | 0.0 | 29.0 | 36.1 | 0.0 | 45.9 | 27.7 | 0.1 | 10.9 | 17.6 | 40.3 |
| 17 | 17 | 0.0 | 8.5 | 11.7 | 0.0 | 14.4 | 8.7 | 1.8 | 22.7 | 6.0 | 12.3 |
| 18 | 18 | 0.0 | 3.8 | 6.5 | 0.0 | 6.6 | 2.9 | 2.1 | 42.4 | 2.5 | 4.7 |
| 19 | 19 | 0.0 | 5.4 | 6.9 | 0.0 | 10.2 | 4.3 | 0.6 | 25.8 | 5.4 | 6.6 |
| 20 | 20 | 0.0 | 2.9 | 3.0 | 0.0 | 5.4 | 5.2 | 0.1 | 2.5 | 3.1 | 3.4 |
| 21 | 21 | 0.0 | 1.9 | 2.0 | 0.0 | 4.6 | 3.7 | 0.0 | 0.1 | 2.3 | 2.4 |
| 22 | 22 | 6.2 | 92.6 | 90.4 | 19.5 | 86.3 | 100.0 | 0.6 | 13.0 | 91.9 | 93.9 |
| 23 | 23 | 100.0 | 100.0 | 100.0 | 34.8 | 100.0 | 92.3 | 19.9 | 64.2 | 100.0 | 100.0 |
| 24 | 24 | 0.0 | 41.2 | 42.3 | 47.2 | 56.5 | 76.6 | 7.8 | 37.0 | 39.8 | 44.6 |
| 25 | 25 | 0.0 | 22.1 | 23.5 | 5.0 | 37.5 | 42.9 | 2.6 | 11.4 | 22.5 | 26.5 |
| 26 | 26 | 0.0 | 18.1 | 21.9 | 100.0 | 35.8 | 28.2 | 46.2 | 45.9 | 18.2 | 21.5 |
| 27 | 27 | 0.0 | 9.5 | 11.9 | 4.5 | 21.3 | 14.1 | 34.4 | 29.3 | 7.9 | 10.9 |
| 28 | 28 | 0.0 | 7.3 | 10.4 | 0.3 | 15.7 | 10.0 | 32.3 | 35.5 | 5.5 | 9.0 |
| 29 | 29 | 0.0 | 5.5 | 11.8 | 0.0 | 11.1 | 6.1 | 100.0 | 100.0 | 3.3 | 7.1 |

TABLE 3.6A: Factor Analysis Results:
'Spectra'

| MIX NO. :- | 1 | 2 | 3 | 4 | 5 | 6 |
|---|---|---|---|---|---|---|
| GROUP NO. V | | | | | | |
| 1 | 0 | 0 | 0 | 0 | 54 | 0 |
| 2 | 0 | 0 | 0 | 0 | 53 | 0 |
| 3 | 0 | 0 | 0 | 0 | 52 | 0 |
| 4 | 0 | 0 | 0 | 0 | 100 | 0 |
| 5 | 0 | 0 | 0 | 0 | 92 | 0 |
| 6 | 0 | 0 | 0 | 0 | 74 | 0 |
| 7 | 0 | 0 | 0 | 0 | 63 | 0 |
| 8 | 100 | 0 | 0 | 0 | 0 | 0 |
| 9 | 1 | 0 | 0 | 9 | 0 | 7 |
| 10 | 0 | 0 | 0 | 14 | 0 | 1 |
| 11 | 0 | 0 | 0 | 8 | 0 | 0 |
| 12 | 0 | 0 | 0 | 15 | 0 | 0 |
| 13 | 0 | 2 | 0 | 3 | 0 | 0 |
| 14 | 0 | 1 | 0 | 1 | 0 | 0 |
| 15 | 0 | 0 | 48 | 2 | 0 | 17 |
| 16 | 0 | 0 | 100 | 4 | 0 | 38 |
| 17 | 0 | 0 | 1 | 15 | 0 | 10 |
| 18 | 0 | 0 | 6 | 29 | 0 | 2 |
| 19 | 0 | 0 | 36 | 17 | 0 | 6 |
| 20 | 0 | 5 | 0 | 1 | 0 | 3 |
| 21 | 0 | 4 | 0 | 0 | 0 | 2 |
| 22 | 0 | 0 | 0 | 0 | 0 | 89 |
| 23 | 13 | 0 | 0 | 39 | 0 | 100 |
| 24 | 40 | 100 | 0 | 22 | 0 | 32 |
| 25 | 0 | 59 | 0 | 6 | 0 | 22 |
| 26 | 92 | 0 | 0 | 39 | 0 | 15 |
| 27 | 0 | 0 | 0 | 30 | 0 | 9 |
| 28 | 0 | 0 | 0 | 34 | 0 | 7 |
| 29 | 0 | 0 | 0 | 100 | 0 | 0 |

TABLE 3.6B: Factor Analysis Results:
'Concentrations'

| FACTOR :- | 1 | 2 | 3 | 4 | 5 | 6 |
|---|---|---|---|---|---|---|
| MIX NO. V | | | | | | |
| 1 | 6 | 0 | 0 | 56 | 0 | 38 |
| 2 | 2 | 7 | 0 | 22 | 0 | 70 |
| 3 | 2 | 7 | 0 | 27 | 0 | 64 |
| 4 | 81 | 1 | 0 | 0 | 0 | 18 |
| 5 | 5 | 8 | 0 | 30 | 0 | 57 |
| 6 | 4 | 10 | 0 | 17 | 0 | 69 |
| 7 | 17 | 0 | 3 | 59 | 0 | 20 |
| 8 | 4 | 0 | 0 | 87 | 0 | 8 |
| 9 | 3 | 6 | 0 | 18 | 0 | 74 |
| 10 | 2 | 8 | 0 | 25 | 0 | 66 |

analysis results do show factor spectra which may be attributed to 'naphthalenes' (factor 1) and to 'phenanthrenes' (factor 4), also these factors are high in the relavent mixtures spectra. However, exactly what chemical significance we are to attach to these results it is difficult to say. Certainly the 'concentrations' produced by the factor analysis program only compare with the standard type analysis results in a very approximate fashion - the factor analysis results for example appear to suggest that all of the mixtures contain significant concentrations of phenanthrenes, just how approximate the identification of factor 4 to the chemical type 'phenanthrenes' is can be seen when we observe that 56% of mixture 1 is attributed to factor 4, mixture 1 was in fact, pure m-xylene.

An examination of the original mass group data yields as much information as the results of the factor analysis program when we attribute to each mass group the principal compound type we would expect to contribute most to that group.

It may also be mentioned here that in those factor analysis runs in which both aromatic and saturates samples where included, no conclusive separation into aromatic and non-aromatic components was achieved by the program. This illustrates the failing of the program where 'overlap' types are concerned as aromatics and saturates would be severe cases of mutual overlap - which is the reason that conventional type analysis requires the separation of the oil samples by HPLC into their aromatic and saturate components.

### 3.3.1 CONCLUSIONS: CHEMOMETRICS AND TYPE ANALYSIS

The conclusions which may be gained from the above experiments in some respects parallel those made in chapter 2. The summation of mass peaks into mass groups had two purposes. The main purpose was to manipulate the raw data into a form most appropriate to the analysis in terms of chemical compound TYPES. A secondary, but still very important purpose, was to enable significant data compression to take place. One of the main reasons for the poor performance of the factor analysis program is due to the simplicity of this data preparation step. A more sophisticated pre-anlysis of the data may be possible.

Virtually all of the chemical literature (14 - 19) that has considered the use of chemometrics for the analysis of compound types has been aimed at the classification of pure compounds into one of several chemical classes. Generally pattern recognition techniques are used with a 'training' set of chemical compounds to define the class structure to which specific 'unknown' compounds are to be classified.

It may be possible to use similar techniques to perform type analysis of mixtures. Pattern recognition may be used to define the class structure, in effect define the target vectors, and factor analysis may be used to decompose the mixture data in terms of these target vectors. Problems may arise because some pattern recognition procedures require that non-linear transformations are carried out on the data (for example the use of binary encoded spectra, where a mass channel can have either the value 0 or 1, is often used (20) ). The mixture data could not then be resolved in terms of the concentrations

of compound types since this requires that the mixture data is a concentration-weighted linear combination of the data for the 'pure' classes.

In conclusion, the application of factor analysis to chemical type analysis of mixtures does seem to offer some prospect of yielding useful results, given the sophistication and number of factor analysis and related techniques that are now avialable. However, oil fractions, being at the same time extremely complex and relatively chemically homogeneous, do present a very large problem, and it is doubtful that this particular problem will easily be tackled.

## 3.3 METASTABLE IONS AND COLLISION INDUCED DECOMPOSITION

In a conventional mass spectrum, occasionally one observes low intensity, broad, diffuse peaks, often at non-integral mass. The origin of these peaks are the so-called 'metastable ions'. These are fragment ions which are produced by fragmentations which occur within a field free region after the 'parent' ion has left the source, but before the ion reaches the detector.

In order for the metastable ions to be detected at a discrete mass, they must be produced by fragmentations which occur in either the first field free region, or the second field free region of the mass spectrometer. Fragmentations which occur within the magnetic analyser or the electric sector produce metastable ions which are detected as a continuum throughout an extended mass range. The most commonly observed metastable ions are produced in the first field free region, i.e.

between the acceleration region and the electric sector (21).

The metastable ions which appear in a mass spectrum appear at an apparent mass, $M^*$, which is related to both the parent mass, $M_1$, and the daughter mass, $M_2$:-

$$M^* = M_2^2/M_1$$

It is for this reason that the study of metastable ions finds use in the analysis of mixtures and unknown organic compounds. Of a more fundamental nature, metastable ion studies also yield information on reaction mechanisms of ions in the ion source.

For those compounds or mixtures which display few or no peaks arising from metastable ions, the technique of collision induced dissociation may be used (22). In this technique, a buffer gas is passed into a collision cell in first field free region. The ion beam from the source passes through this cell, and some of the ions undergo collision induced fragmentation.

In the analysis of an unknown compound, metastable transitions or collision induced transitions may occur which are characteristic of particular functional group or groups, thus giving additional information about the chemical nature of the sample.

The use of collision induced decomposition techniques for the analysis of complex mixtures usually involves the use of soft ionisation techniques, such as chemical ionisation. Chemical ionisation produces a spectrum which consists, in favourable cases, mainly of molecular ions - giving information about the relative concentrations of each of the compounds in the mixture and their relative molecular weights. As no

fragmentation ions are produced, no information is available to allow one to identify these compounds. When, however, the collision gas is present, the collisionally induced fragment ions provide this structural information. It is important to note, that this technique for analysis of complex mixtures requires that the molecular ions are singlet peaks, i.e. a mixture of isomeric compounds could not be analysed unless the ionisation technique used gives rise to a different pseudo-molecular ion for each of the isomers in the mixture.

The normal operating conditions for a double focusing mass spectrometer are not optimum for the observation and analysis of ions due to metastable or collision induced fragmentation ions. A number of operating procedures are possible, including linked scans and metastable mapping (to be discussed below).

Other types of mass spectrometer may be more suited to the study of metastable/collision induced fragmentation of ions, instruments such as the FTMS machines and multiple sector instruments mentioned in chapter 1, (see also section 4.11, below).

### 3.3.1 METASTABLE MAPS

Early workers studying the metastable and collision induced decomposition of ions used techniques that attempted to map out all the metastable transitions occurring in the B-E or B-V plane i.e. as a function of magnetic field and electric sector voltage, or magnetic field strength and acceleration voltage (23, 24, 25). Recently this technique has regained favour, especially as alternative methods of presentation of the data make interpretation easier. In the method used

at the University of Warwick the B-E plane is scanned in a manner similar to that used by Kiser (23). The procedure originally developed at Warwick for use on the MS-50 (26, 27), can also be used on the MS-80 using a programmable voltage supply as a reference source for the electric sector. The programmable voltage supply is under software control from the DS-55 data system. In the earlier work reported here, the data system incorporated a Data General NOVA II computer, in later work, this was replaced by a Data General ECLIPSE S120 computer.

In acquiring metastable map data the magnetic field of the instrument is scanned in the normal way; however, the electric sector voltage is decremented by a constant fraction of the original voltage $E_o$.

If an ion $m_1^+$ undergoes a metastable transition to give the ion $m_2^+$ in the first field free region, i.e. before the magnetic sector, the $m_2^+$ ion will retain the velocity, $v_1$, of the $m_1^+$ ion. The $m_2^+$ ion will be transmitted at a lower magnetic field, $B^*$, and will appear at an apparent mass $m^*$ :-

$$(B^*Re)^2 = (m_2 v_1)^2$$
$$= 2m^*Ve = 2m^* m_1 v_1^2/2$$
$$= m^* m_1 v_1^2$$

from which:-

$$m^* = m_2^2/m_1$$

This equation is valid if effects due to energy release are relatively small. Where kinetic energy release is important, this leads to a broadening of the observed peak and to changes in the peak shape

depending upon the kinetics of the fragmentation. Studies of the kinetic energy release are important in themselves as they yield information about the kinetics of the fragmentation process.

Using the above equations in conjunction with the equation:-

$$E/E_0 = m_2/m_1$$

it is possible to process the acquired scans and display them as metastable maps with the parent ion mass and daughter ion mass as dependent and independent variables respectively. Additionally, it is possible to display a three dimensional projection which gives not only the positions of the metastable transitions, but also their relative intensities.

An alternative style of presentation is possible for metastable map data, this is to simulate various types of linked scans. Three types of simulated scan are possible, they are, the 'daughter scan', the 'parent scan' and the 'constant neutral loss scan'. All these simulated scans are displayed as intensity versus mass/charge ratio similar to conventional mass spectra.

The 'daughter scan' gives the intensities of all daughter ions, $M_2^+$, from a given parent ion, $M_1^+$.

Similarly, the 'parent scan' gives all parent ions which contribute to a given daughter ion.

In the 'constant neutral loss scan', as the name implies, all ions which arise from a fragmentation in which a neutral fragment of given mass, $M_n$, is lost, are displayed. The independent variable can be either $M^*$, $M_1$ or $M_2$.

PAGE NUMBERING AS ORIGINAL

# n-hexadecane metastable map.

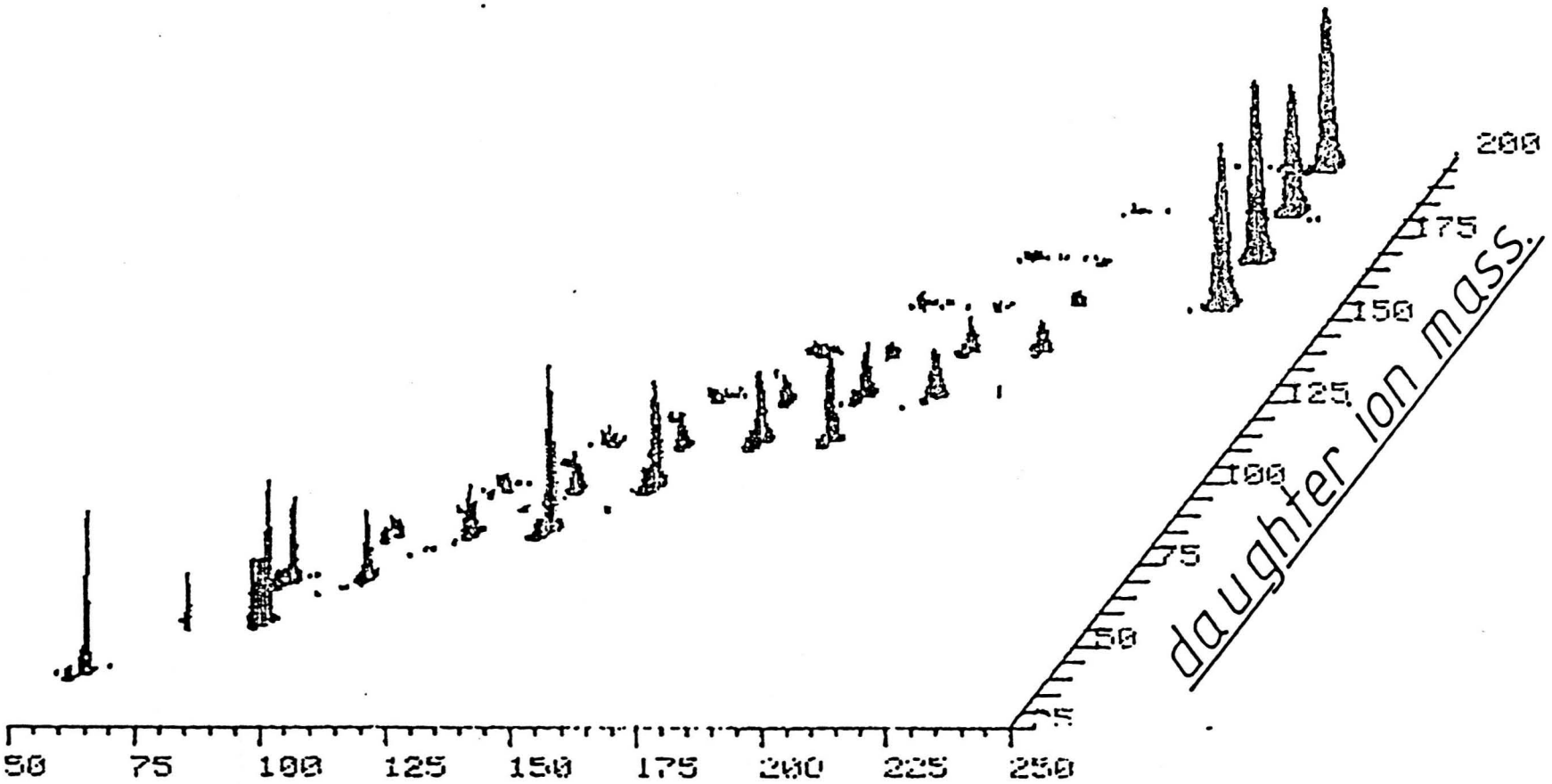


figure 3.5

# n-hexadecane: EI Spectrum

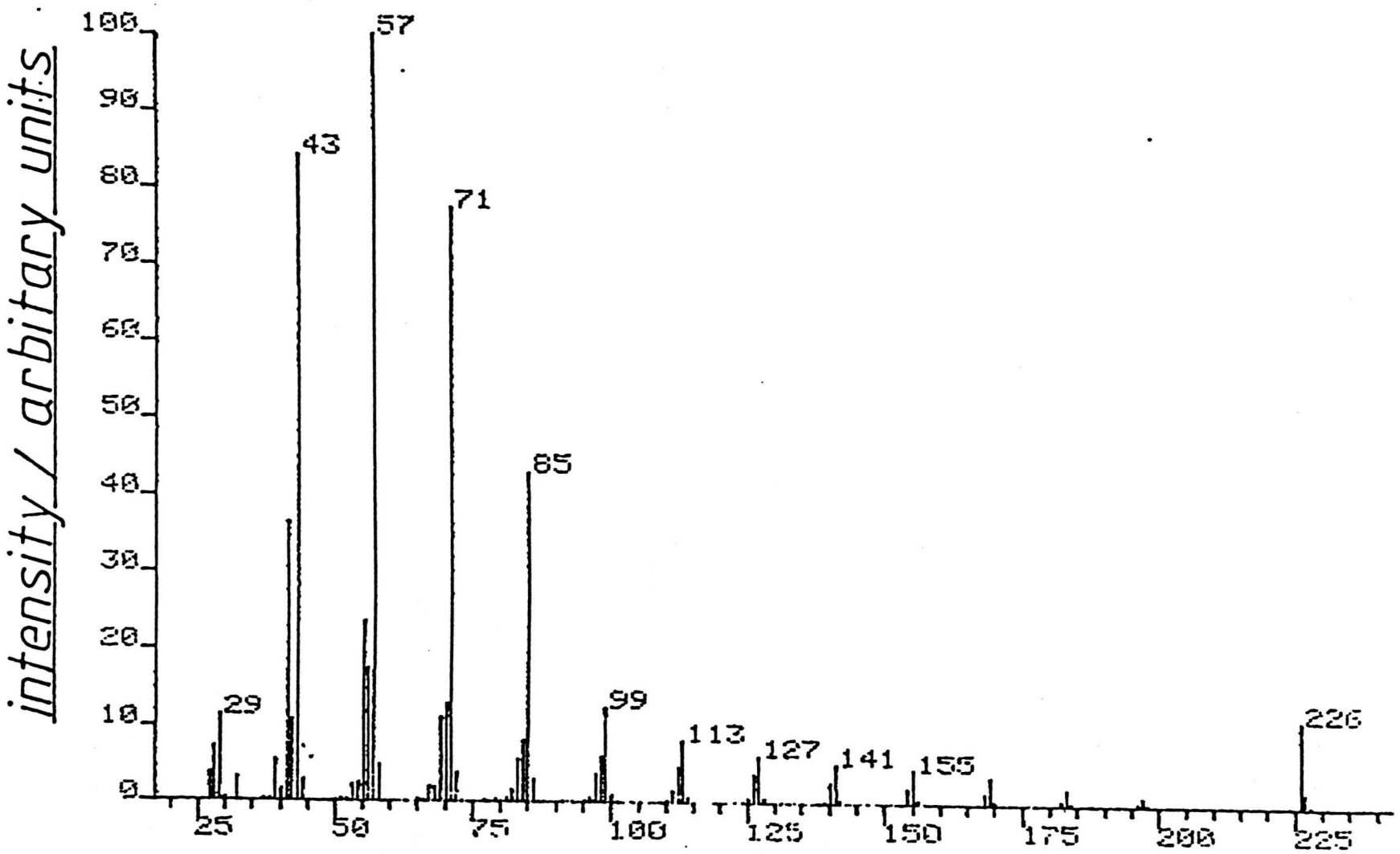


Figure 3.5b

metastable map.

Sample: G1

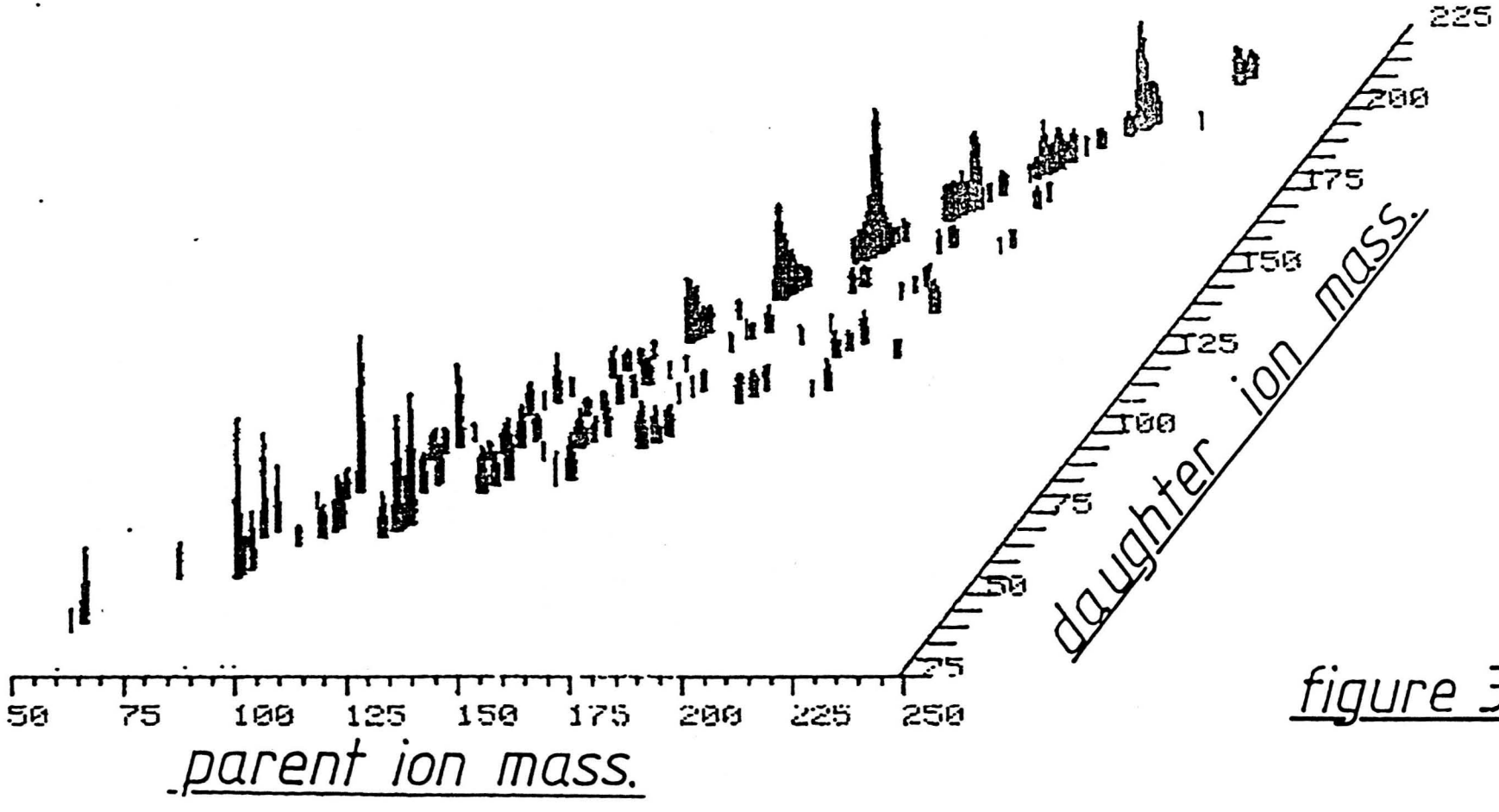


figure 3.6

# EI Spectrum: Sample G1

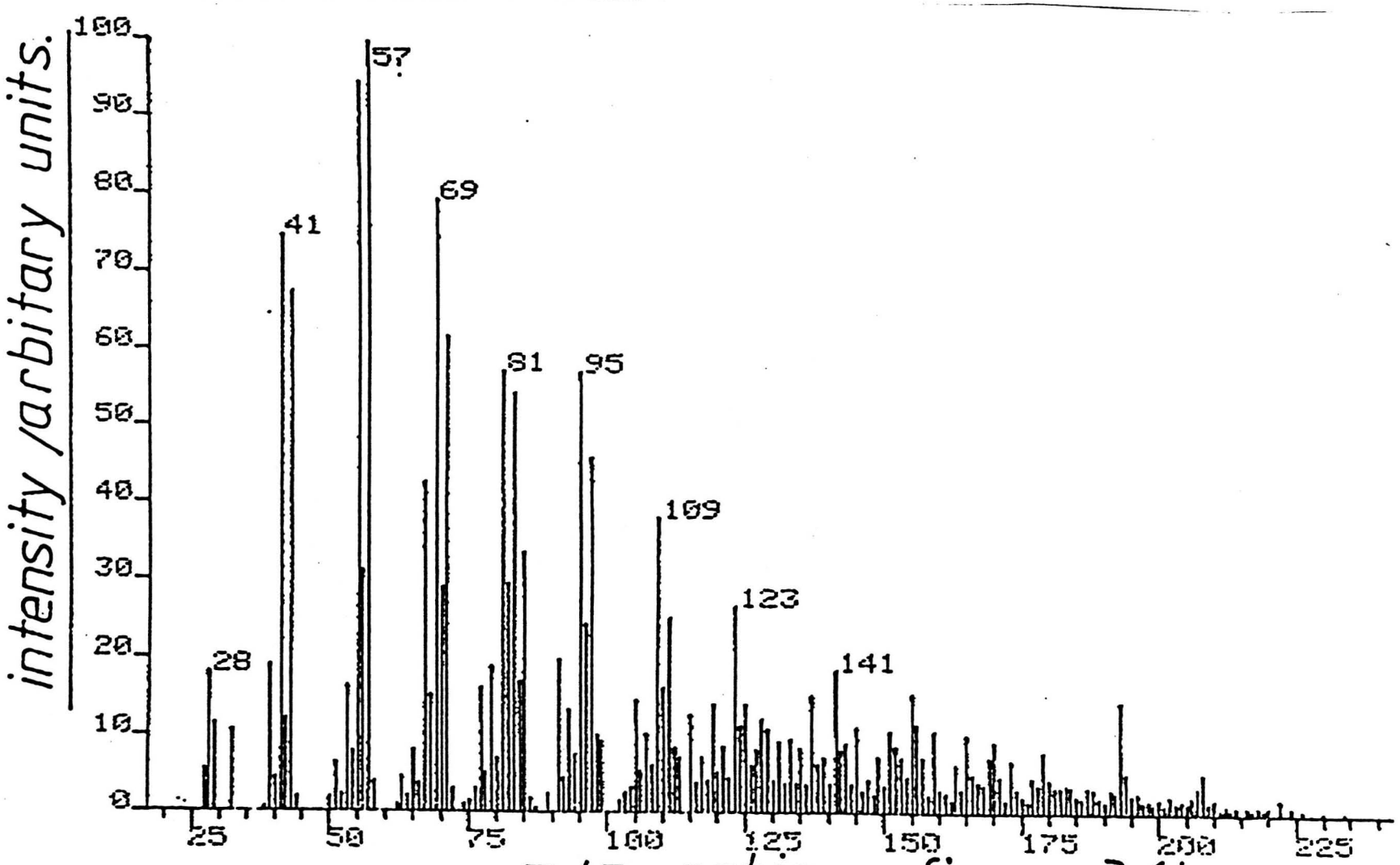


figure 3.6b

metastable map.

Sample: G2

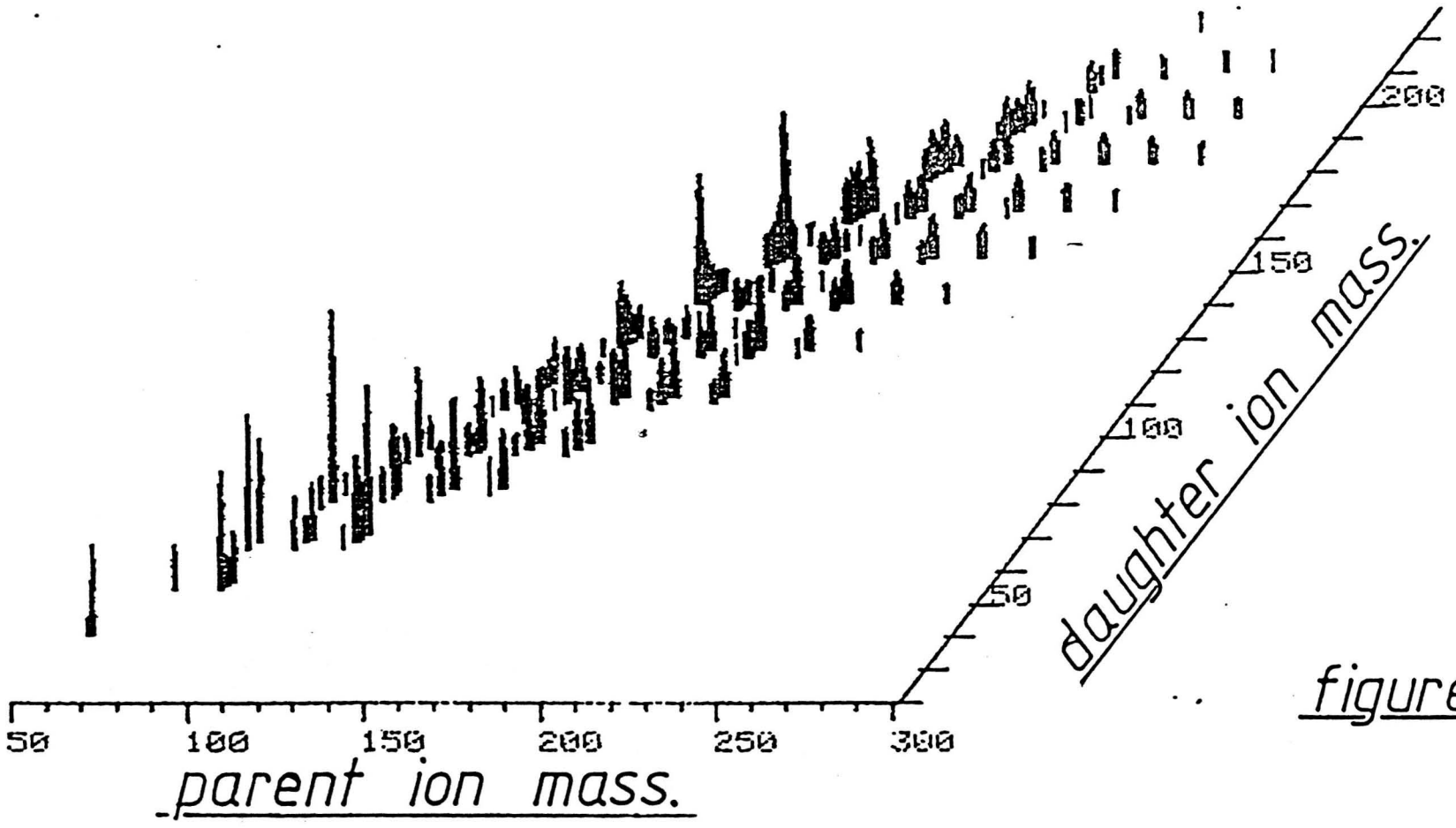


figure 3.7

# EI Spectrum: Sample G2

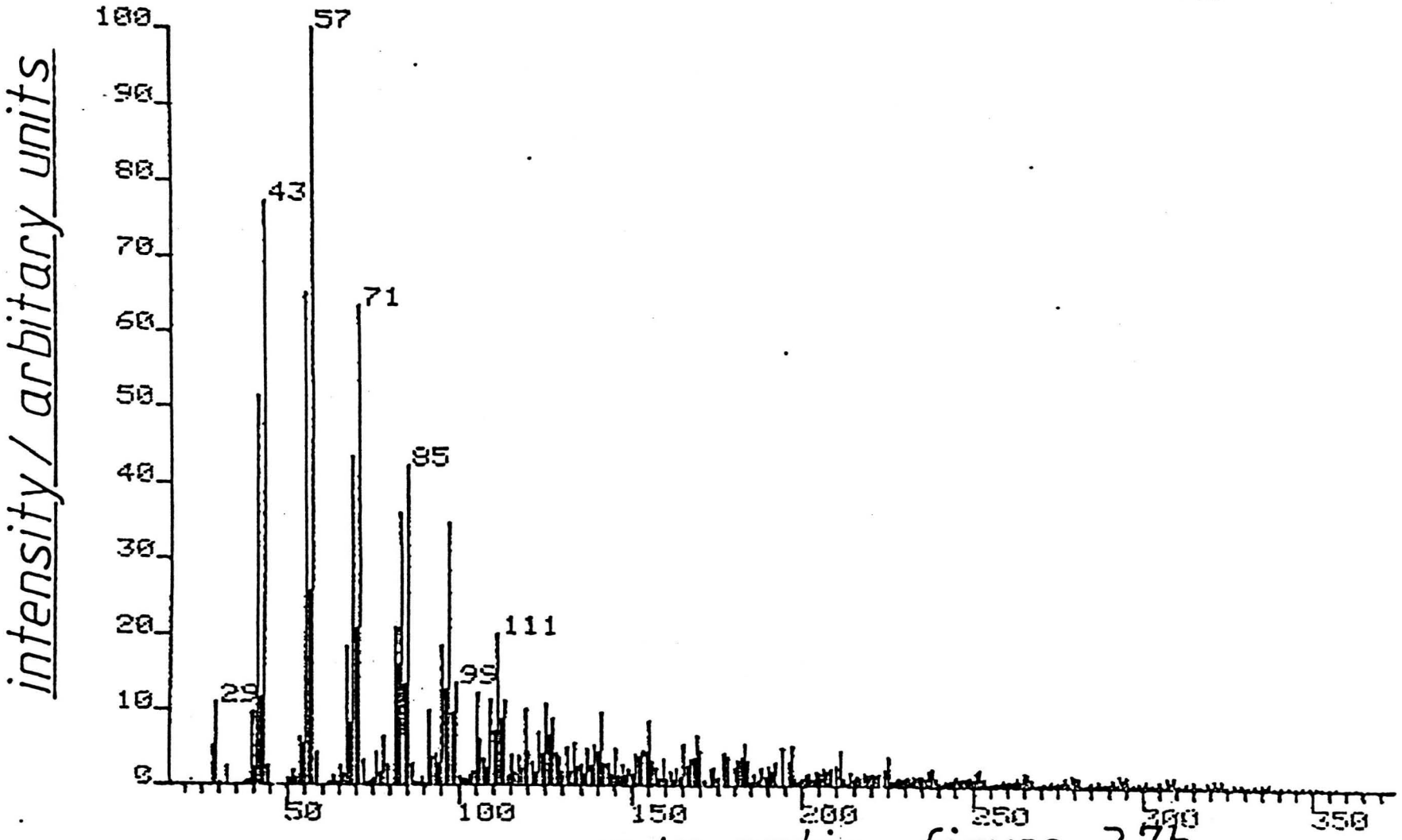


figure 3.7b

## 3.4 CHEMICAL IONISATION ANALYSIS OF ENGINE OIL FRACTIONS

In an ideal situation, metastable mapping would be used to examine the daughter ions from a given parent ion, and then on the basis of the daughter ions present, this would enable one to determine the nature of the component, ( in a mixture ), that gave rise to that parent ion. This requires, however, that the parent ion chosen is unique to that one component. Furthermore, we have seen that the statistical technique of factor analysis requires that a unique peak exists for each component.

In electron impact ionisation, this situation arises only if we are very fortunate. We can hope to increase the likelihood that we achieve the above conditions by using a less energetic method of ionisation. The obvious choice is CI.

### 3.5.1 METHANE AND ISO-BUTANE CI OF ENGINE OIL SAMPLES

Preliminary experiments were carried out on the MS-80 mass spectrometer at Warwick using positive CI with methane and iso-butane as CI reagents. The samples used were n-hexadecane and n-hexatriacontane, n-$C_{36}H_{74}$.

These initial experiments were designed to establish the best operating conditions for the mass spectrometer.

The first set of experiments using methane CI of n-hexadecane showed $(M-1)^+$ peaks which had a much lower intensity relative to the $M^+$ peak in comparison to the relative intensity published in the literature (Field et. al. methane CI of paraffins (28), and methane CI of cyclo-paraffins (29)). A repeat experiment was performed in which the source temperature was set at 150 $^oC$ and allowed to warm-up to 200 $^oC$ during the course of the experiment. This was done in order to ascertain the effect of temperature variations on the spectra. The results show that at the lower temperature, the relative intensity of the $(M-1)^+$ peak is increased compared to that at higher temperatures. Further at the highest temperature most of the ion current is carried by low mass ions.

The next set of experiments involved the methane and isobutane CI of n-hexadecane and n-$C_{36}H_{74}$ samples at temperatures of 150 $^oC$, 200 $^oC$, and 250 $^oC$. The results of these experiments followed the results of the earlier experiment. For the CI of the n-$C_{36}H_{74}$ at 250 $^oC$, the $(M-1)^+$ peak was not even detectable.

Even at the low temperature, the $(M-1)^+$ intensity is relatively low compared to that described in the literature. The tuning of the mass-spectrometer was carried out under EI conditions using the mass peak of PFK at 219 Daltons. In order to see if the situation could be improved by tuning the mass-spectrometer under CI conditions, another set of experiments was carried out. Initially in this set of experiments the mass-spectrometer was tuned up on the mass peak of n-hexadecane at 225 Daltons whilst operating under CI conditions. Without altering the source setting the mass-spectrometer was switched to EI operation and re-calibrated (the tuning procedure disturbs the calibration). In later experiments it was found that it was just as easy to tune up on the $(M-1)^+$ mass peak of n-$C_{36}H_{74}$, in fact the sample (being a solid) lasted longer than the n-hexadecane samples, making the tuning procedure easier.

It was found that this tuning procedure allowed for much improvement in the quality of the spectra. It became obvious however that the isobutane CI spectra were consistently better than the corresponding methane CI spectra. This observation is understandable as the reagent ions from isobutane, $C_4H_9^+$ are less energetic reagent ions than those of methane, $CH_3^+$.

During these experiments the samples of n-$C_{36}H_{74}$ were introduced on to the probe using three different methods. The first method tried was to melt a little of the sample and allow it to be drawn into a small capillary tube which was then introduced into the sample tube of the DIP. The second method followed essentially the same procedure, except that the sample was dissolved in cyclohexane instead of being melted. This allowed the sample to be drawn up a greater length of

the capillary tube. A third method was to introduce the sample onto the tip of a short length of gold wire, which when inserted into the DIP, would allow the sample to enter the plasma of the source.

Of these methods the second was found to be the most successful. The DIP was heated to 200 $^{o}C$ causing the excess cyclohexane to evaporate off during the first few scans, and the n-$C_{36}H_{74}$ to evaporate several scans later.

The lack of success of the gold wire method is probably due to the very quick vaporisation of the sample.

In order to exploit the improvements observed in a cooler source, an additional experiment was carried out. This experiment was performed with the source heating switched off and with reduced filament current. In this way it was hoped to operate with as cold a source as possible. The results confirm that the observed ion intensity at lower masses is due in the main to the pyrolysis of the sample. As can be seen by comparing the isobutane CI spectra of n-$C_{36}H_{74}$ (figs. 3.8 - 3.10), operation at lower source temperatures improves the quality of spectra significantly. However, as well as an improvement in that the amount of fragmentation observed decreases, there is a decrease in the absolute intensity of the $(M-1)^+$ ion as the source temperature becomes very low, so that for maximum sensitivity, a compromise has to be made between relative fragmentation and intensity of the $(M-1)^+$ peak. This is illustrated in fig 3.11, which shows the ratio I(505)/I(113) and I(505), the intensity of the $(M-1)^+$ peak, as functions of temperature. The ratio, I(505)/I(113), is assumed to be a good measure of the degree of fragmentation.

These spectra may be compared with fig. 3.12, which shows the

# iso-butane CI Spectrum of n-$C_{36}H_{74}$

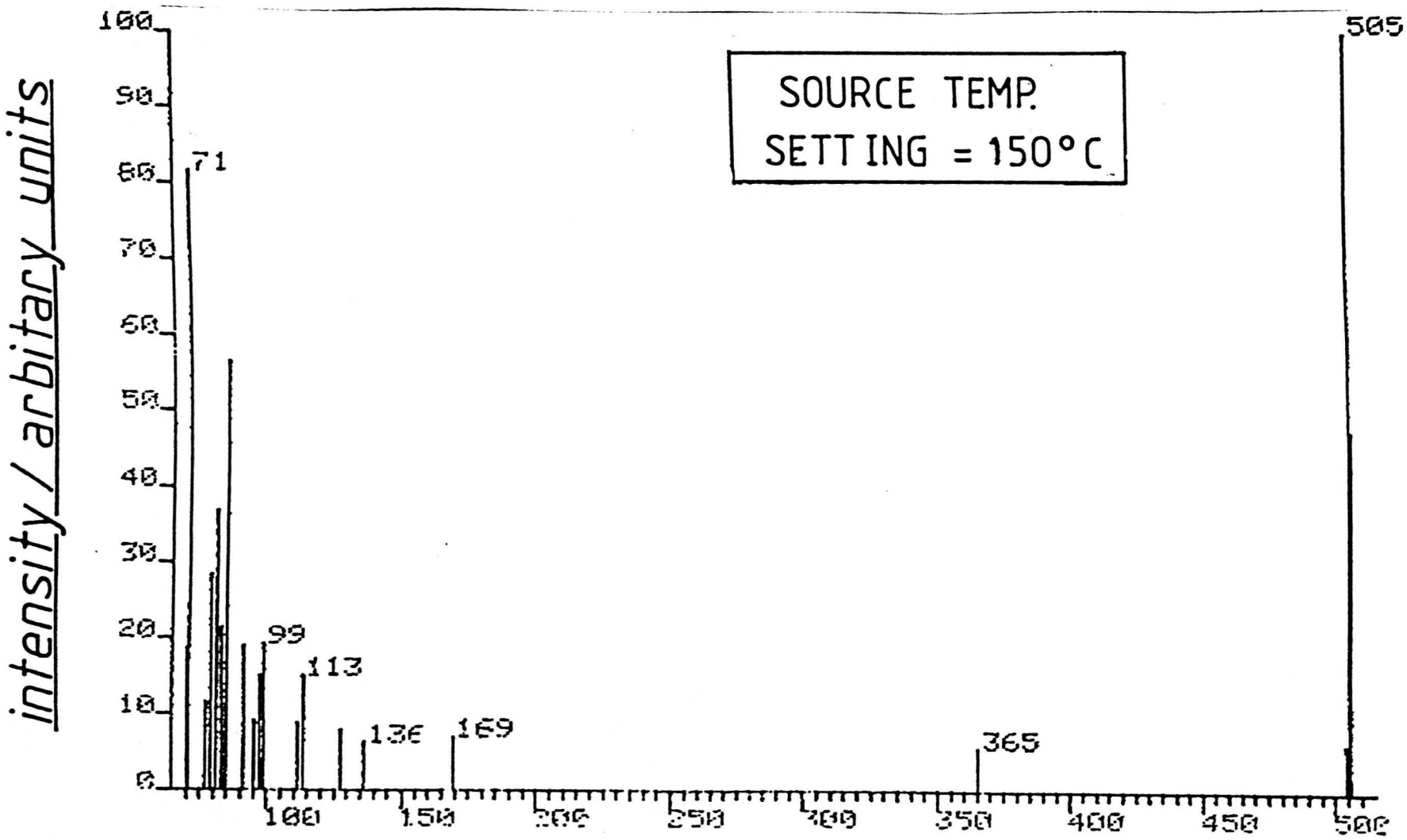


m/z ratio

figure 3.8

# iso-butane CI Spectrum of n-$C_{36}H_{74}$

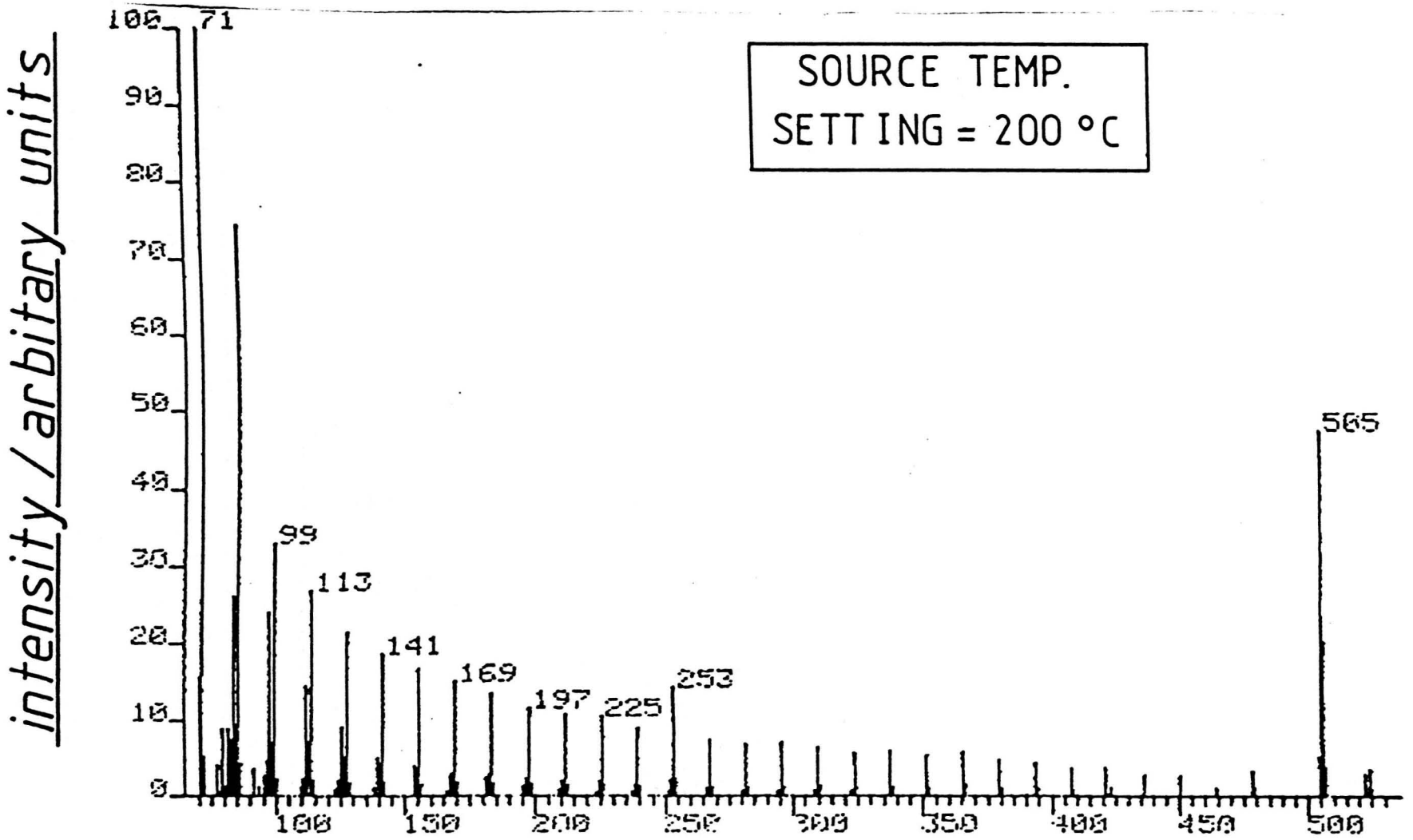


figure 3.9

# iso-butane CI Spectrum of n-$C_{36}H_{74}$

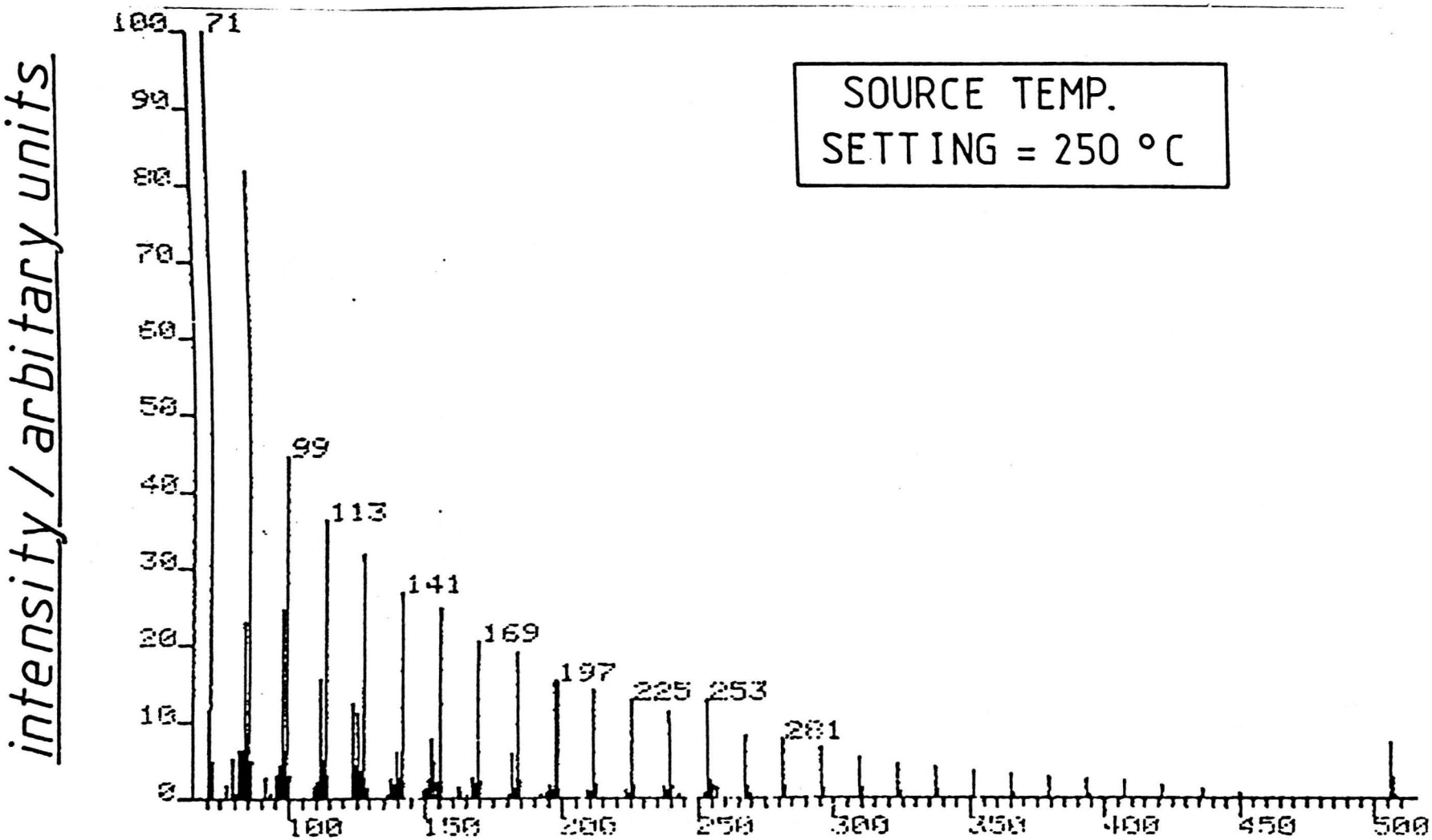


figure 3.10

*figure 3.11*

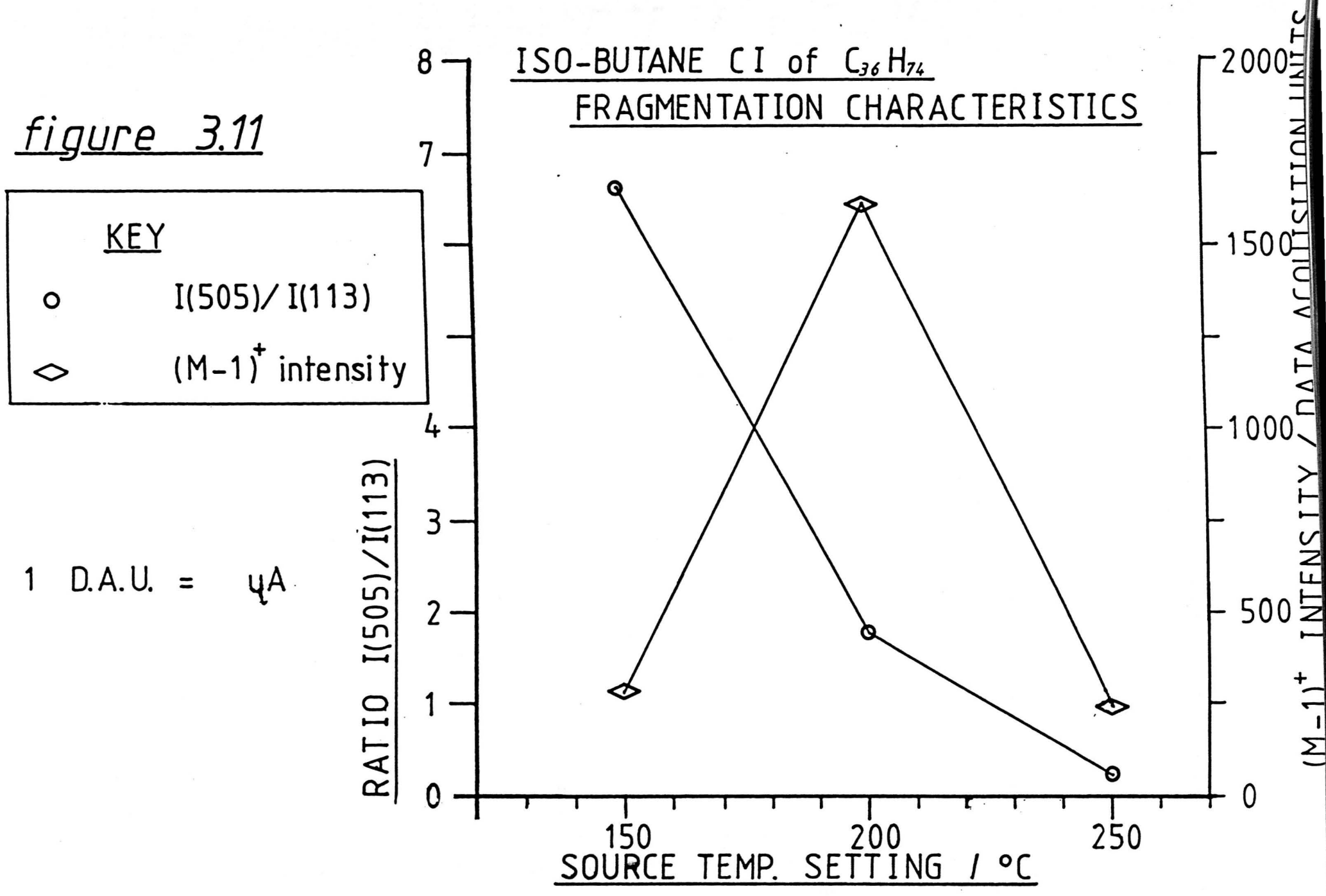
ISO-BUTANE CI of $C_{36}H_{74}$
FRAGMENTATION CHARACTERISTICS
KEY
I(505)/ I(113)
$(M-1)^+$ intensity
1 D.A.U. = μA
RATIO I(505)/I(113)
$(M-1)^+$ INTENSITY / DATA ACQUISITION UNITS
SOURCE TEMP. SETTING / °C
0
1
2
3
4
7
8
0
500
1000
1500
2000
150
200
250

figure 3.12 iso-butane DCI of n-$C_{36}H_{74}$

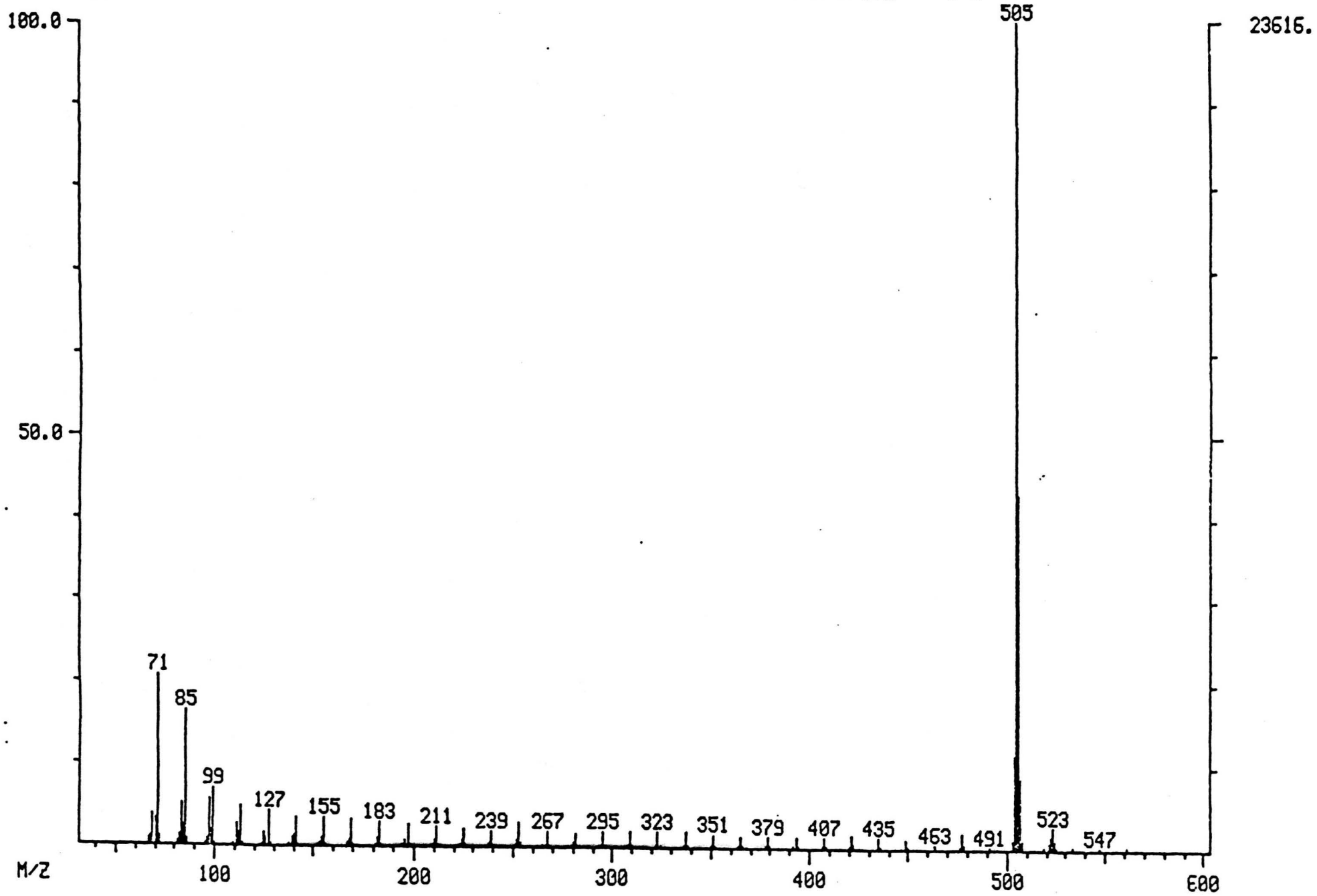

iso-butane CI spectra of n-$C_{36}H_{74}$. This spectrum, provided by the ESSO Research Centre, Abingdon, was run under DCI conditions (30) in which the CI reagent gas is passed through the probe and the sample is allowed to make a more direct contact with the CI reagent gas and with the plasma within the source.

The iso-butane CI spectra of two oil samples are shown in figs. 3.13 and 3.14, sample G3a is the saturates fraction of the oil, and sample G3b is the aromatics fraction of the oil. These were previously separated from the original oil sample using elution chromatography (11). The different positions of the maxima in the relative molecular weight distributions of the EI spectra and the CI spectra is due to the lower molecular weight fractions distilling off the probe tip, so that the molecular weight distribution is not reproducible from scan to scan. The CI spectrum of the aromatics fraction gives major ions at $(M+1)^+$, but fragmentation still occurs, and the over-all sensitivity is lower than the corresponding EI spectrum. The corresponding saturates sample also shows an $(M+1)^+$ series of peaks with iso-butane CI, and shows reduced fragmentation and similar sensitivity. The features are, however, difficult to interpret e.g. comparing fig 3.13b and fig. 3.13c which respectively show the CI and EI spectra of the saturates sample in the region 290 to 320 Daltons, one can see that the odd mass fragment ions may interfere with the odd mass pseudo-molecular ions $(M+1)^+$.

In conclusion, it is difficult to see any clear advantage in using iso-butane CI for the analysis of saturate and aromatic engine oil fractions. Again, it is concluded that it is the extreme complexity of the samples involved which is the root of the problem, making it difficult to interpret the CI spectra.

iso-butane CI, Sample: G3a (saturates)

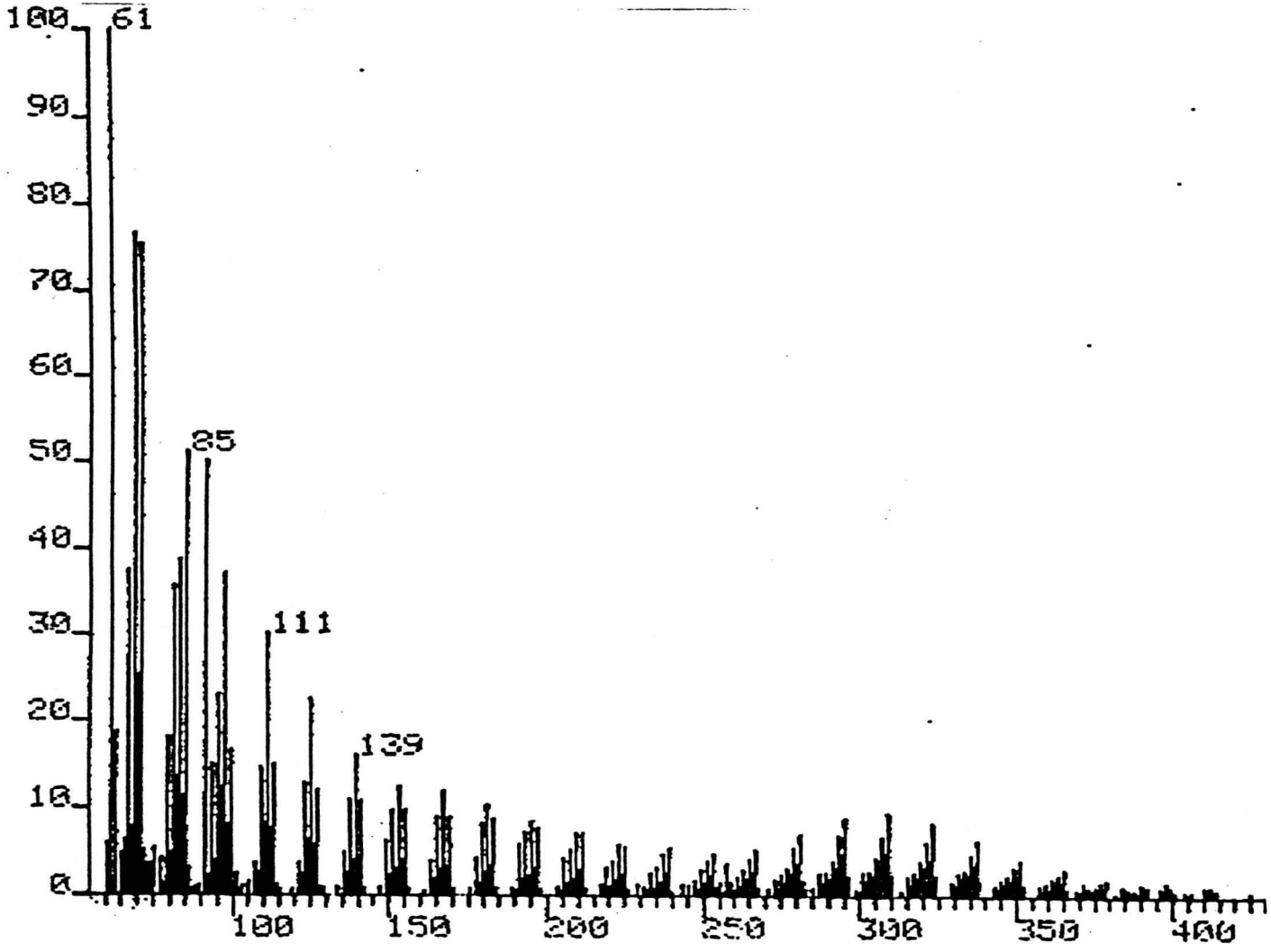


m/z ratio

figure 3.13a

iso-butane CI, Sample: G3a, m/z = 290 - 320 Daltons

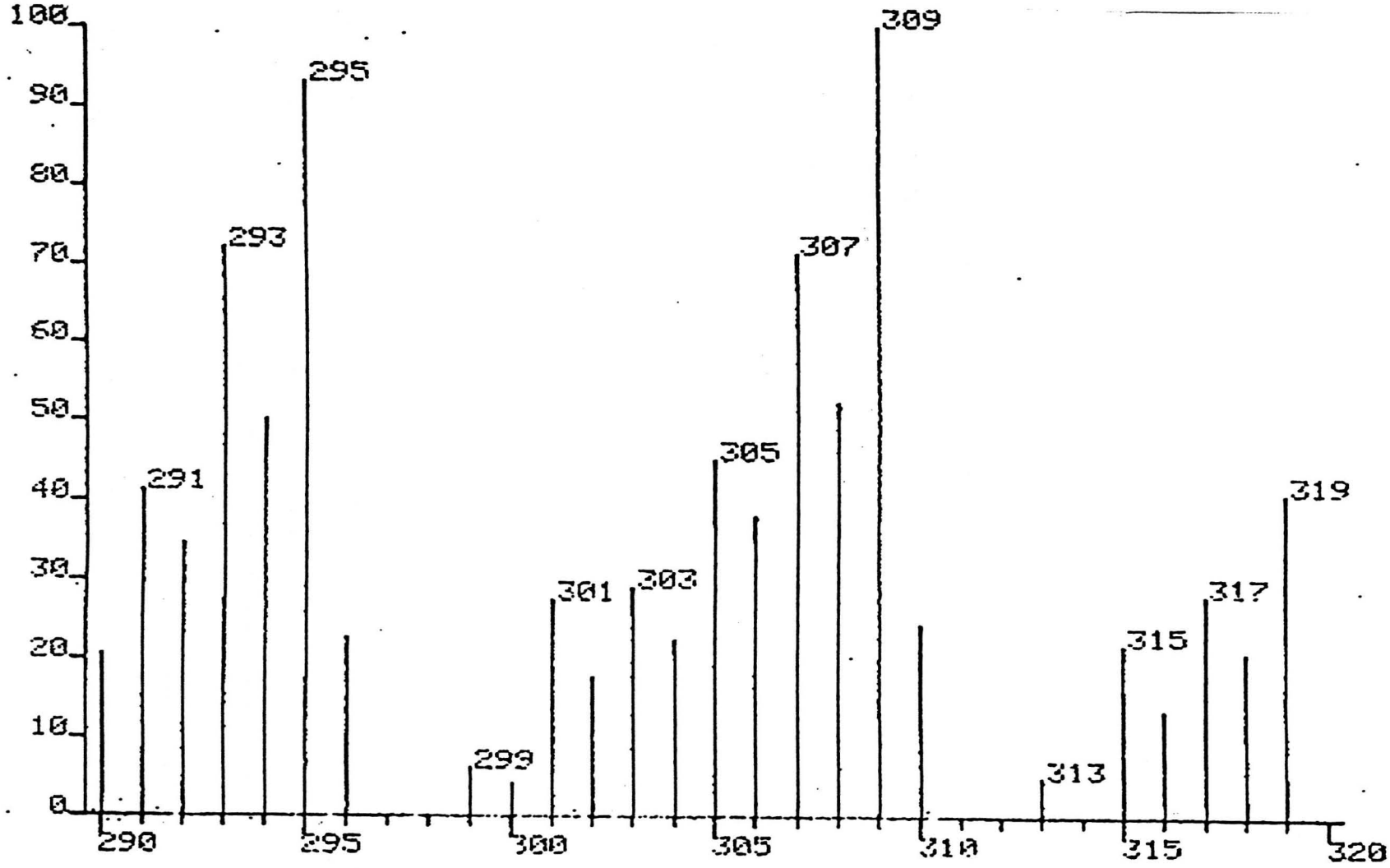


m/z ratio

figure 3.13b

EI Spectrum, Sample: G3a, m/z = 290 - 320 Daltons

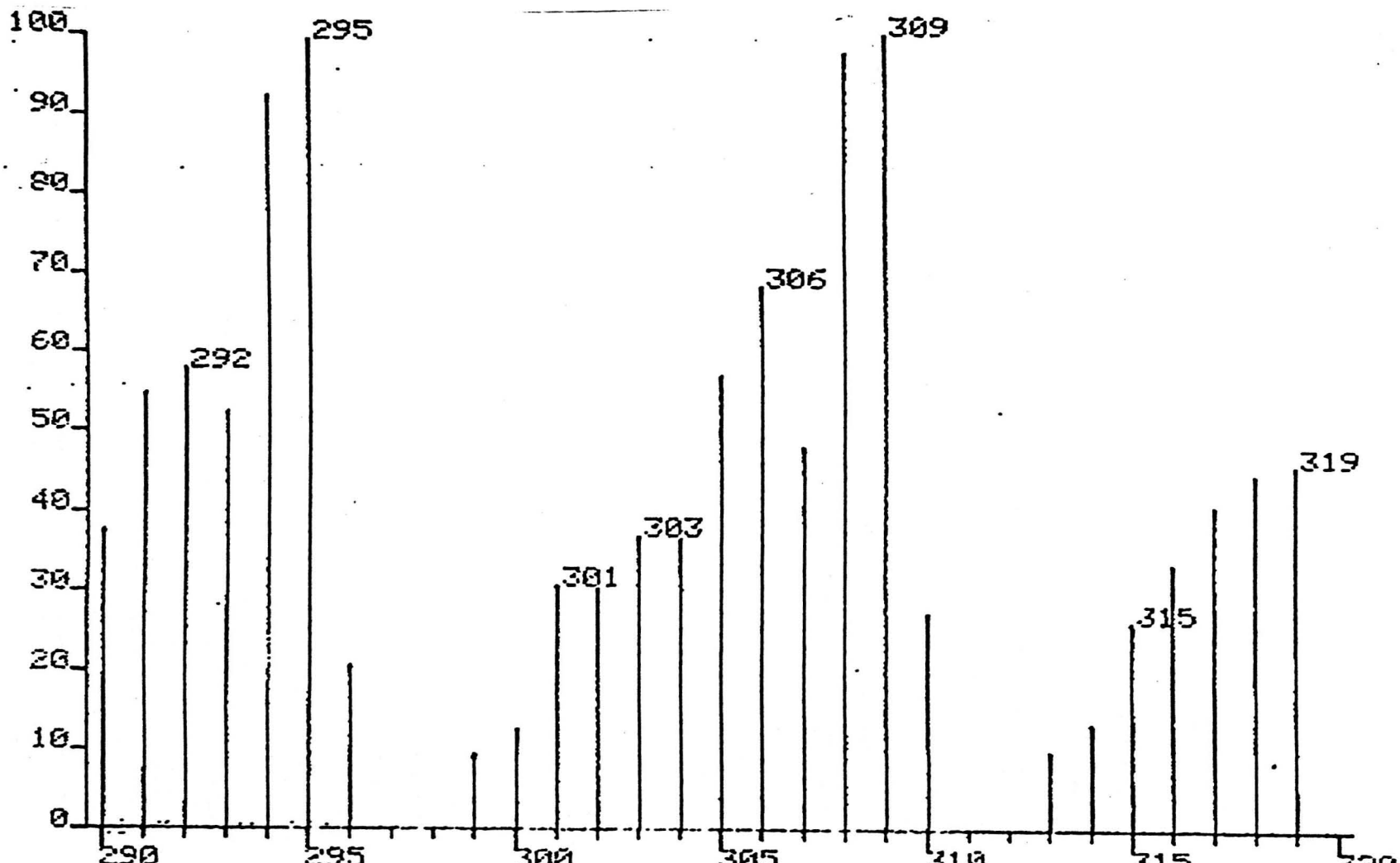


m/z ratio

figure 3.13c

iso-butane CI, Sample: G3b (aromatics)

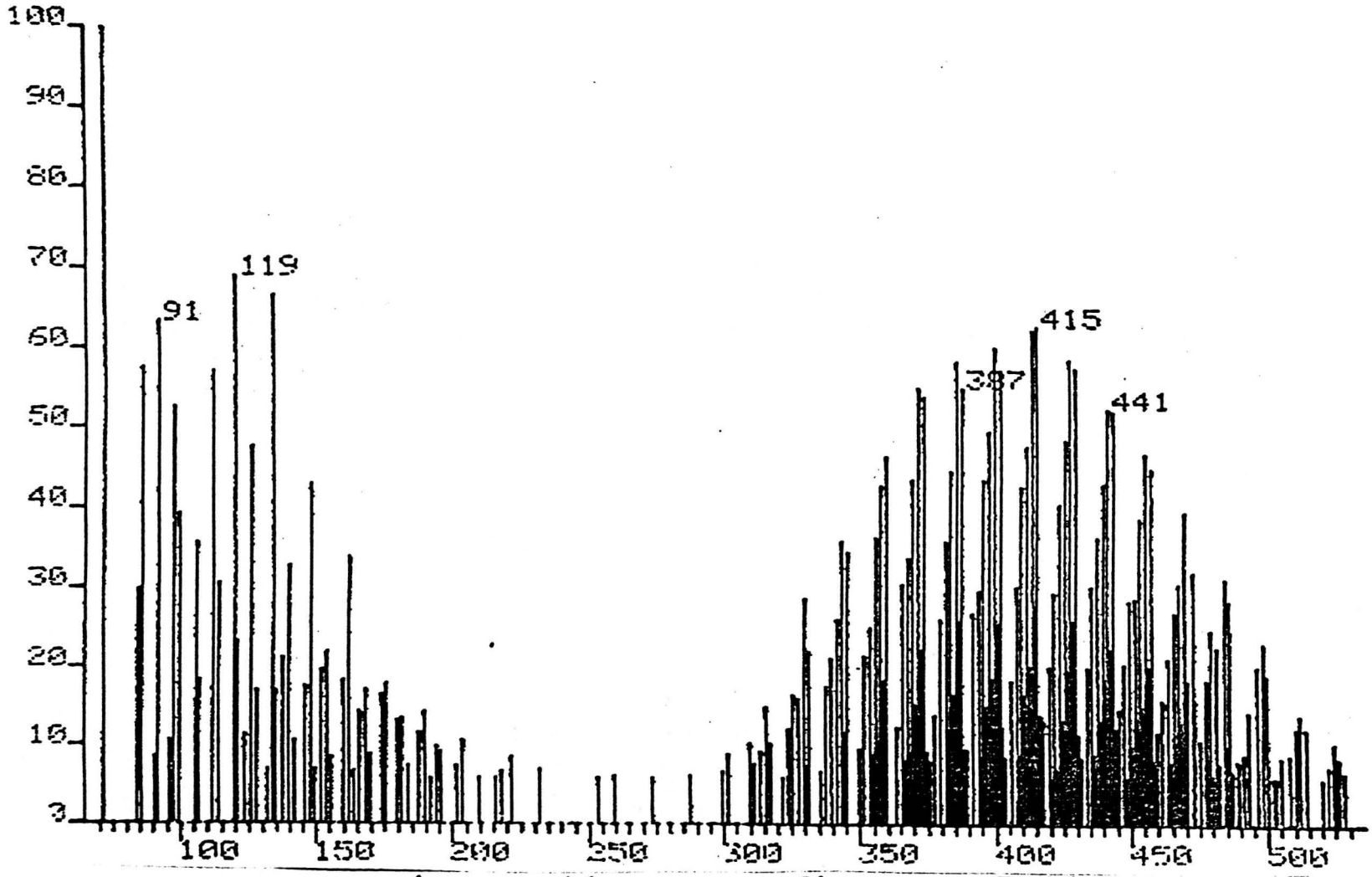


m/z ratio

figure 3.14a

# figure 3.14b iso-butane CI & EI of sample G3b

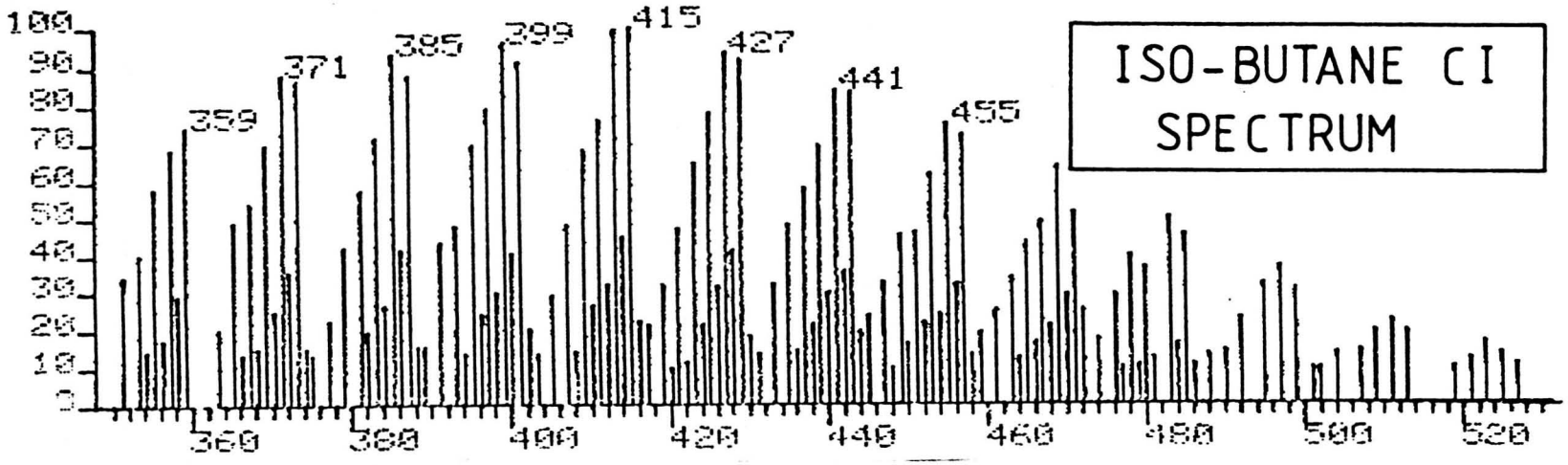


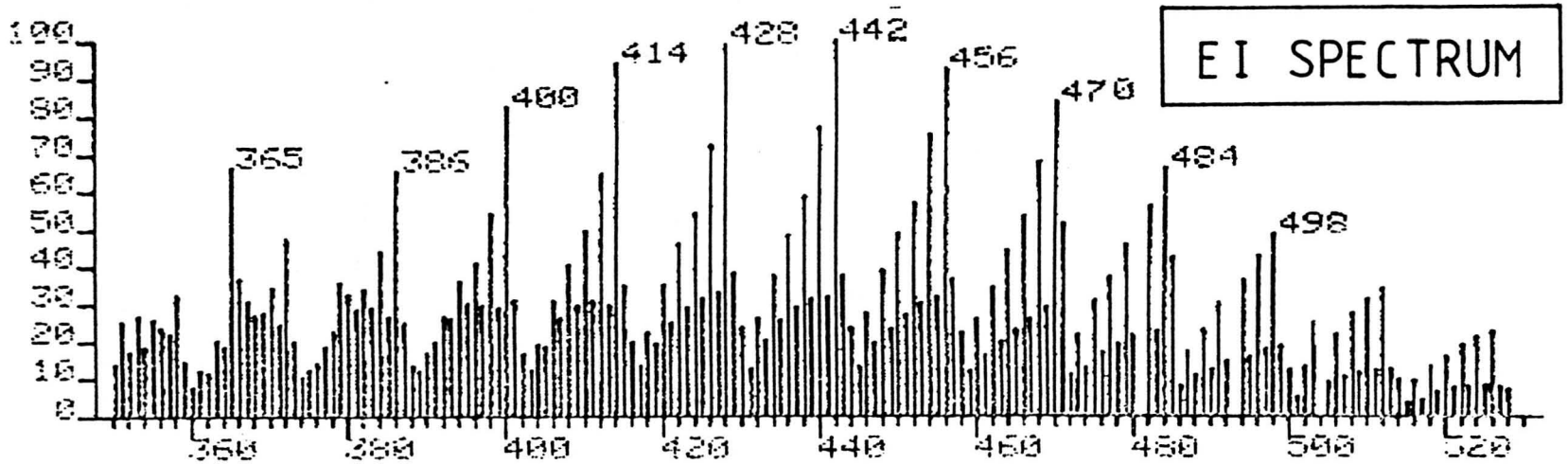

### 3.5.2 OTHER CI REAGENTS

One method that allows one to achieve conditions of soft ionisation is to use a charge transfer reagent with ionisation energy close to that of the sample:-

$$M + R^+ \rightarrow M^+ + R$$

$$\Delta H = IE(M) - IE(R)$$

where M refers to sample molecules and R to reagent molecules.

Table 3.7 shows the ionisation energies of various sample and reagent molecules and from the table, one may infer that charge exchange from $CS_2^+$ should only be important for aromatic hydrocarbons and possibly for high molecular weight alkanes.

Figure 3.15 shows the $CS_2$ CI spectra of n-$C_{36}H_{74}$. The reagent gas was introduced from a 1 litre bulb containing approximately a 2:1 mixture of $CS_2$/nitrogen. Examination of the reagent ions showed very little $N_2^+$, the principal reagent ions being $CS_2^+$ and $S^+$. As can be seen from fig. 3.15, the $CS_2$ CI spectrum of n-$C_{36}H_{74}$ exhibits quite significant fragmentation. Charge exchange from $S^+$ may account for this. It is possible that by finding a suitable mixture of $CS_2$ and an appropriate buffer gas, then the contribution from $S^+$ charge exchange may be reduced, however, no investigation into this area was undertaken as it was felt that $NO^+$ CI offered a greater prospect of yielding results.

The ionisation energy of NO, when compared with that of typical

# $CS_2$ charge exchange spectrum of n-$C_{36}H_{74}$

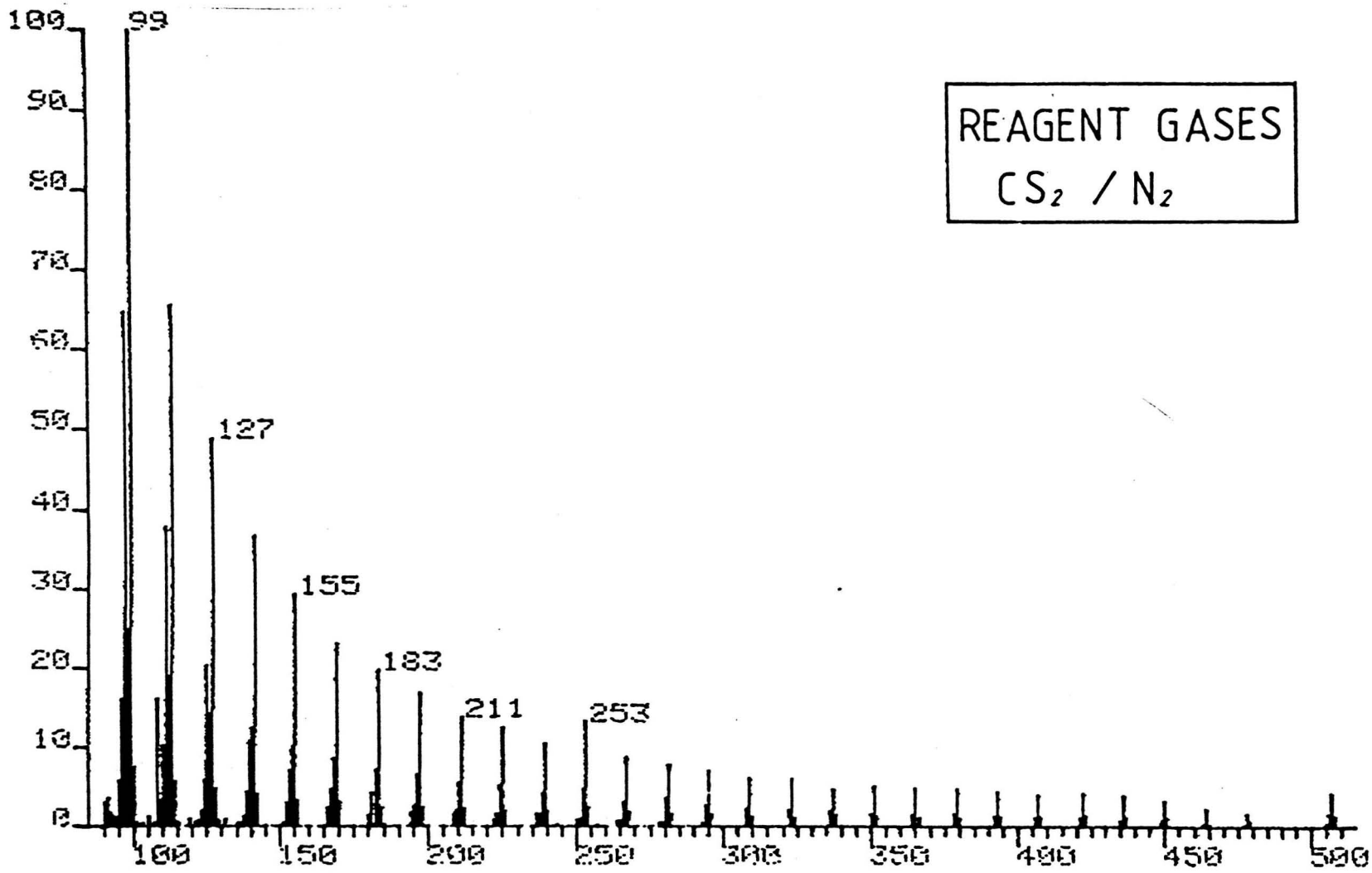


m / z ratio

figure 3.15

TABLE 3.7: Ionisation Energies of Some Species.

| Molecule | IE / eV |
|---|---|
| Benzene | 9.2 |
| Anthracene | 7.4 |
| n-Octane | 10.3 |
| $CS_2$ | 10.1 |
| S | 10.4 |
| NO | 9.3 |

saturated and aromatic hydrocarbons, indicates that charge transfer from $NO^+$ will only be important for aromatic hydrocarbons. One may also expect that there will be little or no fragmentation.

With alkanes, it has been reported (32), $NO^+$ undergoes a hydrogen abstraction reaction:-

$$NO^+ + M \rightarrow (M-H)^+ + HNO$$

This reaction is accompanied by very little fragmentation of the $(M-H)^+$ ion. Thus it should be possible to analyse easily an oil sample containing both saturated and aromatic compounds, as the aromatics should generate molecular ions, $M^+$, at even mass, and the saturate pseudo-molecular ions, $(M-1)^+$, at odd mass.

A complication arises due to the other main reaction path-way available to $NO^+$, the addition reaction:-

$$NO^+ + M \rightarrow (MNO)^+$$

This reaction is important for aromatic hydrocarbons whose ionisation energy is greater than about 8.5 eV (32). One possible answer if this problem arises, is to use collision induced decomposition to identify those ions due the above addition reaction.

The $NO^+$ CI spectrum of 1-methylnaphthalene was used as a test case for setting up the mass spectrometer operating conditions. The NO was introduced from a 1 litre bulb containing a 5% mixture of nitric oxide in hydrogen, as recomended by Chai and Harrison (32). The bulb stagnation pressure was about 600 torr and the gas mixture was admitted

into the mass spectrometer through a needle valve. The gas pressure was adjusted by the needle valve until the measured source chamber pressure was $10^{-4}$ torr. The solenoid valve which is part of the gas introduction system on the MS80 was opened to its normal position, as used in routine methane/iso-butane CI runs. This follows the normal procedure that was adopted for the introduction of reagent gas samples from bulbs.

The EI and $NO^+$ CI spectra of 1-methylnaphthalene are shown in fig. 3.16. The nitric oxide CI spectra show significantly less fragmentation ions than the corresponding EI spectrum. This was also the case for several other simple aromatic hydrocarbons that were tried.

The $NO^+$ CI spectra of a typical aromatic oil fraction, run under the same conditions, proved very disappointing. The $NO^+$ CI spectra of this sample showed very poor sensitivity, virtually no ions above 200 Daltons were observed, and those below 200 Daltons corresponded to low intensity fragment ions, possibly due to residual electron impact ionisation. Increasing and decreasing the reagent pressure had very little effect on the spectra.

The poor sensitivity of the results may be due to impurities in the nitric oxide supply. It was noticed that the bulb containing the gas mixture was of a very pale yellow/brown colour, indicating the presence of nitrogen dioxide. The intensity of the peak at 46 Daltons, however, which would correspond to the $NO_2^+$ ion, is less than 3% of the intensity of the base peak (30 Daltons). Another possibility, if nitrogen dioxide is a contaminant, is generation of the $O^+$ ion. The intesity of the peak at 16 Daltons is negligible. Significant contamination by nitrogen dioxide can therefore be ruled-out.

The reactions occurring in hydrogen/nitric oxide mixture have been shown to be as follows (33):

$$e^- + H_2 \rightarrow H_2^+ + 2e^+$$

$$H_2^+ + H_2 \rightarrow H_3^+$$

$$H_3^+ + NO \rightarrow HNO^+ + H_2$$

$$HNO^+ + NO \rightarrow NO^+ + HNO$$

$$e^- + NO \rightarrow NO^+ + 2e^-$$

The $H_2$ has a very low proton affinity (423 kJ/mol; cf $H_2O$, 724 kJ/mol), so that if the $H_3^+$ ion is present in high concentrations, it will react with the sample molecules to give ions with a high internal energy, leading to extensive fragmentation of the sample ions.

It was not possible to measure the ion abundance at 3 Daltons on the MS-80 mass spectrometer. Due to the reaction of $H_3^+$ with NO to produce $HNO^+$, it is possible to establish whether the $H_3^+$ ion is present. The intensity of the peak at 31 Daltons was ca. 12% of the base peak intensity, and since the natural abundances of $^{15}N$ and $^{17}O$ are negligible, the peak at 31 Daltons may be attributed to be due to $HNO^+$ ions.

Hence, it can be inferred that the poor spectrum was a result of the presence of the $H_3^+$ ion.

Attempts were made to re-fill the reservoir bulb with a fresh

figure 3.16 $NO^+$ CI of 1-methyl-naphthalene

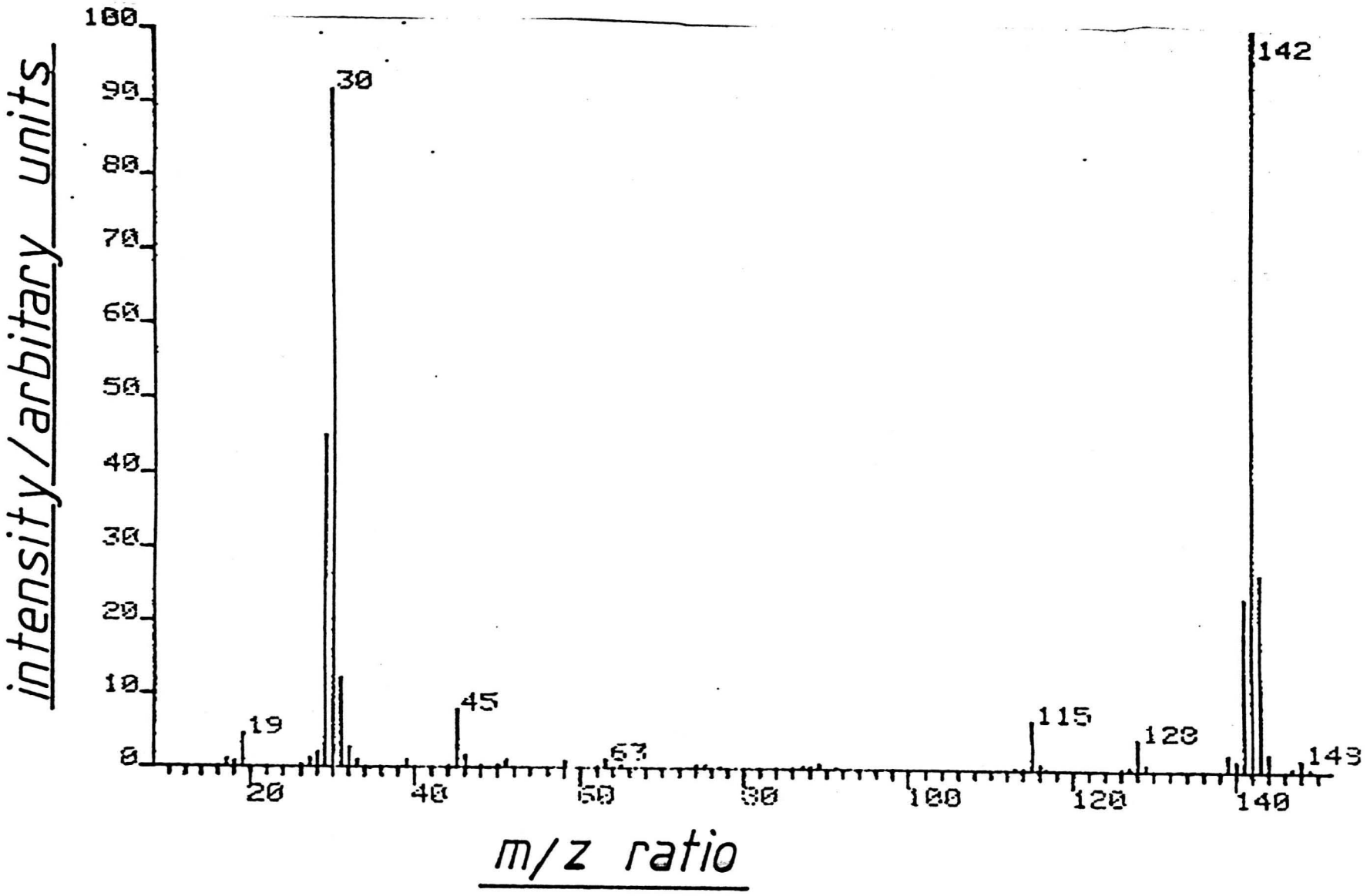

figure 3.16b EI Spectrum: 1-methyl-naphthalene

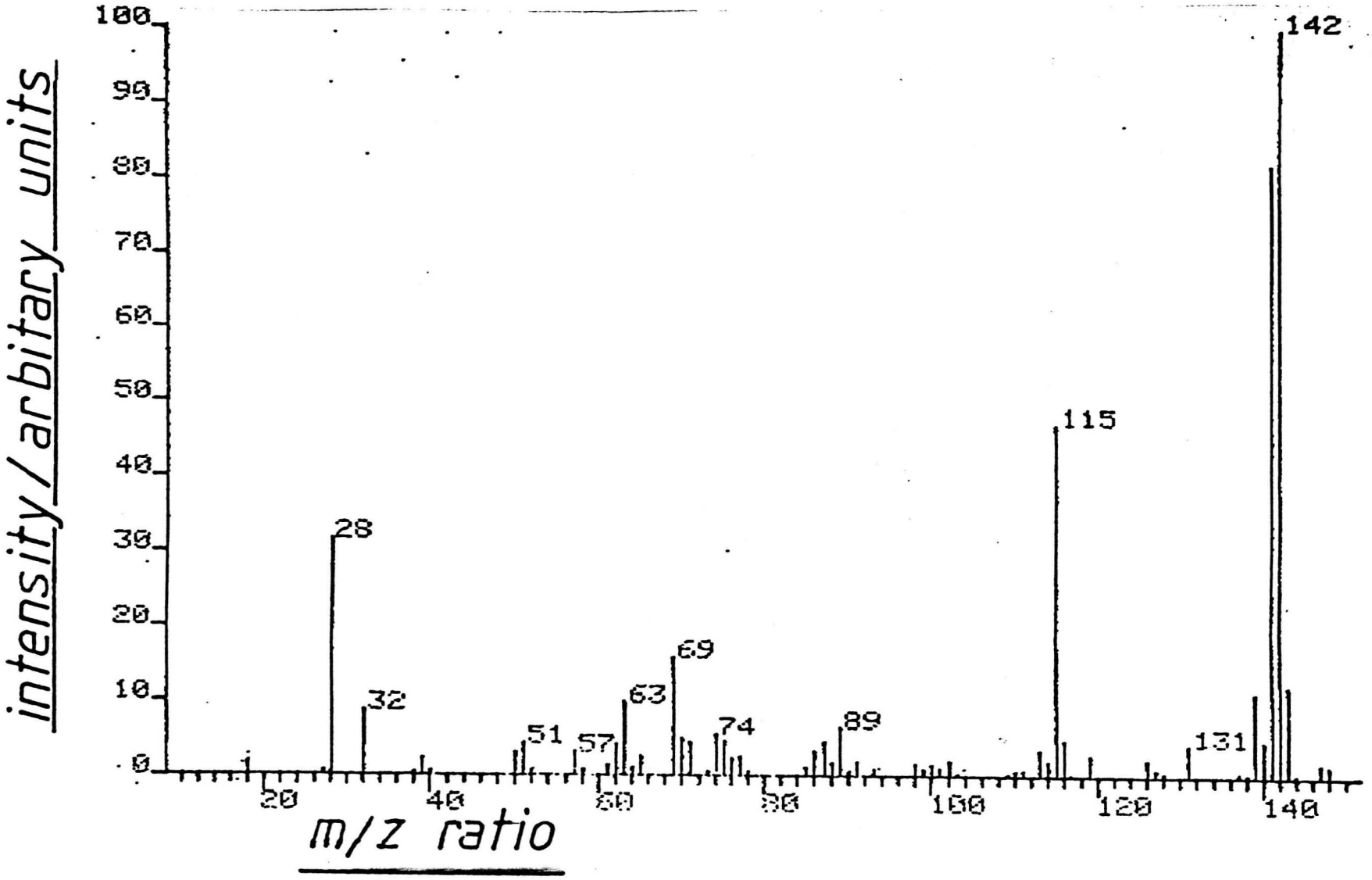

$NO/H_2$ mixture, but the nitric oxide cylinder was found to be exhausted. It was not possible to obtain a replacement nitric oxide cylinder in the time available, so that further experiments were not possible.

### 3.5.3 CONCLUSIONS

It is felt that for saturate and aromatics engine oil fractions, no significant gain is likely with the use of the chemical ionisation techniques investigated. The use of CI for these samples further complicates an already complicated spectrum due to the possibility of two, or more, reaction pathways e.g. hydride abstaction verses addition reactions in the case of $NO^+$ CI.

Where the chemical ionisation techniques may be of use in the analysis of hydrocarbon samples is in the analysis of aromatic hydrocarbon mixtures which contain a smaller number of compounds, or which contain a small number of chemically dissimilar compounds which may be selectively ionised in the presence of a background of other compound types. One interesting example, due to Simonsick and Hites (34), uses combined methane CI / argon CI to characterise high molecular weight polycyclic hydrocarbons in terms of the ratio of $M^+$ to $(M+1)^+$.

Analysis of saturate hydrocarbons is unlikely to benefit from chemical ionisation techniques because those properties which allow selective ionisation - chemical reactivity, or low ionisation energy for example, are generally properties associated with aromaticity of the sample molecules.

The selective ionisation of the aromatic fraction of an engine oil sample would seem quite feasable, but as a part of a quantitative procedure, the use of chemical ionisation poses problems because it is less reproducible than EI. Since it is also required to analyse quantitatively the saturates present in the oil sample, for which an HPLC or elution chromatographic separation is required anyway, then the use of a CI analysis of the aromatics would not seem to be very beneficial.

A chemical ionisation based analysis of aromatics would be of use if quantitative results are not required. One possibility is the use of pattern recognition techniques to 'finger-print' oil samples. This would not require quantitative results because many pattern recognition techniques require the use of binary encoded mass spectra (see above) or use of 'normalised' intensities. A recent example of this type of application involved the use of $OH^-$ chemical ionisation (35) and principle component analysis to fingerprint crude oil samples (36).

## CHAPTER THREE: REFERENCES


1) Carlson, E.G., Andre, M.L. and O'Neal, M.J., Advances in Mass Spectroscopy, 377, (1959).

2) Hood, A. and O'Neal, M.J., Advances in Mass Spectroscopy, 175, (1959).

3) Hood, A., Clerc, R.J. and O'Neal, M.J., J. Inst. Petrol., 45, 168, (1959).

4) O'Neal, M.J. and Hood, A., Abstracts, American Chemical Society, Division of Petroleum Chemistry, Vol. 1, No. 4, (1956).

5) Johnson, J. V., Britton, E. D. & Yost, R. A., Anal. Chem., 58, 1325, (1986).

6) Roboz, J., Introduction to Mass Spectrometry, Interscience, 1968, Chap. 10, p314-318.

7) Brown, R.A., Anal. Chem., 23, 430, (1951).

8) Robinson, C.J. and Cook, G.L., Anal. Chem., 41, 1548, (1969).

9) Hydrocarbon Type Analysis Of Gas-Oil Aromatics By High Ionizing Voltage Mass Spectrometry, ASTM, Book of Standards, D3239.

10) Hydrocarbon Type Analysis Of Gas-Oil Saturates By High Ionizing Voltage Mass Spectrometry, ASTM, Book of Standards, D2786.

11) Separation Of Representative Aromatic And Nonaromatic Fractions Of High-Boiling Oils By Elution Chromatography, ASTM, Book of Standards, D2549.

12) Hydrocarbon Types In Lubricating Oil Basestocks By Preparative High Performance Liquid Chromatography, Institute of Petroleum, Proposed Method, Designation AQ.

13) Kendrick, E.K., ESSO Research Centre, Abingdon, private communication.

14) Rozzett, R.W. and Patersen, E.M., Anal. Chem., 47, 1301, (1975).

15) Rozzett, R.M. and Patersen, E.M., Anal. Chem., 48, 817, (1976).

16) Justice, J.B., and Isenhour, T.L., Anal. Chem. 47, 2286, (1975).

17) Lam, T.F., Wilkins, C.L., Brunner T.R., Saltzberg, L.J. and Kaberline, S.L., Anal. Chem. 48, 1768, (1976).

18) Wold, S., Christie, H.J., Anal. Chim. Acta. 165, 51, (1984).

19) Dromey, R.G., Anal. Chem. 48, 1464, (1976).

20) Grotch, S.L., Anal. Chem. 42, 1214, (1970).

21) Cooks, R.G., Beynon, J.H., Caprioli, R.M. and Lester, G.R., 'Metastable Ions', Elsevier, 1973.

22) Cooks, R.G., 'Collision Spectroscopy', Plenum Press, 1978.

23) Kiser, R.W., Sullivan, R.E. and Lupin, M.S. Anal. Chem., 41, 1958, (1969).

24) Coutant, J.C. and McLafferty, F.W. Int. J. Mass Spectrom. Ion Phys., 8, 323, (1972).

25) Shannon, T.W., Mead, T.E., Warner, C.G. and McLafferty, F.M. Anal. Chem., 39, 1748, (1967).

26) Mason, R.S., Farncombe, M.J., Jennings, K.R. and Scrivens, J., Int. J. Mass Spectrom. Ion Phys., 44, 91, (1982).

27) Warburton, G.R., Stradling, R.S., Mason, R.S. and Farncombe, M.J., Org. Mass Spectrom., 16, 507, (1981).

28) Field, F.H., Munson, M.S.B. and Becker, D.A., Advances in Chemistry, No. 58, 167, (1966).

29) Field, F.H. and Munson, M.S.B., J. Amer. Chem. Soc., 89, 4272, (1967).

30) Kendrick, E.K., ESSO Research Centre, Abingdon, private communication.

31) Hall, G.G., Proc. Roy. Soc., 205a, 541, (1951).

32) Chai, R. and Harrison, A.G., Anal. Chem., 55, 969, (1983).

33) Burt, J. A., Dunn, J. L., McEwan, M. J., Sutton, M. M., Roche, A. E. & Schiff, H. I., J. Chem. Phys., 52, 6062, (1970).

34) Simonsick, W.J. and Hites, R.A., Anal. Chem., 58, 2114, (1986).

35) Smit, A.L.C., Field, F.H., J. Amer. Chem. Soc., 99, 6471, (1977).

36) Burke, P., Jennings, K.R., Morgan, R.P. and Gilchrist, C.A., Anal. Chem., 54, 1304, (1982).

# CHAPTER IV

# MASS SPECTROMETRY OF SULPHURISED PHENOL ENGINE OIL ADDITIVES.

# THE ANALYSIS OF ENGINE OIL ADDITIVES.

## 4.1 INTRODUCTION

Probably the most important additives for lubricating oils are the detergents and dispersants which amount to some 50% of the total amount of additives used.

The purpose of detergents and dispersants is to keep the insoluble combustion products in suspension. These combustion products include soot, lead salt particles and resinous oxidation products which lead to particles and conglomerates from 0.04 to 1.5 um in size which then form deposits on metal surfaces, cause oil thickening, sludge deposition and corrosive wear due to their acidic nature.

The reduced efficiency and increased wear caused by these combustion products is combatted by the use of dispersants, which prevent coagulation of colloidal particles, and detergents, which solubilise the combustion products to form colloidal suspensions. The distinction between dispersants and detergents is a fine one, and any particular additive will probably have a significant role as both detergent and dispersant.

The chemical analysis of these additives is important for two main reasons. On a practical level, the production of these additives requires quality control measures, and therefore accurate adjustment of production parameters in conjunction with reliable analytical procedures. More fundamentally, an understanding of the operation of detergents and dispersants in terms of physical chemical principles requires a detailed knowledge of the molecular structure of these compounds. It will be noted that to date, the production of suitable

additives has relied upon largely empirical observations, although numerous studies of the colloidal properties of lubricating oil particulates has revealed the broad principles of the detergent/dispersant properties of these additives.

Of the numerous detergent/dispersant additives available (1), this study focussed upon the sulphurised phenates, which are commonly used as the calcium or barium salts of 2,2'-bis (4-alkylphenyl) sulphide (I below), where the alkyl groups are an average of twelve carbon atoms long.

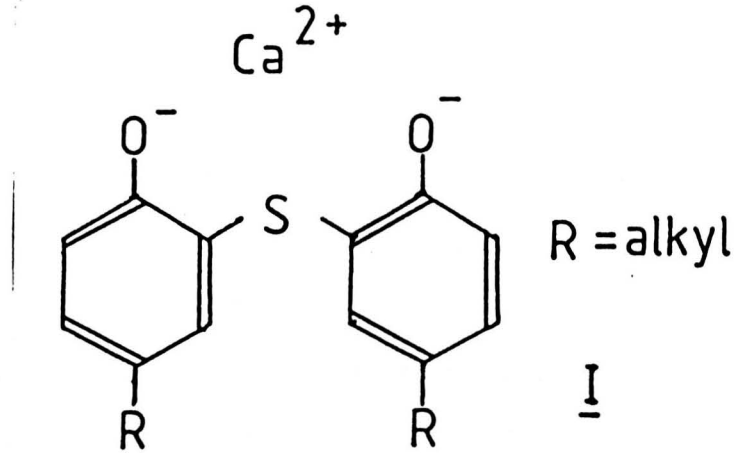


I

These are prepared industrially by methods which result in a complex mixture of compounds containing the product with varying alkyl chain lengths as well as products due to side reactions.

## 4.2 CURRENT ANALYTICAL PROCEDURE.

The analytical procedure currently used in the petroleum industry for analysis of sulphurised phenols consists of the following steps:-

(1) Hydrolysis of the metal salt to the phenol.

(2) Separation of the phenol sulphides mixture using HPLC.

(3) Analysis of the HPLC fractions by EI mass spectrometry and NMR.

The major problems associated with this procedure are the extensive sample pre-treatment involving hydrolysis and HPLC, and the use of EI mass spectrometry.

The electron impact mass spectrum presents problems because it is complicated by the fact that the sample is a complex mixture and because the spectrum exhibits extensive fragmentation. The electron impact spectrum of an HPLC fraction obtained from a sulphurised phenate sample is shown in figure 4.1; the essential features are five groups of fragment ions, all of which can be rationalised in terms of bond rupture in the alkyl chains or in the C-S bonds (see figure 4.2), and a group of low intensity (ca 15% base peak) molecular ions from 456 to 596 Daltons with maximum intensity at 554 Daltons.

## 4.3 POSSIBLE IMPROVEMENTS

The remainder of this chapter is concerned with the attempts to improve the analytical technique for sulphurised phenates.

The use of FAB mass spectrometry and GC/MS mass spectrometry to minimize sample pre-treatment is detailed in section 4.4 and 4.5 respectively.

Various chemical ionization techniques to simplify the mass spectra and to provide additional information on the structure of the sample

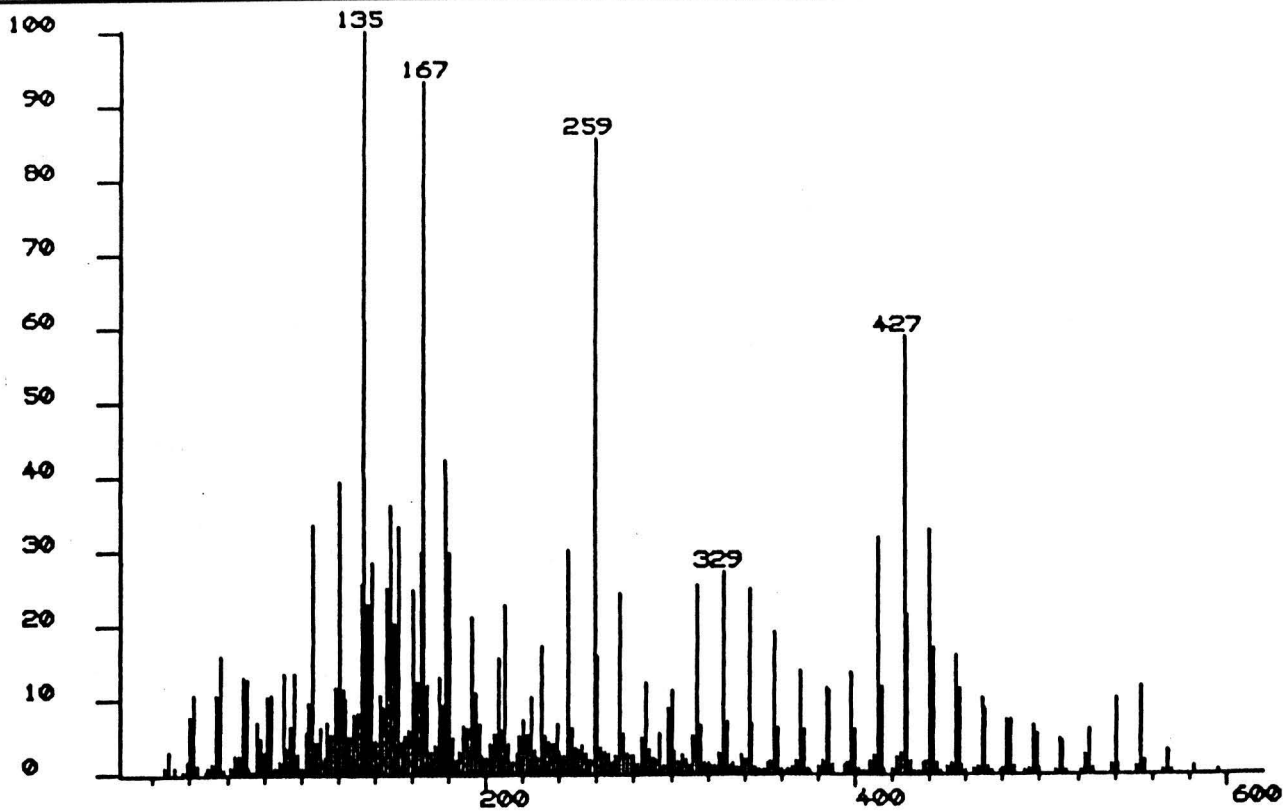


FIGURE 4.1: Electron Ionisation Mass Spectrum of Sulphurised Phenol Sample.

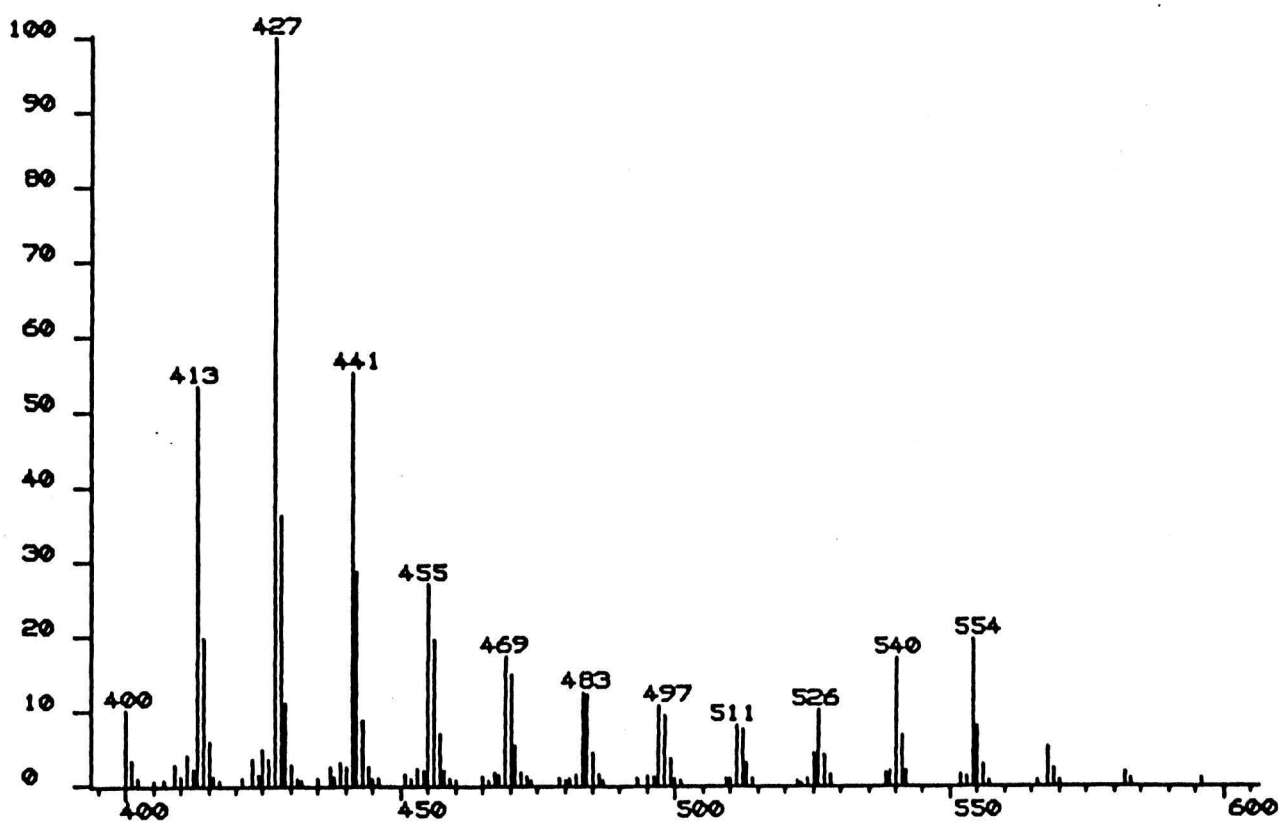


FIGURE 4.1(b): Electron Ionisation Mass Spectrum of Sulphurised Phenol Sample: (400-600) Daltons.

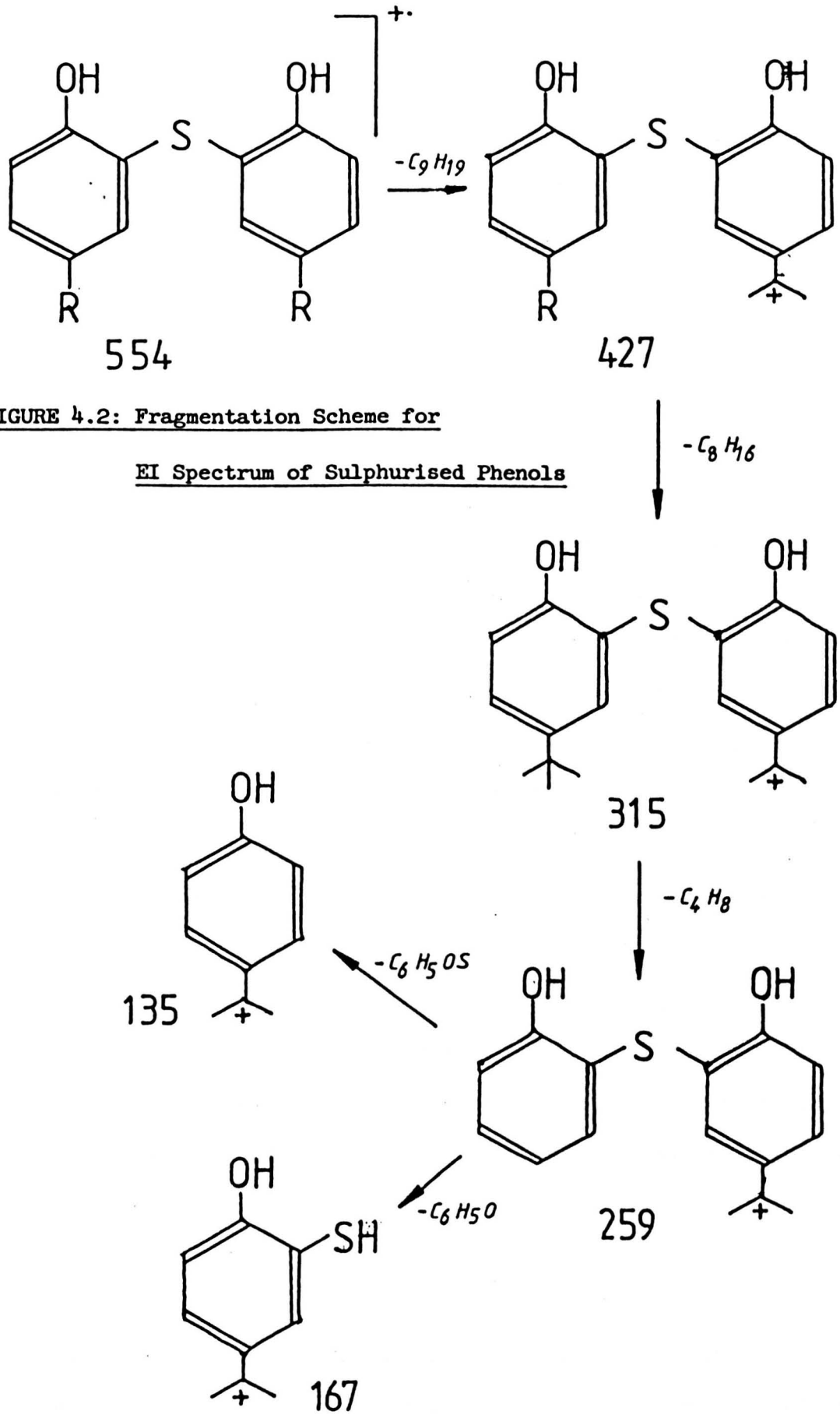


**FIGURE 4.2: Fragmentation Scheme for EI Spectrum of Sulphurised Phenols**

material is the concern of section 4.6.

Finaly, section 4.7 describes the attempts made to utilize metastable mapping techniques to provide structural information.

## 4.4 FAB MASS SPECTROMETRY OF SULPHURISED PHENATES.

### 4.4.1 Introduction

The usefulness of FAB mass spectrometry for the analysis of ionic compounds has already been mentioned, in the case of anionic and cationic surfactants, excellent spectra may be obtained when the surfactant properties of the matrix/sample are such that sample molecules are preferentially concentrated in the surface layers of the matrix. The attainment of such conditions can usually be found by appropriate selection of matrix.

For the common water soluble anionic detergents, glycerol has been recommended for the more soluble surfactants, and triethanolamine has been recommended for those that give poor results in glycerol (2).

The characteristic ions in FAB mass spectrometry can be quite complex due to cluster ion formation. These clusters may sometimes involve matrix molecules and/or metal ions from the sample. For example, the FAB mass spectra of alkylsulphonates (sodium salts) gives rise to $L_nNa_{n+1}^+$ ions in the positive ion FAB spectrum (n=1 to 7) and, $L^-$ and $NaL_2^-$ ions in negative ion FAB spectrum (3). The addition of metal salts to the matrix can influence the FAB spectra of compounds. Occasionally the presence of these metal ions in solution as

impurities can suppress the ion intensity of the sample in the mass spectrum (4), whilst, in some cases, the deliberate addition of metal ions can enhance the intensity of the molecular or pseudo-molecular ions in the mass spectrum (5).

Thus, FAB mass spectrometry, one would expect, is ideally suited to the analysis of sulphurised phenate lubricating oil additives. Circumventing the extensive sample preparation used in the current analytical technique by direct analysis of the metal salts using FAB mass spectrometry would allow one to carry out a more efficient and reliable analysis.

### 4.4.2 Experimental Details

Mass spectra were obtained on an MS-80 mass spectrometer ( Kratos Analytical). An Ion Tech atom gun and a standard Kratos FAB source were used. The sample was dissolved in glycerol, thioglycerol, triethanolamine, triethanolamine / sodium sulphate solution (3:1 triethanolamine / $Na_2SO_4$ soln. ca. 0.4 Molar) or squalane (2,6,10,15,19,23-hexamethyltetracosane) as matrix. Typically, the sample was bombarded with 6-7 keV xenon atoms. The mass spectrometer was operated on the 1200 Dalton mass range (2keV accelerating voltage) scanning at 30 sec/decade. This mass range was chosen because calibration was achieved using the characteristic mass peaks of triazine up to 966 Daltons.

The sample used was a commercial engine oil additive mixture, principally calcium 2,2'-bis (4-alkylphenyl) sulphide. This was kindly provided by the ESSO Research Centre, Abingdon.

### 4.4.3 Results and Discusion

Unfortunately both the positive and negative ion FAB mass spectra of the sample in all of the matrix materials available gave very poor spectra. All the spectra exhibited ions characteristic of the matrix, but, sample ions were either absent, or were present only as low mass low intensity fragment ions.

The poor results obtained were disappointing, especially for triethanolamine matrix which has been recommended for anionic surfactant samples.

If one considers the requirements for good FAB spectra - preferential concentration of the sample in the surface layers of the matrix and pre-formed ions in solution, one can interpret the failure of the current study in terms of these requirements: future FAB studies of these materials should benefit from a better understanding of their behaviour in matrix materials.

The need for pre-formed ions in solution is perhaps not the most important consideration, as the FAB spectrum of the saturated hydrocarbon, squalane illustrates.

It is likely that sulphurised phenate oil additives, being designed to form colloidal aggregates in lubricating oils, show poor solubility in such polar media as glycerol, thioglycerol and triethanolamine. It is probable that in these media the sample is merely held in (non-colloidal) suspension.

In the FAB spectra in which squalane was used as matrix, the poor results may be interpreted differently. Squalane is likely to be sufficiently close to lubricating oils for the additive to form micelles similar to those observed in lubricating oils themselves (6). As

expected, these micelles are reversed with respect to those found in aqueous media in that the oleophilic alkyl chains are on the 'outside' directed towards the bulk solution, whilst the oleophobic parts of the molecule are directed towards the centre.

It is unclear if, in oleophilic media, detergent molecules would be preferentially concentrated in the surface layers or form surface monolayers. Thus, it is possible that for the sulphurised phenate / squalane system, micelles occur in the bulk solution with negative surface concentration effects depleting the surface layers of sample molecules with respect to the bulk solution; in this case FAB mass spectrometry would not perform well.

Furthermore, in squalane the non-occurrence of pre-formed sample ions may or may not present difficulties. The ionisation processes occurring in FAB are not well understood - it is difficult to say why some compounds seem to require the presence of pre-formed ions whereas others do not.

In conclusion, it is felt that despite the failure of the current study, the possibility of using FAB mass spectrometry for the analysis of sulphurised phenate samples still holds promise. The possibility of finding a suitable matrix, perhaps with dielectric properties midway between those of triethanolamine and squalane, is still open. Some alternative matrix materials which have been mentioned in the literature are DAP (2,4-ditert-pentylphenol), TRITON X100 (alkylphenylpolyethyleneglycol) and various polyethyleneglycols (2). These are often used when sample solubility in glycerol and thioglycerol are poor. Some of the polyethyleneglycol mixtures also have the advantage that they can be used for mass calibration.

## 4.5 GC/MS ANALYSIS

### 4.5.1 Introduction

In an attempt to provide additional structural and compositional information on the sulphurated phenate mixture after hydrolysis, GC/MS analysis was used. It was decided however that direct GC/MS analysis of the sample would not be of use because of the relatively high polarity of the phenol groups and the relatively high molecular weight of the compounds involved. For this reason three derivatives were prepared, and prior to GC/MS analysis, their EI spectra were recorded to ascertain the degree of success of the derivatisation.

The GC/MS spectra were taken with both a packed column (OV101) and a 25 metre capillary column. In both cases the GC oven temperature was taken up to 300 $^{o}$C, the maximum working temperature for the columns. The OV101 packed column was used because of its low relative polarity and high working temperature.

### 4.5.2 Derivatives

The three derivatisations attempted were the silyl derivative, the acetyl derivative and the methyl derivative.

#### 4.5.2.1 Silyl Derivative.

The recipe used for the silylation was based upon a commercially available mixture which is recommended for derivatisation of phenol samples.

The silylation mixture consisted of dry pyridine, trimethylchorosilane and hexamethyl disiloxane in proportions 5:1:2. This was added in excess to a small sample of the sulphurised phenol mixture, the resulting solution was then injected directly into the GC inlet to give a GC/MS EI spectrum and, subsequently, a little of the mixture was used for an EI probe sample. The column used for this GC/MS run was the packed column, OV101.

The GC/MS results showed little evidence of sample material eluting through the chromatography column apart from solvent (pyridine).

Examination of the EI spectrum of the probe sample showed evidence of derivatisation: the mass peak corresponding to the monosilyl derivative was ca. 41% of that due to the original phenol (measured at 626 Daltons and 554 Dalton respectively). No ion intensity was observed at the mass peak (698 Daltons) corresponding to the disilyl derivative. The EI spectrum of the probe sample is shown in figure 4.3.

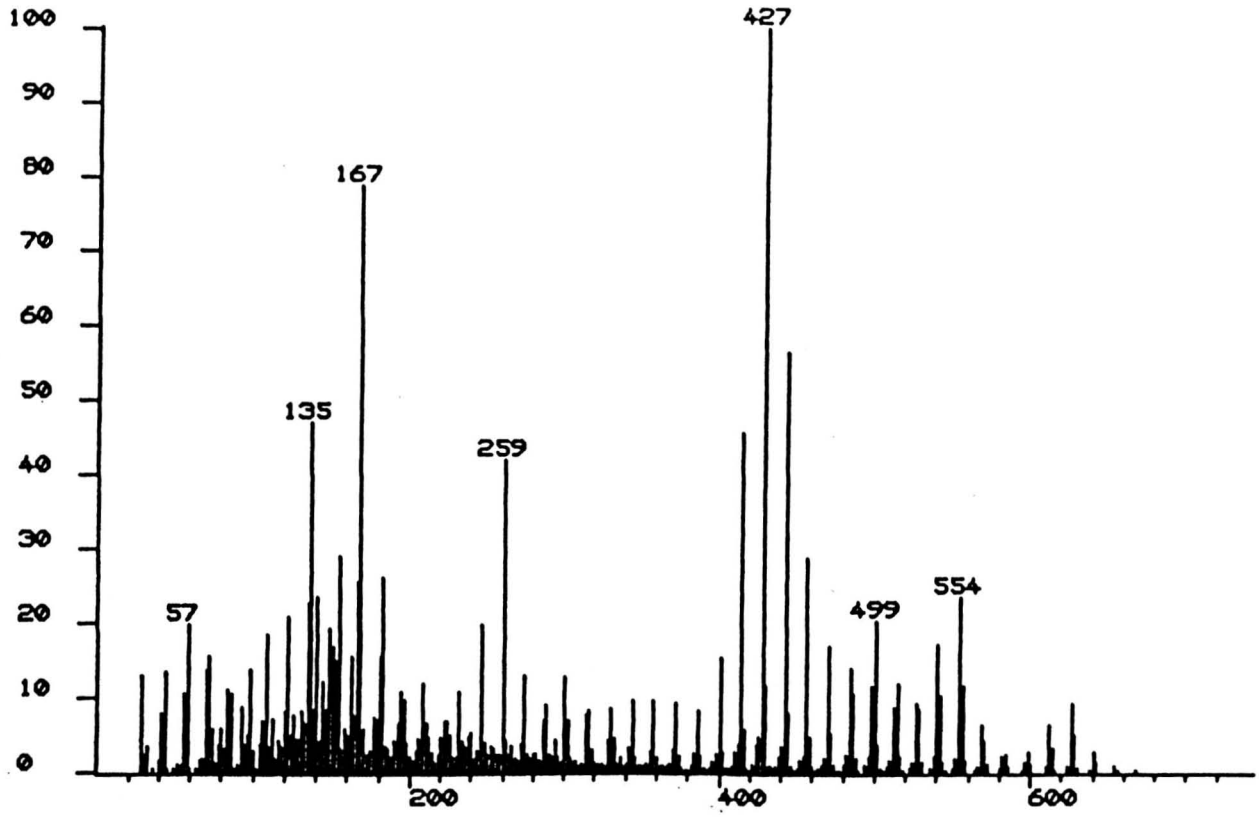


FIGURE 4.3: Electron Ionisation Mass Spectrum of the $Me_3Si$ Derivative of Sulphurised Phenol

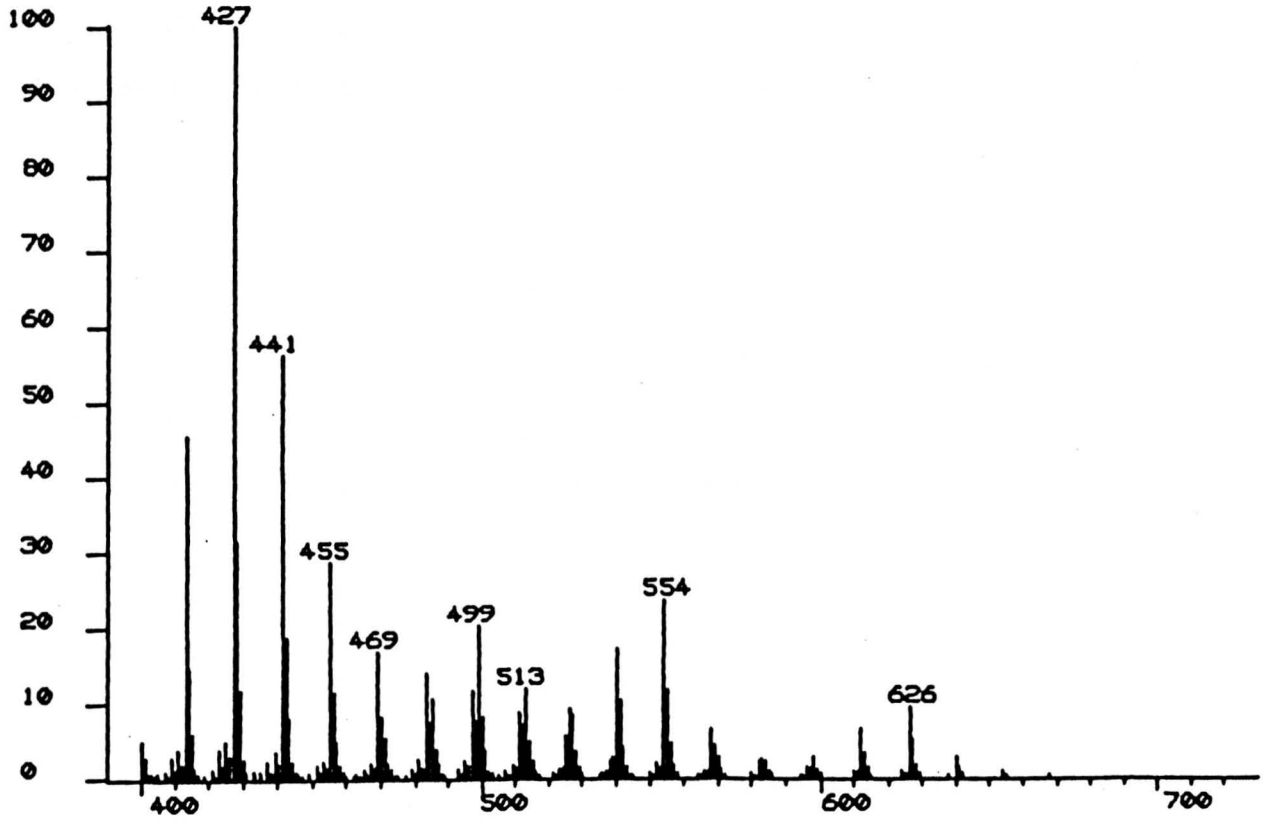


FIGURE 4.3(b): Electron Ionisation Mass Spectrum of the $Me_3Si$ Derivative of Sulphurised Phenol (in the range 400 - 700 Daltons)

#### 4.5.2.2 Acetyl Derivative.

The preparation of the acetyl derivative was as follows. A small sample (ca. 0.1 g) of the sulphurised phenol was dissolved in dry pyridine (ca. 5 ml). The solution was cooled in an ice bath, and acetyl chloride was added drop-wise whilst maintaining the temperature at or below 10 $^{o}$C. Acetyl chloride was added in excess after reaction ceased, to ensure complete derivatisation. The mixture was added to a dilute solution of sulphuric acid, and the organic products extracted into an diethyl ether layer in a separating funnel. The ether was distilled under partial vacuum in a rotary evaporator until the product was isolated as a red/brown tarry liquid. The product was dissolved in methanol to remove it easily from the flask. The solution was then used directly for EI probe samples, and as a dilute solution in methanol for GC/MS analysis using both the packed column and the capillary column.

The EI spectrum showed that, like the silylation, derivatisation only proceeded as far as the mono- derivative. The acetyl derivatisation was more successful, as the mass peak intensity due to the mono-acetyl derivative (596 Daltons) was ca. 500% that of the mass peak due to the sulphurised phenol.

Both GC/MS experiments proved unsuccessful, no ions were observed which could be attributed to the sample.

#### 4.5.2.3 Methyl Derivative.

The methylation proceeded in the same manner as the acetylation, except that the active reagent used was methyl sulphate instead of acetyl chloride, and the product was dissolved in chloroform before being used.

The EI probe sample spectrum is shown in figure 4.4. The peak in the molecular ion region of the spectrum shows a maximum at 582 Daltons (as opposed to a maximum at 554 Daltons in the original sample), however, as the mass peaks of the derivatives overlap those of the original phenol, it is difficult to ascertain the degree of derivatisation. One may, however, conclude that derivatisation was successful.

Again GC/MS analyses were carried out using both packed column and capillary column, and again these were unsuccessful.

### 4.5.3 Discussion.

The failure of the GC/MS experiments is probably due to the relatively high molecular weight of the sample material. In addition, it is possible that since the derivatisations appear to have only proceeded to the mono derivative stage, the derivatives may have remained sufficiently polar to fail to elute through the columns.

A more appropriate mass spectrometric technique would be LC/MS, which though a relatively new technique holds much promise. With the 'thermo-spray' interface technique (7), which may be regarded as an

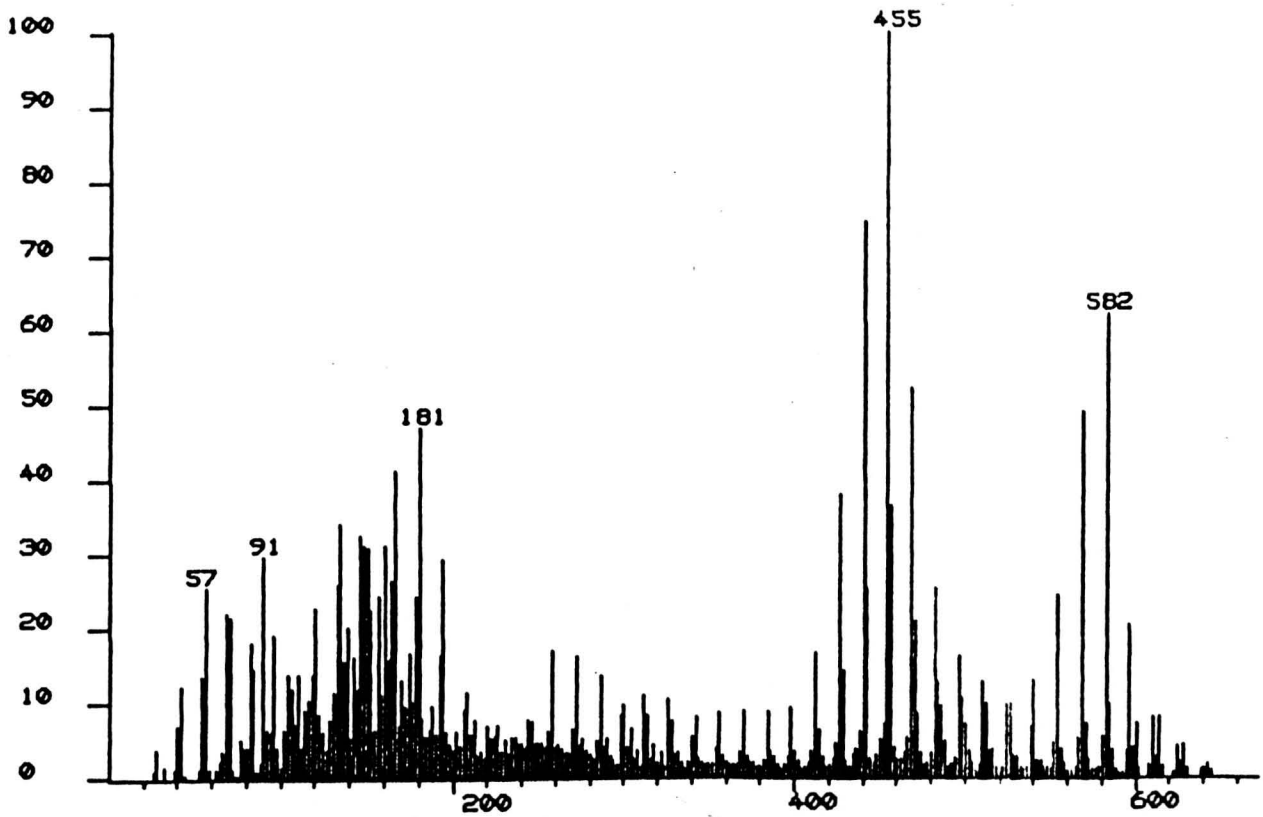


FIGURE 4.4: Electron Ionisation Spectrum of

the Methyl Derivative of Sulphurised Phenol

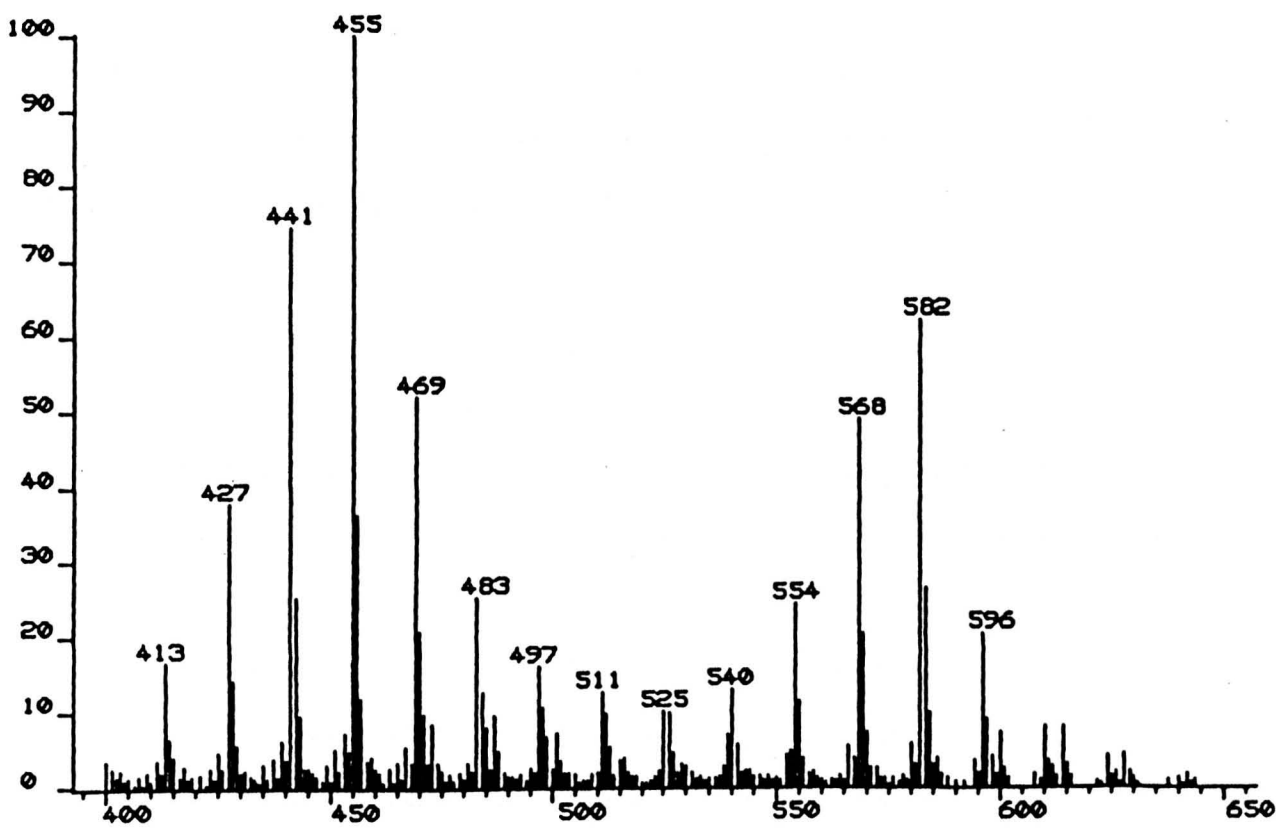


FIGURE 4.4(b): As above, in the range 400 - 650 Daltons.

ionisation technique in its own right, LC/MS should provide useful mixture separation coupled with soft ionisation of sulphurised phenol mixtures.

The alternative LC/MS interface, the moving belt interface (8), may also provide useful mixture separation and soft ionisation for some samples, as it is possible to use the FAB ionisation technique. However, with LC/FABMS it may not be possible to analyse the sulphurised phenate samples because of the failure of FAB ionisation with these samples without an appropriate matrix (see section 4.4 above).

## 4.6 CHEMICAL IONISATION.

### 4.6.1 Introduction.

The promise of CI techniques in mass spectrometry to provide controlled fragmentation and characteristic ionisation modes makes CI techniques second only to EI mass spectrometry in importance.

The main thrust of the CI studies on the sulphurised phenols is to reduce fragmentation to a minimum, thus enabling one to determine the molecular weight distribution of the sample mixture. It will be noted that the EI spectra of these materials does allow one to determine the molecular weight distribution, but the distribution is distorted at the low mass end of the distribution due to interference from C-13 isotope peaks of adjacent fragment ions. Any technique that simplifies the determination of the distribution would therefore make an important contribution to the routine analysis of these lubricating oil additives.

Additionally, it was hoped that CI techniques, in conjunction with

collision induced fragmentation studies, would be able to throw light upon the detailed structure of these molecules, as this information may be relevent to an understanding of their surfactant properties and the reaction mechanisms involved in their commercial preparation.

### 4.6.2 Ammonia CI of Sulphurised Phenols.

Positive CI using proton transfer reagents is the most commonly used CI technique because it is generally applicable to a wide range of sample molecules and because there are several reagent gases available. Of the commonly used reagent gases, (methane, iso-butane and ammonia), ammonia provides reagent ions which if they react with the sample molecules by protonation, transfer the least amount of energy to the product ions. Therefore, there is often little fragmentation of the pseudo-molecular ions produced with ammonia CI:-

$$NH_4^+ + M \rightarrow MH^+ + NH_3$$

$$\& \quad \Delta E = -\Delta H = PA(M) - PA(NH_3)$$

where $\Delta E$ is the exoergicity of the reaction.

The ammonia CI spectrum of a sulphurised phenol probe sample is shown in figure 4.5. It can be seen that protonation gives low intensity pseudo-molecular ions with a maximum intensity at 555 Daltons. Comparing this with the EI spectrum, fig. 4.1, it can be seen that fragmentation is reduced somewhat but is still significant.

It may be concluded that the common proton transfer reagents used

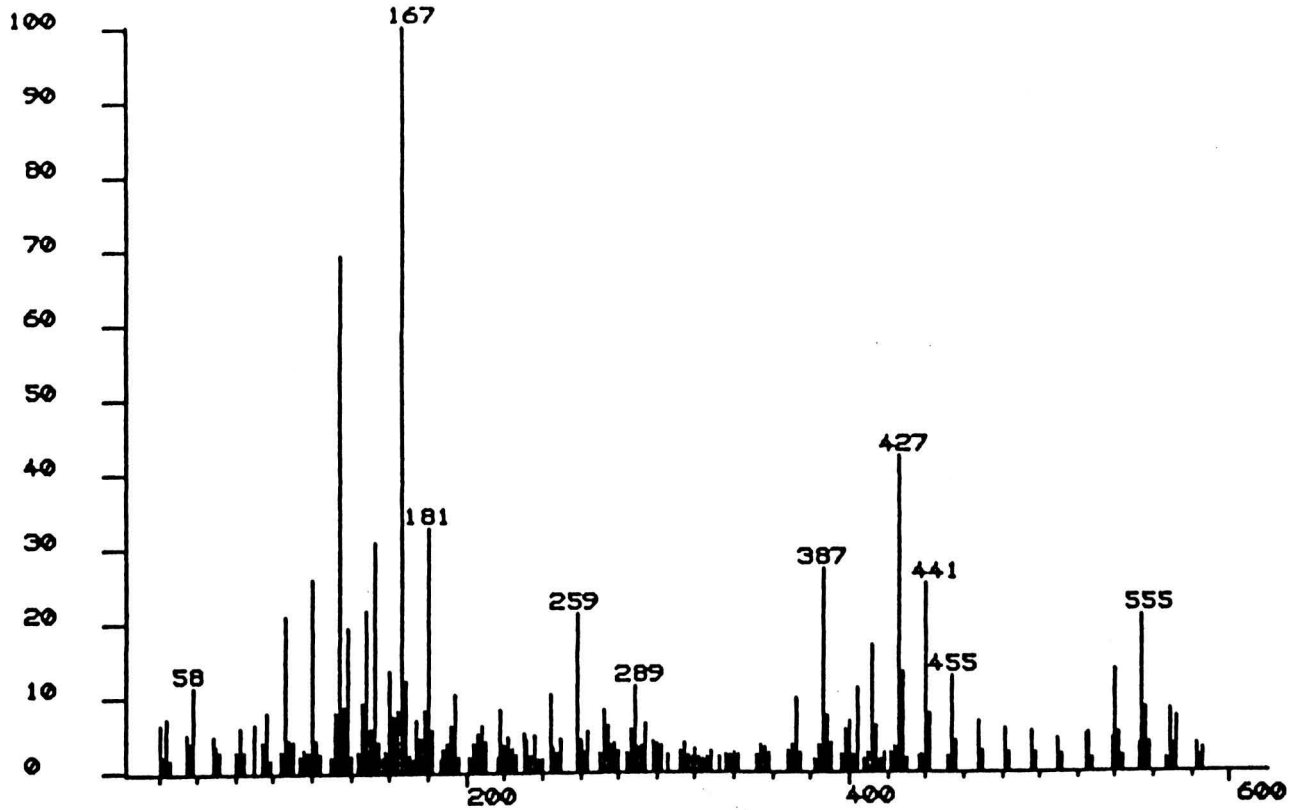


FIGURE 4.5: Ammonia Chemical Ionisation Spectrum of a Sulphurised Phenol Sample.

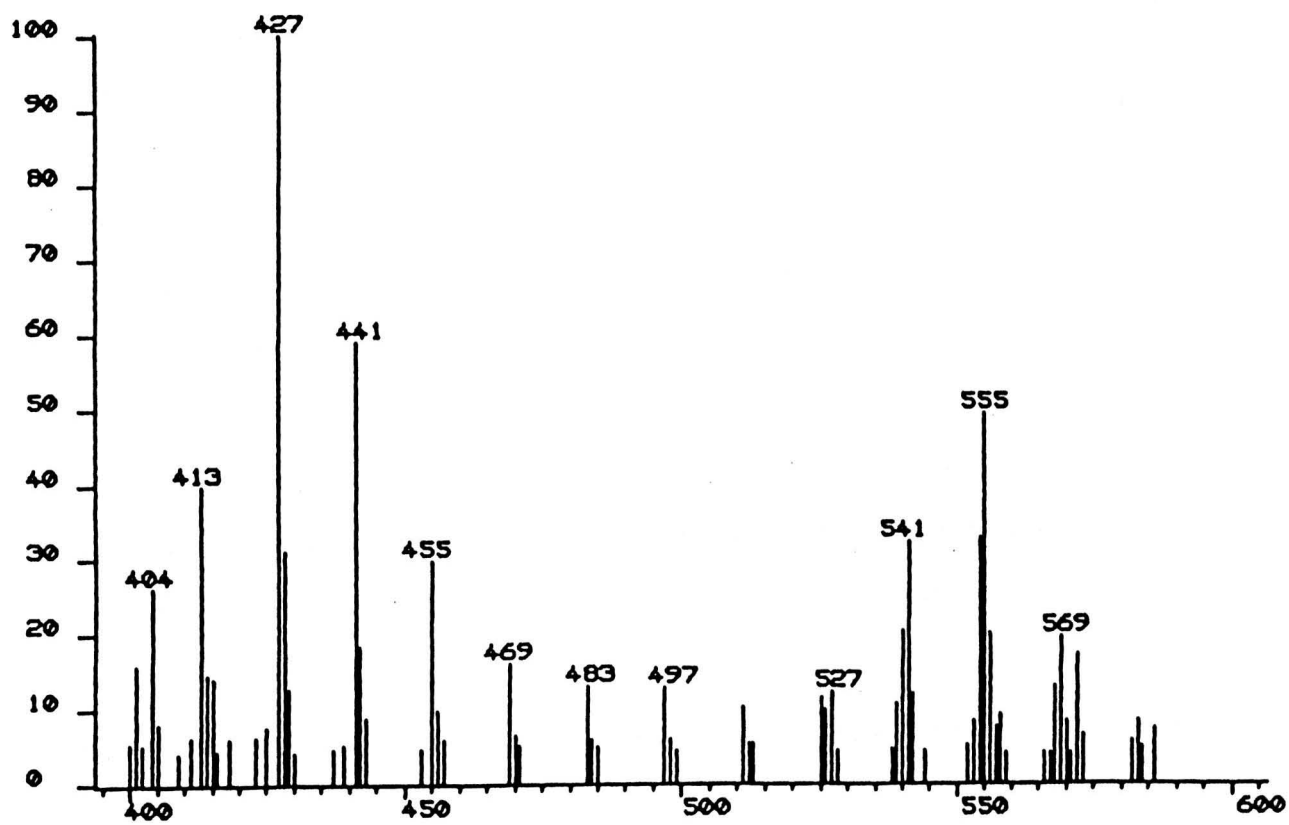


FIGURE 4.5: As above, in the range 400 - 600 Daltons.

in positive CI will be of little use in the analysis of sulphurised phenols.

### 4.6.3 $NO^+$ Charge Transfer CI of Sulphurised Phenols.

In positive CI an alternative technique to proton tranfer ionisation which allows controlled fragmentation is charge transfer ionisation:-

$$R^+ + M \rightarrow R + M^+$$

$$\& \ \Delta E = -H = I(R) - I(M)$$

where R refers to reagent and M to sample molecule, and I(x), is the ionisation energy of x.

The nitric oxide chemical ionisation spectrum of a probe sample of a sulphurised phenol fraction was recorded using a mixture of nitric oxide and hydrogen (5% NO in $H_2$) as reagent gas.

The spectrum showed much fragmentation, and exhibited significant peak intensities at 31 Daltons and at 47 Daltons. It is concluded that the reagent gases were contaminated with oxygen to produce nitrogen dioxide and that therefore, the nitric oxide concentration was too low in comparison with the hydrogen concentration. The extensive fragmentation and the peaks at 31 Daltons and 47 Daltons can be explained by the presence of $H_3^+$ due to the reactions:-

$$H_3^+ + NO \rightarrow HNO^+ + H_2$$

$$H_3^+ + NO_2 \rightarrow HNO_2^+ + H_2$$

$$H_3^+ + M \rightarrow MH^{+*} + H_2$$

and

$$MH^{+*} \rightarrow \text{fragments}$$

Unfortunately it was not possible to carry out further experiments because the nitric oxide cylinder was empty, and a replacement was not available in time.

## 4.7 Electron Capture Ionisation.

Electron capture spectra were recorded using the MS-80 mass spectrometer with ammonia as buffer gas. Several spectra were recorded using iso-butane as buffer gas to check for the presence of mass spectral features specific to the buffer gas; none was observed.

Initially, source tuning and mass calibration was carried out in positive ion mode using PFK, it was assumed that the source tuning parameters did not need adjusting when the instrument was operated in negative ion mode. It was found that this resulted in poor sensitivity and mis-calibration at higher masses. Source tuning and calibration was then achieved using a mixture of PFK and carbon tetrachloride with the instrument operated in negative ion mode. The calibration range was from

35 Daltons to ca. 600 Daltons. With PFK alone as calibrating sample, calibration could be achieved in negative ion mode from 119 Daltons. This mass range was adequate as the ions of interest were of higher relative molecular mass; it also avoided interference of the electron capture spectra due to the presence of residual carbon tetrachloride (see below).

### 4.7.1 Electron Capture Spectrum of Sulphurised Phenols.

The electron capture spectrum of a sulphurised phenol sample is shown in figure 4.6.

Two main groups of ions are observed: high intensity molecular ions from 400 to 582 Daltons, with a maximum intensity at 554 Daltons (ca. 30% of base peak); and a series of ions, presumably fragment ions, from 180 to 320 Daltons, with a maximum at 292 Daltons, these are the most intense ions in the spectrum; the peak at 292 Daltons is the base peak.

A much less intense group of ions occurs with a maxima at 385 Daltons (ca 10% base peak).

Compared with the electron impact spectrum, the electron capture give greater intensity molecular ions and without obscuring fragment ions. The fragment ions in the electron capture spectrum have no corresponding fragment ions in the electron impact spectrum and they are simpler to interpret. The main group of fragment ions in the electron capture spectrum have been tentatively assigned the structure below (II).

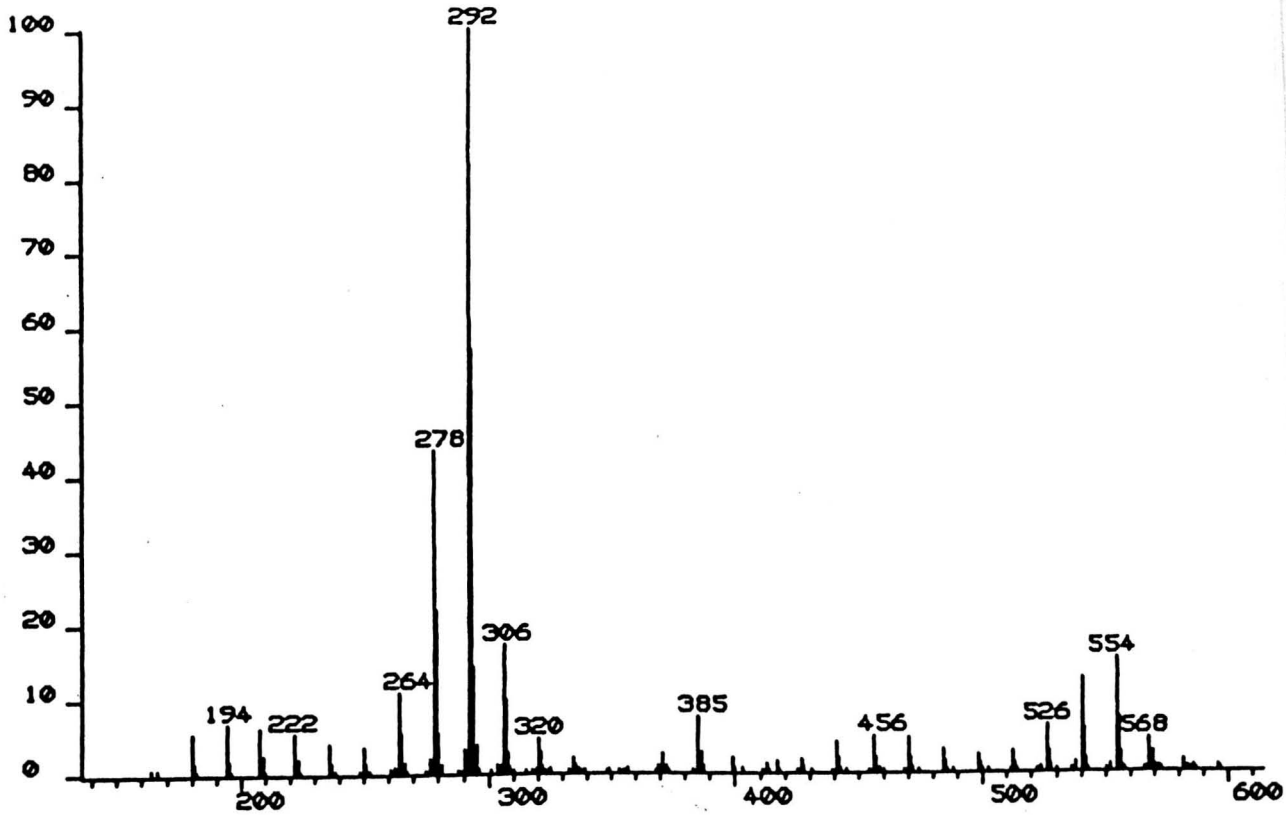


FIGURE 4.6: Electron Capture Ionisation Spectrum of a Sulphurised Phenol Sample.

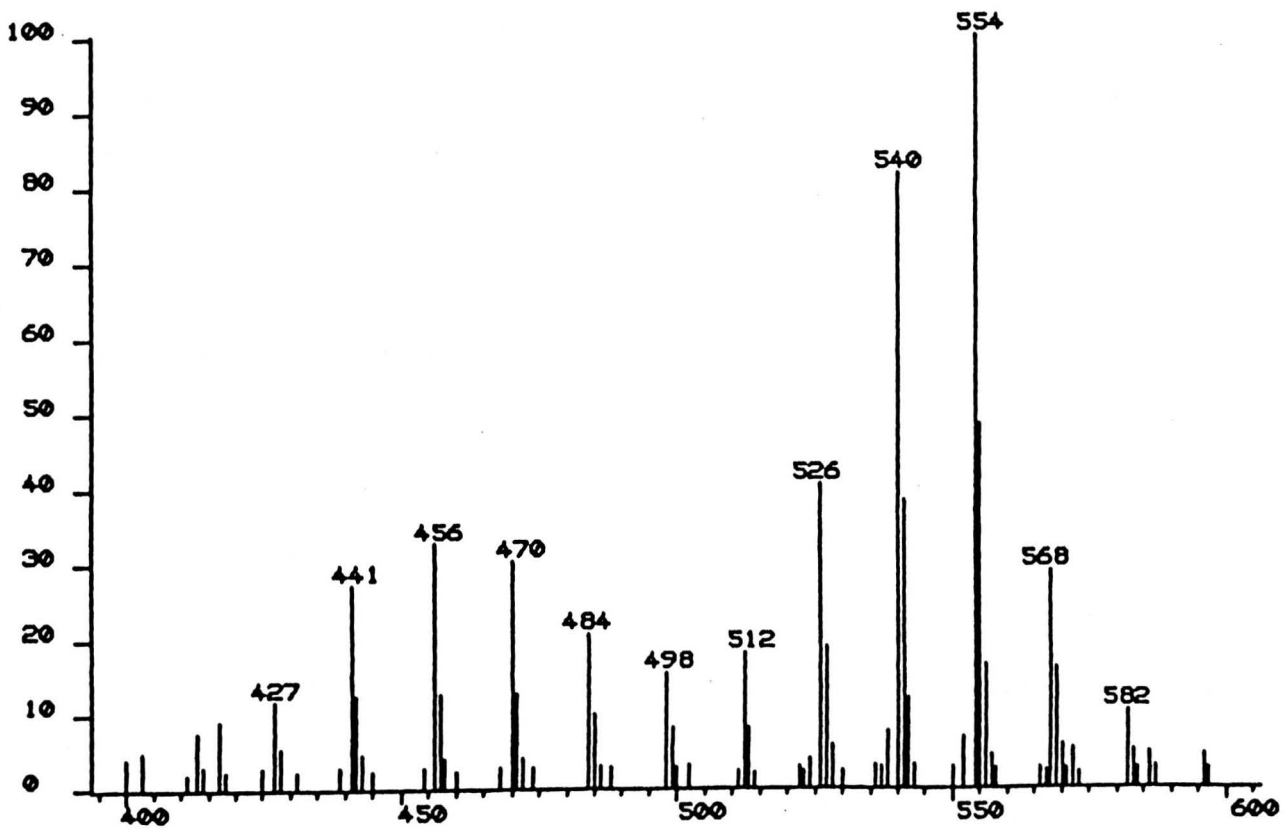


FIGURE 4.6(b): As above, in the range 400 - 600 Daltons.

II 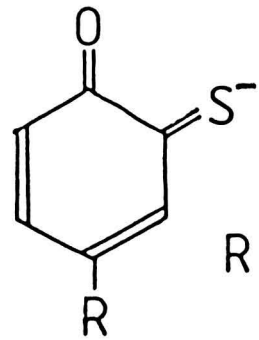


R = alkyl

The group of ions with the maxima at 385 Daltons can be explained by simple chain cleavage with the loss of the whole of one of the alkyl chains.

### 4.7.2 Sulphurised Phenol Derivatives.

The electron capture spectra of the methyl and acetyl derivatives of the sulphurised phenol sample are shown in figures 4.7 and 4.8 respectively.

Both spectra show pseudo-molecular ions at masses which may correspond to either $(M + 32)^-$ or $(M + 18)^-$, these are attributed to ions solvated with one water molecule or one methanol molecule. For the methyl derivative these ions occur at 404 to 656 Daltons, with maximum ion intensity at 586 Daltons; and for the acetyl derivative they occur at 432 to 684 Daltons, with a maximum intensity at 614 Daltons.

To confirm the nature of these pseudo-molecular ions, electron capture spectra of the original sample were recorded. For the first sample, the phenol was mixed with a little water, and for the second sample it was dissolved in methanol. The water/phenol sample gave quite intense $(M + H_2O)^-$ ions, whilst the methanol/phenol sample gave analogous $(M + CH_3OH)^-$ ions. One of the methanol/phenol sample

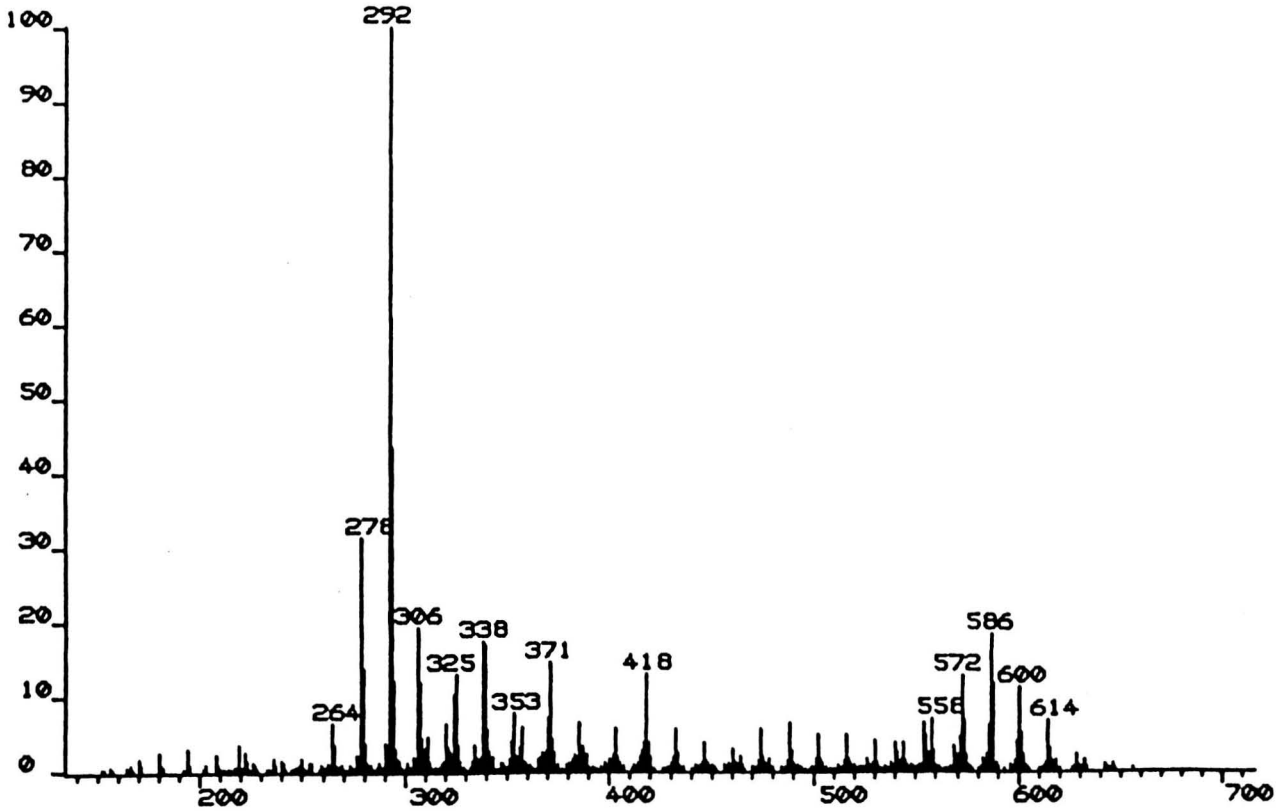


FIGURE 4.7: Electron Capture Ionisation Spectrum of the Methyl Derivative of Sulphurised Phenol

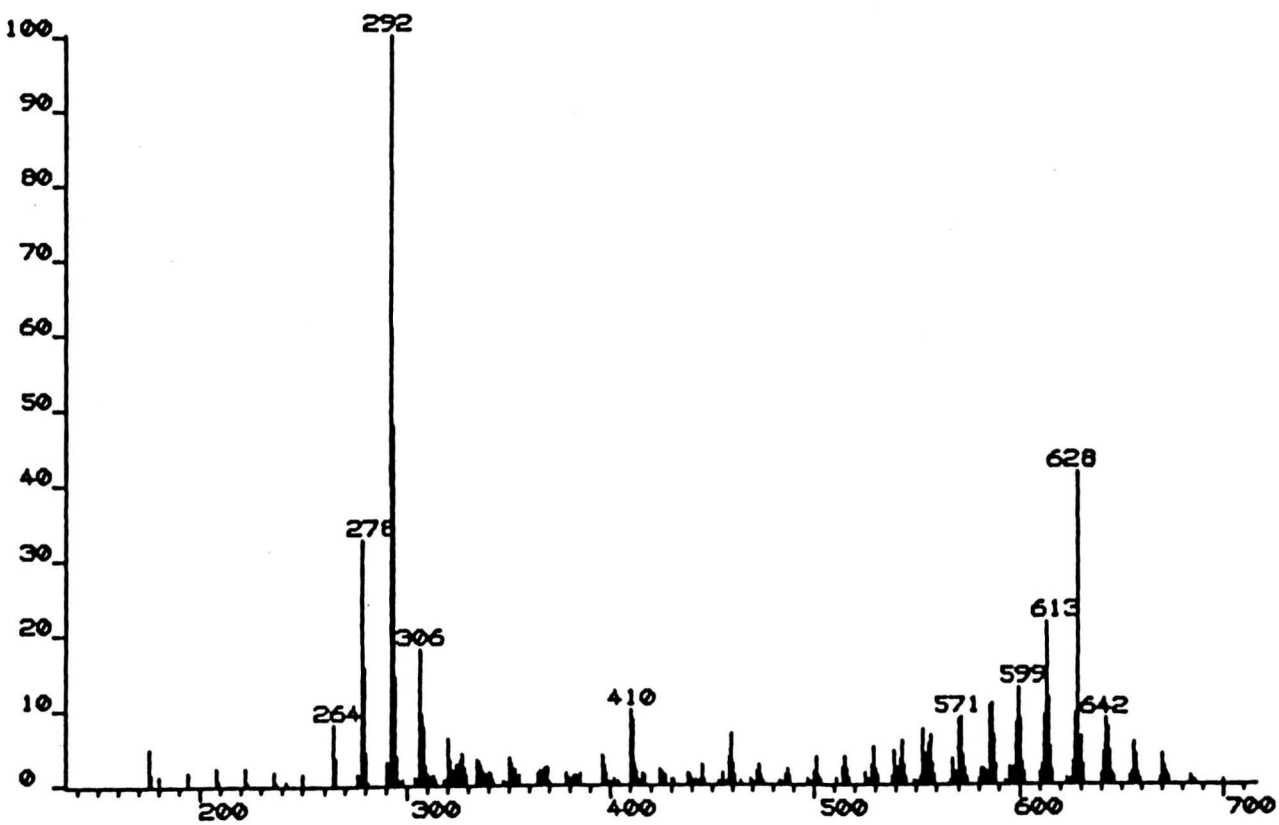


FIGURE 4.8: Electron Capture Ionisation Spectrum of the Acetyl Derivative of Sulphurised Phenol

spectra is shown in figure 4.9. The occurrence of $(M + CH_3OH)^-$ ions presents difficulties when interpreting the electron capture spectra of the methyl derivative of the sulphurised phenol sample, as the methanol solvated ions from the original sample occur at the same masses as the water solvated methyl derivatives, i.e. $(M\text{-}OH + CH_3OH)^-$ and $(M\text{-}OCH_3 + H_2O)^-$ have the same relative molecular mass.

Attempts to dry the derivative samples over dry silica gel in a desiccator and by using molecular sieve granules proved to have little effect on the their mass spectra. It is possible that there is enough water vapour in the CI gas inlet system of the mass spectrometer to account for the presence of these ions.

The other feature of the electron capture spectra of the derivatives is the occurrence of the fragment ions, these occur at the same masses as in the underivatised sample (with maximum intensity at 292 Daltons). Fragment ions containing the substituted phenol group appear only in relatively low intensities, e.g. in the electron capture spectrum of the methyl derivative the fragment ion at 338 Daltons may be attributed to $(M'\text{-}OCH_3 + CH_3OH)^-$, where M'-OH corresponds to the fragment ion observed in the electron capture spectrum of the underivatised phenol occurring at 292 Daltons.

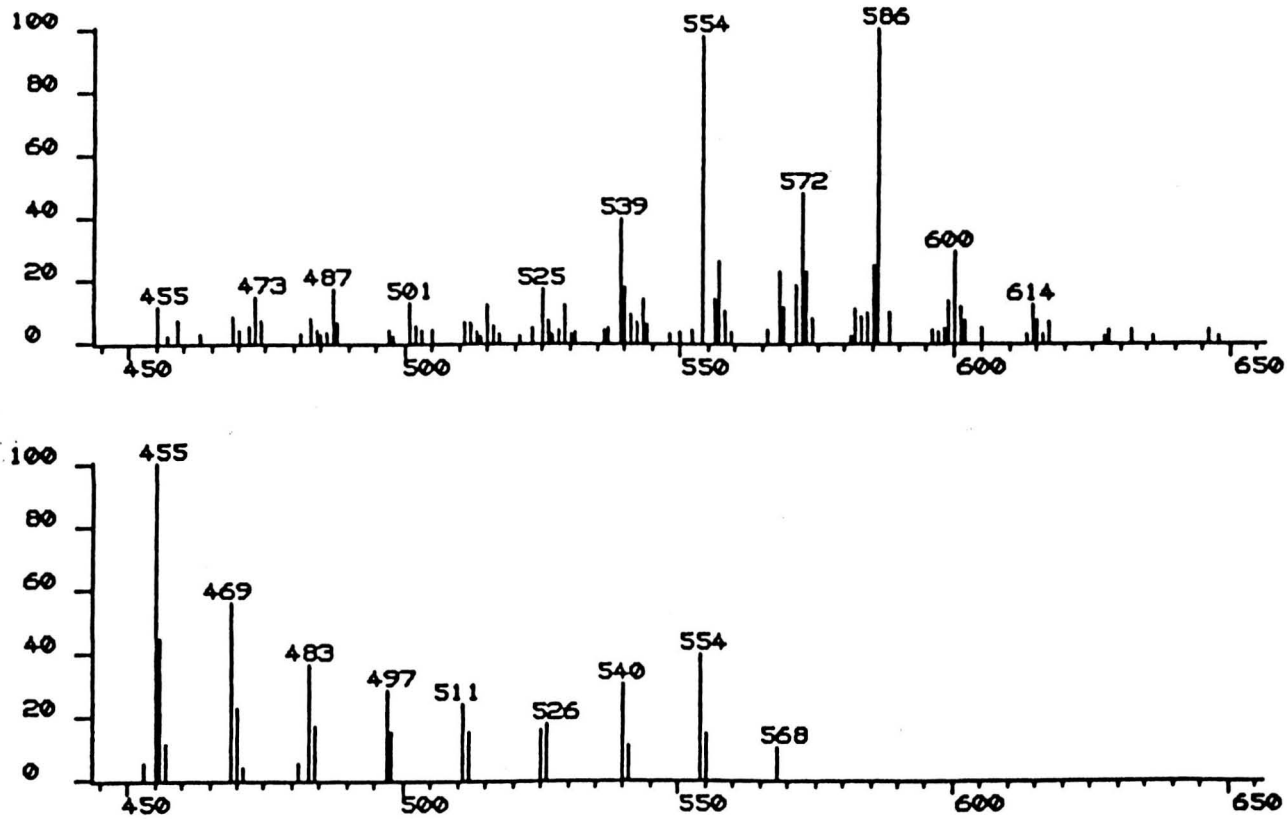


FIGURE 4.9: Mass Spectra of Methanol / Sulphurised Phenol Mixture.

Comparison of the EC spectrum (top) and the EI spectrum of sulphurised phenol / methanol mixtures, shows the presence of solvated negative ions, $(M+MeOH)^-$, in the EC spectrum at 572, 586, 600 and 614 Daltons. Analogous ions due to $(M+H_2O)^-$ are also observed in the EC spectra of sulphurised phenol / water mixtures.

### 4.7.3 Effects of Temperature & Pressure on Spectra.

A set of electron capture spectra were recorded in which the buffer gas pressure was varied. Figure 4.10 shows the ratio I(292)/I(554) as a function of source housing pressure. The observed effect upon the spectra at the higher pressures, where the ratio I(292)/I(554) decreases slowly, is not significant, as it appears to be more related to the sample pressure than to the buffer gas pressure. To illustrate this, figure 4.11 shows the ratio of I(292)/I(554) as a function of the total ion current due to sample ions, which is assumed to be proportional to the sample pressure.

The over-all sensitivity was optimum when the buffer gas pressure was such that the source housing pressure was in the range $10^{-4}$ to $10^{-3}$ torr.

Changes in the probe temperature had a more dramatic effect. Figure 4.12 shows the summed ion intensities for two mass ranges during a run in which the probe temperature setting was changed. The summation of the higher masses, which incorporate the molecular ion intensities, shows very little change during the run. The low mass ions, corresponding to fragment ions, shows a marked increase in intensity with probe temperature. It may be concluded that the fragment ions are primarily produced by pyrolysis.

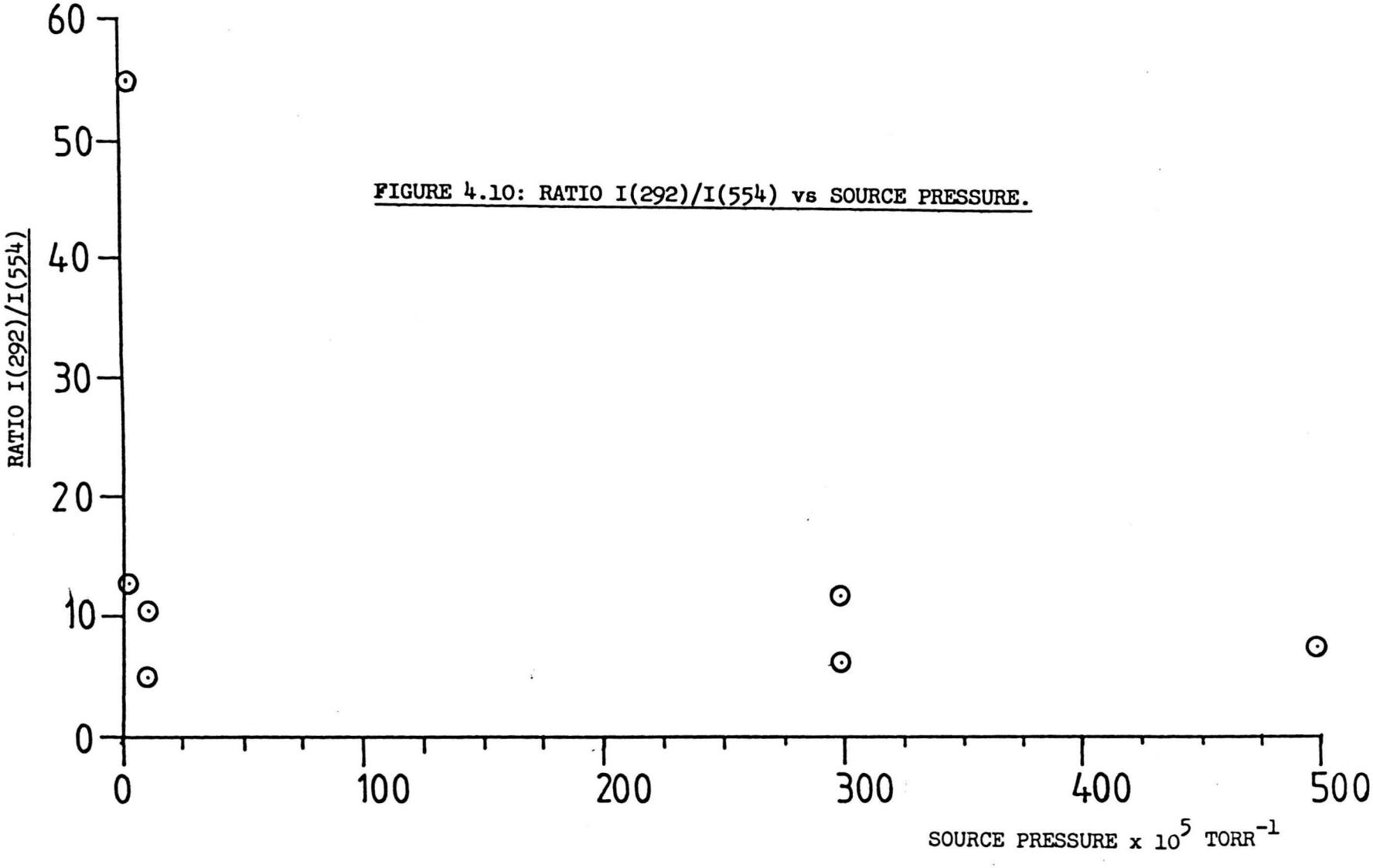


FIGURE 4.10: RATIO I(292)/I(554) vs SOURCE PRESSURE.

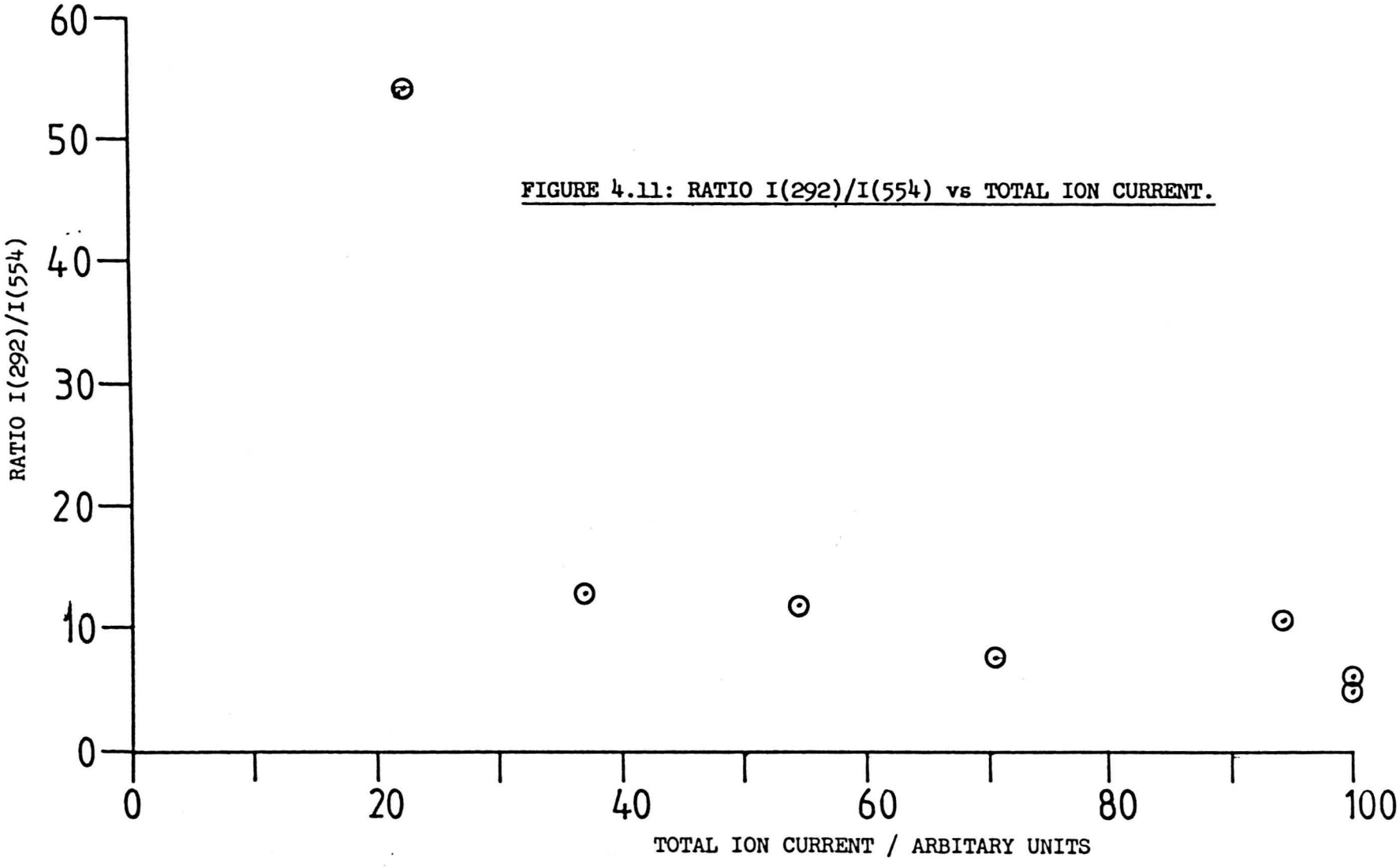


FIGURE 4.11: RATIO I(292)/I(554) vs TOTAL ION CURRENT.

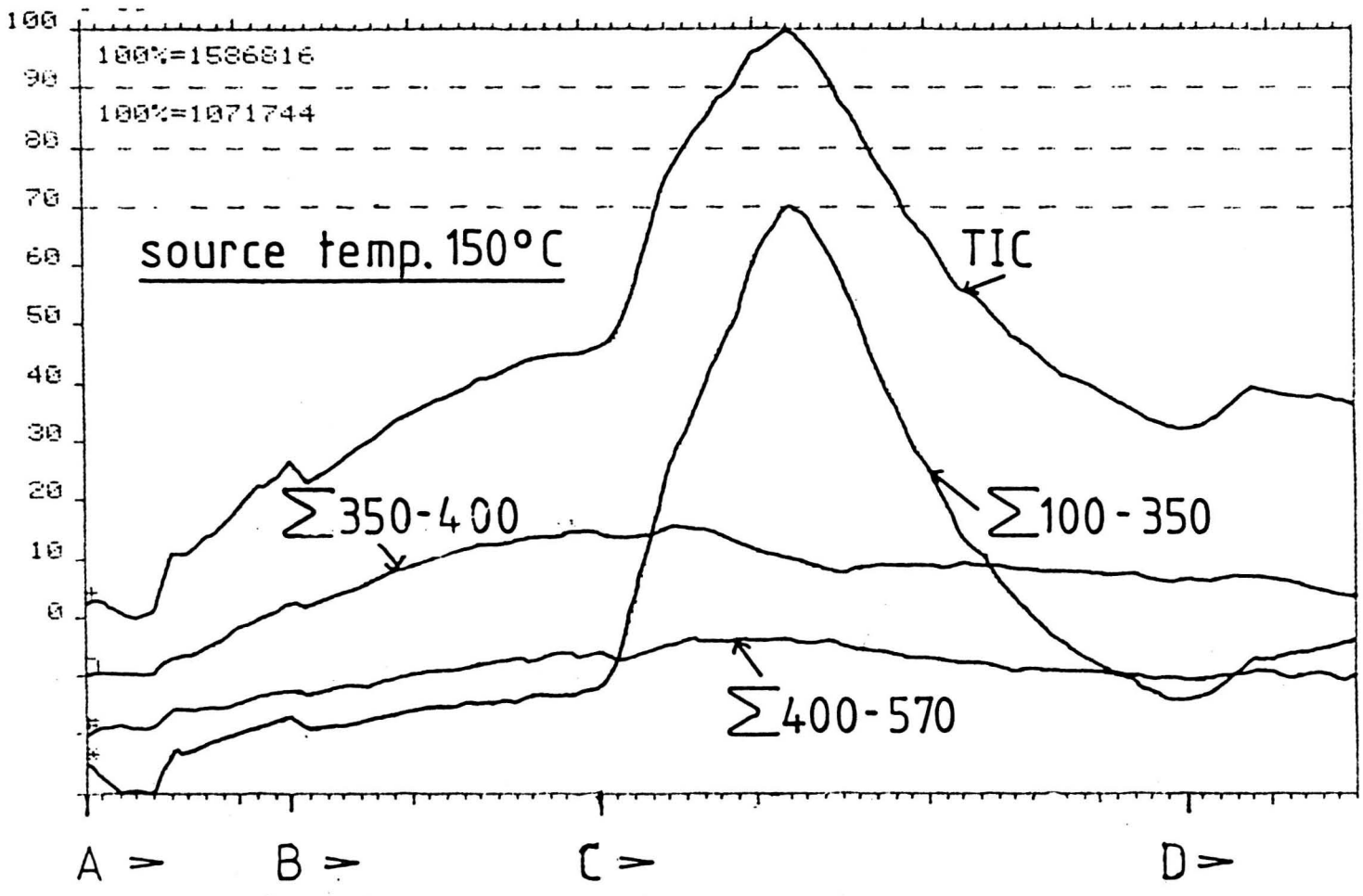


**FIGURE 4.12: Summed Ion Currents Cross-Scan Plot:**

KEY: A - Probe temp. 150°C, B - Probe temp. increasing to 200°C,

C - Probe temp. increasing to 300°C, D - Source temp. increasing to 200°C.

### 4.7.4 Conclusions.

The technique of electron capture ionisation offers a simple and efficient method for the qualitative analysis of sulphurised phenol samples. For these samples it is very sensitive, and gives intense molecular ions; the peak at 554 Dalton in EC spectrum is typically ten to twenty times the intensity of the peak at 554 Daltons in the EI spectrum for the similar sample sizes. The relative molecular weight distribution of ions in the molecular ion region are shown in table 4.1. This table also shows the distribution found in the EI spectrum; both distributions are corrected for contributions due to heavy isotopes of carbon, hydrogen and sulphur in the preceding (M-H) peaks. No correction was made for heavy isotopes of carbon, hydrogen and oxygen contributing to the intensity from (M-2H) peaks, but contributions to the intensities from $^{34}S$ was allowed for as the natural abundance of $^{34}S$ is relatively high at 4.2%. As can be seen from the table, inteference due to heavy isotopes is more of a problem in the EI spectrum.

The relative molecular weight distributions in the two spectra are quite different; unfortunately, there is no alternative analytical technique which can allow one to decide which mass spectrum gives the most reliable results.

Assuming that the EC spectrum yields ions which correctly reflect the relative molecular mass distribution of the sample, then the simple fragmentation also enables the relative molecular weight distribution of the alkyl side chains to be determined.

The technique is not sensitive to buffer gas pressure, but the

TABLE 4.1(A)

| N+M | MASS | INT | INT(CORR.) |
|---|---|---|---|
| 6 | 330 | 0.00 | 0.00 |
| 7 | 344 | 0.00 | 0.00 |
| 8 | 358 | 0.00 | 0.00 |
| 9 | 372 | 0.00 | 0.00 |
| 10 | 386 | 0.00 | 0.00 |
| 11 | 400 | 0.00 | 0.00 |
| 12 | 414 | 54.35 | 19.69 |
| 13 | 428 | 100.00 | 28.62 |
| 14 | 442 | 79.11 | 57.29 |
| 15 | 456 | 53.71 | 55.06 |
| 16 | 470 | 41.08 | 46.88 |
| 17 | 484 | 34.02 | 41.27 |
| 18 | 498 | 25.51 | 27.75 |
| 19 | 512 | 20.75 | 23.50 |
| 20 | 526 | 28.09 | 44.43 |
| 21 | 540 | 46.87 | 84.16 |
| 22 | 554 | 54.28 | 100.00 |
| 23 | 568 | 14.15 | 25.93 |
| 24 | 582 | 4.72 | 8.93 |
| 25 | 596 | 2.27 | 4.29 |
| 26 | 610 | 0.00 | 0.00 |
| 27 | 624 | 0.00 | 0.00 |

**TABLE 4.1(A):** Relative molecular weight distribution of sulphurised phenols calculated from the EI spectrum. The 'INT(CORR)' values are calculated from the intensities at the $(M)^+$ peaks and the isotope contributions from the corresponding $(M-H)^+$ and $(M-2H)^+$ peaks, taking into account $^{13}C$, $^{2}H$, $^{17}O$ and $^{33}S$ isotopes from (M-H); and the $^{34}S$ and $^{18}O$ isotopes from (M-2H). The fraction of molecules containing more than one heavy isotope was assumed to be negligible.

TABLE 4.1(B)

| N+M | MASS | INT | INT(CORR.) |
|---|---|---|---|
| 6 | 330 | 0.63 | 0.40 |
| 7 | 344 | 0.00 | 0.00 |
| 8 | 358 | 0.00 | 0.00 |
| 9 | 372 | 1.24 | 0.39 |
| 10 | 386 | 2.32 | 0.69 |
| 11 | 400 | 1.76 | 1.86 |
| 12 | 414 | 1.50 | 1.52 |
| 13 | 428 | 1.92 | 1.42 |
| 14 | 442 | 2.90 | 2.77 |
| 15 | 456 | 3.52 | 3.71 |
| 16 | 470 | 3.79 | 3.71 |
| 17 | 484 | 4.61 | 4.57 |
| 18 | 498 | 3.78 | 3.53 |
| 19 | 512 | 7.18 | 6.88 |
| 20 | 526 | 21.13 | 20.94 |
| 21 | 540 | 62.48 | 62.83 |
| 22 | 554 | 100.00 | 100.00 |
| 23 | 568 | 32.73 | 32.61 |
| 24 | 582 | 13.88 | 13.57 |
| 25 | 596 | 7.26 | 7.08 |
| 26 | 610 | 1.21 | 1.28 |
| 27 | 624 | 0.00 | 0.00 |

**TABLE 4.1(B):** Relative molecular weight distribution of sulphurised phenols calculated from the EC spectrum.

relative intensities of the fragment ions and the molecular ions are affected by the probe temperature, as noted above. It is suggested that the lower mass ions are primarily the result of pyrolysis. The electron capture spectra of the sulphurised phenol derivatives give essentially the same fragment ions as the underivatised sample; this could be because the fragmentation involves the transfer of a phenolic hydrogen to the neutral fragment:

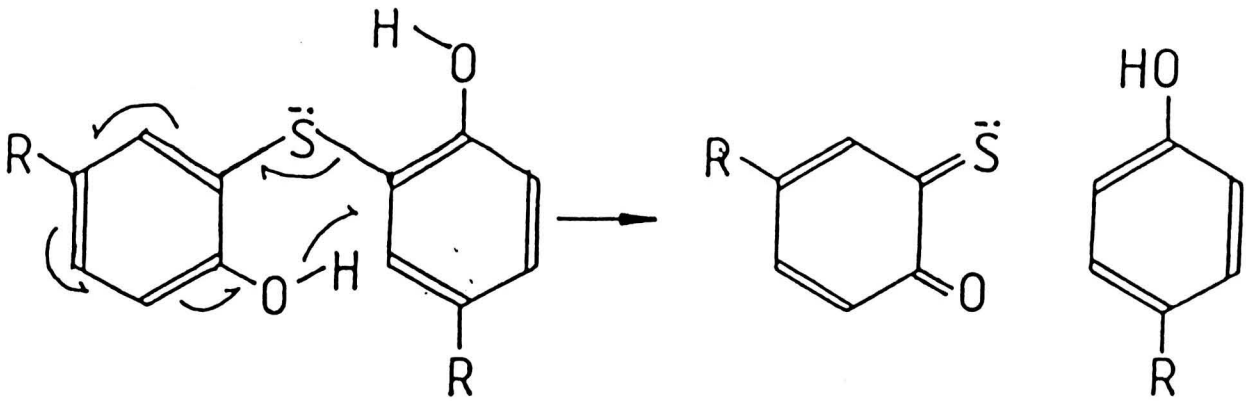


It may be noted that dipole moment measurements (9) suggest that the phenolic hydrogens are strongly hydrogen bonded to the sulphur, this may facilitate the proposed mechanism. In the derivatised sulphurised phenols, which appear to be mainly the mono-derivatives, fragmentation would, by the proposed mechanism, occur preferentially such that the un-derivatised side of the molecule becomes the fragment ion.

Pyrolysis of the sample molecules and subsequent ionisation of the products could also account for the observed low mass ions:

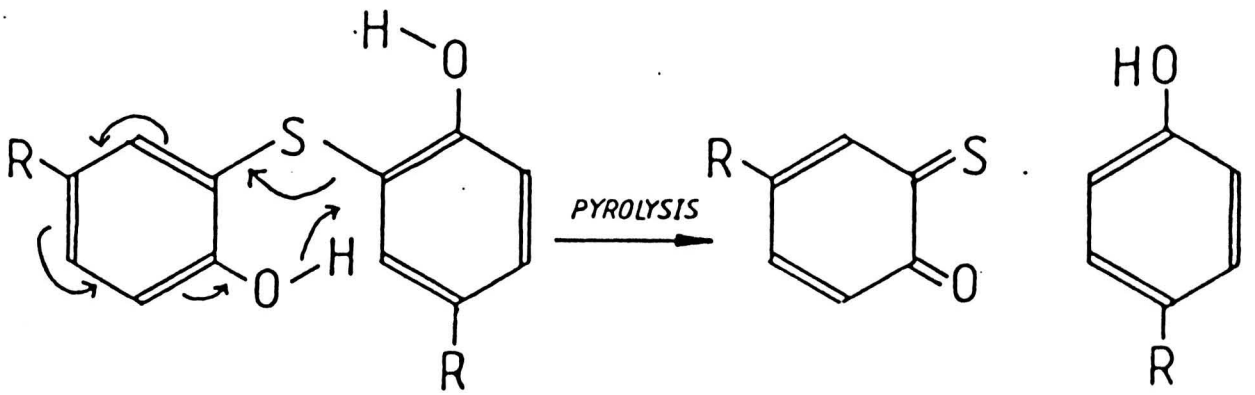

$$\text{alkyl-}C_6H_3OS \xrightarrow{EC} \text{alkyl-}C_6H_3OS^{-\cdot}$$

$$\text{alkyl-PhOH} \xrightarrow{EC} \text{alkyl-PhOH}^{-\cdot}$$

However, one would then expect to observe ions produced from the ionisation of both products of the reaction. Furthermore, one would also expect to observe an analogous reaction to take place under electron impact conditions.

One possible problem with the electron capture spectra of sulphurised phenols is the ease with which solvents containing hydroxyl groups can cause interference in the spectra due solvent adduct ions. This has been noted above for adducts involving water and methanol.

## 4.8 Chloride Chemical Ionisation.

Chloride chemical ionisation was achieved using carbon tetrachloride contained in a glass bulb at its room temperature vapour pressure. This was admitted to the instrument via a needle valve. The needle valve was adjusted until the source housing pressure reached the usual CI operating pressure ($10^{-4}$ torr). The instrument was tuned and calibrated in negative ion mode using a mixture of PFK and carbon tetrachloride.

### 4.8.1 Results and Conclusions.

The $Cl^-$ CI spectrum of a sulphurised phenol sample is shown in figure 4.12.

The main features of the spectrum are pseudo-molecular ions, fragment ions due to C-S bond rupture, and fragment ions due to bond rupture in the alkyl chains.

Pseudo-molecular ions occur at $(M-1)^-$, presumably formed by addition of $Cl^-$ followed by loss of HCl, although no evidence of an adduct $(M+Cl)^-$ was observed. Chloride adduct ions were observed at very high reagent gas pressures, but these were adducts of neutral fragments and $Cl^-$. Most prominent was an adduct ion at 297 Daltons, corresponding to the chloride adduct with alkyl-phenol.

Fragment ions are more extensive than in the electron capture spectra. The group of fragment ions with a maximum at 292 Daltons in the electron capture spectra is replaced by a group of ions with maximum at 293 Daltons, the 292 peak about half as intense as the 293 peak. This difference may be due to fragmentation occurring with more excess energy in the chloride chemical ionisation compared to electron capture ionisation, perhaps by the direct fragmentation of the $(M-H)^-$ ion:

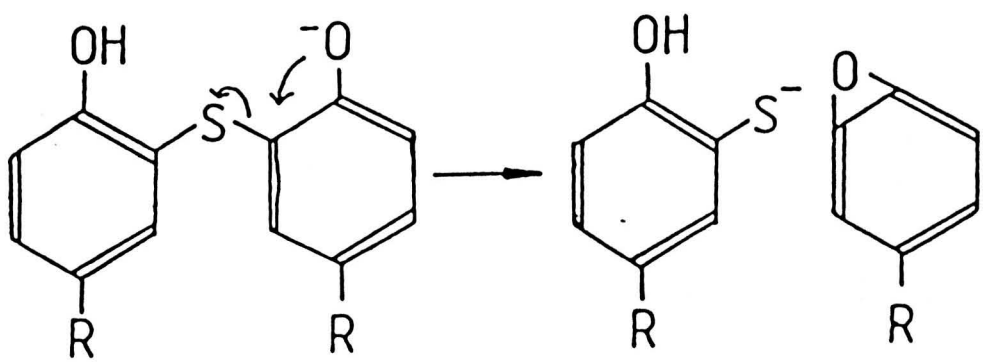

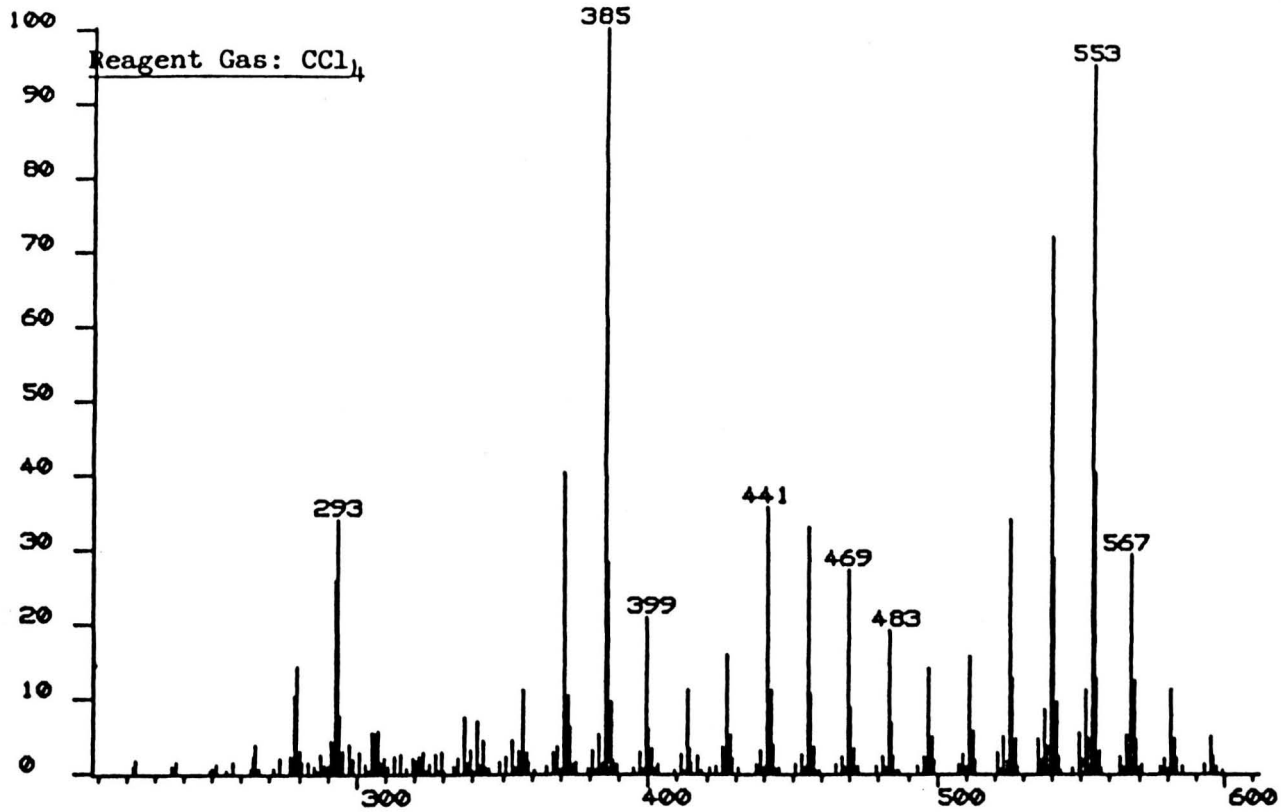


FIGURE 4.13: $Cl^-$ CI Mass Spectrum of a Sulphurised Phenol Sample.

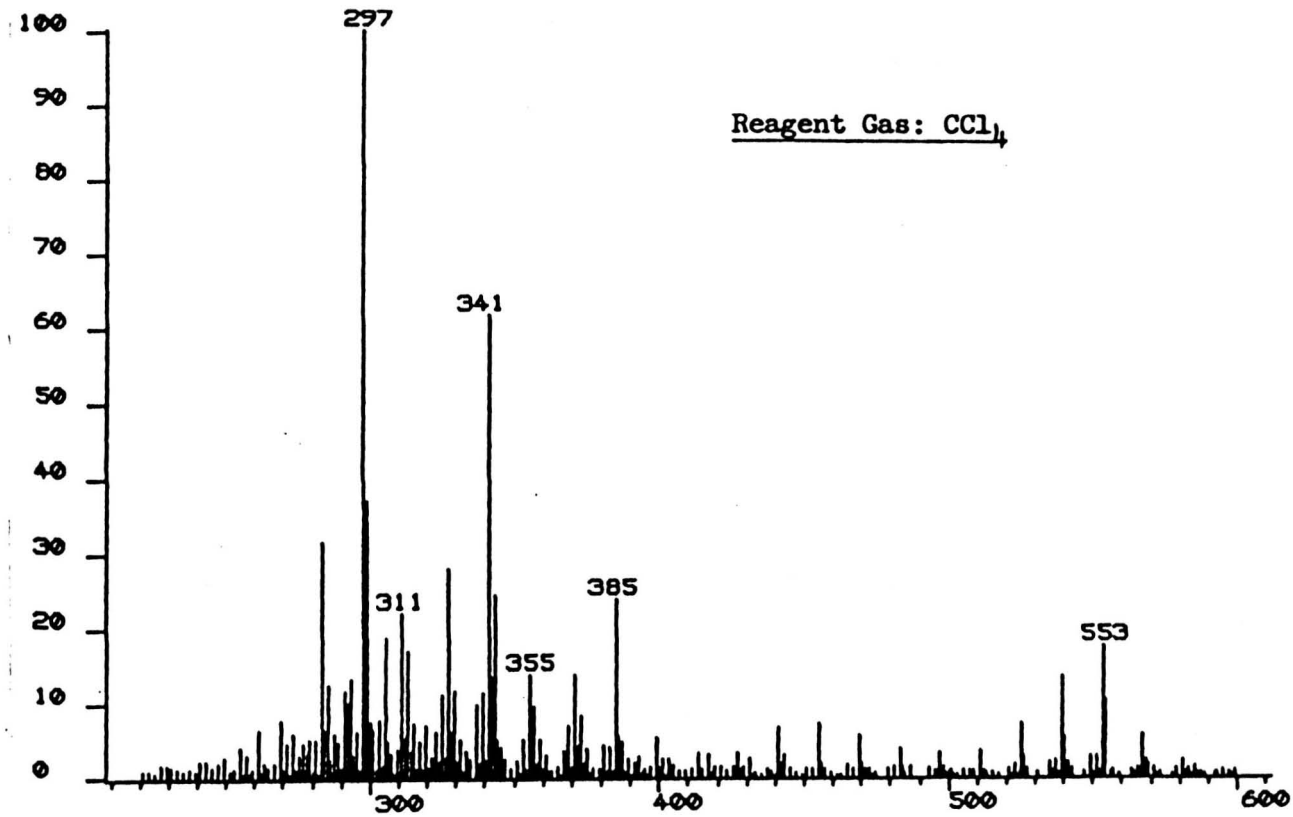


FIGURE 4.13(b): As above, but with high reagent gas pressure.

In conclusion, the chloride chemical ionisation of sulphurised phenol samples offers no obvious advatages over electron capture spectra.

## 4.9 METASTABLE ION MEASUREMENTS.

### Introduction.

One of the problems often encountered in mass spectrometry when using a soft ionisation technique is that the spectrum has not enough structurally significant features to enable one to identify an unknown sample. An elegant approach to overcome this problem is the measurement of metastable ions - or, if these are absent, the measurement of fragment ions formed by collision-induced decomposition.

One of the other main uses of metastable ion measurements is the confirmation of hypothesised fragmentation mechanisms. If a metastable ion corresponding to the fragmentation:

$$M_1^+ \rightarrow M_2^+ + M_3$$

(or a similar negative ion fragmentation)

is present, then this fact is proof that the fragmentation occurs in one step.

Thus it was hoped that metastable mapping and collision induced decomposition studies of the EC and the EI spectra of sulphurised phenol samples would provide confirmation of the proposed fragmentation schemes in EI and EC spectra.

### 4.9.1 Experimental.

The technique of metastable mapping (see chapter one) was used to make measurements of metastable and collisionally induced fragment ions from the electron capture spectrum of a sulphurised phenol sample.

In the initial experiments, the metastable ion intensities were very low, so that subsequent experiments were performed with the instrument set up for collision induced fragmentation.

Several experiments were carried out to optimise the experimental conditions.

For the purposes of finding the optimum settings for the instrument when operating in the collision induced fragmentation mode, the instrument was set up so that metastable ion measurements could be made manually. This involved the use of an external reference voltage for the electric sector. This was provided by a nine volt battery fed via a 10k ohm precision potentiometer to the external reference input for the electric sector. The electric sector voltage was measured using a digital voltmeter, the ESA voltage being set to the required voltage calculated from:-

$$E/E_o = m_2/m_1$$

where $E_o$ is the full ESA voltage and E the ESA voltage required to observe the collision induced fragmentation.

The simple reference voltage supply used enabled measurements to be made; it did however, suffer from significant drift over extended

periods of time (ca. 0.1V/Min.). This meant that the ESA voltage periodically had to be re-adjusted to the required voltage.

Table 4.2 and figure 4.14 shows the percentage transmission of the peak at 554 daltons from a sulphurised phenol sample produced under electron ionisation conditions and source pressure as functions of the dial setting of the collision gas inlet valve. The signal intensity was measured by manually adjusting the magnet to the appropriate peak which was easily distinguishable on the oscilloscope. With the amplifier bandwidth set at 10Hz, the signal intensity was measured on the collector monitor.

TABLE 4.2

| DIAL SETTING | TRANSMISSION (%) | PRESSURE X $10^6$ |
|---|---|---|
| 0 | 100 | 1.5 |
| 1 | 90 | 1.6 |
| 2 | 60 | 3.5 |
| 3 | 20 | 10. |
| 4 | 0 | 20. |

The recommended transmission of 30% (9) corresponds to a vernier dial setting of about 2.5.

Using the potentiometer to set the ESA voltage allows one to measure the signal intensity due to a collisionally induced fragmentation.

Examination of the electron impact spectrum of the sulphurised phenol shows that fragment ions occurring at 427 Daltons are the most abundant ions resulting from simple loss of part of the alkyl chain from the molecular ion.

The signal intensity arising from the collisionally induced

FIGURE 4.14: Transmission of Peak at 554 Daltons vs Collision Gas Valve Setting.

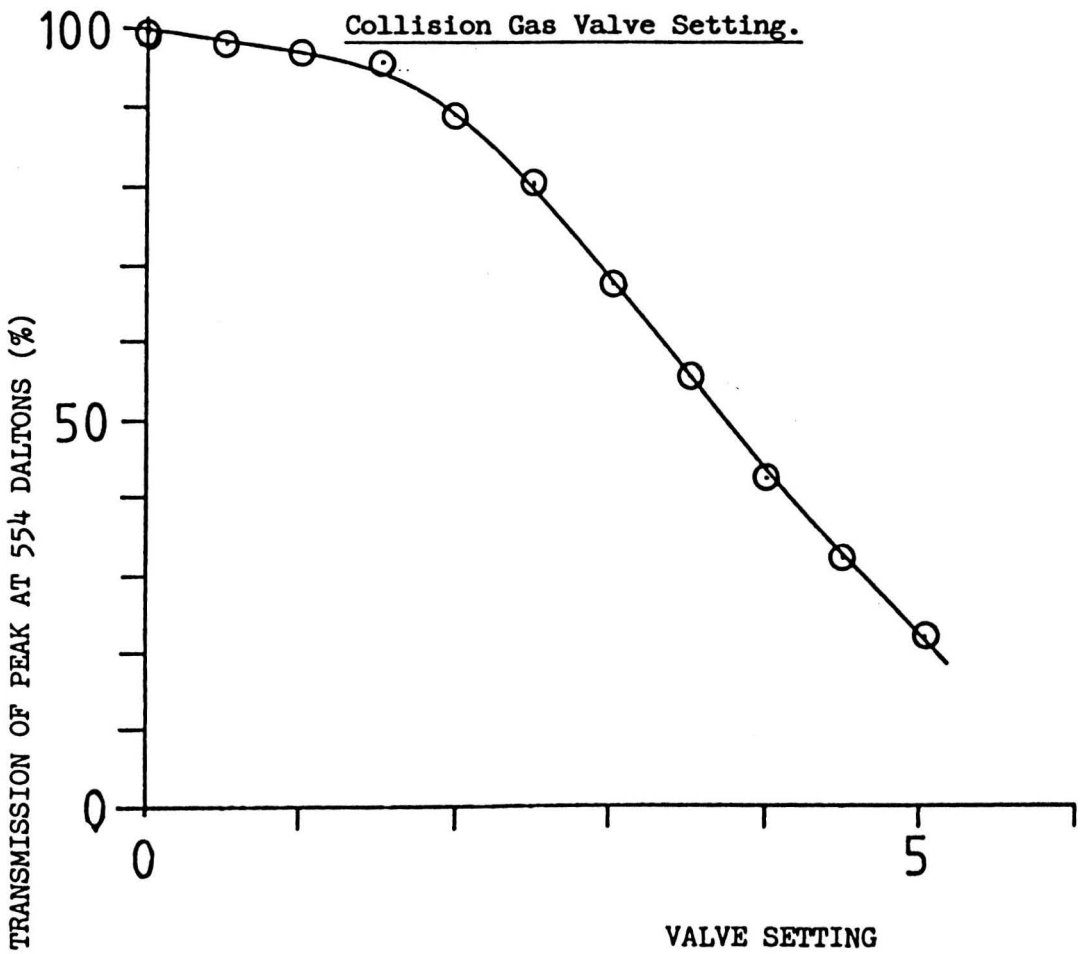

fragmentation:-

$$M_1(554)^+ + G \rightarrow M_2(427)^+ + C_9H_{19} + G$$

was measured by setting the ESA voltage to 77.07% $E_0$ (200.4V), and acquiring data by scanning the magnet in the normal manner. Table 4.3 shows the signal intensity arising from these ions as a function of collision gas vernier setting.

TABLE 4.3

| DIAL SETTING | SIGNAL INTENSITY (ARBITARY UNITS) |
|---|---|
| 0.0 | 15 |
| 0.5 | 15 |
| 1.0 | 25 |
| 1.5 | 45 |
| 2.0 | 70 |
| 2.5 | 65 |
| 3.0 | 40 |
| 3.5 | 18 |

These results are also shown in figure 4.14.

Comparison of the results in tables 4.2 and 4.3 shows that the optimum vernier dial setting for the collision gas inlet valve is 2.0 to 2.5 and that the recommended transmission of the parent ion (30%) does correspond to the approximate maximum in the abundance of the ions produced by collisionally induced fragmentation.

Following these optimisation experiments several attempts were made to produce acceptable metastable maps of collisionally induced fragment ions both from electron ionisation and electron capture ionisation of the sulphurised phenol sample.

**FIGURE 4.15: Intensity of the Peak Due to Collision Induced Fragmentation $M(554)^+ \rightarrow M(427)^+$ vs Collision Gas Valve Setting**

ESA: 200.4 V (77.1%)

GAIN: 6

BANDWIDTH: 10HZ

Estimated error ± 15 %

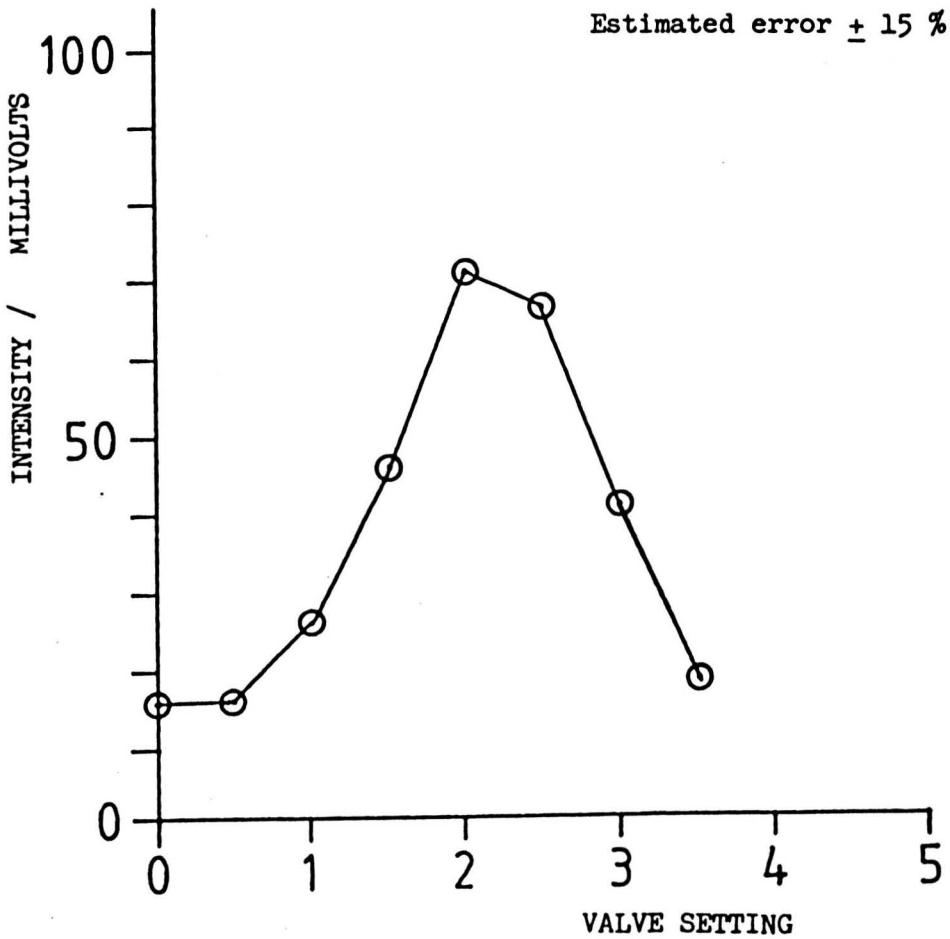

During these experiments the following points were noted:-

(1) When scanning at 3 sec/decade, the signal intensities due to the ion produced by collision induced decomposition (electron impact mode, but especially electron capture mode) do not record on the data system, although peaks can be discerned on the oscilloscope. Increased gain (higher voltage on the electron multiplier) does enable the data system to pick up the peaks, but noise peaks are numerous and the results are not very reproducible. This was due to the data system rejecting the peaks as noise, rather than because the peaks were below the threshold level.

(2) Changing the scan rate to 10 sec/decade does improve signal acquisition, but prolonged run times (about 90 minutes) for maps makes it difficult to maintain sample pressure at an adequate level.

(3) The variability in the quality of the maps seems to be due to variations in sample pressure and sample life-time.

(4) The source and probe temperatures do not affect the quality of the metastable maps except in so far as they affect sample life-time.

(5) Signal intesities from collisionally induced fragment ions from electron ionisation of sulphurised phenols are approximately 3 to 5 times more intense than those generated from electron ionisation of sulphurised phenols and approximately the same intensity as those generated from the electron ionisation of hydrocarbon samples. It is note-worthy that, for hydrocarbon samples, sample life-time and sample pressure stability are very good when compared to sulphurised phenols.

(6) The intensities of the fragment ions formed by collision induced decomposition were much lower under electron capture conditions than they were under positive electron impact conditions. This may be due to the ease with which negative ions undergo collision induced electron loss:-

$$M^- + G \rightarrow M + e^- + G$$

## 4.92 METASTABLE MAP RESULTS

Figure 4.16 shows part of the positive EI metastable map for ions produced by collision induced decomposition. Alkyl chain fragmentation can clearly be seen from loss of $C_2H_5$ to $C_{10}H_{21}$. It may be noted that the most intense peaks correspond to loss of $C_8H_{17}$ and $C_9H_{19}$. In EI, this region gave the most intense metastable intensities.

Unlike the EI metastable map, the EC metastable map gave very poor metastable intensities at the high parent mass end of the map. The most

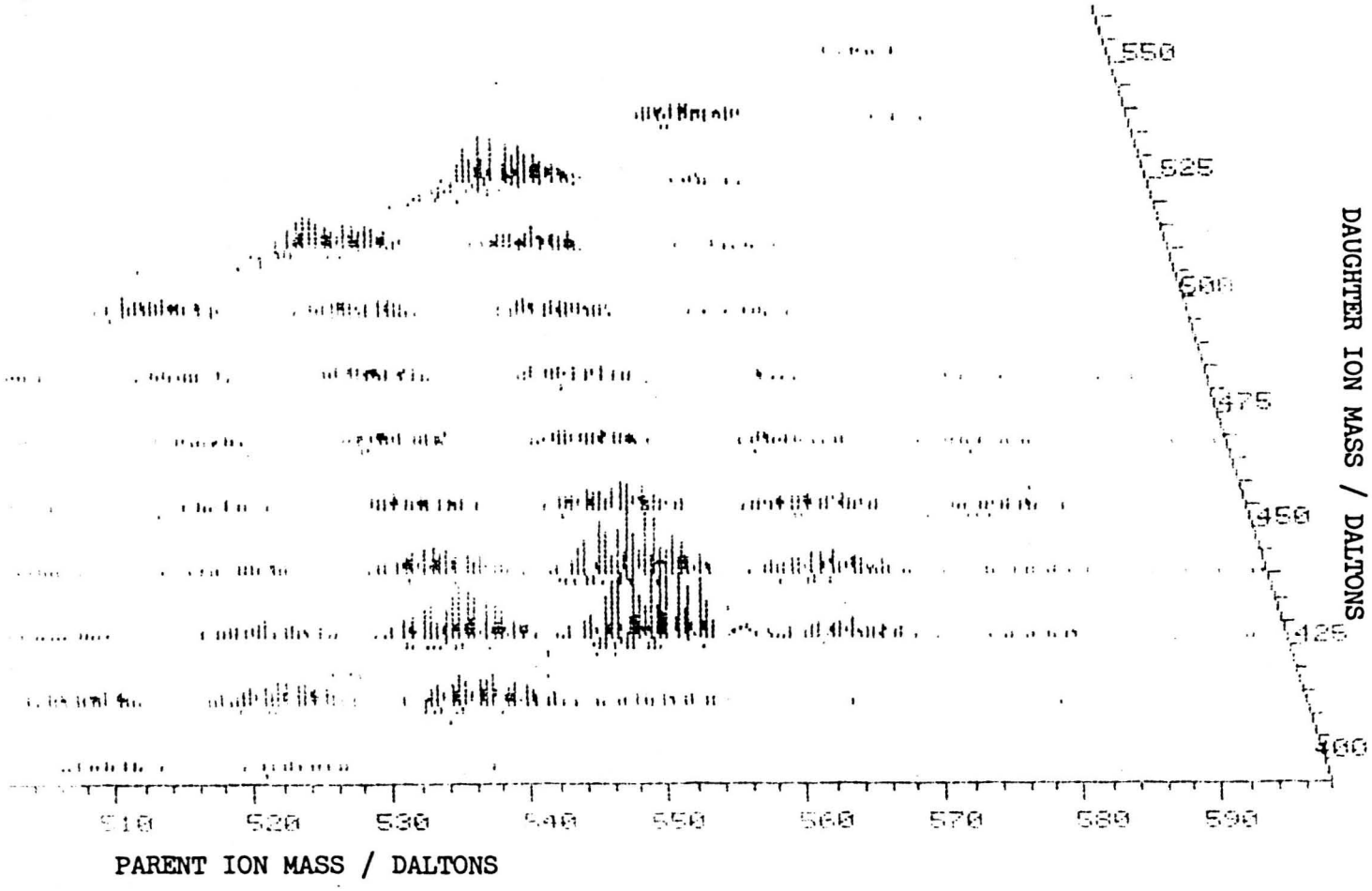


**FIGURE 4.16: Part of the Metastable Map from the Electron Ionisation of a Sulphurised Phenol sample.**

intense metastable ions in the EC case are shown in figure 4.17. Alternatively, part of the same data is presented in figure 4.18 as a simulated linked scan. One may notice a problem here; if the ion at 292 Daltons corresponds to the structure given above, then it should be an even electron species, and one would expect it to fragment via the elimination of alkanes, and figure 4.18 suggests that alkyl fragments are lost, eg metastable peak at 249 Daltons corresponding to loss of $C_3H_7$ from $M(292)^-$. However, referring to figure 4.17, there is clearly an overlap between metastable ions from the fragmentation of $M(292)^-$ and $MH(293)^-$.

This result shows up one of the main disadvantages with metastable mapping and linked scanning techniques: poor resolving power.

The poor resolving power of the technique is also evident in figure 4.19 which shows the simulated linked scan of daughter ions from mass 586 in the EC spectrum of the methylated sulphurised phenol sample. Although the groups of ions clearly arise from the loss of parts of the alkyl chain and fission of the C-S bond, the 'linked scan' is quite noisy.

It is interesting to note that the loss of $H_2O$ from what is presumed to be the solvated molecular ion, $(M+H_2O)^-$ can not explain the masses which occur in figure 4.19, however, losses of alkane from the parent ion corresponding to the ion $(M'+H_2O-Me)^-$, where M' represents the next homologue of M, do give the correct masses.

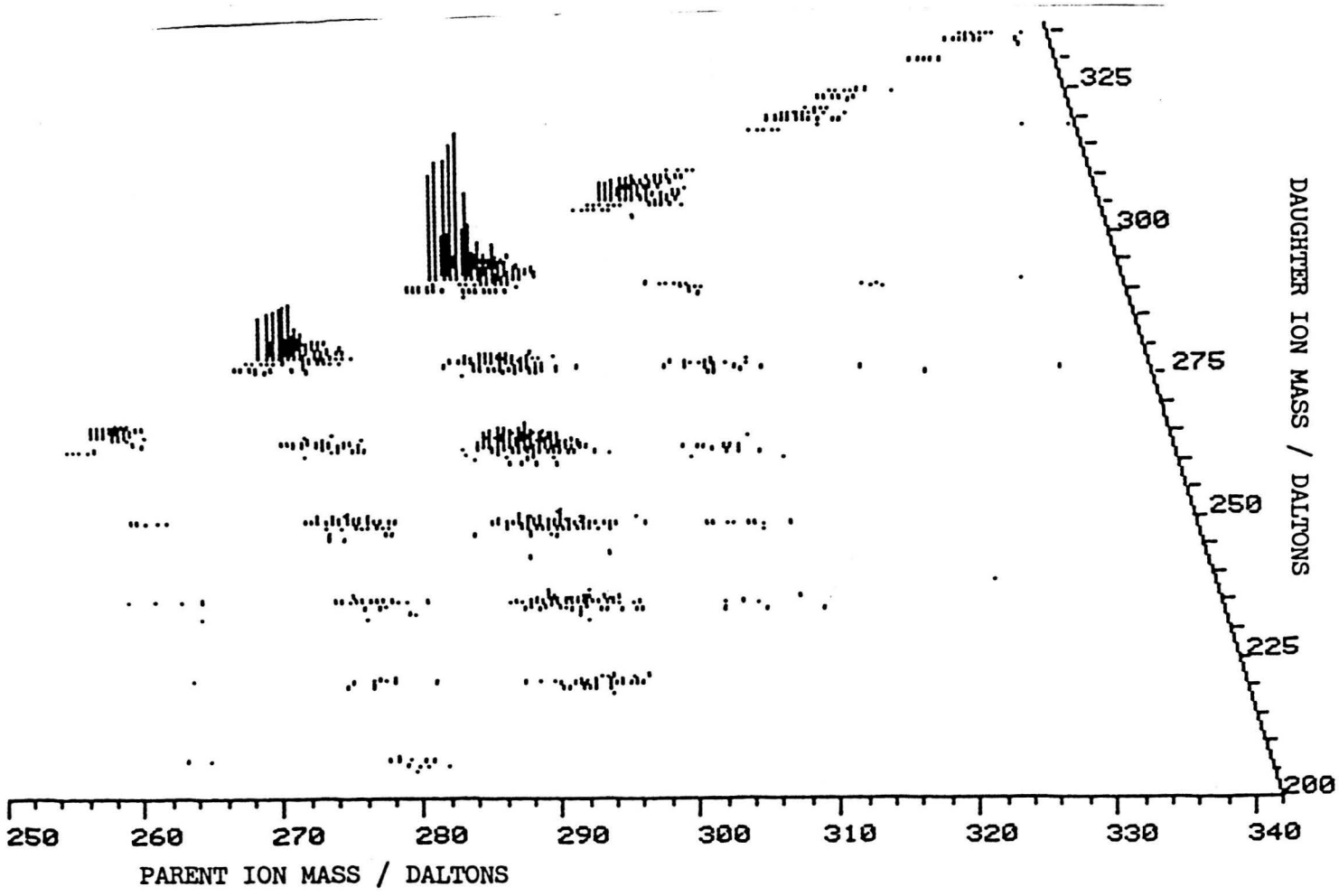


FIGURE 4.17: Part of the Metastable Map from the Electron Capture Ionisation of a Sulphurised Phenol sample.

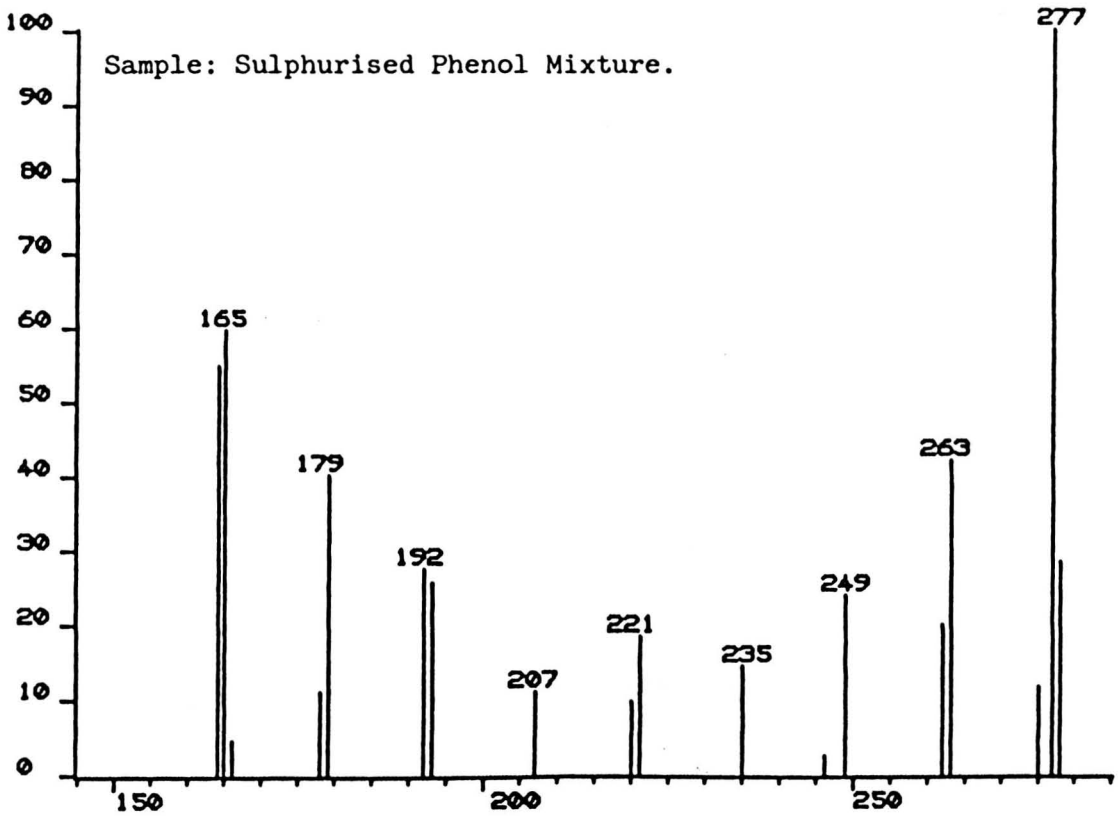


FIGURE 4.18: Simulated Linked Scan Showing Daughter Ions from Parent Ions at 292 Daltons Produced by Electron Capture Ionisation.

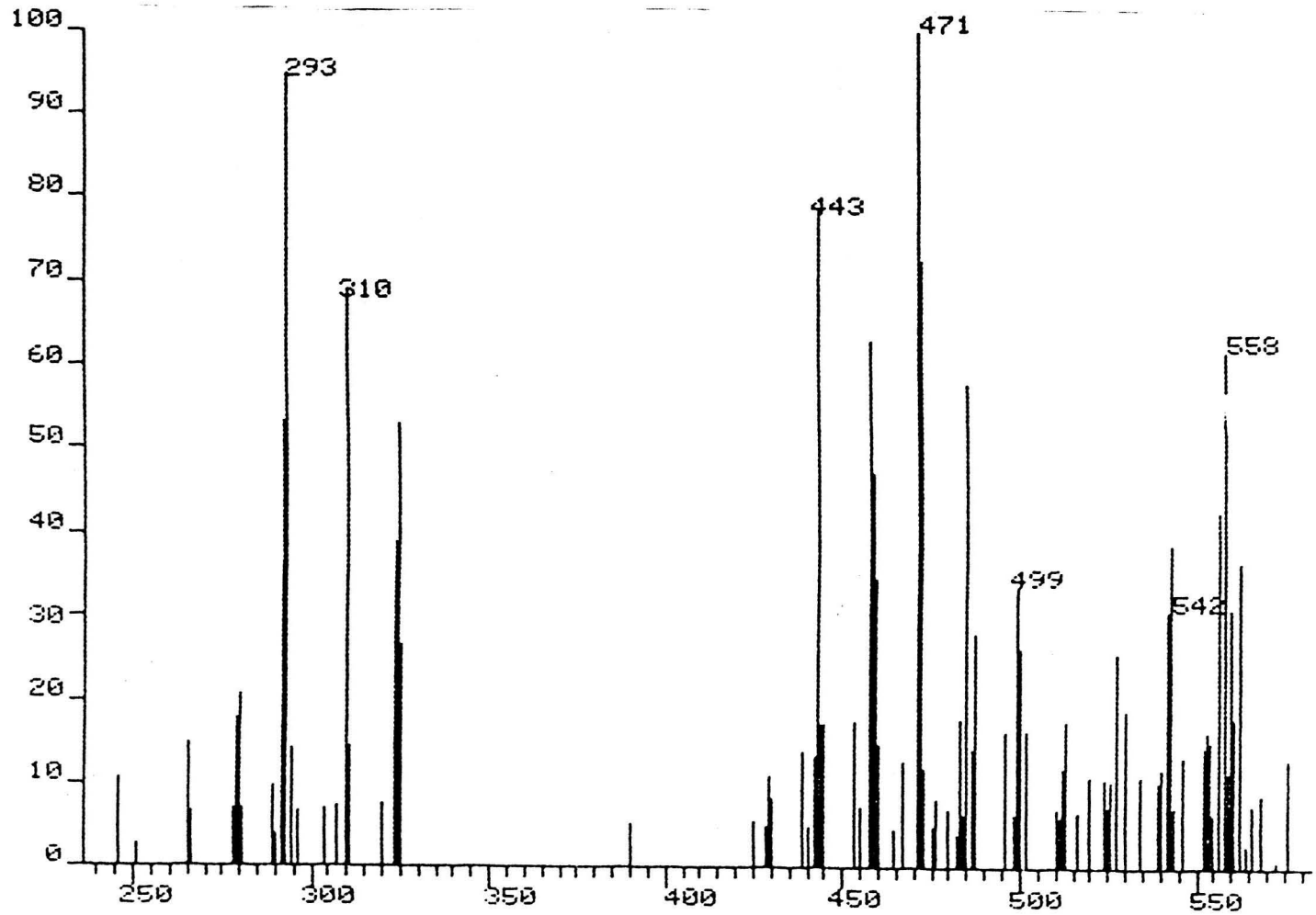


FIGURE 4.19: Simulated Linked Scan Showing Daughter Ions from Parent Ions at 586 Daltons Produced by Electron Capture Ionisation of the Methyl Derivative.

Thus, the daughter ions from the parent ion at 585 Daltons are interfering with those from the parent at 586 Daltons. Most of the peaks in figure 4.18 are attributable to loss of neutrals from ions at 585 Daltons, whilst only a few are attributable to loss of neutrals from ions at 586 Daltons.

This can be explained thus; since the ions at 586 Daltons are odd electron species, the collisionally induced loss of an electron should be the favoured process, whereas, the ions at 585 Daltons, being fragment ions, are even electron species, so that collision induced decoposition is the favoured process. This may also explain why loss of $H_2O$ from the $(M+H_2O)^-$ ion does not seem to occur.

Figure 4.19 shows part of the metastable map for the acetyl derivative recorded under electron capture conditions. Loss of a neutral fragment of relative molecular mass 43, may correspond to the loss of the acetyl group or loss of $C_3H_7$. No metastable peaks are observed which would correspond to loss of $C_2H_5$, which one would expect to see if the metastable ions correspond to loss of parts of the alkyl chain, so that it reasonable to attribute loss of a fragment of relative molecular mass 43 Daltons to loss of the acetyl group. Again it is suprising that no metastable ions are recorded which may be attributed to loss of $H_2O$.

Unfortunately, the sample did not last sufficiently long to allow more of the metastable map to be recorded.

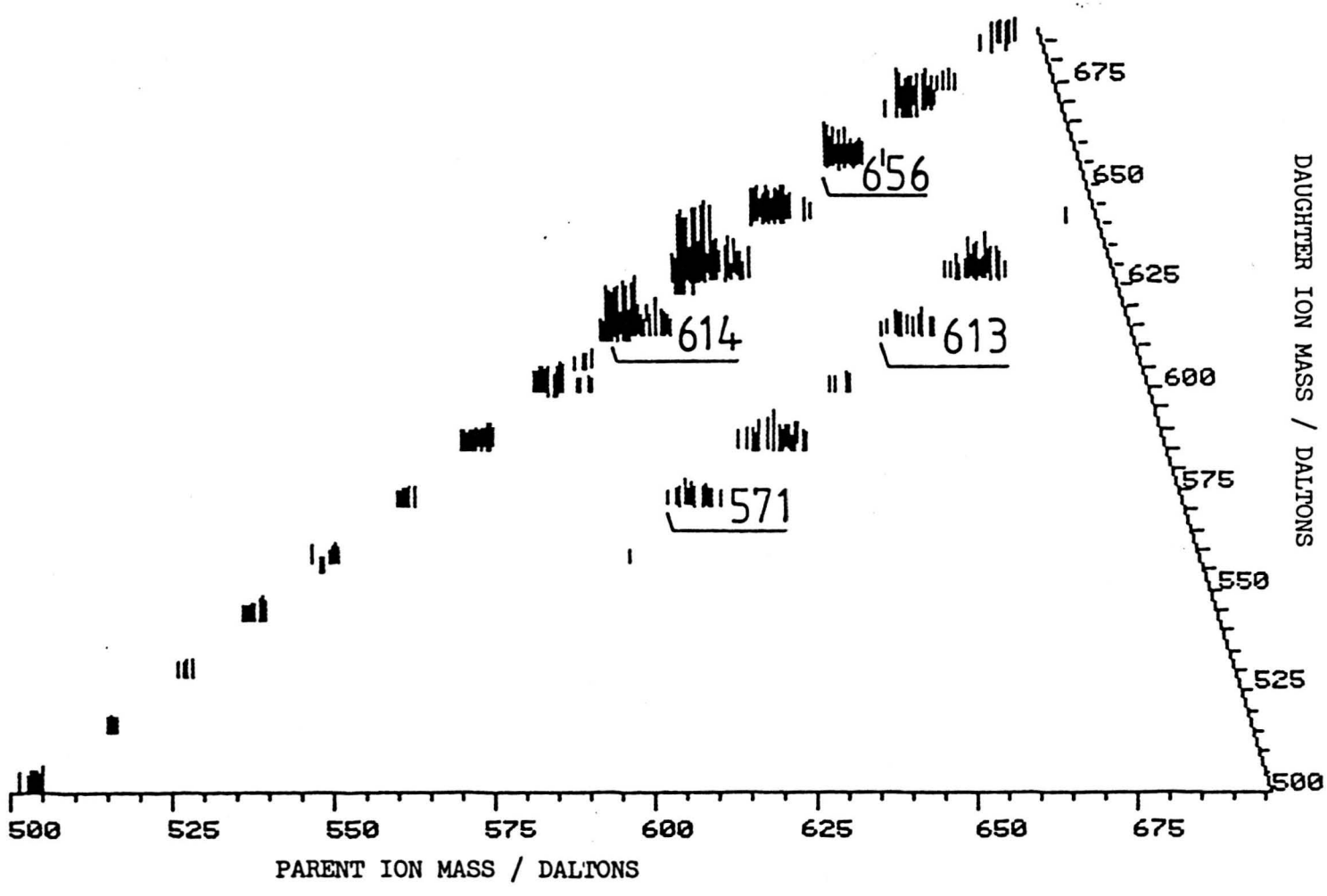


**FIGURE 4.20: Part of the Metastable Map from the Electron Capture Ionisation of the Acetyl Derivative of the Sulphurised Phenol.**

## Conclusions

It may be concluded that the poor results obtained from the metastable mapping of the sulphurised phenol sample are due mainly to the short sample life time compared to the run times of the measurements. In addition, for the metastable mapping of negative ions produced by collision induced fragmentation of parent ions produced under electron capture conditions, it is likely that collision induced electron loss competes with collision induced fragmention, resulting in low metastable ion abundances.

In addition, it was found that the poor resolving power for parent ion mass caused considerable inteference from the metastable fragmentations from adjacent parent ions, thus making interpretation of the results more difficult.

## 4.10 Some Metastable Ion Measurements.

In view of the poor results obtained with the metastable mapping studies, it was decided to make several metastable ion / collision induced fragment ion measurements manually using the external reference voltage for the ESA. This technique has the advantage of speed and can be carried out within the sample life time. The major disadvantage of using this technique is that one has to know in advance the metastable transitions which are likely to be present, since the ESA voltage has to be calculated appropriately. Furthermore, the technique will still suffer from poor resolving power for parent ion mass.

It has been noted (6) that NMR measurements suggest that in the

sulphurised phenol molecules, the alkyl chains are attached to the aromatic ring such that they are branched at the 1'- position by one or more methyl groups. It is possible that collision induced fragmentation studies may provide data to support this. The relative abundances of collision induced fragment ions produced by chain rupture should reflect the relative stability of the daughter ion produced. This is because the energy threshold to the transition state of the reaction leading to fragmentation should be small, so that the activation energy of the reaction is the nearly the same as the endothermicity of the reaction. Therefore those features which stabilise the daughter ion with respect to the parent ion should result in a lower activation energy of reaction.

### 4.10.1 Experimental

The procedure adopted for the collision induced fragmentation measurements was to scan the magnet as normal (3 sec/decade) and manually alter the ESA voltage during the run. Once the ESA voltage was adjusted such that the first set of collision induced fragment ions were being detected, the gain was adjusted to give reasonable signal intensities, the gain was then used at that setting for the remainder of the measurements. The latter procedure was required because the 'normal' signal intensities recorded at 100% $E_o$ are approximately two orders of magnitude greater than the signal intensities encountered when recording collision induced fragment ions.

The collision induced fragment ions produced from the reaction are recorded at an apparent relative molecular mass $m^*$, given by:-

$$m^* = (M_2)^2/M_1$$

Table 4.4 shows the results of the collision induced fragmentation of a sulphurised phenol sample under electron ionisation conditions. The parent ion chosen was the ion at 554 Daltons in the normal spectrum, as this was the most intense molecular ion.

TABLE 4.4 Collision induced fragments from ions at 554 Daltons, electron ionisation of sulphurised phenol.
(intensities - mean value of 3 scans)

| mass daughter | ESA (%) | mass m* | intensity (arbitary units) |
|---|---|---|---|
| 399 | 72.0 | 287 | 25 |
| 413 | 74.5 | 308 | 69 |
| 427 | 77.1 | 329 | 100 |
| 441 | 79.6 | 351 | 23 |
| 455 | 82.1 | 374 | 11 |

estimated error in intensities ± 20%

From the above table, the most abundant collision induced fragment occcurs at 427 Daltons corresponding to the loss of $C_9H_{19}$, the parent ion at 554 Daltons must however have a mean chain length of twelve carbons. This may be rationalised by assuming that the chains have two methyl groups at the 1'- position leading to the formation of the relatively stable ion at 427 Daltons by chain fission:-

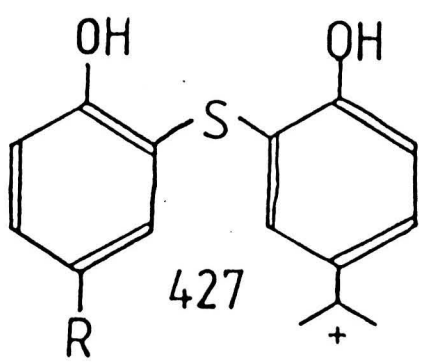


In retrospect, observation of the fragmentation pattern in the electron ionisation spectrum of the sulphurised phenols more easily

yields the results obtained by the collision induced fragmentation experiments.

## 4.11 General Conclusions.

If the metastable mapping technique had proved more successful, it is possible that more unexpected, more structuraly significant, metastable fragmentations could have been observed.

One must conclude that a major draw-back with the metastable mapping technique is the long run times encountered. Perhaps this would not have been such a problem if sample introduction was more controlled, for example as it is with an all glass heated inlet system.

The poor resolution, however, is a problem which is insumountable without extensive modification of the instrument. A complete discussion of linked techniques and metastable mapping is to be found in reference (11).

For collision induced decomposition studies the techniques of tandem mass spectrometry (12) and Fourier transform mass spectrometry (13) are much more appropriate, as they allow more versatility, have greater sensitivity and have better resolving power.

These comments apart , the technique of metastable mapping does allow the analytical chemist access to metastable / collision induced fragment ion measurements where the more exotic and expensive instruments such as multiple sector instruments or FTMS instruments are not available.

## CHAPTER FOUR: REFERENCES


1) Klamann, D., 'Lubricants and related products: synthesis, properties, applications & international standards', Verlag Chemie GmbH, 1984.

2) Gower, J. L., Poster presentation: 'Matrix Compounds for FAB mass spectrometry: An interim review', British Mass Spectrometry Society, Thirteenth meeting, University of Warwick, Sept. 1983.

3) Lyon, P. A. Stebbings, W. L., Crow, F. W., Tomer, K. B., Lippstreu, D. L. & Gross, M. L., Anal. Chem., 56, 8, (1984).

4) Martin, S. A., Costello, C. E. & Blemann, K., Anal. Chem., 54, 2362, (1982).

5) Barber, M., Bordoli, R. S., Elliott, G. J., Sedgwick, R. D. & Tyler, A. N., Anal. Chem., 54, 645A, (1982).

6) Kendrick, E. K., ESSO Research Centre, Abingdon, Oxon., U.K., private communication.

7) Blakley, C. R. & Vestal, M. L., Anal. Chem., 55, 750, (1983).

8) Rose, M. E. & Johnston, R. A. W., 'Mass Spectrometry for Chemists and Biochemists', Cambridge University Press, 1982.

9) Garnovskii, A. D., Ismailov, Kh. M. & Osipov, O. A., Azerb. Khim. Zh., 6, 87, (1965). [Russ.]; also Chem. Abstracts, 64:18583a.

10) Moore, C., University of Warwick, private communication.

11) Jennings, K. R. & Mason, R. S., 'MS/MS From Linked Scanning of Double-Focussing Mass Spectrometers', in 'Tandem Mass Spectrometry', Ed. McLafferty, F. W., Wiley-Interscience Publication, (1983).

12) Yost, R. A. & Fetterolf, D. D., Mass Spectrom. Rev., 2, 1, (1983).

13) McIver Jr., R. T. & Bowers, W. D., 'Tandem Mass Spectrometry', Ed. McLafferty, F. W., p287, Wiley-Interscience Publication, (1983).

# APPENDIX A

## ENGINE OIL FRACTIONS - TYPE ANALYSIS RESULTS.

TYPE ANALYSIS D-2786-71
SAMPLE: G3A

| | SATS |
|---|---|
| ALKANES(O-RING) | 37.52 |
| 1-RING NAPHTHENES | 24.67 |
| 2-RING NAPHTHENES | 18.61 |
| 3-RING NAPHTHENES | 12.56 |
| 4-RING NAPHTHENES | 4.10 |
| 5-RING NAPHTHENES | 0.75 |
| 6-RING NAPHTHENES | 0.00 |
| MONO-AROMATICS | 1.80 |

MS AROMATICS ANALYSIS ASTM D3239
SAMPLE: G3B

| FRACTION IS 28.5 % OF OIL | VOLUME % OF FRACTION | |
|---|---|---|
| MONOAROMATICS | | 75.5 |
| ALKYLBENZENES | 42.7 | |
| NAPHTHENEBENZENES | 17.8 | |
| DINAPHTHENEBENZENES | 15.0 | |
| DIAROMATICS | | 12.1 |
| NAPHTHALENES | 3.9 | |
| ACENAPHTHALENES-DIBENZOFURANS | 4.2 | |
| FLUORENES | 4.0 | |
| TRIAROMATICS | | 2.3 |
| PHENANTHRENES | 2.3 | |
| NAPHTHENPHENANTHRENES | 0.0 | |
| TRETRA-AROMATICS | | 0.3 |
| PYRENES | 0.3 | |
| CHRYSENES | 0.0 | |
| PENTA-AROMATICS | | 0.3 |
| PERYLENES | 0.2 | |
| DIBENZANTHRACENES | 0.1 | |
| THIOPHENO-AROMATICS | | 5.1 |
| BENZOTHIOPHENES | 3.5 | |
| DIBENZOTHIOPHENES | 1.5 | |
| NAPHTHOBENZOTHIOPHENES | 0.1 | |
| UNIDENTIFIED-AROMATICS | | 4.4 |

MS AROMATICS ANALYSIS ASTM D3239
SAMPLE: G4

| FRACTION IS 30.7 % OF OIL | VOLUME % OF FRACTION | |
|---|---|---|
| MONOAROMATICS | | 73.4 |
| ALKYLBENZENES | 43.7 | |
| NAPHTHENEBENZENES | 16.6 | |
| DINAPHTHENEBENZENES | 13.1 | |
| DIAROMATICS | | 13.4 |
| NAPHTHALENES | 4.0 | |
| ACENAPHTHALENES-DIBENZOFURANS | 4.7 | |
| FLUORENES | 4.7 | |
| TRIAROMATICS | | 5.1 |
| PHENANTHRENES | 5.1 | |
| NAPHTHENPHENANTHRENES | 0.0 | |
| TRETRA-AROMATICS | | 0.4 |
| PYRENES | 0.4 | |
| CHRYSENES | 0.0 | |
| PENTA-AROMATICS | | 0.3 |
| PERYLENES | 0.2 | |
| DIBENZANTHRACENES | 0.1 | |
| THIOPHENO-AROMATICS | | 4.4 |
| BENZOTHIOPHENES | 1.9 | |
| DIBENZOTHIOPHENES | 2.5 | |
| NAPHTHOBENZOTHIOPHENES | 0.0 | |
| UNIDENTIFIED-AROMATICS | | 3.0 |

MS AROMATICS ANALYSIS ASTM D3239
SAMPLE: G5

| FRACTION IS 42.3 % OF OIL | VOLUME % OF FRACTION | |
|---|---|---|
| MONOAROMATICS | | 58.3 |
| ALKYLBENZENES | 26.6 | |
| NAPHTHENEBENZENES | 16.7 | |
| DINAPHTHENEBENZENES | 15.0 | |
| DIAROMATICS | | 16.2 |
| NAPHTHALENES | 4.7 | |
| ACENAPHTHALENES-DIBENZOFURANS | 6.3 | |
| FLUORENES | 5.2 | |
| TRIAROMATICS | | 4.6 |
| PHENANTHRENES | 3.0 | |
| NAPHTHENPHENANTHRENES | 1.6 | |
| TRETRA-AROMATICS | | 2.6 |
| PYRENES | 1.6 | |
| CHRYSENES | 1.1 | |
| PENTA-AROMATICS | | 0.8 |
| PERYLENES | 0.4 | |
| DIBENZANTHRACENES | 0.3 | |
| THIOPHENO-AROMATICS | | 8.9 |
| BENZOTHIOPHENES | 6.5 | |
| DIBENZOTHIOPHENES | 2.2 | |
| NAPHTHOBENZOTHIOPHENES | 0.2 | |
| UNIDENTIFIED-AROMATICS | | 8.6 |

MS AROMATICS ANALYSIS ASTM D3239
SAMPLE: G7

| FRACTION IS 8.9 % OF OIL | VOLUME % OF FRACTION | |
|---|---|---|
| MONOAROMATICS | | 76.6 |
| ALKYLBENZENES | 31.0 | |
| NAPHTHENEBENZENES | 27.6 | |
| DINAPHTHENEBENZENES | 18.1 | |
| DIAROMATICS | | 10.4 |
| NAPHTHALENES | 2.1 | |
| ACENAPHTHALENES-DIBENZOFURANS | 4.4 | |
| FLUORENES | 3.9 | |
| TRIAROMATICS | | 2.1 |
| PHENANTHRENES | 1.5 | |
| NAPHTHENPHENANTHRENES | 0.5 | |
| TRETRA-AROMATICS | | 3.4 |
| PYRENES | 2.1 | |
| CHRYSENES | 1.3 | |
| PENTA-AROMATICS | | 0.5 |
| PERYLENES | 0.4 | |
| DIBENZANTHRACENES | 0.1 | |
| THIOPHENO-AROMATICS | | 2.9 |
| BENZOTHIOPHENES | 1.2 | |
| DIBENZOTHIOPHENES | 1.5 | |
| NAPHTHOBENZOTHIOPHENES | 0.2 | |
| UNIDENTIFIED-AROMATICS | | 4.2 |

MS AROMATICS ANALYSIS ASTM D3239
SAMPLE: G8

| FRACTION IS 50.6 % OF OIL | VOLUME % OF FRACTION | |
|---|---|---|
| MONOAROMATICS | | 58.7 |
| ALKYLBENZENES | 25.5 | |
| NAPHTHENEBENZENES | 16.9 | |
| DINAPHTHENEBENZENES | 16.4 | |
| DIAROMATICS | | 20.8 |
| NAPHTHALENES | 6.2 | |
| ACENAPHTHALENES-DIBENZOFURANS | 7.9 | |
| FLUORENES | 6.8 | |
| TRIAROMATICS | | 4.4 |
| PHENANTHRENES | 3.6 | |
| NAPHTHENPHENANTHRENES | 0.8 | |
| TRETRA-AROMATICS | | 1.8 |
| PYRENES | 1.3 | |
| CHRYSENES | 0.5 | |
| PENTA-AROMATICS | | 0.4 |
| PERYLENES | 0.2 | |
| DIBENZANTHRACENES | 0.2 | |
| THIOPHENO-AROMATICS | | 7.9 |
| BENZOTHIOPHENES | 5.8 | |
| DIBENZOTHIOPHENES | 1.8 | |
| NAPHTHOBENZOTHIOPHENES | 0.3 | |
| UNIDENTIFIED-AROMATICS | | 6.0 |

MS AROMATICS ANALYSIS ASTM D3239
SAMPLE: G11

| FRACTION IS 22.3 % OF OIL | VOLUME % OF FRACTION | |
|---|---|---|
| MONOAROMATICS | | 77.8 |
| ALKYLBENZENES | 48.1 | |
| NAPHTHENEBENZENES | 16.5 | |
| DINAPHTHENEBENZENES | 13.2 | |
| DIAROMATICS | | 8.1 |
| NAPHTHALENES | 2.2 | |
| ACENAPHTHALENES-DIBENZOFURANS | 3.2 | |
| FLUORENES | 2.7 | |
| TRIAROMATICS | | 1.5 |
| PHENANTHRENES | 1.1 | |
| NAPHTHENPHENANTHRENES | 0.4 | |
| TRETRA-AROMATICS | | 1.7 |
| PYRENES | 0.8 | |
| CHRYSENES | 0.9 | |
| PENTA-AROMATICS | | 0.5 |
| PERYLENES | 0.4 | |
| DIBENZANTHRACENES | 0.2 | |
| THIOPHENO-AROMATICS | | 6.3 |
| BENZOTHIOPHENES | 3.9 | |
| DIBENZOTHIOPHENES | 2.3 | |
| NAPHTHOBENZOTHIOPHENES | 0.2 | |
| UNIDENTIFIED-AROMATICS | | 4.0 |

TYPE ANALYSIS D-2425-83
SAMPLE: G6

| | AROMS | SATS |
|---|---|---|
| PARAFFINS | 0.2 | 0.0 |
| CYCLOPARAFFINS | 0.0 | 0.0 |
| DICYCLOPARAFFINS | 0.0 | 0.0 |
| TRICYCLOPARAFFINS | 0.0 | 0.0 |
| ALKYL BENZENES | 20.0 | 0.0 |
| INDANES/TETRALINS | 20.4 | 0.0 |
| INDENES ETC | 4.7 | 0.0 |
| NAPHTHALENE | 4.2 | 0.0 |
| NAPHTHALENES | 47.5 | 0.0 |
| ACENAPHTHENES | 2.4 | 0.0 |
| ACENAPHTHYLENES | 0.2 | 0.0 |
| TRICYCLIC AROMATICS | 0.4 | 0.0 |

TYPE ANALYSIS D-2425-83
SAMPLE: G9

| | AROMS | SATS |
|---|---|---|
| PARAFFINS | 0.1 | 0.0 |
| CYCLOPARAFFINS | 0.0 | 0.0 |
| DICYCLOPARAFFINS | 0.0 | 0.0 |
| TRICYCLOPARAFFINS | 0.0 | 0.0 |
| ALKYL BENZENES | 1.5 | 0.0 |
| INDANES/TETRALINS | 0.2 | 0.0 |
| INDENES ETC | 0.2 | 0.0 |
| NAPHTHALENE | 0.0 | 0.0 |
| NAPHTHALENES | 20.8 | 0.0 |
| ACENAPHTHENES | 17.2 | 0.0 |
| ACENAPHTHYLENES | 22.3 | 0.0 |
| TRICYCLIC AROMATICS | 37.7 | 0.0 |

TYPE ANALYSIS D-2425-83
SAMPLE: G10

| | AROMS | SATS |
|---|---|---|
| PARAFFINS | 1.3 | 0.0 |
| CYCLOPARAFFINS | 6.9 | 0.0 |
| DICYCLOPARAFFINS | 0.0 | 0.0 |
| TRICYCLOPARAFFINS | 0.0 | 0.0 |
| ALKYL BENZENES | 7.3 | 0.0 |
| INDANES/TETRALINS | 4.1 | 0.0 |
| INDENES ETC | 1.2 | 0.0 |
| NAPHTHALENE | 0.5 | 0.0 |
| NAPHTHALENES | 15.4 | 0.0 |
| ACENAPHTHENES | 11.7 | 0.0 |
| ACENAPHTHYLENES | 21.1 | 0.0 |
| TRICYCLIC AROMATICS | 30.5 | 0.0 |

# APPENDIX B

## FACTOR ANALYSIS PROGRAMS AND SUBROUTINES.

```
C
C       MASS SPECTROMETRIC FACTOR ANALYSIS PROGRAM
C
        DIMENSION DAT(10,30),COV(10,10),EVECT(10,10),EVALS(10),
     +          V(10,30),PU(10),A(10,10),CONC(10,10),CCT(30,10),
     +          INVCCT(30,10),R(10,30),M(10,10),CTCCT(10,10)
C
        REAL INVCCT,MAX,M
        INTEGER FT,PU,ZP
        LOGICAL FLAG
C
        COMMON /LAB/ DAT
        COMMON /LAB0/ NMX,NPK
        COMMON /LAB1/ CONC
        COMMON /LAB2/ V,N
        COMMON /LAB3/ EVALS
        COMMON /LAB4/ COV,C,S
        COMMON /LAB5/ PU
        COMMON /LAB6/ EVECT
C
        EQUIVALENCE (V,CCT,INVCCT,R),(COV,A,CTCCT),
     +          (CONC,M)
C
        THR=1.0E-09
C
        FLAG=.FALSE.
        TYPE
        CALL GTDATA
C
C       FORM THE COVARIANCE MATRIX FROM THE DATA
C
        DO 100 I=1,NMX
        DO 100 J=1,NMX
        COV(J,I)=0.0
        DO 100 K=1,NPK
        COV(J,I)=COV(J,I)+DAT(I,K)*DAT(J,K)
 100    CONTINUE
        CALL NODDY(COV,NMX,NMX,10,10)
C
C       CALCULATE THE EIGENVECTORS & EIGENVALUES
C
        CALL EIGEN
        TYPE ' EIGENVECTORS'
        TYPE
        TYPE
        CALL NODDY(EVECT,NMX,NMX,10,10)
C
C       CALCULATE RE & 'IND' FUNCTION.
C
 180    N=0
        IF (FLAG) GOTO 195
        DO 190 FT=1,2
        CALL REIND(FT)
 190    CONTINUE
 195    TYPE
```

```
2830    ACCEPT ' NUMBER OF FACTORS ? ',N
        IF (N.LE.0) TYPE ' YOU MUST HAVE AT LEAST ONE FACTOR !'
        IF (N.GT.NMX) TYPE ' YOU CANNOT HAVE MORE FACTORS THAN SPECTRA.'
        IF ((N.LE.0).OR.(N.GT.NMX)) GOTO 2830
        TYPE
        TYPE ' NUMBER OF FACTORS CHOSEN ',N
        FLAG=.TRUE.
C
C       CALCULATE THE [V] MATRIX.
C       [V]=[D].[EVECT] FOR FIRST N EIGENVECTORS
C
        DO 200 I=1,NPK
        DO 200 J=1,N
        V(J,I)=0.0
        DO 200 K=1,NMX
        V(J,I)=V(J,I)+DAT(K,I)*EVECT(K,J)
 200    CONTINUE
C
C       NORMALISE [V].
C       SUM OF SQUARES ACROSS EACH ROW IS UNITY.
C
        DO 220 I=1,NPK
        SUM=0.0
        DO 210 J=1,N
        SUM=SUM+V(J,I)*V(J,I)
 210    CONTINUE
        SUM=SQRT(1/SUM)
        DO 220 J=1,N
        V(J,I)=V(J,I)*SUM
 220    CONTINUE
        TYPE ' [V] MATRIX'
        CALL NODDY(V,NPK,N,30,10)
C
C       FIND PURE PEAKS
C
        TYPE ' SELECTION OF PURE PEAKS'
        TYPE
        TYPE ' 1...MANUAL SELECTION'
        TYPE
        TYPE ' 2...MALINOWSKY METHOD (AUTOMATIC)'
        TYPE
3510    ACCEPT ' WHICH METHOD (1 OR 2) ? ',METHOD
        IF ((METHOD.NE.1).AND.(METHOD.NE.2)) GOTO 3510
        IF (METHOD.EQ.1) CALL MANUAL
        IF (METHOD.EQ.2) CALL MALIN
        TYPE ' PEAKS UNIQUE TO FACTORS '
        IF (METHOD.EQ.1) TYPE ' (MANUALLY SELECTED)'
        IF (METHOD.EQ.2) TYPE ' (AUTOMATICALLY SELECTED)'
        TYPE
        TYPE ' FACTOR#          PEAK#'
        TYPE
        DO 280 I=1,N
        WRITE(10,5060) I,PU(I)
5060    FORMAT(I4,10X,I3)
 280    CONTINUE
```

```
C
C       FILL ROTATION MATRIX
C
        DO 290 J=1,N
        DO 290 I=1,N
        A(I,J)=V(J,PU(I))
 290    CONTINUE
        TYPE ' ROTATION MATRIX'
        CALL NODDY(A,N,N,10,10)
C
C
C       FORM CONCENTRATION MATRIX
C
        DO 300 I=1,N
        DO 300 J=1,NMX
        CONC(J,I)=0.0
        DO 300 K=1,NMX
        CONC(J,I)=CONC(J,I)+EVECT(K,I)*A(J,K)
 300    CONTINUE
        TYPE ' CONCENTRATION MATRIX'
        CALL NODDY(CONC,N,NMX,10,10)
C
C       GET CCT FROM C DIRECTLY
C
        DO 310 I=1,N
        DO 310 J=1,N
        CCT(J,I)=0.0
        DO 310 K=1,NMX
        CCT(J,I)=CCT(J,I)+CONC(K,I)*CONC(K,J)
 310    CONTINUE
C
C       INVERT CCT -> INVCCT
C
        CALL INVERT
C
C       GET CCT.CCTINV
C
        DO 320 I=1,NPK
        DO 320 J=1,N
        CTCCT(J,I)=0.0
        DO 320 K=1,N
        CTCCT(J,I)=CTCCT(J,I)+CONC(I,K)*INVCCT(J,K)
 320    CONTINUE
C
C       SPECTRA
C
        DO 330 I=1,NPK
        DO 330 J=1,N
        R(J,I)=0.0
        DO 330 K=1,NMX
        R(J,I)=R(J,I)+DAT(K,I)*CTCCT(J,K)
 330    CONTINUE
```

```
C
C       NORMALISE SPECTRA - BASE PEAK = 100%
C
        DO 360 I=1,N
        MAX=0.0
        DO 340 J=1,NPK
        IF (R(I,J).LT.0) R(I,J)=0.0
        IF (R(I,J).LT.MAX) GOTO 340
        MAX=R(I,J)
 340    CONTINUE
        IF (MAX.GT.0) GOTO 345
        TYPE
        TYPE ' SPECTRUM ',I,' IS FULL OF ZEROS'
        TYPE ' SO DO NOT TRUST THE RESULTS !!!'
        TYPE
        MAX=100.0
 345    MAX=100.0/MAX
        DO 350 J=1,NPK
        R(I,J)=R(I,J)*MAX
 350    CONTINUE
        DO 360 J=1,NMX
        CONC(J,I)=CONC(J,I)/MAX
 360    CONTINUE
        TYPE
        TYPE ' CONCENTRATIONS'
        TYPE ' --------------'
        TYPE
        DO 390 I=1,NMX
        SUM=0.0
        DO 370 J=1,N
        IF (CONC(I,J).LT.0) CONC(I,J)=0.0
        SUM=SUM+CONC(I,J)
 370    CONTINUE
        IF (SUM.NE.0) SUM=100.0/SUM
        DO 380 J=1,N
        CONC(I,J)=CONC(I,J)*SUM
        WRITE(10,5070) CONC(I,J)
5070    FORMAT(F8.1,Z)
 380    CONTINUE
        TYPE
 390    CONTINUE
        PAUSE
```

```
      TYPE
      TYPE ' SPECTRA'
      TYPE ' -------'
      TYPE
      DO 410 I=1,NPK
      DO 400 J=1,N
      ZP=INT(10*R(I,J)+0.5)
      IF (ZP.EQ.0) WRITE(10,5080)
5080  FORMAT(7X,'-',Z)
      IF (ZP.GT.0) WRITE(10,5090) R(I,J)
5090  FORMAT(F8.1,Z)
 400  CONTINUE
      TYPE
 410  CONTINUE
      TYPE
      PAUSE
C
C     REPEAT ?
C
      TYPE
 420  TYPE ' DO YOU WISH TO REPEAT THE CALCULATION'
      TYPE ' USING A DIFFERENT NUMBER  OF  FACTORS'
      ACCEPT ' OR DIFFERENT PURE PEAKS ? (Y/N)',ANSWER
      IF (ANSWER.EQ.'Y') GOTO 180
      IF (ANSWER.EQ.'N') GOTO 500
      GOTO 420
 500  END
```

```
C
C       EIGENVECTOR SUBROUTINE.
C
        SUBROUTINE EIGEN
        REAL COV(100),TEMP(100),EVEC(100),EVALS(10),
     +          DUM(10,30),NI,NF,MAX
        INTEGER AA,AB,AC,AD
C
        COMMON /LAB0/ NMX,NPK
        COMMON /LAB2/ DUM,N
        COMMON /LAB3/ EVALS
        COMMON /LAB4/ COV,C,S
        COMMON /LAB6/ EVEC
C
        THR=1.0E-9
C
C       CONVERT COVARIANCE MATRIX INTO TRIANGULAR FORM TO
C       CONFORM WITH THE EIGENVECTOR ANALYSIS.
C
        K=0
        DO 100 I=1,NMX
        I2=(I-1)*10
        DO 100 J=1,I
        IJ=I2+J
        K=K+1
        COV(K)=COV(IJ)
 100    CONTINUE
        K=K+1
        DO 110 I=K,100
        COV(I)=0.0
 110    CONTINUE
C
C       CALCULATE EIGENVECTORS AND EIGENVALUES.
C
C       INITIALISE EIGENVECTOR ARRAY.
C
        DO 120 I=1,NMX
        I2=(I-1)*NMX
        DO 120 J=1,NMX
        IJ=I2+J
        EVEC(IJ)=0.0
        IF (I.EQ.J) EVEC(IJ)=1.0
 120    CONTINUE
C
C       CALCULATE EIGENVALUES:
C       GENERATE INITIAL AND FINAL NORMS.
C       NI IS THE MEAN SQUARE VALUE OF THE
C       OFF-DIAGONAL ELEMENTS.
C
        NI=0.0
        DO 130 I=1,NMX
        DO 125 J=I,NMX
        IF (I.EQ.J) GOTO 125
        IA=(J*J-J)/2+I
        NI=NI+COV(IA)*COV(IA)
 125    CONTINUE
 130    CONTINUE
```

```
      IF (NI.LE.0.0) GOTO 2280
      NI=SQRT(2.0*NI)
      NF=NI*THR/NMX
      IND=0
      TH=NI
1870  TH=TH/NMX
1880  L=1
1890  M=L+1
1900  MQ=(M*M-M)/2
      LQ=(L*L-L)/2
      LM=L+MQ
      IF (ABS(COV(LM)).LT.TH) GOTO 2230
      IND=1
      LL=L+LQ
      MM=M+MQ
      X=(COV(LL)-COV(MM))/2
      W=-COV(LM)/SQRT(COV(LM)*COV(LM)+X*X)
      IF (X.LT.0) W=-W
      S=W/SQRT(2*(1+SQRT(1-W*W)))
      S2=S*S
      C=SQRT(1-S2)
      C2=C*C
      CS=C*S
      AA=NMX*(L-1)
      AB=NMX*(M-1)
C
C     ROTATE L AND M COLUMNS.
C
      DO 140 I=1,NMX
      IQ=(I*I-I)/2
      IF ((I.EQ.L).OR.(I.EQ.M)) GOTO 2120
      IF (I.GT.M) IM=M+IQ
      IF (I.LT.M) IM=I+MQ
      IF (I.LT.L) IL=I+LQ
      IF (I.GT.L) IL=L+IQ
      X=COV(IL)*C-COV(IM)*S
      COV(IM)=COV(IL)*S+COV(IM)*C
      COV(IL)=X
2120  AC=AA+I
      AD=AB+I
      X=EVEC(AC)*C-EVEC(AD)*S
      EVEC(AD)=EVEC(AC)*S+EVEC(AD)*C
      EVEC(AC)=X
 140  CONTINUE
```

```
C
C       CLEAR UP AND BACK FOR NEXT.
C
        X=2*COV(LM)*CS
        W=COV(LL)*C2+COV(MM)*S2-X
        X=COV(LL)*S2+COV(MM)*C2+X
        COV(LM)=(COV(LL)-COV(MM))*CS+COV(LM)*(C2-S2)
        COV(LL)=W
        COV(MM)=X
2230    IF (M.EQ.NMX) GOTO 2240
        M=M+1
        GOTO 1900
2240    IF (L.EQ.(NMX-1)) GOTO 2250
        L=L+1
        GOTO 1890
2250    IF (IND.NE.1) GOTO 2260
        IND=0
        GOTO 1880
2260    IF (TH.GT.NF) GOTO 1870
C
C       SORT THE EIGENVECTORS.
C
2280    IQ=-NMX
        DO 150 I=1,NMX
        IQ=IQ+NMX
        LL=I+(I*I-I)/2
        JQ=NMX*(I-2)
        DO 150 J=I,NMX
        JQ=JQ+NMX
        MM=J+(J*J-J)/2
C
C       SWAP THE EIGENVALUES ?
C
        IF (COV(LL).GE.COV(MM)) GOTO 150
        X=COV(LL)
        COV(LL)=COV(MM)
        COV(MM)=X
```

```
C
C       SWAP CORRESPONDING EIGENVECTORS.
C
        DO 145 K=1,NMX
        AC=IQ+K
        AD=JQ+K
        X=EVEC(AC)
        EVEC(AC)=EVEC(AD)
        EVEC(AD)=X
 145    CONTINUE
 150    CONTINUE
        J=0
        DO 160 I=1,NMX
        J=J+I
        EVALS(I)=COV(J)
        IF (EVALS(I).LE.0.0) EVALS(I)=1.0E-30
 160    CONTINUE
        MAX=0.0
        N=0
        TYPE ' EIGENVALUES'
        WRITE(10,5000) EVALS(1)
5000    FORMAT(1X,F12.0,10X,'RATIO')
        DO 170 I=2,NMX
        RATIO=EVALS(I-1)/EVALS(I)
        IF (RATIO.LE.MAX) GOTO 2560
        MAX=RATIO
        N=I-1
2560    WRITE(10,5010) EVALS(I),RATIO
5010    FORMAT(1X,F12.0,10X,F12.0)
 170    CONTINUE
        WRITE(10,5020) N
5020    FORMAT(11X,'SUCCESSIVE EIGENVALUE RATIO'/
     +          11X,'SUGGESTS',I3,' FACTORS')
        DO 180 I=1,NMX
        IF (EVALS(I).LT.THR) EVALS(I)=0.0
 180    CONTINUE
        K=0
        DO 190 I=1,NMX
        I2=(I-1)*10
        DO 190 J=1,NMX
        IJ=I2+J
        K=K+1
        TEMP(IJ)=EVEC(K)
 190    CONTINUE
        DO 200 I=1,100
        EVEC(I)=TEMP(I)
 200    CONTINUE
        RETURN
        END
```

```
      SUBROUTINE INVERT
C
      DIMENSION CCT(30,10),INVCCT(30,10)
C
      REAL INVCCT
C
      COMMON /LAB2/ CCT,N
C
C     INITIALLY [INVCCT] IS SET TO A UNIT MATRIX.
C
      DO 100 I=1,N
      DO 100 J=1,N
      INVCCT(J,I)=0.0
      IF (I.EQ.J) INVCCT(J,I)=1.0
 100  CONTINUE
C
C     TRIANGULATE CCT
C
      I2=N-1
      DO 110 I=1,I2
      DO 110 J=I,N
      Z=CCT(I,I)/CCT(J,I)
      DO 110 K=1,N
      CCT(K,J)=CCT(K,I)-Z*CCT(K,J)
      INVCCT(K,J)=INVCCT(K,J)-Z*INVCCT(K,J)
 110  CONTINUE
C
C     BACK SUSTITUTE
C
      DO 130 I=1,N
      I2=N+1-I
      DO 130 K=1,N
      IF (I.EQ.N) GOTO 125
      J2=I+1
      DO 120 J=J2,N
      INVCCT(K,I)=INVCCT(K,I)-CCT(J,I)*INVCCT(K,J)
 120  CONTINUE
 125  INVCCT(K,I)=(INVCCT(K,I)+1.0E-18)/(CCT(I,I)+1.0E-18)
 130  CONTINUE
      RETURN
      END
```

```
      SUBROUTINE DETER(ORDER,RESULT)
C
      DIMENSION M(10,10),TEMP(10,10)
C
      REAL M
      INTEGER ORDER
C
      COMMON /LAB1/ M
C
      DO 100 I=1,ORDER
      DO 100 J=1,ORDER
      TEMP(J,I)=M(J,I)
 100  CONTINUE
C
C     TRANSFORM INTI TRIANGULAR ARRAY BY
C     ROW/COLUMN OPS.
C
      MM=ORDER-1
      DO 110 K=1,MM
      M2=K+1
      IF (ABS(TEMP(K,K)).GT.1.0E-30) GOTO 108
      DO 105 L=M2,ORDER
      IF (ABS(TEMP(K,L)).LE.1.0E-30) GOTO 105
      DO 102 L2=1,ORDER
      TEMP(L2,K)=TEMP(L2,K)+TEMP(L2,L)
 102  CONTINUE
      GOTO 108
 105  CONTINUE
      RESULT=0.0
      RETURN
 108  DO 110 I=M2,ORDER
      Z=TEMP(K,I)/TEMP(K,K)
      DO 110 J=K,ORDER
      TEMP(J,I)=TEMP(J,I)-TEMP(J,K)*Z
 110  CONTINUE
C
C     THE DETERMINANT IS THE PRODUCT OF THE ELEMENTS
C     ALONG THE MAIN DIAGONAL OF THE TRIANGULAR MATRIX.
C
      RESULT=1.0
C
      DO 120 I=1,ORDER
      RESULT=RESULT*TEMP(I,I)
 120  CONTINUE
      RETURN
      END
```

```
C
C       MALINOWSKY PURE PEAKS ALGORITHM.
C
        SUBROUTINE MALIN
        DIMENSION V(10,30),PU(10),M(10,10)
        REAL M,MIN,MAX
        INTEGER PU,P
        COMMON /LAB0/ NMX,NPK
        COMMON /LAB1/ M
        COMMON /LAB2/ V,N
        COMMON /LAB5/ PU
        MIN=1.0E-30
C
C       FIND FIRST PURE PEAK.
C
        DO 230 I=1,NPK
        IF (V(1,I).GE.MIN) GOTO 230
        MIN=V(1,I)
        PU(1)=I
 230    CONTINUE
C
C       FIND SECOND PURE PEAK.
C
        MIN=1.0E-30
        V2=V(2,PU(1))
        DO 240 I=1,NPK
        IF (I.EQ.PU(1)) GOTO 240
        DP=V2*V(2,I)
        IF (DP.GE.MIN) GOTO 240
        MIN=DP
        PU(2)=I
 240    CONTINUE
C
C       THIRD TO NTH PURE PEAK.
C
        IF (N.LT.3) RETURN
        DO 270 I2=3,N
        MAX=0.0
        I3=I2-1
        DO 250 J=1,I3
        DO 250 P=1,I2
        M(P,J)=V(P,PU(J))
 250    CONTINUE
        DO 270 L=1,NPK
        DO 260 P=1,I2
        M(P,I2)=V(P,L)
 260    CONTINUE
        CALL DETER(I2,DET)
        IF (ABS(DET).LE.MAX) GOTO 270
        MAX=ABS(DET)
        PU(I2)=L
 270    CONTINUE
        RETURN
        END
```

```
      SUBROUTINE MANUAL
C
      DIMENSION PU(10),DUM(10,30)
C
      INTEGER PU
C
      COMMON /LAB2/ DUM,N
      COMMON /LAB5/ PU
C
      DO 100 I=1,N
   90 WRITE(10,1000) I
 1000 FORMAT(' PURE PEAK FOR COMPONENT ',I4,' ? ',Z)
      ACCEPT PU(I)
      IF ((PU(I).LT.1).OR.(PU(I).GT.N)) GOTO 90
  100 CONTINUE
      TYPE
      RETURN
      END
```

```
C
C       RE & 'IND' FUNCTION SUBROUTINE.
C
        SUBROUTINE REIND(FT)
C
C
        DIMENSION EVALS(10)
        REAL MIN
        INTEGER FT
        LOGICAL FLAG1,FLAG2
C
        COMMON /LAB0/ NMX,NPK
        COMMON /LAB3/ EVALS
C
        FLAG1=(FT.EQ.1)
        FLAG2=(FT.EQ.2)
        IF (FLAG1) WRITE(10,1000)
        IF (FLAG2) WRITE(10,1010)
1000    FORMAT(//' REAL ERROR - COMPARE WITH EXPTL. ERROR.'/)
1010    FORMAT(//' IND FUNCTION - LOOK FOR MINIMUM.'/)
        MIN=1.0E38
        K=NMX-1
        DO 100 I=1,K
        SUM=0.0
        L=I+1
        DO 90 J=L,NMX
        SUM=SUM+EVALS(J)
  90    CONTINUE
        RE=SQRT(SUM/NPK*(NMX-I))
        IF (FLAG1) FU=RE
        IF (FLAG2) FU=RE/(NMX-I)**2
        IF (FLAG1) WRITE(10,1020) I,FU
        IF (FLAG2) CALL INDS(MIN,FU,N,I)
 100    CONTINUE
1020    FORMAT(I8,10X,F12.4)
        IF (FLAG1) RETURN
        IF (N.EQ.1) TYPE N,' FACTOR INDICATED'
        IF (N.GT.1) TYPE N,' FACTORS INDICATED'
        TYPE
        PAUSE
        RETURN
        END
```

```
      SUBROUTINE INDS(MIN,FU,N,I)
C
      REAL MIN,FU
      INTEGER N,I
      IF (FU.GE.MIN) GOTO 10
      MIN=FU
      N=I
   10 IF (FU.EQ.0) GOTO 20
      WRITE(10,1000) I,FU
 1000 FORMAT(I8,10X,F12.4)
   20 RETURN
      END
```

```
      SUBROUTINE YESNO(ANSWER)
C
      INTEGER REPLY
C
      LOGICAL ANSWER
C
  100 READ(11,1000) REPLY
 1000 FORMAT(A1)
C
C                NOTE: 22816 CORRESPOND TO "Y" AND
C                        20000 CORRESPONDS TO "N".
C
      IF ((REPLY.NE.22816).AND.(REPLY.NE.20000)) GOTO 100
      ANSWER=.FALSE.
      IF (REPLY.EQ.22816) ANSWER=.TRUE.
      RETURN
      END
```

```
      SUBROUTINE NODDY(MATRIX,ROWS,COLS,RSZ,CSZ)
C
      INTEGER ROWS,COLS,RSZ,CSZ
C
      REAL MATRIX(CSZ,RSZ)
C
      DO 110 I=1,COLS
      DO 100 J=1,ROWS
      WRITE(10,1000) MATRIX(J,I)
 1000 FORMAT(E16.8,2X,Z)
  100 CONTINUE
      WRITE(10,1010)
  110 CONTINUE
      WRITE(10,1010)
 1010 FORMAT(/)
      PAUSE
      RETURN
      END
```

```
      SUBROUTINE GTDATA
C
      DIMENSION DAT(10,30)
C
      INTEGER SPEC,PEAK,ANSWER
C
      COMMON /LAB/ DAT
      COMMON /LAB0/ NMX,NPK
C
 100  ACCEPT ' HOW MANY SPECTRA (MAX 10) ? ',NMX
      IF ((NMX.GT.10).OR.(NMX.LT.2)) GOTO 100
 110  ACCEPT ' HOW MANY PEAKS IN EACH SPECTRUM (MAX 30) ? ',NPK
      IF ((NPK.GT.30).OR.(NPK.LT.1)) GOTO 110
      TYPE
      DO 120 J=1,NMX
      DO 115 I=1,NPK
      WRITE(10,1020) J,I
1020  FORMAT(1X,'SPECTRUM ',I4,'; MASS PEAK ',I4,' ? ',Z)
      ACCEPT DAT(J,I)
 115  CONTINUE
      TYPE
 120  CONTINUE
 125  TYPE
      DO 140 I=1,NPK
      DO 130 J=1,NMX
      WRITE(10,1030) DAT(J,I)
1030  FORMAT(F12.4,Z)
 130  CONTINUE
      TYPE
 140  CONTINUE
 150  WRITE(10,1040)
1040  FORMAT(1X,'ANY CORRECTIONS (Y/N) ? ',Z)
      READ(11,2020) ANSWER
2020  FORMAT(A1)
X     TYPE ' VALUE PUT INTO ANSWER IS ......',ANSWER
C     NOTE: INTEGERS 22816 & 20000 CORRESPOND TO "Y" & "N" RESP.
      IF ((ANSWER.NE.22816).AND.(ANSWER.NE.20000)) GOTO 150
      IF (ANSWER.EQ.20000) RETURN
 160  ACCEPT ' CHANGE WHICH SPECTRUM ? ',SPEC
      IF ((SPEC.LT.1).OR.(SPEC.GT.NMX)) GOTO 160
 170  ACCEPT ' CHANGE WHICH MASS PEAK ? ',PEAK
      IF ((PEAK.LT.1).OR.(PEAK.GT.NPK)) GOTO 170
      WRITE(10,1020) SPEC,PEAK
      ACCEPT DAT(SPEC,PEAK)
      GOTO 125
      END
```

```
C       SUBROUTINE TO SAVE DATA TO DISK
C
        SUBROUTINE SVDAT(FNAME)
        DIMENSION DAT(10,30)
        LOGICAL MSFLG
        INTEGER FNAME(4),MASS(30)
        COMMON /LAB/ DAT
        COMMON /LAB0/ NMX,NPK
        COMMON /LAB7/ MASS,MSFLG
C
 200    WRITE(10,1010)
1010    FORMAT(" FILE NAME (6 CHARS. MAX.) ? "Z)
        READ(11,5010) (FNAME(I), I=1,4)
5010    FORMAT(4S2)
        CALL DIR("DP0",IER)
        IF (IER.NE.1) GOTO 9000
        CALL CFILW(FNAME,1,IER)
        IF (IER.NE.1) GOTO 9000
        CALL OPEN(8,FNAME,3,IER)
        IF (IER.NE.1) GOTO 9000
C
        WRITE BINARY(8) MSFLG,NMX,NPK
        IF (.NOT.MSFLG) GOTO 5
        DO 5 I=1,NPK
        WRITE BINARY(8) MASS(I)
   5    CONTINUE
        DO 10 I=1,NPK
        DO 10 J=1,NMX
        WRITE BINARY(8) DAT(J,I)
  10    CONTINUE
        CALL CLOSE(8,IER)
        IF (IER.NE.1) GOTO 9000
        RETURN
C
C
C
9000    TYPE
        TYPE "RDOS ERROR"
        IF (IER.EQ.4) TYPE " ILLEGAL FILE NAME"
        IF (IER.EQ.12) TYPE " FILE ALREADY EXISTS"
        IF ((IER.NE.12).AND.(IER.NE.4)) GOTO 9010
        WRITE(10,1020)
1020    FORMAT(/" NEW "Z)
        GOTO 200
9010    TYPE
        TYPE " SYSTEM ERROR NUMBER ",IER," RUN TERMINATED"
        TYPE
        CALL EXIT
        END
```

```
C       SUBROUTINE TO LOAD SAVED DATA FROM DISK.
C
        SUBROUTINE LDDAT(FNAME)
C
        DIMENSION DAT(10,30)
C
        LOGICAL MSFLG
C
        INTEGER FNAME(4),MASS(30)
C
C
        COMMON /LAB/ DAT
        COMMON /LAB0/ NMX,NPK
        COMMON /LAB7/ MASS,MSFLG
C
 200    WRITE(10,1010)
1010    FORMAT(' FILE NAME (6 CHARS. MAX.) ? 'Z)
        READ(11,5010) (FNAME(I),I=1,4)
5010    FORMAT(4S2)
        CALL DIR("DP0",IER)
        IF (IER.NE.1) GOTO 9000
        CALL OPEN(8,FNAME,1,IER)
        IF (IER.NE.1) GOTO 9000
C
        READ BINARY(8) MSFLG,NMX,NPK
        IF (.NOT.MSFLG) GOTO 5
        DO 5 I=1,NPK
        READ BINARY(8) MASS(I)
   5    CONTINUE
        DO 10 I=1,NPK
        DO 10 J=1,NMX
        READ BINARY(8) DAT(J,I)
  10    CONTINUE
        CALL CLOSE(8,IER)
        IF (IER.NE.1) GOTO 9000
        RETURN
C
C
C
9000    TYPE
        TYPE "RDOS ERROR"
        IF (IER.EQ.4) TYPE "ILLEGAL FILE NAME"
        IF (IER.EQ.16) TYPE "FILE DOES NOT EXIST"
        IF ((IER.NE.16).AND.(IER.NE.4)) GOTO 9010
        WRITE(10,1020)
1020    FORMAT(/" NEW "Z)
        GOTO 200
9010    TYPE
        TYPE " SYSTEM ERROR ",IER," RUN TERMINATED"
        TYPE
        CALL EXIT
        END
```

```
C
C       PROGRAM TO GENERATE TEST DATA
C
        DIMENSION DAT(10,30),R(10,30),C(10,10)
        INTEGER FDUM(4)
        COMMON /LAB/ DAT
        COMMON /LAB0/ NMX,NPK
        TYPE " HOW MANY MIXTURES ? "
        ACCEPT NMX
        TYPE " HOW MANY COMPONENTS ? "
        ACCEPT N
        TYPE " HOW MANY PEAKS ? "
        ACCEPT NPK
        DO 10 I=1,NMX
        DO 10 J=1,N
        TYPE " CONCENTRATION OF COMP.",J," IN MIXTURE",I," ? "
        ACCEPT C(I,J)
 10     CONTINUE
        DO 20 I=1,N
        DO 20 J=1,NPK
        TYPE " INTENSITY OF PEAK",J," IN COMP.",I," ? "
        ACCEPT R(I,J)
 20     CONTINUE
        DO 30 I=1,NPK
        DO 30 J=1,NMX
        DAT(J,I)=0.0
        DO 30 K=1,N
        DAT(J,I)=DAT(J,I)+R(K,I)*C(J,K)
 30     CONTINUE
        CALL SVDAT(FDUM)
        CALL NODDY(DAT,NPK,NMX,30,10,12,'DATA MATRIX')
        CALL NODDY(C,N,NMX,10,10,12,' CONCENTRATION MATRIX')
        CALL NODDY(R,NPK,N,30,10,12,' [R] MATRIX')
        DO 40 I=1,N
        SUM=0.0
        DO 35 J=1,NMX
        SUM=SUM+C(I,J)
 35     CONTINUE
        SUM=SUM/100.0
        DO 40 J=1,NMX
        C(I,J)=C(I,J)/SUM
 40     CONTINUE
        CALL NODDY(C,N,NMX,10,10,12,' CONC.  MATRIX - NORMALISED')
        DO 50 I=1,N
        SUM=0.0
        DO 45 J=1,NPK
        IF (R(I,J).GT.SUM) SUM=R(I,J)
 45     CONTINUE
        SUM=SUM/100.0
        DO 50 J=1,NPK
        R(I,J)=R(I,J)/SUM
 50     CONTINUE
        CALL NODDY(R,NPK,N,30,10,12,' [R] MATRIX - NORMALISED')
        CALL EXIT
        END
```

```
C
C                 FACTOR ANALYSIS DATA PREP.  PROGRAM
C
      CHANTASK 16,1
      PARAMETER IRPCH=1                          ;REPORT DEVICE CHANNEL
      PARAMETER BUFSZ=825,NBUF=3                 ;I/O WORK AREA SIZE
      PARAMETER RPTSZ=24,DFTSZ=20                ;ARRAY SIZES
      PARAMETER QSIZE=100
C
C
C
      PARAMETER RNMSK=400K
      PARAMETER MSMSK=4K
      PARAMETER STATL=4
      PARAMETER SNPKS=2
      PARAMETER SRECL=3
C
C
C
      COMMON IRPT(RPTSZ),IDFT(DFTSZ),DEFECT,INQU(QSIZE),MHI,MLO,ISWIT(2)
C
C
C
      COMMON /APNAM/ IDQNAM(RPTSZ)
      COMMON /IOP/ LINENO,IPAGENO,IFULLPG
C
      COMMON /LAB/ DAT(10,30)
      COMMON /LAB0/ NMX,NPK
      COMMON /LAB7/ MASS,MSFLG
      INTEGER FDUM(4),MASS(30),IOBUFF(BUFSZ),NSCAN,
     + RUNNAM(8),ISTAT(64),IPK(4)
      DOUBLE PRECISION DEFECT
      LOGICAL ANSWER,MSFLG
C
C
      CALL CINIT(ISWIT)
      CALL DINIT(IOBUFF,NBUF)
      CALL TYPSNT(10,"$VDU",.FALSE.)
      MSFLG=.TRUE.
      TYPE ' ENTER MASSES:-   "-1" TO FINNISH (MAX 30)'
      DO 10 I=1,30
      NPK=I
      WRITE(10,1000) I
1000  FORMAT(" MASS OF PEAK NO. "I3" > "Z)
      ACCEPT MASS(I)
      IF (MASS(I).EQ.-1) GOTO 12
  10  CONTINUE
      GOTO 15
  12  NPK=NPK-1
  15  NSCAN=0
      NMX=0
      TYPE " DO YOU WANT TO NORMALISE THE INTENSITIES ? "
      CALL YESNO(ANSWER)
```

```
  2     CALL DQ(NSCAN,INQU,QSIZE,RSC,RUNNAM,$2,$300)
C
        CALL DQOPN(ISCH,RUNNAM,NSCAN,MSMSK,ISTAT,$500,IER)
        IF (IER.NE.0) GOTO 500
        IF (ISTAT(8).NE."L") GOTO 700
        NPKS=ISTAT(SNPKS)
        IF (NPKS.EQ.0) GOTO 100
        CALL P4SR(ISTAT(10),ISTAT(9),STIC)
        STIC=STIC/1.0E06                                  ; TIC IN MILLIONS
        NMX=NMX+1
        DO 16 I=1,NPK
        DAT(NMX,I)=0.0
  16    CONTINUE
        DO 50 I=1,NPKS
        CALL DREAD(ISCH,IPK,$510,IER,ISTAT(SRECL))
        IF (IER.NE.0) GOTO 510
        CALL SCNVT(IPK,J1,10000K,RMASS,SIZE,J2,J3,J4,1.0,$50,$50)
        JJ=IDINT(DBLE(RMASS)+DEFECT)
        IF (.NOT.(ANSWER)) SIZE=SIZE/STIC        ; CORRECT FOR TOTAL ION
        DO 20 J=1,NPK                            ; CURRENT
        IF (JJ.NE.MASS(J)) GOTO 20
        DAT(NMX,J)=DAT(NMX,J)+SIZE
 20     CONTINUE
 50     CONTINUE
100     CALL DQCLS(ISCH,IER)
        IF (IER.NE.0) GOTO 500
        IF (NMX.EQ.10) GOTO 300
        GOTO 2
300     DO 70 I=1,NPK
        SUM=0.0
        DO 60 J=1,NMX
        SUM=SUM+DAT(J,I)
  60    CONTINUE
        IF (SUM.GE.1.0E-06) GOTO 70
        TYPE " WARNING...."
        TYPE " PEAK NO.",I," HAS NO ENTRIES"
  70    CONTINUE
        CALL SVDAT(FDUM)
C
C
C
400     CALL EXIT
C
C
C
500     TYPE " ERROR IN OPENING FILE"
        GOTO 550
510     TYPE " ERROR IN READING FROM FILE"
550     CALL CRNAM(RUNNAM,0,"MS",IDFT,ERRNAM)
        CALL RDOSER(.TRUE.,IER,NSCAN,ERRNAM)
        GOTO 400
C
C
C
700     TYPE " MUST BE LOW RES DATA"
        GOTO 400
C
        END
```